Metabolic Modulator Effects of Inorganic Nitrate and Nitrite, and Therapeutic Potential in Patients with Chronic Heart Failure

By

Brodie L Loudon

MBBS

A Thesis Presented in Fulfilment of the Requirements for the Degree of

Doctor of Philosophy

To

Norwich Medical School

University of East Anglia

December 2020

Abstract

Nitric oxide (NO) is a crucial signalling molecule within almost all aspects of human physiology. In the cardiovascular system, NO reduces blood pressure and vascular tone, prevents thrombus formation via platelet activation/aggregation, prevents inflammation by impairing leukocyte adherence to the endothelium, and prevents blood vessel thickening and pulmonary hypertension by impairing vascular smooth muscle cell proliferation. Inorganic nitrate (NO_3) and nitrite (NO_2) were historically considered to be inert byproducts of NO metabolism (i.e. oxidation within the tissues). The recently characterised nitrate-nitrite-NO pathway however, has revealed an important NO storage pool within the body that, importantly, is highly active in hypoxic tissues where typical mechanisms for NO production (i.e. via L-arginine) are impaired.

In a series of studies we have sought to explore the effects of inorganic nitrate and nitrite on a less explored effect of NO in the cardiovascular system, cardiac metabolism. In a basic science study in mice supplemented with 7 days of oral inorganic nitrate or nitrite, we explore the effects of nitrite on the rate-limiting enzyme of glucose metabolism, pyruvate dehydrogenase (PDH), and on the formation of the oxidative dimer of protein kinase G-1α, a newly-characterised downstream transducer of reactive oxygen species and inflammation that may have beneficial effects acutely but detrimental effects if chronically activated. We also explore these effects in human cardiac biopsy samples obtained from patients undergoing coronary artery bypass surgery. Although nitrite increased PKG1α dimer content, this was not statistically significant, except for in patients with type 2 diabetes, a pro-inflammatory state, in whom there was a robust *reduction* in dimer formation. This is in-keeping with the known anti-inflammatory effects of nitrite. Nitrite also dephosphorylated PDH but did not increase its activity in mouse or human heart tissue.

Given the potential for nitrite to affect metabolism, either via NO or via a direct effect of its own, we also investigated whether nitrite could affect the metabolic profile of 786-0 renal cell carcinoma cells, which is unique to cancers and involves a switch away from oxidative phosphorylation towards aerobic glycolysis (termed the Warburg effect), and whether this might increase susceptibility to chemotherapy. Interestingly, nitrite slightly improved cancer cell survival at lower doses of chemotherapy, but did not have any effects on PDH or other metabolic proteins such as Akt or LDH, and may have also occurred via effects on redox signalling.

We also designed a large, randomised controlled clinical trial to investigate the effect of oral inorganic (sodium) nitrate (to increase plasma nitrite levels) on exercise capacity in patients with heart failure with reduced ejection fraction. Inflammation, NO deficiency, and reduced cardiac metabolism are key features of heart failure, and correction of these features with nitrite have the potential to improve exercise tolerance, as well as potential effects on cardiac function, serum biomarkers, quality of life score, serum glucose and insulin levels, and inflammatory markers. Unfortunately, the study was halted prematurely by the study Sponsor, with only 19 patients recruited from a target of 56. However, our results showed a fall in exercise tolerance in the group receiving the placebo medication, and a small increase in the nitrate arm, and the difference was statistically significant. The fall in the placebo group was likely due to disease progression and worsening heart failure given the better baseline function in this arm compared to the nitrate arm, and the change in echocardiographic data such as V100.

Finally, by analysing data previously obtained by others in patients with symptomatic non-obstructive hypertrophic cardiomyopathy (often considered a unique subphenotype of heart failure with preserved ejection fraction), we assessed whether impaired resting cardiac energetic status (measured via resting 31P cardiovascular magnetic resonance spectroscopy and dynamic change in vasculoventricular coupling with exercise) was associated with the dynamic diastolic

dysfunction and impaired Frank-Starling mechanism that is largely responsible for the profound exercise intolerance in HCM. We demonstrate modest correlations between cardiac energetic impairment and exercise intolerance and vasculoventricular coupling in HCM, identifying energetic impairment as a key therapeutic target in HCM. Given the recent equivocal results of a definitive trial of nitrite in heart failure with preserved ejection fraction, and the results of our other studies, nitrite is unlikely to be a clinically useful treatment in these patients, however other metabolic modulators remain attractive.

Contents

List of Figures

List of Tables

Statement of Contribution

Chapter 3: Effects of Nitrite on Protein Expression in the Myocardium

The "Effect of Nitrite on Cardiac Muscle and Blood Vessels in Patients Undergoing Coronary Artery Bypass Grafting Surgery" Study, clinicaltrials.gov identifier: NCT04001283, was conceived by Professor Michael Frenneaux and completed at the University of Aberdeen. I undertook the molecular biology studies on the patient cardiac biopsy samples collected in this study, under the Supervision of Dr Melanie Madhani, Senior Lecturer Cardiovascular Medicine at the University of Birmingham, and Dr Nathan Procter, Senior Research Associate at the University of East Anglia. Professor Frenneaux, Dr Madhani and I designed the animal studies, and I performed the molecular studies on murine cardiac samples.

Chapter 4: Effects of Nitrite on Chemotherapy Sensitivity in 786-0 Renal Cell Carcinoma Cells

Professor Frenneaux and I conceived and designed the studies to investigate the effects of nitrite on chemotherapy sensitivity in 786-0 Renal Cell Carcinoma (RCC) cells. I performed the cell culture and viability studies, and performed the molecular biology studies under the Supervision of Dr Nathan Procter, Senior Research Associate at the University of East Anglia.

Chapter 5: The Nitrite In Chronic HEart failure (NICHE) Trial

The Nitrite In Chronic HEart failure (NICHE) Study (*Registered Title*: Effects of inorganic nitrite on cardiac and skeletal muscle), ISRCTN clinical trial registration number: 16356908, was conceived by Professor Michael Frenneaux. The study was first set up at the University of Aberdeen by Dr Konstantin Schwarz, but was later put on hold due to issues with sourcing the study drug. I transferred the study to the University of East Anglia/Norfolk and Norwich University Hospitals NHS Foundation Trust, and undertook the trial registration and compliance activities to commence the trial in England under the new HRA system. I set up the study at the Royal

Brompton Hospital, and completed the study recruitment, study drug management, and patient visits. Although I received training in transthoracic echocardiography and cardiopulmonary exercise testing, these were completed by cardiac physiologists the non-invasive cardiac imaging department as a condition of the Royal Brompton Hospital for their participation in the trial.

Chapter 6: Myocardial Energetic Deficiency in Non-obstructive Hypertrophic Cardiomyopathy and Association with Vasculoventricular Coupling and Exercise Capacity

The data for chapter 6, "Myocardial Energetic Deficiency in Non-obstructive Hypertrophic Cardiomyopathy and Association with Vasculoventricular Coupling and Exercise Capacity", was previously collected by Dr Khalid Abozguia, Dr Ibrar Ahmed, and Dr Thanh Phan at the University of Birmingham. Professor Michael Frenneaux and I designed the study and data analysis. A sub-analysis of this data has been included previously in a thesis presented by Dr Ibrar Ahmed to the University of Birmingham. I completed the data analysis and wrote the manuscript, which is currently under review by the American Heart Journal.

Acknowledgements

My thanks to the Medical Research Council (MRC) in the UK for funding the programme grant awarded to Professor Michael Frenneaux that funded the studies. I want to thank all the patients who participated in the studies for giving up their time and reminding me of the critical importance of research in improving lives. Many thanks to my wonderful supervisors Professor Michael Frenneaux and Dr Vassilios Vassiliou for inspiring a lasting passion for research in me, and for their unending guidance and patience. Thanks also to my supervisor in the basic science work, Dr Melanie Madhani, for her kind support and dedication, and to my supervisor and Principal Investigator for the NICHE clinical trial at the Royal Brompton Hospital, Professor Sanjay Prasad. I would also like to thank my amazing colleagues Dr Nicholas Gollop, Mrs Crystal Lowery, Dr Donnie Cameron, and Dr Nathan Procter for their emotional support and friendship. Finally, to my family, without whom this wouldn't have been possible, thank you for all that you have done and continue to do for me, I am truly blessed.

Chapter 1: Background

1.1 Introduction

Nitric oxide (NO) is a gaseous free-radical that acts as a signalling messenger in many critical cellular processes (1). NO is neutrally-charged and permeates across the phospholipid cell membrane, and was originally thought to have a half-life of milliseconds in the vasculature (due to rapid binding to oxyhaemoglobin) (2) but has since been shown to be transported across much greater distances within the circulation *in vivo*, in the form of NO metabolites or bound to proteins (RXNO), with release of NO at distal sites (3). Reactive oxygen species (ROS) levels within tissues are an important determinant of NO consumption and degradation, and the balance between synthesis and oxidation determines resting activity. NO is synthesised by the conversion of the non-essential amino acid l-arginine to l-citrulline in a reaction catalysed by nitric oxide synthase (NOS) in the presence of a number of enzymatic cofactors including oxygen (O_2), calcium (Ca^{2+}), tetrahydrobiopterin (BH4), and nicotinamide adenine dinucleotide phosphate (NADPH) (4). There are 3 known isoforms of the NOS enzyme, endothelial NOS (eNOS), inducible NOS (iNOS), and neuronal NOS (nNOS) (4). The membrane-bound eNOS isoform is constitutively expressed and was first derived from vascular endothelial cells (now known to be present in many tissues) (5), and NO derived from the NOS isoforms plays in integral role in a number of functions within the cardiovascular system including vasodilatation, platelet aggregation and leukocyte interaction, leukocyte adherence to the endothelium, and vascular smooth muscle cell proliferation (6) (**Table 1-1**). Constitutive expression of eNOS and nNOS is also a feature of the myocardium, however their subcellular positions are tightly regulated (7). These enzyme isoforms may undergo post-translational modulation/regulation (8), indicating the need to carefully balance the beneficial and detrimental effects of NO (and related reactive nitrogen/oxygen species) in the heart. A deficiency of bioavailable NO is a key feature of cardiovascular disease (9,10), the leading cause of mortality worldwide (11), and interventions to correct NO deficiency have been extensively studied, but with mixed results.

NO in tissues classically binds to the haem moiety of soluble guanylate cyclase (sGC) to activate the enzyme, which catalyses the conversion of guanosine triphosphate (GTP) to cyclic guanosine 3',5'-monophosphate (cGMP) (1). Cyclic GMP activates cGMP-dependent protein kinase (PKG), which is an effector protein in the cascade that activates many downstream targets (including calcium signalling proteins and transcription factors) via protein phosphorylation to cause the aforementioned cardiovascular effects. The intracellular levels of cGMP are also regulated by various classes of phosphodiesterase (PDE), the enzyme that degrades cGMP to the inactive guanosine 5'-monophosphate (GMP). Alternative mechanisms by which NO exerts its cardiovascular effects include post-translational S-nitrosylation of sulphur atoms (thiols) within cysteine residues of various proteins (either increasing or decreasing their activity) (12), and cGMP-independent activation of Ca^{2+}-dependent potassium (K^{+}) channels via membrane hyperpolarisation, to decrease cytosolic Ca^{2+} levels (13). Additionally, elevated levels of cGMP inhibit PDE3, leading to increased intracellular levels of cyclic adenosine monophosphate (cAMP), which in turn activates protein kinase A (PKA) (14).

The oxidation of NO within the tissues produces nitrite (NO_2^-) and nitrate (NO_3^-), which were previously considered to be physiologically inactive (15,16). Nitrate and nitrite levels in the plasma are partly a result of the oxidation of NO within the blood, mainly via oxyhaemoglobin and ceruloplasmin (17,18), however they are also largely determined by the dietary intake of inorganic nitrate and nitrite. In this way, plasma nitrite levels following a nitrate-deplete diet for at least 4 days, have been proposed as a method of detecting basal NO production by vascular NOS isoenzymes, and plasma nitrate levels obtained following a similar nitrate-deplete period have been proposed as a measure of the body's total NO turnover (15). Whereas higher-order organisms lack the ability to reduce nitrate to nitrite and NO, there are many nitrite reductases that have been identified in humans that can liberate NO from nitrite, usually under hypoxic conditions (16,19,20). Therefore interventions that increase

plasma nitrite levels have the potential to increase the bioavailable NO pool (independent of production via NOS), potentially correcting any NO deficit as seen in cardiovascular disease or inflammatory states, as described above.

Table 1-1: Cardiovascular Effects of Nitric Oxide at Physiological Levels

Target Tissue/Cell	Effect of NO at Physiologic Levels	Reference(s)
Vascular Smooth Muscle Cells	↓ VSMC contraction/tone (i.e. vasodilatation) ↓ VSMC proliferation	(21,22)
Platelets	↓ Platelet aggregation ↓ Platelet activation	(23-25)
Leukocytes	↓ Leukocyte adherence ↓ Monocyte chemotaxis ↓ ROS	(26,27)
Endothelial Cells	↑ Angiogenesis ↓ ROS	(28-30)
Fibroblasts	↓ Fibrosis	(31,32)
Myocardium/ Cardiomyocytes	↑ Contractility (unstimulated healthy heart) ↑ Contractility (stimulated healthy heart) ↑ Lusitropy ↑ Chronotropy ↑ Ischaemic preconditioning ↑ Hypoxia sensing ↑ Myocardial efficiency ↑ FFA β-oxidation (healthy heart) ↑ FFA β-oxidation (diseased heart) ↑ Glucose oxidation (diseased heart) ↓ Hypertrophy ↓ Apoptosis ↓ Myocardial oxygen consumption ↓ Glucose oxidation (healthy heart)	(33,34)

Cardiovascular effects of nitric oxide in different tissues/cells. FFA, free fatty acids; ROS, reactive oxygen species; VSMC, vascular smooth muscle cells.

1.2 Dysfunctional Nitric Oxide Signalling is a Key Feature of Heart Failure

Cardiovascular diseases (CVD) are the leading cause of death worldwide, however, a dramatic reduction in age-specific rates of cardiovascular disease in affluent countries (that is only partly explained by advances in treatment/preventive strategies) have led to it being overtaken recently by cancer in many of these countries (35). Heart failure is a clinical syndrome defined as an inability of the heart to pump sufficient blood to meet the metabolic needs of the body, or to do so only by raising left ventricular end diastolic pressure (LVEDP) (36), and occurs commonly as a final result of various forms of CVD. The cardinal symptoms of heart failure are dyspnoea and exercise intolerance, and the 5-year prognosis is as poor as many cancers (37). It is estimated that more than 900,000 people in the United Kingdom are affected by heart failure, and this number is likely to rise as the population ages and treatments for acute heart diseases (such as coronary heart disease) improve (38). Heart failure also poses a large budgetary strain on the National Health Service (NHS), with heart failure related hospital admissions (some 5% of all emergency medical admissions) accounting for 2% of NHS inpatient bed-days each year (39). Conventionally, heart failure groups are classified on the basis of left ventricular (LV) ejection fraction (EF), i.e. the percentage of blood in the left ventricle at the end of diastole that is ejected with each beat during systole. A normal EF is considered to be 55% or greater (or 60% or greater when calculated via cardiovascular magnetic resonance imaging from LV volumes derived from established reference values for age and sex) (36). Historically, research has focused on patients with heart failure with a reduced ejection fraction (HFrEF) of less than 40%, also known as ‘systolic heart failure’, and there is now an established evidence-base for treatments in HFrEF that can robustly reduce patient morbidity and mortality. However, the real-world initiation and optimisation of these medications is often complicated by intolerable side effects, resulting in many patients remaining symptomatic and well below the beneficial doses used in clinical trials (36). For patients with heart failure symptoms but an EF >50%, these treatment approaches have consistently failed to significantly

improve patient outcomes. In the past ~20 years, our understanding of the pathophysiology of heart failure in these patients has advanced greatly, and heart failure with a preserved ejection fraction of greater than 50% (HFpEF), previously known as 'diastolic heart failure', is now considered to be the most prevalent form of heart failure worldwide (40). However, despite carrying a similar morbidity and mortality burden to HFrEF, there are currently no proven treatments for patients with HFpEF.

1.2.1 Pathophysiology of Heart Failure

The established definition for heart failure focuses on impaired pump function of the LV, and reflects the conventional thinking of heart failure as a disease of altered haemodynamics. The term 'systolic heart failure' was used for HFrEF as patients presented with heart failure signs and symptoms and had a reduced LVEF on admission echocardiogram, whereas 'diastolic heart failure' was used for patients with HFpEF as they had a 'normal' LVEF (41). The signs and symptoms of acute decompensated heart failure can be attributed to acute rises in LVEDP (and subsequently in RVEDP) resulting in pulmonary and peripheral oedema and/or to an inadequate cardiac output (22). Whereas HFrEF may simply be considered as a 'failure to squeeze', HFpEF may be considered a 'failure to fill'. The increase in LVEDP (and therefore pulmonary congestion) in 'diastolic heart failure' results from a failure of LV active relaxation and an increase in LV passive stiffness from a stiff and non-compliant LV, together with an increased afterload due to increased stiffness of the aorta and other large vessels (42). However, whilst this dichotomy makes it clear that the underlying pathophysiology differs between these two forms of heart failure (explaining the differences in response to therapies), the taxonomy was called into question after multiple studies demonstrated impairments in LV systolic function, particularly in the long axis, in patients with diastolic heart failure (43). Although imperfect, the classification of heart failure syndromes by where they sit on an 'EF spectrum' is now standard practice, and in HFpEF 'preserved EF' is preferred over

'normal EF' to indicate that, whilst LVEF is normal, LV contractile function may nevertheless be impaired. This has prompted the characterisation of a further group of patients with heart failure who have a mid-range EF (HFmrEF) of 40-49%. HFmrEF is thought to share many similarities with HFpEF, importantly sharing with HFpEF the paucity of evidence for use of the interventions that have been established for patients with HFrEF (44).

In the healthy heart, there is a substantial capacity for augmentation of cardiac output (e.g. on exercise) by increasing stroke volume (the volume of blood ejected with each beat) and heart rate. In heart failure, the ability to increase cardiac output (CO) is reduced as a result of one or both of these mechanisms being impaired. In haemodynamic terms, LV pump performance is determined by the intrinsic contractile state of the myocardium (inotropy), and the loading conditions under which it functions, known as preload and afterload (45). Stroke volume can be augmented by directly increasing inotropy, or by increasing preload (i.e. increasing LV diastolic volume, and thereby, through the Frank-Starling mechanism, the force of contraction), or by decreasing afterload. Whilst it is extremely difficult to assess the force generated by each shortening myofilament *in vivo*, there are many methods for assessing 'chamber level' LV contractility. The gold standard involves simultaneous measurement of pressure and volume via a conductance catheter placed inside the LV cavity to derive pressure-volume (PV) loops (45). A schematic of a PV loop is shown in **Figure 1-1**. Occlusion of the inferior vena cava (IVC) with a balloon can be used to alter RV (and by extension LV) preload, allowing the calculation of important measures of LV contractility and afterload (46). A straight line can then be drawn connecting the end systolic points from each PV loop obtained at varying preloads, to give the end systolic pressure volume relationship (ESPVR). The slope of the ESPVR is the end systolic elastance (Ees), which is a useful load-independent measure of contractility that is linear except at its very extremes (**Figure 1-1**) (47). The area of each PV loop is a measure of LV stroke work. A fall in contractility is demonstrated by a flatter gradient of the ESPVR and reduced PV loop area (stroke work) for a given

preload, representing a downwards and rightwards shift of the Frank-Starling relationship (48). Whilst the ESPVR is a useful measure of contractility it is, to some extent, afterload dependent, and non-linear at its extremes (47). A better measure, also derived from conductance catheter pressure-volume data, is the preload recruitable stroke work relationship (PRSW). PRSW describes the relationship between LV end diastolic volume (EDV) and stroke work (PV loop area), and is therefore a direct measure of the Frank-Starling mechanism of the LV (49). Similar to the ESPVR, the PRSW is characterised by a slope (Mw) and an x-axis (volume) intercept (Lw).

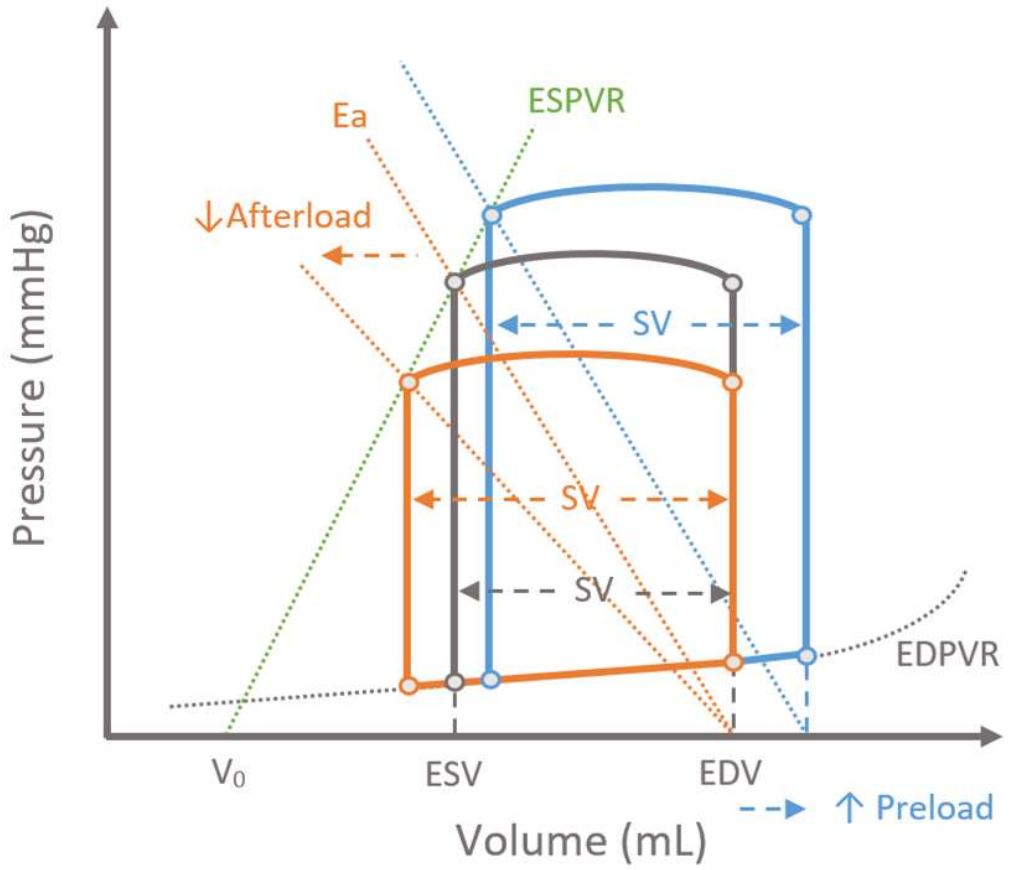

Figure 1-1: Schematic of a Pressure Volume (PV) Loop Obtained from a Conductance Catheter Positioned in the Left Ventricle.

A pressure-volume loop is derived from pressure-time and volume-time measurements taken within the left ventricle via a conductance catheter (grey). Altering preload shifts the PV loop up and down the end systolic pressure volume relationship (ESPVR) line by altering EDV (blue). Changes in afterload are reflected by changes in the slope of Ea, moving the PV loop along the ESPVR (orange). Ea, arterial elastance; EDPVR, end diastolic pressure volume relationship; EDV, end diastolic volume; ESPVR, end systolic pressure volume relationship; ESV, end systolic volume; SV, stroke volume; V_0, theoretical left ventricular volume when pressure is 0mmHg (i.e. x-axis intercept).

1.2.1.1 Heart Failure with Reduced Ejection Fraction

1.2.1.1.1 Left Ventricular Contractile Function

A reduction in LV contractility is considered the primary lesion in HFrEF and may result from a number of direct cardiac insults including ischaemia, deposition diseases, and toxins (50). Whatever the initial insult, a process of maladaptive remodelling typically takes place due to neurohumoral activation. Renal hypoperfusion results from the reduced CO, which activates the renin angiotensin aldosterone system (RAAS). The tissue RAAS system is also activated. A reduction in cardiac baroreflex sensitivity, together with increased activity of cardiac sympathetic efferent activity, result in increased sympathetic and reduced vagal neural efferent activity and increased release of catecholamines by the adrenal glands (51). This neurohormonal response is a 'primitive' response to a low CO, designed to acutely increase LV contractility via β-adrenergic stimulation of the myocardium, and LV preload via renal water and sodium retention (i.e. blood volume expansion), and to maintain blood pressure via systemic vasoconstriction (which increases afterload). Furthermore, thrombotic and platelet aggregation pathways are activated in an attempt to reduce bleeding and consequent hypovolaemia which would have been a common cause of low CO historically. However, chronic neurohumoral activation, as in heart failure, has severe adverse consequences. Chronically increased afterload results in a compensatory hypertrophic response in the left ventricle. RAAS and sympathetic activation result in interstitial and focal cardiac fibrosis (structural remodelling) and myocyte apoptosis and necrosis (52). These changes result in progressive dilation of the left ventricle and progressive worsening of left ventricular function. Therefore, even if the initial insult was insufficient to result in clinical heart failure, it may develop as a result of this remodelling process (51).

The contractile apparatus is controlled by the β-adrenergic pathway, and stimulation of β-receptors (membrane-bound G-protein coupled receptors), stimulates calcium

(Ca^{2+}) influx via L-type Ca^{2+} channels and increases intracellular cAMP to activate protein kinase A (PKA) (52). PKA activates the ryanodine receptor and inhibits phospholamban (the inhibitor of the sarcoplasmic reticulum (SR) Ca^{2+} ATPase 2a (SERCA2a) pump), leading to greater levels of Ca^{2+} entering the SR to increase the force generated by the next contraction. PKA also phosphorylates troponin I and myosin binding protein C to improve myofilament uncoupling (relaxation), enhancing cardiac lusitropy (53). Chronic elevation of catecholamines is deleterious for the myocardium however, due to toxic Ca^{2+} accumulation and myocyte apoptosis, further impairing LV contractility (54,55). Chronic sympathoexcitation also results in downregulation and uncoupling of β-receptors, and, whilst this may serve to ameliorate the toxicity, it also reduces the ability to increase CO when it needs it (e.g. on exercise). Finally, the pro-coagulant and platelet aggregatory effects of neurohumoral activation explain some of the increased risk of cerebrovascular accidents in heart failure (56).

1.2.1.1.2 Pharmacotherapy in HFrEF

Blockade of neurohumoral activation has been the cornerstone of treatment of heart failure for approximately 30 years. Beta-blockers are used to treat HFrEF to counteract the effects of chronic sympathoexcitation, and have been shown to reduce mortality by ~30% in clinical trials (57-60), however the treatment should 'start low and go slow' because acute withdrawal of sympathetic tone may cause an acute decompensation due to their negatively inotropic effects. Similar mortality benefits have been demonstrated with angiotensin converting enzyme (ACE) inhibitors (61-64) or angiotensin receptor blockers (ARBs) (65-67), and the combination of beta-blockers and ACE-inhibitors is now the mainstay of therapy for chronic heart failure, with diuretics used to counteract symptomatic volume overload. As per the European Society of Cardiology (ESC) guidelines for the diagnosis and management of heart failure, maximally tolerated evidence based doses of these neurohormonal blockers is the first-line therapy for patients with HFrEF (36). For

patients with persistent symptoms of breathlessness (New York Heart Association (NYHA) Class III breathlessness) and an EF ≤35%, mineralocorticoid receptor antagonists (MRAs) are indicated as additive therapy (68,69). Should these symptoms persist, ACE-inhibitors should be replaced with the angiotensin receptor blocker-neprilysin inhibitor combination drug sacubitril/valsartan to maximise neurohormonal blockade. The neprilysin enzyme degrades natriuretic peptides (i.e. atrial natriuretic peptide, brain natriuretic peptide, and C-type natriuretic peptide) and vasoactive substances such as bradykinin that are released as a compensatory mechanism during neurohormonal activation (70). Inhibitors of neprilysin therefore increase circulating levels of these substances. Sacubitril/valsartan therapy was recently associated with a further 16% reduction in mortality in symptomatic patients with HFrEF on optimised medical therapy (OMT) (71). Symptomatic patients with a wide QRS complex duration on electrocardiogram (ECG) of ≥130ms should be considered for cardiac resynchronisation therapy (CRT) using a biventricular pacemaker to reduce intraventricular dyssynchrony. CRT improves mortality by a further 30% in eligible symptomatic patients on OMT (72-74). If the EF is persistently ≤35% despite OMT or if there is a history of symptomatic ventricular tachycardia/ventricular fibrillation, an implantable cardiac defibrillator should be implanted (i.e. CRT-D). Beyond this, treatments for HFrEF may be limited especially for patients with symptoms but an EF >35%, or those unable to tolerate optimisation (to evidence based doses) of medical therapy. There is some evidence that patients with a resting heart rate ≥70 bpm and sinus rhythm on ECG may benefit from heart rate reduction using Ivabradine, a blocker of the 'funny current' (If) of the sinoatrial node (75,76). Similarly, the sodium/potassium (Na^+/K^+) ATPase pump inhibitor digoxin may reduce hospitalisation in patients with HFrEF possibly by reducing arrhythmic events (77). In HFrEF patients with atrial fibrillation (AF), rate control is therefore preferentially achieved with digoxin, for the added benefit of reduced heart failure hospitalisations. In patients with resistant symptoms despite these therapies, or in whom these therapies cannot be initiated or uptitrated due to intolerable side effects, there are very few options left for symptom management. Left ventricular

assist device (LVAD) therapy or heart transplantation are reserved only for those patients with persistent significant LV impairment.

Most recently, inhibitors of the renal sodium-glucose cotransporter 2 (SGLT2) have shown promise in heart failure for reducing the risk of cardiovascular death or heart failure hospitalisation, independent of the presence of type 2 diabetes mellitus (78). SGLT2 inhibitors reduce renal glucose reabsorption at the proximal convoluted tubule inducing glycosuria, which has a potent diuretic effect. Diuretics improve left ventricular performance in patients with heart failure by reducing ventricular preload (discussed in section 1.2.1.1.3). Interestingly, SGLT2 inhibitors also reduce afterload in a mechanism not yet fully elucidated, which corresponds to a fall in arterial elastance with reduced serum glucose levels, decreasing the vasculoventricular coupling ratio and improving myocardial efficiency (see section 1.2.1.1.4) (79). This is of particular importance in heart failure with preserved ejection fraction (HFpEF). Another important mechanism behind the effect of SGLT2 inhibitors includes its inhibition of the sodium-hydrogen exchanger (NHE), a mechanism that is shared with many other heart failure medications (80). The benefits of NHE blockade (NHE3 in the kidney and NHE1 in the heart and vasculature) include antihypertensive and natriuretic effects, and reduced cardiac hypertrophy and fibrosis (80). However, importantly, natriuresis does not appear to be a significant effect of SGLT2 inhibition. Indeed, the diuretic effect of the SGLT2 inhibitor Empagliflozin appeared to occur without a significant natriuretic effect when co-administered with a loop diuretic in patients with HFrEF and type 2 diabetes (i.e. electrolyte-free water rather than urinary sodium excretion was increased) (81); this is a beneficial effect profile considering the risk of hyponatraemia with high-dose loop diuretics or in combination with thiazide diuretics. Another risk with loop diuretics, hyperuricaemia (with its associated negative cardiovascular effects), is also reduced with SGLT2 inhibition via promotion of uricosuria, likely via blocked of NH3 (82). Finally, SGLT2 inhibitors may also activate sensors of nutrient deprivation such as sirtuin-1 (SIRT1) and AMP-activated protein kinase (AMPK) as a consequence of the ‘fasting state’ induced by

sustained hypoglycaemia, which increase autophagy, reduce oxidative stress, and more (discussed in more detail in section 1.2.2.2) (83).

1.2.1.1.3 Left Ventricular Preload

Increases in LV preload lead to improvements in the force of contraction via the Frank-Starling mechanism. Contractility/inotropy itself is unchanged, but the ventricle moves up along the slope of the PRSW relation to generate a more forceful contraction. True LV preload (i.e. the load on the LV prior to systole) is given by the effective distending pressure called the transmural LVEDP (TLVEDP), which is estimated clinically by LVEDP and is directly related to myocardial stretch (84). The Frank-Starling mechanism couples LV stroke work to LV end diastolic volume in the healthy heart, such that a larger LV end diastolic volume/pressure results in a stronger contraction due to greater stretch (i.e. shifting along the PRSW relation) (85). This preload-dependent contractile function of the LV is particularly important on exercise, when RV preload increases due to increased venous return and heart rate increases due to sympathetic activation and parasympathetic inactivation, reducing the diastolic filling period (86,87). Impairment of the Frank-Starling mechanism is a hallmark feature of heart failure, and a major contributor to reduced cardiovascular reserve and exercise intolerance (88). In HFrEF, systolic dysfunction raises LVEDP which recruits the Frank-Starling mechanism in an attempt to maintain contractility. Recruitment of preload is limited at the onset of pulmonary and peripheral oedema, however LV cavity dilatation may compensate for this by allowing for increases in LVEDV, minimising increases in LVEDP.

However, external factors have also been shown to increase LVEDP in situations associated with right ventricular pressure and volume overload, including heart failure. In these situations, the LVEDP is no longer a reliable marker of transmural LVEDP. The LV and RV are contained within the pericardium, which exhibits a 'J-shaped' stress-strain relationship, such that changes in pressure are small when the

pericardium is only mildly stretched, but pericardial pressure increases exponentially when the pericardium is progressive stretched as in patients with heart failure associated with right ventricular enlargement and substantially increased RVEDP (89). LV filling can therefore be constrained by the pericardium (pericardial constraint) and by the RV through the interventricular septum (diastolic ventricular interaction, DVI), which becomes shifted to the left resulting in a flattened or D-shaped septum. Right atrial pressure (RAP) and pericardial pressure are almost identical in humans, and therefore the following formula can be used to calculate true LV preload: TLVEDP = LVEDP – RAP (90). This demonstrates that large acute changes in right ventricular volume (i.e. RAP) could affect LVEDP without affecting TLVEDP, and explains the paradoxical increase in LV stroke volume seen in some patients with chronic heart failure following acute preload reduction (91,92). Frenneaux et al. demonstrated significant DVI (diagnosed by a paradoxical increase in LV stroke volume when lower body negative pressure was applied to unload the RV) in as many as 40% of patients with systolic heart failure, and this was predicted by a LVEDP ≥15mmHg (93). The same group also demonstrated that DVI is responsible for "the apparent descending limb of the Frank-Starling curve in heart failure", whereby early measures of the Frank-Starling mechanism using LVEDP vs. SW showed a fall in SW (i.e. reduced contractility) with volume loading past a certain point in patients with heart failure, and a sudden paradoxical increase in SW with volume unloading back to this point (i.e. increased contractility) (92). They showed that DVI accounted for this sudden change slope of the LVEDP-SW relationship (Frank-Starling curve), and that plotting TLVEDP-SW instead maintained a positive slope, demonstrating that contractility was, in fact, not depressed.

1.2.1.1.4 Left Ventricular Afterload

Finally, LV afterload is increased in HFrEF and contributes to disease progression. Afterload reflects ventricular 'wall stress' and denotes the load against which the myocardium must eject its stroke volume (94). A reduction in afterload for a given

EDV results in an increase in stroke volume, as demonstrated by a widening of the PV loop (**Figure 1-1**), and underlies the beneficial effects attributed to vasodilator therapies. The acute/semi-acute myocardial response to increased afterload is to increase contractility in an attempt to maintain stroke volume, known as the Anrep effect or 'stress-stimulated contractility'/'homeometric autoregulation', and occurs via stretch-activated-receptor mediated increases in intracellular Ca^{2+} currents (95). Such mechano-sensitive channels may include the angiotensin type 1 (AT1) receptor and channels from the transient receptor potential (TRP) superfamily (96,97). Neurohormonal activation and volume overload contribute to ventricular remodelling. In chronic pressure overload states, the left ventricle remodels to reduce wall stress, typically in the form of concentric hypertrophy. According to LaPlace's law, wall stress is proportional to LV pressure and cavity radius, but inversely proportional to wall thickness (98). In volume overload states such as longstanding HFrEF, eccentric hypertrophy (LV dilatation) occurs as described above, which maintains stroke volume via preload but increases wall stress by LaPlace's law. Afterload is acutely and critically elevated in acute decompensated HFrEF in association with severe endothelial dysfunction, and this has led some experts to reclassify the condition an 'acute endothelitis' (99).

A measure of LV afterload known as arterial elastance (Ea) can be obtained from PV loops in a manner similar to Ees, and is given by the slope of a straight line drawn from the end systolic point to the end diastolic volume (EDV) on the volume axis (**Figure 1-1**) (100). Ea encompasses both pulsatile and static afterload, but is primarily determined by systemic vascular resistance (SVR) and heart rate. The ratio of Ea to Ees is known as the vasculoventricular coupling (VVC) ratio, which describes the efficiency with which blood is ejected from the LV is transmitted to the vasculature (101). A normal resting VVC ratio in man is between 0.7-1.0, and this range reflects a state in which LV output and energetic efficiency are optimised (102). During exercise, Ea increases slightly (with heart rate) in association with a much greater increase in Ees, causing the VVC ratio to fall (103). This maximises LV stroke work to

achieve the increase in CO required with exercise but sacrifices energetic efficiency such that myocardial energy consumption increases. When the VVC ratio departs substantially from normal values efficiency is markedly reduced, and, as active relaxation of the LV is a highly energy dependent process (104), this compounds the energetic impairment that is typically present in the failing heart. In HFrEF, Ees is reduced at rest due to depressed LV contractility, yet neurohumoral activation (in the absence of adequate neurohumoral blockade) results in an increase in vascular tone, resulting in an increase in Ea and consequently vasculoventricular mismatch (101). Indeed in acute HFrEF, afterload excess (endothelitis) greatly elevates the VVC ratio leading to decompensation. This can be successfully managed with vasodilator therapies.

1.2.1.2 Heart Failure with Preserved Ejection Fraction

1.2.1.2.1 Left Ventricular Afterload and Contractility

The pathophysiology of HFpEF is complex. Excessive LV afterload is considered by many to be a cardinal cause of the haemodynamic impairment, and this is supported by a near-ubiquitous history of systolic hypertension in patients who develop the disease (105). Similarly, the other common risk factors for HFpEF such as old age, female sex, diabetes, renal dysfunction, and obesity, are known to contribute to an increase in afterload. An EF within the 'normal' range is frequently assumed to indicate 'normal' contractile function, however most of these patients exhibit impairment of long axis contractile function (43). There is currently no way to predict those patients who will progress to HFpEF from hypertensive heart disease (106). Recent studies in these populations however, have demonstrated important reductions in 'myocyte level' LV contractility that do not translate to impairments in Ees or EF, but the mechanism was not defined (107).

Both pulsatile and static afterload are raised in HFpEF. Progressive vascular calcification and increased basal tone increase SVR, and stiffening of the aorta and other great vessels leads to increased afterload through the 'Windkessel' effect and an associated increase in pulse wave velocity (108). When blood is ejected from the LV, a large forward wave is propagated into the elastic aorta which acts like a 'Windkessel' (an air chamber used in old fire hoses to produce a steady flow of water transmitted from a pump) to dampen pulsatility and transmit steady flow to the muscular distal arteries (109). At areas of impedance mismatch, such as branch points of the aorta, blood is reflected back towards the LV. Normally, this backwards wave arrives at the beginning of diastole when the aortic valve is closed, and enters the coronary ostia, perfusing the coronary arteries (110). When pulse wave velocity is increased (e.g. due to aortic calcification), the backwards propagating wave arrives earlier in the cardiac cycle when the aortic valve is open, causing this wave to be transmitted to the LV and augmenting LV late systolic load (111). Shorter stature also results in earlier return of the reflecting waves due to shorter distances to arterial branch points (112), perhaps partly explaining the greater prevalence of HFpEF in women. To maintain VVC, Ees rises in response to increased Ea (103). Whilst acute increases in Ees reflect improved contractility (the Anrep effect), the chronic increase seen in HFpEF also reflects increased diastolic passive stiffness. Together with impaired active relaxation, this limits increases in LVEDV on exercise, and thereby stroke volume and cardiac output, and greatly increases exercise LVEDP (107).

Diastolic dysfunction on PV loops is demonstrated by an increased slope of the end diastolic pressure volume relationship (EDPVR) (**Figure 1-1**), the shape of which is predominantly determined by the phosphorylation status of the giant cytoskeletal protein titin (phosphorylation reduces passive stiffness) (113). Indeed, genetic variants of titin that produce a truncated protein (TTNtv), result in dilated cardiomyopathy and HFrEF (114). These variants have a relatively low penetrance, but also appear to amplify the risk of other causes of DCM including peripartum cardiomyopathy. The two isoforms of titin, N2BA (larger and more compliant) and

N2B, are present in roughly equal amounts in human myocardium. An increased N2BA:N2B ratio has been shown in ischaemic and non-ischaemic DCM, as well as in LV pressure overload due to aortic stenosis (115) but an isoform switch was not demonstrated in HFpEF (116). However, titin PKA/PKG phosphorylation status is greatly reduced in HFpEF compared to normal myocardium, and contributes to diastolic dysfunction. Impairment of the Frank-Starling mechanism in HFpEF contributes to the reduced cardiovascular reserve, the hallmark feature of the disease, and for this reason, patients may be asymptomatic at rest when LVEDP is not elevated but become severely symptomatic on exertion (36). The increased slopes of Ees and Ea also contribute to blood pressure lability, such that acute reductions in afterload result in significant falls in systolic blood pressure, putting patients at risk of symptomatic hypotension with the use of diuretic and vasodilator therapies (117).

1.2.1.2.2 Sub-phenotypes in HFpEF

An important reason for the failure of therapies to improve patient outcomes in HFpEF is the notable differences between patient cohorts included in clinical trials (118). To minimise this and better select patients for whom these therapies may be of benefit, HFpEF should be considered a disease of multiple sub-phenotypes, each with a unique clinical profile, set of risk factors, and priority list of therapeutic targets. It is hoped that improved patient phenotyping will ensure that the correct patient group is matched to the correct intervention and, for research, match patients to therapies that are most like to succeed and improve outcomes. Whilst the key medications in HFrEF (beta-blockers, ACE-inhibitors, and MRAs) have proven unsuccessful in the management of HFpEF (119-123), there is hope that newer studies utilising enhanced patient phenotyping may yet yield success. Currently however, management is targeted at symptom control with cautious use of diuretics and minimisation of cardiovascular risk factors, including statins for hypercholesterolaemia, targeted weight loss for obesity, and antihypertensives (with ACE-inhibitors, beta-blockers, and MRAs preferred) and anti-diabetic medications as

indicated (124). There is clear evidence that primary prevention of CVD risk factors reduces the risk of patients developing heart failure (although the evidence for HFpEF specifically is limited), however such approaches to management are insufficient in patients with established disease, and novel therapies are sorely needed.

1.2.1.2.3 Left Ventricular Preload

An example of a novel therapy for HFpEF involves delineating the contribution of external constraint to LVEDP at rest and with exercise. The raised preload that characterises this disease is considered by many to be solely related to LV stiffening, and whilst this is certainly the predominant mechanism, others are likely to be important, especially with exercise. Exercise-induced pulmonary hypertension is very common in HFpEF, and the origin may be multifactorial, including reduced LV compliance, energetic impairment (i.e. impaired LV active relaxation), and pulmonary arterial dysfunction (125). These mechanisms result in acute increases in LVEDP that are then transmitted back into the pulmonary vasculature raising RVEDP and thus pericardial pressure. We recently showed that this leads to significant DVI and pericardial constraint on exercise in ~50% of a sub-phenotype of patients with HFpEF and normal LVEDP at rest, and that this impaired augmentation of exercise stroke volume via the Frank-Starling mechanism (126). This is important, as although the contribution of LV stiffness to this increase in preload is a difficult therapeutic target, pericardial constraint may be targeted with surgical or transcatheter pericardiotomy (127). Similarly, biventricular pacemaker therapy may also present a viable option. In HFrEF, triggering LV filling ahead of RV filling prevented the RV from constraining LV filling, relieving DVI (128).

1.2.1.3 The Pro-Inflammatory Paradigm of Heart Failure and NO

Although this haemodynamic paradigm accurately describes and predicts changes in clinical parameters of patients with heart failure, it does not easily lend itself to

determining underlying cellular mechanisms. Recently, Paulus and Tschöpe proposed a novel paradigm that unifies the pathophysiologies of HFpEF and HFrEF under the umbrella of cardiac inflammation (129). The authors propose that HFpEF results from systemic inflammation which is secondary to a slew of cardiovascular risk factors. Interstitial fibrosis and myocyte NO consumption results from coronary endothelial ROS. NO consumption reduces PKG signalling, which increases pro-hypertrophic signalling and resting myocyte tension via hypophosphorylation of titin (116). HFrEF on the other hand, results in this paradigm from various insults to myocytes leading to toxic intracellular ROS, causing myocyte loss and replacement fibrosis. However, the proposition that heart failure is a pro-inflammatory state is not new. Indeed RAAS activation, central to the neurohormonal hypothesis, has been associated with high intracellular ROS via activation of NADH oxidase by angiotensin II and aldosterone (130). The level of shear-stress induced activation of the ROS-quenching superoxide dismutase (SOD) has also been shown to be related to exercise capacity in patients with HFrEF, and may underlie the beneficial effects of physical training (131). Inflammatory markers such as interleukin 6 (IL-6) and high sensitivity C-reactive protein (hsCRP) have been shown to predict death and correlate with exercise capacity in HFrEF (132). Although blockade of tumour necrosis factor α (TNFα) has proved unsuccessful in HFrEF trials (133), a recent exploratory analysis of the Canakinumab Anti-Inflammatory Thrombosis Outcomes Study (CANTOS) demonstrated reduced hospitalisations for heart failure in the active arm in patients with a history of myocardial infarction and elevated hsCRP (134) and has rekindled interest in inflammation as a therapeutic target. This new paradigm by Paulus and Tschöpe (129) importantly centralises perturbed canonical NO signalling due to inflammation in the pathogenesis of HFrEF and HFpEF, and suggests that therapies that restore myocardial PKG content may hold the key to successfully improving patient outcomes where others have failed.

1.2.2 Alterations in Cardiac Metabolism

The heart cycles vast amounts of energy each day to power its continued pumping to meet the incessant oxygen demands of the body. This translates to as much as 6kg of adenosine triphosphate (ATP, the chemical energy molecule used to fuel cellular processes) cycling per day (135). Therefore, impairments in energy metabolism can have profound effects on all aspects of LV performance. The healthy heart is omnivorous, allowing it to utilise multiple alternative energy substrates to minimise energetic deficiency when certain substrates are scarce or insufficient (136). Oxidation of free fatty acids (FFAs), and glucose and lactate, normally provide roughly 60-90% and 10-40% of the energy needed to meet the adult heart's metabolic requirements, respectively in the fasting state (137). More than 98% of the energy produced in the heart comes from oxidative phosphorylation, with <2% being derived from glycolysis.

1.2.2.1 Cardiac Metabolism in Health

Cellular metabolism involves the interplay of many complex pathways (**Figure 1-2**). We have reviewed the basics of cardiac metabolism and touched on the alterations observed in heart failure previously (138,139). Briefly, long chain FFAs enter myocytes via fatty acid translocase (FAT/CD36), and are esterified by acyl-CoA synthetase to form long-chain fatty acyl-CoA. The enzyme carnitine palmitoyltransferase 1 (CPT1) is the rate-limiting enzyme for the transport of FFAs into mitochondria via the 'carnitine shuttle' (140). CPT1 adds a carnitine group so that fatty acyl-CoA can be transferred across the mitochondrial membrane, where the carnitine is removed by the enzyme CPT2. Cytoplasmic long chain fatty acyl-CoA that is not transported into the mitochondria enters the triacylglyceride (TAG) storage pool (141). Fatty acyl-CoA in the mitochondrion undergoes β-oxidation to generate acetyl-CoA, and high energy nicotinamide adenine dinucleotide (NADH) and flavin adenine dinucleotide ($FADH_2$). Acetyl-CoA enters the tricarboxylic acid (TCA) cycle to produce NADH and $FADH_2$ (from succinate dehydrogenase), which donate electrons that are transferred between the complexes of the electron transport chain (ETC)

located on the inner mitochondrial membrane (142). This powers extrusion of hydrogen ions (H^+) across the membrane via these complexes and generates an electrochemical gradient, which is used to power the synthesis of ATP via phosphorylation of ADP by ATP synthase (oxidative phosphorylation). Although necessary for the formation of ATP, superoxide and other ROS production is a consequence of the actions of the ETC. While these usually react with H^+ ions to form H_2O, uncoupling proteins (UCP) and adenine nucleotide translocases (ANT) may dissipate the electrochemical gradient in a controlled fashion to prevent overwhelming ROS-related damage (143). UCPs also importantly mediate thermogenesis by brown fat and can export free fatty acids outside of mitochondria when present in excess. Uncontrolled ROS-related damage includes the oxidation of NO to form peroxynitrite ($ONOO^-$), which leads to lipid peroxidation and DNA damage, culminating in the opening of the mitochondrial permeability transition pore (mPTP), release of cytochrome *c*, and ultimately, cellular apoptosis (144).

Glucose is transported into the myocyte via the glucose transporter (predominantly GLUT4) where it is phosphorylated by hexokinase to glucose-6-phosphate (G6P) (145). G6P then enters the glycolytic pathway to produce pyruvate. G6P may also enter the pentose phosphate pathway (PPP) via oxidation by the glucose-6-phosphate dehydrogenase (G6PD) enzyme, culminating in the production of ribonucleotides and reduced nicotinamide adenine dinucleotide phosphate (NADPH). NADPH is critical for quenching cellular ROS and is also required for fatty acid synthesis (146). Excess G6P may also be stored as glycogen (glycogenesis). The phosphofructokinase (PFK) enzyme catalyses the next, 'committed' step of glycolysis (the irreversible conversion of fructose-6-phosphate to fructose-1,6-bisphosphate), and is therefore the most important regulator of glycolysis (147). The substrate of PFK, fructose-6-phosphate, may also be funnelled away from glycolysis into the hexamine biosynthesis pathway (HBP). The HBP consumes glutamine, acetyl-CoA and ATP, and ultimately, transfers N-acetylglucosamine to many cellular proteins (O-GlcNAcylation), an important form of post-translational modification (148). Indeed,

O-GlcNAcylation of PFK-1 occurs in response hypoxia and shunts glucose towards the PPP, increasing NADPH to quench cellular ROS (147).

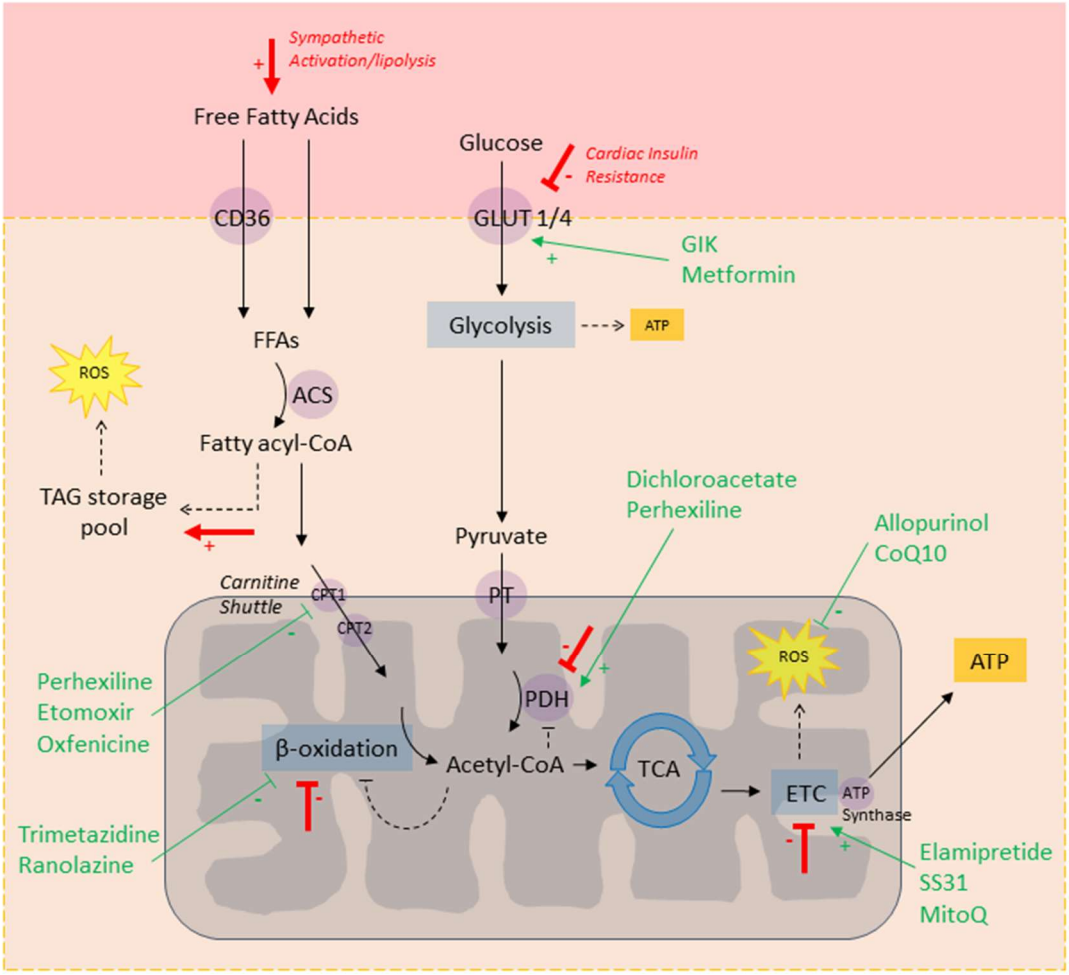

Figure 1-2: A Simplified Illustration of Cardiac Metabolism and the Effects of Metabolic Modulator Drugs in Heart Failure.

The healthy heart derives almost all of its energy (ATP) from oxidative phosphorylation, predominantly of free fatty acids (smaller pathways, such as ketone metabolism, not included). Heart failure is associated with a number of pathological changes in cardiac metabolism (red arrows) and an increase in ROS. Many metabolic modulator drugs inhibit fatty acid oxidation or transport of FFAs into the mitochondrion, which increases glucose metabolism via the Randle Cycle (green arrows). Other mechanisms include directly increasing glucose metabolism, or stabilising the mitochondrial electron transport chain (ETC). ACS, acyl-CoA synthetase; ATP, adenosine triphosphate; CD36, fatty acid translocase; CoQ10, co-enzyme Q10; CPT, carnitine palmitoyltransferase; ETC, electron transport chain; FFA, free fatty acid; GIK, glucose, insulin, potassium; GLUT, glucose transporter; PDH, pyruvate dehydrogenase; PT, pyruvate translocase; TCA cycle, tricarboxylic acid cycle.

Pyruvate is actively transported into the mitochondrion by pyruvate translocase, where the pyruvate dehydrogenase (PDH) complex catalyses its decarboxylation into acetyl-CoA, which enters the TCA cycle with the acetyl-CoA produced by the β-oxidation of fatty acyl-CoA. PDH controls the rate-limiting step in glucose oxidation, and is allosterically inhibited by its products, acetyl-CoA and NADH, and activation of pyruvate dehydrogenase kinases (PDK) (149). In this way, fatty acid oxidation inhibits glucose oxidation, termed the Randle cycle (150). Conversely, activating phosphatases (PDP) are upregulated by insulin and Ca^{2+}, increasing the activity of PDH leading to a net increase in glucose oxidation (151). The myocardium also extracts plasma lactate (produced elsewhere in the body) and can oxidise this to pyruvate, with lactate and glycolysis representing roughly equal contributions to myocardial pyruvate in health (152). The inhibitory kinases (predominantly PDK1), as well as PFK and GLUT4 are upregulated in hypoxia by hypoxia inducible factor 1α (HIF1α) (153). This prevents oxidation of pyruvate in low O_2 conditions, which would uncouple oxidative phosphorylation causing toxic cellular ROS, but increases glucose uptake for energy production via anaerobic glycolysis.

Even during acute myocardial ishaemia, the heart derives most of its energy from fatty acid oxidation, the products of which further inhibit pyruvate oxidation via the Randle cycle. Indeed, the partial restoration of pyruvate oxidation underpins the success of fatty acid oxidation inhibitors in the treatment of *angina pectoris* (154). Hypoxia shunts pyruvate to the final pathway of anaerobic glycolysis catalysed by lactate dehydrogenase (LDH) to generate ATP and lactate (i.e. a switch to lactate production), and increases the precursors of the HBP and PPP (to modify proteins and detoxify hypoxia-generated ROS). Pyruvate may also be consumed to replenish TCA cycle intermediates, termed ‘anaplerosis’ (155).

1.2.2.2 Heart Failure

Failing (and indeed hypertrophic) hearts have reduced cardiac energetic status compared to healthy hearts as demonstrated by reduced phosphocreatine (PCr) to adenosine triphosphate (ATP) ratio on 31-phosphorus cardiovascular magnetic resonance spectroscopy (31P CMRS), and this is related to disease severity (135). PCr represents a pool of ATP that can be drawn upon during short bursts of intense work in muscle (e.g. first minutes of exercise) and later replenished, and a reduced PCr/ATP ratio indicates a chronic deficit requiring consumption of energy reserves. Reduced ATP production in heart failure is multifactorial and affects all levels (**Figure 1-2**). Catecholamine release results in lipolysis and release of FFAs into the bloodstream from peripheral adipocytes, resulting in increased long chain FFAs entering myocytes (156). Despite the increased supply of FFAs, their oxidation is impaired in heart failure due to both downregulated expression and reduced activity of peroxisome proliferator-activated receptor α (PPARα), a ligand-activated transcriptional factor that regulates the expression of β-oxidation enzymes and CPT1 (157). Expression of PPARα and its transcriptional co-factor, PPARγ co-activator 1α (PGC-1α), are directly upregulated by NO-sGC-cGMP signalling in skeletal muscle, and modulated by ROS and HIF1α during hypoxia (158).

Reduced oxidation of FFAs in heart failure leads to cytosolic accumulation of long-chain fatty acid intermediates, including toxic/arrhythmogenic acyl-carnitines and ceramide (159), and a substrate switch towards the neonatal metabolic phenotype, characterised by increased glucose uptake rather than reliance on FFAs. Glucose metabolism carries a lower oxygen cost than fatty acid oxidation, however the amount of ATP generated per mole of substrate is also less (160). However, glucose oxidation in heart failure is either unchanged or reduced at the level of PDH due to PDK (potentially from ROS or chronic subtle hypoxia), and this low ATP state further stimulates glucose uptake, glycolysis, and glycogenolysis, uncoupling glucose oxidation from glucose uptake (152). Cardiac insulin resistance is also a common

feature of heart failure (with or without peripheral insulin resistance), and is closely related to activation of mammalian target of rapamycin complex 1 (mTORC1) and its substrate, ribosomal S6 kinase by ROS (161). Indeed, there is an increased incidence of type 2 diabetes mellitus in heart failure, and this is known to be associated with poorer long-term prognosis (162).

Low ATP production from reduced substrate oxidation causes the cellular ATP/AMP ratio to decline and activates 5' AMP-activated protein kinase (AMPK). AMPK is the negative regulator of mTOR and an insulin-independent mediator of GLUT4 expression (163), but signalling via this pathway is impaired by high ROS, shifting the balance in favour of mTORC1/S6 kinase signalling. NO is an activator AMPK (with AMPK then increasing NO production via eNOS phosphorylation, particularly in response to vascular shear stress (164)), and may normalise AMPK signalling in the setting of high ROS, given its anti-inflammatory effects. Nutrient deficiency, by activating AMPK and inhibiting mTOR, is also an important mechanism for activation of autophagy in healthy cells (161). A basal level of autophagy allows cells to continuously 'recycle' and replace damaged components, including mitochondria (mitophagy) (165). This is critically important in terminally differentiated cells, including cardiac myocytes. Autophagy may be upregulated via multiple mechanisms in cardiovascular disease. In heart failure, high redox and haemodynamic stress increase mTORC1 signalling, activating maladaptive autophagy and contributing to pathological ventricular remodelling and dilatation (166). Similarly, basal autophagy may be affected, such that defective mitochondria and other important structures are no longer recycled and replaced. The low-energy state of heart failure, via an increased cellular NAD^+/NADH ratio, also activates sirtuins, a group of critical NAD^+-dependent deacetylases with a range of positive effects on energy metabolism, oxidative stress, and cellular 'aging' (167). SIRT1 increases expression of catalase and manganese superoxide dismutase (Mn-SOD), important mechanisms for quenching cellular ROS (168), SIRT1 also deacetylates and activates PPARα, eNOS, and PGC-1α (the master regulator of mitochondrial biogenesis), among others, whereas SIRT3

deacetylates and activates the fatty acid oxidation enzyme long chain acyl-CoA dehydrogenase (LCAD) (169). SIRT1 and SIRT6 also importantly activate nuclear factor erythroid 2-related factor 2 (Nrf2) and inhibit nuclear factor-kappa B (NF-κB), protecting the endothelium (169). Therefore, given the complex positive regulatory interplay between NO and sirtuins, interventions that increase NO and/or activate sirtuins (such as resveratrol) are likely to be beneficial in heart failure.

Finally, mitochondrial dysfunction is a key feature of heart failure, contributing significantly to energetic impairment and excessive ROS generation. Downregulation and hypophosphorylation of PGC-1α leads to decreased mitochondrial biogenesis, and mitochondrial quality is also affected as a result of reduced basal autophagy and increased catecholamine toxicity (170). Most importantly however, the mitochondria in heart failure produce excess levels of ROS (produced at complexes I and III) compared to those from healthy hearts, and produce less ATP (171). These toxic levels of ROS are responsible for damage to mitochondrial DNA via peroxynitrite as well as important morphological changes. The mitochondrial respiratory complexes are organised together in supercomplexes at the inner mitochondrial membrane called 'respirasomes' (142). These respirasomes are stabilised by cardiolipin, which also functions to retain cytochrome c (a key cellular apoptotic signal) at the inner mitochondrial membrane. Peroxidation of cardiolipin may also cause cellular apoptosis (172). Drugs that stabilise cardiolipin, such as Elamipretide, could therefore hold great promise in the treatment of mitochondrial dysfunction in heart failure. However, whilst in the phase 1 clinical trial in patients with HFrEF, Elamipretide was shown to be well-tolerated (173), the phase 2 randomised controlled trial from the same group, powered to detect changes in end diastolic and end systolic volumes on cardiovascular MRI, failed to demonstrate a significant improvement in left ventricular end systolic volume (LVESV) following 28 days of either 4mg or 40mg of Elamipretide compared to placebo (174). Similarly, drugs that directly or indirectly target ROS production are likely to be hugely beneficial in heart failure. An important action of NO is to bind to complex I of the ETC, preventing cellular respiration and

ROS production, particularly in hypoxia (175). In keeping with the inflammatory paradigm (129), this once again centralises restoration of NO-signalling in the treatment of heart failure. NO from plasma nitrite, thought previously to be an inert chemical formed by oxidation/consumption of NO within the body, is unique to other methods of NO administration in that it is liberated in hypoxic tissues, representing a method for blockade of mitochondrial ROS that is targeted, and occurs at physiological levels (16). Nitrite may also directly inhibit complex I via S-nitrosylation of cysteine residues, and this is thought to be an important mechanism behind its cytoprotective effects against ischaemia/reperfusion injury (176). Furthermore, energy transport through the creatine kinase (CK) system from the mitochondria to sites of utilisation in the cytosol is reduced in heart failure; mitochondrial creatine levels are reduced due to downregulation of the transporter and oxidative stress reduces cytosolic CK activity (177). Xanthine oxidase derived ROS appears particularly important, since Allopurinol acutely increased CK flux in patients with DCM (178).

1.3 The Nitrate-Nitrite-NO Pathway

NO derived from the recently characterised Nitrate-Nitrite-NO pathway provides an alternative (and supplementary) supply of NO to the action of the eNOS isoenzyme (16,179). Importantly, the liberation of NO from nitrite occurs under conditions of low oxygen tension (180), whereas the metabolism of l-arginine is reliant on oxygen (1). Inorganic nitrate from the diet, particularly found in green leafy vegetables, is almost completely absorbed in the proximal gastrointestinal tract. Nitrate within the blood reaches the salivary glands, where it is concentrated 10-fold and secreted onto the dorsum of the tongue (181). Commensal bacteria within the oral cavity possess nitrate reductase activity not found in humans (182), and reduce nitrate to nitrite which is then swallowed. Around 5% of the ingested nitrate from the diet is reduced to nitrite via this 'enterosalivary circulation' (16). A small proportion of the nitrite within the stomach is also reduced by the acidic environment to NO, and is important for gastric mucosal vasodilatation/integrity, as well as the antibacterial properties of gastric secretions (183). The remaining nitrite is absorbed into the bloodstream and delivered to the tissues. The importance of the enterosalivary circulation was elegantly demonstrated in a recent randomised controlled trial investigating the antihypertensive benefits of inorganic nitrate (as beetroot juice) (184). The beneficial effects of inorganic nitrate on blood pressure were lost when patients were asked to spit out all saliva following ingestion of beetroot juice rather than swallowing. Interestingly the use of mouthwash also abrogated the vasodilator effects of inorganic nitrate (185), reinforcing the important role of healthy commensal oral bacteria, which may also partly explain the increased cardiovascular risk associated with poor dentition, where bacterial overgrowth causes the natural oral microbiota to be replaced.

1.3.1 Nitrite Reductases

Highly acidic environments, as in the stomach, may reduce nitrite to NO spontaneously in a process termed 'acid disproportionation' (186). This reduction is enhanced in the presence of dietary ascorbic acid and polyphenols (187,188). Within other tissues, where such extreme environments do not exist, a number of 'nitrite reductases' necessary for NO release have been identified with maximal rates during hypoxia (i.e. nitrite reduction is inhibited by oxygen) (189). These include xanthine oxidoreductase (XOR) (190), mitochondrial aldehyde dehydrogenase (ALDH2) (191), eNOS (192), deoxymyoglobin and deoxyhaemoglobin (193-195), and cytochrome C oxidase of the mitochondrial electron transport chain (ETC) (196,197). The ubiquitous carbonic anhydrase enzyme has been shown to release NO from nitrite via nitrite-anhydrase activity (198). Neuroglobin and cytoglobin may also play a role in the reduction of nitrite to bioactive NO (199,200). The proposition that the haem-containing globins may function as nitrite reductases is regarded as controversial by some however, as NO avidly binds oxyhaemoglobin, which would prevent release of any NO produced from nitrite in erythrocytes (189,201). This has been countered by proponents of this theory however, who have postulated that nitrite binds with deoxyhaemoglobin to produce methaemoglobin and NO (via the intermediate formation of iron-nitrosyl-Hb) (20). The methaemoglobin would then further bind with nitrite to produce an intermediate $NO_2^{\bullet}$ (with radical properties). NO produced by the reaction is displaced via haem oxidation (termed 'oxidative denitrosylation'), and reacts with the $NO_2^{\bullet}$ radical in a fast 'radical-radical' reaction to form N_2O_3 before the NO can bind nearby oxyhaemoglobin and be oxidised to nitrate. The N_2O_3 then diffuses out of the erythrocyte into other tissues, where it breaks down into NO or directly S-nitrosylates thiols (20). This dual activity of haemoglobin, based on oxygen binding state, may in this way contribute to the selectivity of nitrite for the venous circulation and metabolically active tissues.

Importantly, the liberation of NO from nitrite may also occur independently of ambient tissue O_2 tension and is not subject to the development of tolerance, a recognised barrier to chronic organic nitrate therapy (202). In addition, while nitrite may function as a reservoir of NO and therefore act via the aforementioned mechanisms, it may also directly S-nitrosylate cysteine residues in proteins in a manner similar to NO, increasing or decreasing their activity (203). During hypoxia, nitrite reduction to NO in the presence of nitrite reductases is rapid, however in normoxia the release of NO from nitrite is much slower, and there is mounting evidence that the normoxic action of nitrite may in fact be independent of NO. Nitrite (as intravenous sodium nitrite) has been shown to dilate conduit arteries in healthy volunteers in a manner which was independent of NO but dependent on cGMP, however the mechanism was not identified (204). A potential explanation may be nitrite oxidation to dinitrogen trioxide (N_2O_3), however this has not been adequately explored (20).

1.3.2 Historical Uses of Inorganic Nitrate and Nitrite

Inorganic nitrate from the diet may present a method for nitrite supplementation that is acceptable to many patients, and has been shown to underlie much of the beneficial effects observed from diets associated with lower cardiovascular risk, such as the Mediterranean diet (205,206). The Dietary Approaches to Stop Hypertension (DASH) diet has been shown to reduce blood pressure in patients both with and without hypertension (207). In a clinical trial investigating the effects of eight weeks of the DASH diet (following three weeks of a control diet) on blood pressure in 459 adults with resting blood pressures of <160/80-95mmHg, systolic blood pressure was reduced by ~11.5mmHg in the hypertensive-group in the intervention arm (207). Further analysis of the DASH diet suggests that inorganic nitrate and nitrite levels are likely responsible for the antihypertensive effects (206), with the high vegetable content resulting in a nitrate intake of up to 1222mg per day, which exceeds the WHO recommendations for a 60kg adult almost 5-fold (208). In light of these findings, there

has been ongoing interest in dietary supplementation with inorganic nitrate, which can achieve similar antihypertensive effects via dietary supplementation, for example with beetroot juice, which contains around 40mg (or ~6.4mmol) of nitrate in a single 250 mL dose (209).

Various chemical compounds containing the nitrate ion have in fact been used in medicine since ancient times and may increase plasma nitrite levels. A particular example of this is the mineral potassium nitrate (KNO_3), which occurs naturally (known as nitre or saltpetre) and was prescribed by Chinese physicians, who advised placing the powder under the tongue and swallowing the saliva produced (210). Nitrate compounds have also been used commercially in the synthesis of gun powder and in the agricultural sector as fertiliser (211). Potassium nitrate, as a potassium salt, is also a well-known diuretic that was used before the advent of modern, more effective diuretics (212). Other nitrate containing drugs, such as sodium nitrate, have been proposed as alternative drug candidates that lack diuretic properties, which may be unattractive in many cardiovascular disease states, whilst still increasing plasma nitrite levels. In contrast, nitrite-containing compounds are used commercially as food preservatives due to potent antibacterial effects (213), and were once used in medicine in the form of inhaled amyl nitrite for the treatment of heart failure and *angina pectoris* (214), however the effects were often short-lived causing this to go out of favour.

1.3.3 Safety of Inorganic Nitrate and Nitrite

1.3.3.1 Reported Risk of Gastrointestinal Cancers

The health effects of nitrate and nitrite have fallen in and out of favour over their long history of use, as there have been concerns regarding the use of nitrite as a preservative for meats, linked to a potential increased risk of methaemoglobinaemia and some gastrointestinal cancers (215,216). The putative mechanism for the latter

was nitrosation of consumed amines (such as diphenhydramine, chlorpheniramine, or N,N-dimethyldodecylamine-N-oxide) to form N-nitrosamines, and this was demonstrated in animal models (217). Difficulties in heterogeneities between studies in humans assessing risk of cancer from nitrite/nitrate consumption led to inconclusive results with the dispute remaining largely unresolved. The World Health Organisation (WHO) recommendation states *"ingested nitrate or nitrite under conditions that result in endogenous nitrosation is probably carcinogenic to humans (Group 2A)"* (218). More recently however, this has been called into question considering that the primary source of dietary inorganic nitrate is vegetables, and large prospective studies have demonstrated an inverse association between fruit, vegetable, and fibre intake and gastrointestinal/hepatic cancer risk, with no association for other cancers (219).

Shedding further light on this, the large EPIC (European Prospective Investigation into Cancer and nutrition) Study of 477,312 men and women across 23 centres in Europe showed no association between vegetable intake and gastric adenocarcinoma, but did show a protective effect from citrus fruits (likely linked to high levels of ascorbate/vitamin C, a potent antioxidant) (220). In fact, a meta-analysis into the risk of nitrosamines and gastric cancer demonstrated a reduced risk of gastric cancer with high nitrate intake, but a mild increase with high nitrite and N-nitrosodimethylamine (NDMA) levels (221). Similarly, a study of 120,852 men from the Netherlands over 16.3 years demonstrated an association between oesophageal squamous cell carcinoma (SCC) and high dietary NDMA (222). A further study from the Shanghai Women's Health Study investigated the association between dietary nitrate/nitrite intake and the risk of colorectal cancer. In this cohort of 73,118 women from Shanghai, there was found to be no association between nitrate intake and cancer, but there was a trend towards increasing prevalence with increasing nitrate intake in those women with low ascorbate intake (<83.9mg/day) (223). Concerns from oral sodium nitrite persist however, as single doses of sodium nitrite in mice (at 20, 40, 60, and 75mg per kg bodyweight) were associated with significant intestinal

inflammation (216). Taken together, these data imply a localised effect of nitrosamines, and a potential risk from ingested nitrite and NDMA, but insufficient evidence for risk from dietary inorganic nitrate in the presence of normal ascorbate ingestion.

1.3.3.2 Methaemoglobinaemia

The major side effect from the ingestion of inorganic nitrate in the diet or in drinking water (mainly from agricultural 'run-off') is methaemoglobinaemia, which is related to its conversion to nitrite (224). Nitrite oxidises the iron component of haemoglobin from the ferrous to ferric state (Fe^{2+} to Fe^{3+}), which causes a conformational change to methaemoglobin (MetHb), preventing binding with oxygen (20). This low oxygen state may cause cyanosis and hypoxia, which may be fatal. Methemoglobinaemia may manifest as cyanosis at levels of around 10% in the plasma in healthy adults, but is present at levels from 0-2% in the physiological state (225). Significant methaemoglobinaemia has mainly been reported in children from communities with high levels of inorganic nitrate in the drinking water due to fertiliser run-off from nearby agricultural areas. This is more likely to occur in infants under the age of 3 months (termed 'blue baby syndrome' due to cyanosis), in whom conversion of nitrate to nitrite occurs at an increased rate (up to 80%) (226). This is thought to be due to differences in gut microbiota, lower acidity of stomach acid, higher foetal haemoglobin levels, and lower levels of methaemoglobin reductases (226), and this may be potentiated in infants with gastroenteritis. In addition to this, salivary nitrate reductase activity is absent in infants during the first 2 weeks of life, despite the presence of nitrate-reducing oral bacteria, resulting in almost no nitrite reaching the infant gut (227). In a recent study of 188 infants, salivary nitrate reductase capacity measured at 4 months of age was still significantly lower than adult levels, but increased dramatically by 12 months (228). There were no differences between the sexes, whereas formula-fed infants had higher nitrite levels than breastfed infants at 4 months, but this difference disappeared at 12 months (228).

In adults, the conversion of oral nitrate to nitrite is around 5% (i.e. 25% of the ingested nitrate reaches the salivary glands, and 20% of this is reduced to nitrite by oral flora) (16). Although blood pressure lowering effects with inorganic nitrate have been shown in predominantly Caucasian cohorts, South East Asian patients were resistant to these effects, highlighting potential differences based on ethnicity (229). Similarly, females have been shown to have higher basal plasma nitrite levels than males, in association with higher nitrate-reducing activity of oral bacteria (230). The WHO Acceptable Daily Intake (ADI) is set at 3.7mg nitrate/kg body weight/day (4.2mmol/day for a 70kg adult) (231). Interestingly, the DASH diet reaches levels of nitrate over 1200 mg/day (nearly 20mmol), and has been used safely and effectively without methaemoglobinaemia in non-'at-risk' groups (207). However, human intoxications from sodium nitrite have been reported as a result of its presence in food, mainly as a preservative in cured meats (232). It is possible that there is a difference in risk profile between dietary sources of nitrate and nitrate from drinking water, but this may be more related to contamination of some sources of drinking water, such as wells, with anaerobic bacteria that possess nitrate reductase activity (233).

1.3.3.2.1 Congenital MetHb and G6PD Deficiency

Some patient groups may be at greater risk than others of developing methaemoglobinaemia following exposure to inorganic nitrate or nitrite. Rare hereditary forms of autosomal recessive congenital methaemoglobinaemia have been identified, which result in cyanosis in the milder form, and life-limiting neurological impairment in the severe form (234). Genetic mutations in the NADH-cytochrome b5 reductase gene have been identified as the causative mechanism (235). The NADH-cytochrome b5 reductase enzyme is critically responsible for reducing methaemoglobin to haemoglobin in erythrocytes via important reductive and oxidative reactions between the glycolytic and pentose phosphate pathways

(235), and is thus also known as 'methaemoglobin reductase'. These patients have elevated baseline levels of methaemoglobin, and even slight elevations may cause clinically relevant cyanosis. Similarly, lesions of the glycolytic pathway may also result in raised methaemoglobin levels following exposure to nitrite. Glucose-6-phosphate dehydrogenase (G6PD) deficiency, caused by an X-linked chromosomal mutation, is common to many areas of the Mediterranean, Asia, and Africa, and is thought to affect some 400 million people worldwide (236). The G6PD enzyme catalyses the first step of the pentose phosphate pathway (PPP), which produces the nucleotide precursor ribose-5-phosphate and, critically, the reduced form of nicotinamide adenine dinucleotide phosphate (NADPH) (237). NADPH produced from the PPP is used by the glutathione pathway to remove cellular ROS. In erythrocytes (red blood cells) this is the only source of reducing equivalents. In an unstressed state, patients with G6PD deficiency are generally asymptomatic. Exposure to some substances however, classically antimalarials and fava beans (238,239), results in a haemolytic crisis caused by extensive erythrocyte destruction from toxic levels of intracellular ROS. Interestingly, this is thought to offer a key evolutionary advantage for people living in malaria endemic areas, as the uncontrolled surge in hydrogen peroxide (H_2O_2) and resultant apoptosis of the infected erythrocyte may critically interrupt the parasite lifecycle and prevent reproduction/spread (240). Sodium nitrite is currently licenced for clinical use as an antidote for cyanide poisoning, at a considerable intravenous dose of 300mg (4.35mol) (241). Cyanide avidly binds the Ferric (Fe^{3+}) iron within cytochrome C oxidase (complex IV of the mitochondrial ETC), disrupting critical mitochondrial respiration (241). High dose sodium nitrite converts large amounts of haemoglobin to methaemoglobin, which increases available Ferric (Fe^{3+}) iron to compete with that of cytochrome C oxidase as a substrate for cyanide binding. This is co-administered with sodium thiosulfate to convert cyanide to thiocyanate which can be eliminated by the kidneys (241). At the high dose used in this scenario, sodium nitrite increases intracellular ROS and may precipitate haemolytic crisis and increase methaemoglobin in patients with G6PD deficiency.

1.4 Alternative Methods for NO supplementation

1.4.1 Inhaled Nitric Oxide

Despite the known salubrious effects of saltpetre centuries ago, increasing plasma nitrite has remained a relatively unexplored method for increasing bioactive NO since it's characterisation as the endothelium dependent relaxing factor in the 1980s (242). However, direct methods of NO supplementation have been investigated extensively in the literature, as have interventions that act at varying levels of the NO cascade (**Figure 1-3**). As a gaseous molecule, it seems intuitive that NO may be directly delivered via administration of purified NO gas, which would act locally in the pulmonary circulation and also improve respiratory function. Indeed this method of NO supplementation has been used for many years (243). Acting locally, inhaled NO acts via NO-sGC-cGMP signalling and RSNO (S-nitrosothiol) to cause pulmonary vasodilatation and bronchodilation, and has important anti-inflammatory and anti-proliferative effects.

Following administration, NO reacts with oxyhaemoglobin in the blood and is oxidised to nitrate, with 70% excreted as nitrate in the urine by 48hours (244). Inhaled NO is therefore an effective therapy for pulmonary hypertension and acute respiratory distress syndrome (ARDS), enhancing ventilation-perfusion matching (and therefore oxygenation) by preferentially acting in well-ventilated airways (245). Although pulmonary hypertension is common in many diseases of the cardiovascular system, much of the inhaled NO is quickly oxidised following administration to nitrate, which cannot be reduced as previously described, leaving only a proportion of bioavailable NO following an inhaled dose. The production of nitrite following administration of inhaled NO is relatively low. Larger doses may therefore be required for systemic effects, which may be problematic due to the potent vasodilatory effects of NO with high doses (246). There may be a role for the administration of inhaled sodium nitrite (**Figure 1-3**) as an alternative therapy for

cardiovascular diseases, particularly those of which pulmonary hypertension is a feature, due to the dual benefits of the localised action of nitrite and the increase in systemic plasma nitrite levels, and this is under investigation (247,248). Interestingly, ultra-violet A illumination of the skin also results in non-enzymatic NO formation, and can even induce a drop in systolic and diastolic blood pressure of around 11% at 30 minutes (249). However, the time course of NO formation with prolonged exposure is unknown, and the significant ethical concerns surrounding sun exposure as a medical intervention require further examination.

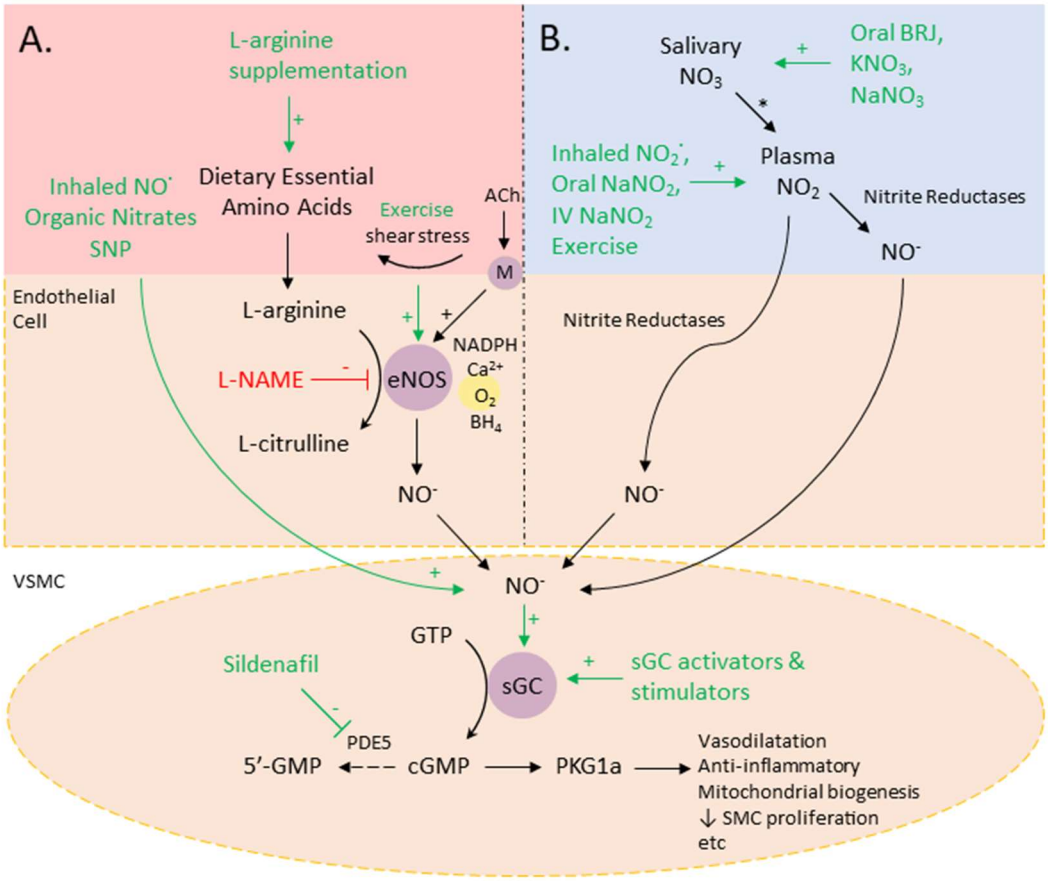

Figure 1-3: Augmentation of the Nitric Oxide Pathway in the Vascular Endothelium. In normoxia (**A**), such as in the arterial circulation, nitric oxide (NO) production occurs via the conversion of l-arginine to l-citrulline by eNOS in the presence of co-factors. Vascular shear stress also mediates the phosphorylation status of eNOS to increase NO production, and this is increased during exercise. Under hypoxic conditions (**B**), low oxygen tension reduces NO production by eNOS. However, plasma nitrite can be reduced to NO in hypoxia, supplementing NO production. Plasma nitrite levels are primarily determined by conversion of ingested inorganic nitrate by the enterosalivary circulation, but also a small part by the oxidation of NO in normoxic tissues. ACh, acetylcholine; BH_4, tetrahydrobiopterin; BRJ, beetroot juice; Ca^{2+}, calcium; cGMP, cyclic guanosine monophosphate; eNOS, endothelial nitric oxide synthase; KNO3, potassium nitrate; LNAME, L-N^G-Nitro arginine methyl ester; M, muscarinic receptor; NaNO3, sodium nitrate; NO, nitric oxide; NO_2, nitrite; PDE5, phosphodiesterase 5; PKG1a, protein kinase G 1 alpha; sGC, soluble guanylyl cyclase; VSMC, vascular smooth muscle cell.

1.4.2 Organic Nitrates and Sodium Nitroprusside

NO-donor drugs that could act in the circulation, close to their therapeutic targets, provide an attractive intervention for diseases of the cardiovascular system. Indeed, GTN (glyceryl trinitrate) has been used in medicine for ~140 years and is known to be an effective relief for *angina pectoris* and heart failure (210). GTN is an organic nitrate, a group of drugs with complex structures that donate NO following bioactivation in metabolically active tissues (**Figure 1-3**) (250). The exact mechanisms for NO release from organic nitrates have not yet been fully elucidated, however it appears that mitochondrial ALDH2 plays an important role in the enzymatic bioactivation of high potency nitrates (such as GTN) (251). Lower potency nitrates (such as isosorbide mononitrate and isosorbide dinitrate) are predominantly bioactivated by CYP450 enzymes in the endoplasmic reticulum (252). An important issue following organic nitrate administration however, is the development of tolerance when the drug is continuously used for 24hours of more, whereby tissues become progressively desensitised to the drug's effects (202). The mechanisms underlying tolerance to organic nitrates involve the formation of ROS and reactive nitrogen species (RNS) and a hypersensitivity to vasoconstrictive substances (202,253). Increased response to vasoconstrictors is also due to ROS as well as upregulation of protein kinase C (PKC), likely due to increased expression of Endothelin-1 receptors (254,255). In the case of the high potency nitrates such as GTN, an inhibition of ALDH2 activity has also been demonstrated, and is secondary to ROS/RNS produced in the cytosol and mitochondria, which oxidise thiols within the enzyme and alter its activity (251). Given the integral role of ROS in nitrate tolerance, concomitant use of drugs that reduce the effects of ROS may therefore effectively reduce the incidence of organic nitrate tolerance. This was attempted with the concurrent use of N-acetylcysteine (NAC) with GTN administration in the hope of replacing depleted sulfhydryl (thiol) bonds within ALDH2 and reducing tolerance. This approach markedly enhanced the vasodilatory and antiplatelet effects of GTN in patients undergoing cardiac catheterisation for investigation of chest pain (256). In a

larger randomised control trial of 112 patients undergoing primary percutaneous coronary intervention, low dose GTN was administered with high dose NAC or placebo, with a reduction in infarct size seen on CMR in the NAC arm (257). A similar positive step towards preventing tolerance was fortuitously discovered for lower potency nitrates, with the use of hydralazine coupled with isosorbide dinitrate therapy in patients with heart failure. Hydralazine was originally used as a selective arteriolar vasodilator to complement the large arteriolar and venodilator effects of isosorbide dinitrate, yet the ancillary effects of hydralazine as an antagonist of NADPH oxidase resulted in increased intracellular levels of NADPH (a scavenger of ROS) and ameliorated nitrate tolerance (258).

The intravenous NO-donor drug sodium nitroprusside has also been used extensively in medicine, but differs significantly from organic nitrates, in that it donates NO upon mixing with oxyhaemoglobin (to also produce cyanide and methaemoglobin) without the requirement for bioactivation (**Figure 1-3**) (259). Sodium nitroprusside causes profound dilatation of both resistance and capacitance vessels, making it an attractive therapy for patients in hypertensive crisis or to induce hypotension to stabilise haemodynamics as in acute aortic dissection (260). This profile however, may predispose to adverse events such as vascular steal syndromes and must therefore be used with caution. An example of this is coronary steal in patients with coronary artery disease (CAD), where dilatation of collateral arteries downstream from the atheromatous plaque causes an increase in blood flow to both the ischaemic and normal regions of the myocardium, interrupting the ability of the circulation to couple flow with O_2 demand (260). For this reason, nitrates that are bioactivated such as GTN, are preferred in patients with atheromatous disease. Additionally, the molecular structure of sodium nitroprusside is comprised of 5 cyanide molecules, and their liberation and subsequent accumulation is a further risk with sodium nitroprusside administration (259).

1.4.3 L-Arginine Supplementation

It may be that dietary supplementation is more acceptable to both patients and clinicians, and inorganic nitrate has gained increasing interest as a candidate therapeutic agent in cardiovascular disease. This may be particularly so in light of the mixed results from randomised controlled trials (RCTs) of supplementation with l-arginine (to increase eNOS-derived NO, **Figure 1-3**) and l-citrulline (which is recycled by the endothelium into l-arginine) in the field. In a small crossover study of fifteen patients with heart failure, l-arginine therapy at a dose of 5.6-12.6g/day and matching placebo were administered for 6 weeks in random order. Forearm blood flow during exercise significantly improved, from 5.1±2.8mL/min/dL to 6.6±3.4mL/min/dL ($p<0.05$), and functional status also significantly improved (261). A single intravenous infusion of l-arginine (30g over 60 minutes) has also been shown to be beneficial in 10 male patients with peripheral vascular disease, with a significant increase in femoral blood flow (increase of 42.3±7.9%, $p<0.05$) compared to no increase with placebo (increase of 4.3±13.0%, p=NS) (262). However, when added to standard therapies for the treatment of acute ST-elevation myocardial infarction (STEMI) in a RCT involving 153 patients, l-arginine therapy at a dose of 3g three times per day (TDS) resulted in six deaths in the treatment arm vs. no deaths in the placebo arm triggering early termination of the study (263). There were no improvements in left ventricular ejection fraction or measures of arterial stiffness at the close of the study.

1.5 Augmentation of the Canonical NO-sGC-cGMP Cascade

1.5.1 Soluble and particulate GC, PDE, and cGMP

NO canonically binds to the haem-containing form of the α/β heterodimer sGC to stimulate production of cGMP (242). This form of sGC can also be 'stimulated' to produce cGMP in a manner independent of NO by drugs such as Riociguat, a class known as sGC stimulators (**Figure *1-3***) (264). Stimulators of sGC also stabilise NO-sGC signalling by sensitising sGC to NO. Under oxidative stress however, the haem moiety may be oxidised and subsequently lost from sGC, and this is a key mechanism by which ROS may impair NO-sGC-cGMP signalling (265). In this haem-free form, sGC is unresponsive to NO and sGC stimulators, but can be 'activated' by sGC activators (such as Cinaciguat), which mimic NO-bound haem, resulting in increased cGMP production (264). These drugs are fairly new, having been engineered only some 10 years ago by Bayer Pharmaceuticals, but have already been tested rather extensively as potential therapies for cardiovascular disease. Riociguat has found a place as a treatment for patients with inoperable chronic thromboembolic pulmonary hypertension (CTEPH) (266). Whilst dyspnoea and exercise intolerance from CTEPH is troubling for patients, the most feared complication is progression to right ventricular failure and death. Riociguat has been shown to improve 6 minute walking distance, N-terminal pro hormone of brain natriuretic peptide (NT-proBNP, released in ventricular failure), measures of pulmonary vascular resistance, and WHO functional class (267). Cinaciguat however, an activator of sGC, was tested as a therapy for acute heart failure, but was found to be limited by significant hypotension at doses that reduced pulmonary capillary wedge pressure (PCWP) but failed to improve cardiac output (268). Newer drugs in these classes are being developed and studies investigating this intriguing and effective method of targeting the NO pathway in cardiovascular disease continue.

The phosphodiesterase (PDE) isoenzymes convert intracellular cGMP to 5'-GMP and/or cAMP to 5'-AMP, reducing activation of Protein Kinase G (PKG) and/or Protein Kinase A (PKA) (**Figure *1-3***). There are many isoforms of the enzyme throughout the cardiovascular system, each classified based on their inhibition or activation in the presence of cGMP and cAMP (269). PDE5 co-localises with the soluble cGMP pool, whereas PDE2 controls the particulate pool, which resides close to the plasma membrane (270). The NO-sGC-cGMP pathway contributes to the soluble cGMP pool, whereas natriuretic peptides activate particulate GC to supply the particulate pool (270). In this way, despite their common action of raising intracellular cGMP, the separation of cGMP into discrete pools plays a role in the different myocardial response to NO vs. natriuretic peptides. Drugs that inhibit PDE5 raise intracellular cGMP, whereas PDE3 inhibitors raise intracellular cAMP (269). PDE5 inhibitors have been extensively studied in the context of cardiovascular disease, and famously, successfully marketed in the form of Sildenafil by Pfizer for the treatment of erectile dysfunction and pulmonary hypertension (271). PDE3 inhibitors, such as Milrinone and Inamrinone, have positive inotropic, lusitropic, and vasodilator effects, making them attractive drugs for the management of acute heart failure (272). They are contraindicated in chronic heart failure however, as long-term use of PDE3 inhibitors was associated with increased morbidity and mortality in a large RCT (273), related to the increased energetic cost of altered calcium signalling with inotropes in CHF (274). These effects are not seen with PDE5 inhibitors however, which have been shown to improve exercise tolerance in patients with chronic heart failure and secondary pulmonary hypertension, mainly due to effects on the pulmonary vasculature (275). Sildenafil also has anti-fibrotic and anti-hypertrophic effects in the myocardium, but these have been shown to be related to myocardial redox status, with a loss in cardioprotective effects demonstrated in the absence of oxidative dimerization of PKG1α (276).

1.5.2 Protein Kinase G1α Activation and Oxidative Dimer Formation

1.5.2.1 The PKG1α Dimer in the Vasculature

Protein Kinase G1α is the predominant PKG isoform in the cardiovascular system (277). PKG1α is activated by cGMP and transduces signals from the upstream NO-sGC-cGMP pathway. In addition to being activated by intracellular cGMP, intracellular ROS can oxidise a cysteine residue (C42) within PKG1α, causing homodimer formation via disulfide bonds between two PKG1α molecules (278). This homodimer has a diffuse cytosolic distribution compared to the monomer, which remains close to the phospholipid membrane (278). The PKG1α dimer and cGMP-activated monomer appear to directly antagonise the effects of one another, as pre-treatment with cGMP attenuates, whereas depletion sensitises, PKG1α oxidation (279). In addition, although the dimer is an active form of PKG1α and has many similar effects to the monomer, other dimer-mediated effects are unique.

The vascular sequelae of raised PKG1α dimer content have received great attention, as they appear to be important in ameliorating arterial hypertension, an important modifiable risk factor for cardiovascular disease. The aorta distributes blood to the arterial tree after receiving the stroke volume ejected by the LV with each heartbeat. The elastic properties of the aorta absorb and dampen the pulse pressure of the ejected blood, and contribute to diastolic blood pressure (280). The small arteries and arterioles are primarily responsible for regulation of vascular resistance and thereby regulate systolic blood pressure and organ perfusion (280). In cardiovascular disease, stiffening of the aorta impairs dampening of systolic pressure and increases pulse wave velocity augmenting late systolic afterload. Changes within resistance vessels also result in increased baseline vascular tone. Whilst aortic compliance is a difficult pharmacological target, resistance vessels, as the primary regulators of blood pressure, respond to a range of pharmacological agents including NO. Following blockade of endogenous NO and prostacyclin, vasodilatation in the intact

endothelium in response to acetylcholine persists, termed endothelium derived hyperpolarising factor (EDHF), and this is shown to be largely due to hydrogen peroxide (H_2O_2) (281). The mechanism underlying this was found to be formation of the PKG1α dimer as a result of H_2O_2 (278). This prompted the creation of a C42S knock-in mouse model (in which C42 is altered to a serine residue via single atom substitution of oxygen in place of sulphur) to characterise the importance of this mechanism *in vivo* (282).

Using this model, the Eaton group showed that the PKG1α dimer is responsible for much of the action of GTN as a vasodilator, and interestingly, that tolerance to GTN was associated with a loss of oxidative dimer formation, as the onset of critical ALDH2 oxidation prevented further bioactivation of GTN associated with an abrupt fall in H_2O_2/ROS (283). The same group have demonstrated that the PKG1α dimer is involved in the vasodilator responses to the reducing agent hydrogen sulfide (H_2S), via intermediate polysulfides (284), and the antioxidant resveratrol (285). The dimer has also been shown to be important in reducing resting small artery tone in response to browning of perivascular adipose tissue (286), an adaptation which is thought to be beneficial in a range of cardiovascular diseases due to the net increase in energy expenditure (287). These beneficial effects have sparked the development of a novel class of antihypertensive drugs that activate PKG1α via oxidative dimerization (280). Redox signalling is therefore critically important at physiological levels, but this must be closely regulated in order to balance the salubrious and damaging effects. Uncontrolled oxidation that overwhelms quenching mechanisms may lead to a feed-forward generation of ROS, as occurs with the oxidation of BH4 to 7,8-dihydrobiopterin (BH2), which leads to eNOS 'uncoupling' and rampant superoxide free-radical generation in the place of NO (288). This is particularly pertinent in endotoxaemia, where excessive redox-related PKG1α dimerization is a major cause (in addition to inducible NOS upregulation from bacterial lipopolysaccharide (289)) of the profound hypotension and calcium-related cardiac dysfunction responsible for sepsis-related multiple organ damage (290). Whilst this is deleterious in the systemic

circulation, it may be a beneficial adaptation in the pulmonary circulation in response to pulmonary hypertension (291).

Recently, Madhani et al. have demonstrated, using the same knock-in mouse model, that nitrite can precipitate PKG1α disulfide dimer formation in resistance vessels, but not conduit vessels, of wild-type mice at 24 hours (292). Importantly, knock-in mice were resistant to the vasodilator effects of nitrite compared to their wild-type littermates, and nitrite-mediated vasodilatation in wild-type mice was NO- and cGMP-independent. The authors demonstrated that nitrite inhibited catalase, increasing hydrogen peroxide generation, and that this resulted in generation of persulfides and polysulfides, resulting in dimerization of PKG1α. This pathway appeared to be responsible for the delayed (1hr) and sustained (24 hours) blood pressure lowering effects of a single intraperitoneal injection of nitrite in mice. This blood pressure lowering effect was not observed in the 'redox-dead' PKG1α knock-in mouse (292). Similarly, inorganic nitrate can 'brown' perivascular adipose tissue (PVAT) via PGC1α, activated by NO-sGC signalling (293), and the ROS from brown PVAT can dimerize PKG1α as discussed above. However, whether these nitrite-mediated alterations in cellular redox state are beneficial or detrimental requires further investigation. Given the critical role of dietary inorganic nitrate in increasing the plasma nitrite pool, nitrite levels fluctuate in peaks (occurring 2-3 hours after each meal) and troughs, and it may be that trough periods are just as important, and allow redox levels to be 'reset'.

1.5.2.2 The PKG1α Dimer in the Myocardium

In a phosphoproteomics study, the Eaton group showed that the PKG1α dimer and monomer share affinity for multiple phosphorylation targets within the myocardium, with the exception of serine 16 of phospholamban (294). Phospholamban (PLN) is the physiological inhibitor of the SERCA2a pump, which is responsible for Ca^{2+} sequestration to modulate contractile force (295). The dimer is formed by oxidation

from ROS produced by myocardial stretch and phosphorylates PLN at serine 16, relieving inhibition of SERCA2a and increasing the force of the subsequent contraction, thereby fine-tuning the Frank-Starling mechanism in response to cyclical changes in stretch (294). However, whilst increased activation of the PKG1α monomer by cGMP is responsible for the cardioprotective effects of NO, sustained formation of the dimer is associated with impaired cardioprotection. In a study investigating the differing effects of PDE5 inhibitors and sGC activators in the high redox state following trans-aortic constriction (TAC) to promote LV failure, the dimer was found to be less effective at inhibiting transient receptor potential canonical channel 6 (TRPC6) than the monomer, blunting the anti-fibrotic/anti-hypertrophic effects (276). Similarly, co-administration of a PDE5 inhibitor ameliorated doxorubicin mediated cardiotoxicity, by increasing cGMP levels to inhibit disulfide dimer formation (296). The dimer is unable to phosphorylate RhoA, an important signalling molecule for enhancing cellular survival, and indeed impairs the ability of the monomer to phosphorylate this target, impairing a key cardioprotective mechanism against doxorubicin toxicity (296).

It is unknown whether nitrite can induce PKG dimerization in the myocardium in a manner analogous to the effects seen in resistance vessels, however, as the dimer was not demonstrated in conduit vessels, this seems unlikely (292). The myocardium and large arteries produce more NO and contain higher levels of peroxiredoxins than resistance vessels, which can detoxify and quench intracellular H_2O_2/persulfides, thus preventing PKG dimerization with moderate increases in ROS (279). As the PKG dimer has been principally demonstrated in 'hyperoxidising' redox states, induction of myocardial PKG1α dimerization with interventions that increase plasma nitrite within physiological levels might not be expected in the healthy myocardium. However, in an integrated metabolomics/proteomics study in rat hearts, a single nitrite dose resulted in short-term cardiac redox changes that translated to 'selective' long-term alterations, with lasting reductions in glutathione oxidation (297). Whether these

selective alterations might include or affect PKG1α oxidation requires further investigation.

1.6 Clinical Trials of Inorganic Nitrate and Nitrite in Heart Failure

Given the purported benefits of nitrite and the nitrate-nitrite-NO pathway in pre-clinical studies, numerous clinical trials utilising this therapeutic intervention have been completed across almost all fields of medicine. In 2007, a group from the Karolinska Institute demonstrated a reduction in the oxygen cost of submaximal exercise following 2 days of 0.1mmol/kg/day oral sodium nitrate in a small study of sedentary men (298). Shortly afterwards, the same group showed that this was associated with improved oxidative phosphorylation due to reduced proton leak at the inner mitochondrial membrane, by reducing expression of the enzymes ANT and UCP in human skeletal muscle (299). This piqued interest in inorganic nitrate as a potential treatment for patient groups in whom exercise intolerance is a key feature. A few years earlier, Gladwin et al. had showed that intravenous sodium nitrite was a potent vasodilator and source of NO in the human forearm circulation in the presence of deoxyhaemoglobin (194). Building on this, Frenneaux et al. demonstrated that nitrite is a potent venodilator in both normoxia and hypoxia, but that the vasodilator effects are only modest in normoxia, with hypoxia significantly augmenting nitrite-induced vasodilatation (300). However, clearly the use of an intravenous medication (with a half-life of ~45 minutes) that induces an acute haemodynamic response to achieve the desired lasting proteomic effects (297), presents issues for designing larger randomised controlled trials. An inhaled form of nitrite was therefore developed, and showed promise in early studies as a selective, hypoxic pulmonary vasodilator (301). This is of particular interest to the heart failure community given the high prevalence of pulmonary hypertension; caused by left-sided cardiac failure in HFrEF (302), and pulmonary arterial dysfunction and exercise-induced pulmonary hypertension in HFpEF (303). Pre-clinical studies also began to demonstrate significant improvements with inorganic nitrate and nitrite in key systems involved in the pathogenesis of heart failure. A combination of oral sodium nitrite and metformin was shown to improve hyperglycaemia and normalise pulmonary pressures in a new 2-hit rat model of HFpEF with pulmonary hypertension (304). In this new model, rats

with double-leptin receptor defects with associated metabolic syndrome and obesity, were treated with a vascular endothelial growth factor receptor blocker to induce pulmonary hypertension. The salubrious effects of combined nitrite and metformin therapy in this model were shown to be related to activation of SIRT3 (discussed in section 1.2.2.2) and AMPK in skeletal muscle (304). Inorganic nitrate also prevented progression to heart failure following a toxic dose of doxorubicin in mice, via transient blockade (nitrosylation) of mitochondrial ROS generation at complex I (305). The same mechanism is thought to be responsible for nitrite-induced cardioprotection from ischaemia reperfusion injury. However, in a large randomised controlled trial (The NIAMI trial), 70 µmol intravenous nitrite infused for 5 minutes prior to reperfusion at percutaneous coronary intervention failed to reduce the primary endpoint of myocardial infarct size on cardiovascular magnetic resonance imaging at 6-8 days (306).

It has also been shown that nitrate may play a central role in the salubrious effects of the Mediterranean diet (205). The recently characterised nitro free fatty acids nitro-oleate and nitrolinoleate, formed via the nitration of unsaturated FFAs (e.g. in olive oil), have been shown to inhibit Kelch-like ECH-associating protein 1 (Keap1), the negative regulator of nuclear factor-erythroid 2-related factor 2 (Nrf2) (307). Nrf2 is a potent mediator of cellular antioxidant responses, and inhibits the pro-inflammatory nuclear factor kappa beta (NF-κB) pathway. Additionally, nitro FFAs directly inhibit DNA-binding by NF-κB via covalent alkylation of cysteine residues within its p65 subunit (308). Nitro FFAs also inhibit soluble epoxide hydrolase, preventing the hydrolysis of epoxyeicosatrienoic acid (EET) substrates, which induce vasodilation and lower blood pressure (205). As further evidence of the anti-inflammatory actions of nitrite, a recent study demonstrated that 1 week of inorganic nitrate at a dose of 2mmol/L in the drinking water of mice attenuated weight loss and markers of ROS production following total body irradiation at 5 Gy (309).

In a heart failure clinical study involving 9 patients with HFrEF, inorganic nitrate (as beetroot juice containing 11.2mmol of nitrate) increased knee extension strength (maximal power) on isokinetic dynamometry (310). Frenneaux et al. also demonstrated that HFrEF had a significant impact on the vasodilator effects of intravenous nitrite, with significant vasodilator responses present in HFrEF patients at doses that did not induce effects in controls (311). Despite this, hypotension was not present in either group with prolonged nitrite infusion, and nor did either group develop tolerance. Interestingly, plasma nitrite post-infusion was also cleared at an accelerated rate in HFrEF compared to controls, associated with an increased rate of plasma protein-bound NO accumulation but not in oxidative formation of nitrate (311). Several small studies have now also demonstrated either an improvement or no difference in peak oxygen consumption (peak VO_2) on cardiopulmonary exercise (CPEX) testing with acute doses of oral inorganic nitrate, but these were underpowered and larger studies are needed (312,313). In 25 patients with severe chronic heart failure, intravenous sodium nitrite infusion at 50µg/kg/min for 5 minutes significantly reduced pulmonary vascular resistance (p=0.03) and increased LV stroke volume (p=0.003) (314). Interestingly, the increase in stroke volume correlated with the increase in transmural LVEDP (r=0.67; p=0.003), prompting the authors to suggest that nitrite may be relieving DVI in these patients (previously shown to be present in ~40% of HFrEF patients (93)).

Given the lack of proven therapies in HFpEF, inorganic nitrate and nitrite have received great attention as potential therapies in these patients. Intravenous sodium nitrite (infused at 50µg/kg/min for 5 minutes) improved haemodynamics and LV performance during exercise in 28 patients with HFpEF, associated with significant increases in cardiac output, stroke volume, LV stroke work, and reduced pulmonary pressures at peak exercise (315). In keeping with this, intravenous and inhaled nebulised sodium nitrite, in a group of HFpEF patients with proven increases in wave reflections and arterial elastance on exercise, significantly reduced wave reflections compared to normal saline placebo (111). In a double-blind crossover study of a

single acute dose of oral inorganic nitrate (as beetroot juice containing 12.9mmol of nitrate) in 17 patients with HFpEF, nitrate improved peak VO_2 by 1.0 mmol/kg/min (p=0.005), increased exercise cardiac output (p=0.006), and reduced aortic augmentation index (p=0.03) compared to nitrate-deplete placebo (316). A definitive large scale trial of inhaled nebulised nitrite in HFpEF has now recently concluded. In this study, nitrite failed to demonstrate an improvement in peak VO_2 vs. placebo (13.5 vs. 13.7 ml/kg/min; p=0.27) (317). The 'Inorganic Nitrite Delivery to Improve Exercise Capacity in Heart Failure with Preserved Ejection Fraction' or 'INDIE-HFpEF' study randomised 105 patients in a random-order crossover design to 4 weeks of inhaled nitrite and placebo with a primary end point of peak VO_2. Inhaled nitrite also failed to improve the secondary endpoints of daily activity levels, quality of life scores, diastolic function on echocardiogram (E/E'), or NT pro BNP levels (317). Despite questions related to dosing, route of administration, and duration of therapy, this study has largely quelled interest in nitrite as a therapy for HFpEF, but left the question of its potential use in HFrEF largely unanswered, particularly given the differences in pathophysiology between the two conditions and the longer-lasting effects of oral inorganic nitrate.

Hypothesis

It is hypothesised that the beneficial effects of plasma nitrite in cardiovascular disease models are, at least in part, related to modulation of cardiac metabolism, and that this will translate into increased exercise capacity and improved cardiac function in patients with heart failure due to dilated cardiomyopathy.

Aims and Objectives

Chapter 3: Effects of Nitrite on Protein Expression in the Myocardium

To characterise the mechanisms underpinning the beneficial effects of nitrite, we sought to measure the post-translational modification of metabolic and redox proteins in the myocardium following: 1) 7 days of oral sodium nitrite supplementation in mice; 2) a single, acute intravenous dose of sodium nitrite in diabetic and non-diabetic patients undergoing coronary artery bypass graft surgery.

Chapter 4: Effects of Nitrite on Chemotherapy Sensitivity in 786-0 Renal Cell Carcinoma Cells

To investigate whether the aforementioned mechanisms underpinning the beneficial effects of nitrite translate to hard endpoints such as cell survival, we sought to assess the effect of an acute dose of sodium nitrite on Warburg metabolism in 786-0 renal cell carcinoma cells in normoxia and hypoxia, a model posited to be highly sensitive to the metabolic changes observed in Chapter 1.

Chapter 5: The Nitrite In Chronic HEart failure (NICHE) Trial

To investigate whether nitrite has beneficial effects in patients with chronic heart failure, we sought to measure the effects of long-term oral inorganic nitrate supplementation on exercise capacity and measures of cardiac function, compared to placebo, in patients with chronic heart failure due to dilated cardiomyopathy.

Chapter 6: Myocardial Energetic Deficiency in Non-obstructive Hypertrophic Cardiomyopathy and Association with Vasculoventricular Coupling and Exercise Capacity

To assess the importance of cardiac metabolism as a therapeutic target in patients with cardiomyopathy, we sought to measure in patients with non-obstructive hypertrophic cardiomyopathy, and compare with age-matched controls: 1) measures of resting cardiac energetic impairment on ^{31}P cardiovascular magnetic resonance imaging; 2) the relationship between resting energetic impairment and dynamic diastolic dysfunction, dynamic vasculoventricular coupling, and exercise capacity.

Chapter 2: Methods

2.1 Basic Science Studies

Mouse studies:

Male C57BL/6 mice, aged between 3-5 months, were obtained from the University of East Anglia Disease Modelling Unit for the PDH studies. After an acclimatisation period of 2 weeks, mice were commenced on a nitrate/nitrite-deplete diet for a further 2 weeks. Sodium nitrite, sodium nitrate, or sodium chloride was added to the drinking water of each age- and body-weight-matched group at a concentration of 1g/L for 7 days. Drinking water was available *ad libitum*.

For the PKG1α studies, male wild-type C57BL/6 (i.e. $PKG1\alpha^{WT}$) mice, bred and maintained in-house at the University of Birmingham, were used. All procedures were performed in accordance with the Home Office Guidance on the Operation of the United Kingdom Animals (Scientific Procedures) Act 1986. Protocols and procedures for the study were also reviewed and approved by the Institutional Animal Welfare and Ethical Review Body.

Human Studies:

Human muscle biopsy samples, including left ventricular (LV) myocardium and *rectus abdominus* skeletal muscle, as well as plasma samples obtained at multiple timepoints, were analysed for this study. Samples were obtained from participants in the 'Effect of Nitrite on Cardiac Muscle and Blood Vessels in Patients Undergoing Coronary Artery Bypass Grafting Surgery' study (clinicaltrials.gov identifier NCT04001283). This was a randomised, placebo-controlled, double-blind clinical trial investigating the effects of sodium nitrite infusion on cardiac and skeletal muscle at a molecular level (**Figure *2-1***). A pre-specified analysis of patients grouped by diabetic status was planned. This study was approved by the North Scotland Research Ethics Committee (reference 11/NS/0059), and complied with the Declaration of Helsinki. Part 1 of this study involved treatment at 24 hours prior to sample collection, and was conducted by Dr Konstantin Schwarz at the Royal Infirmary, Aberdeen, Scotland

UK, under the Supervision of Professor Michael Frenneaux, between 21st January 2013 and 31st December 2014. Part 2 involved treatment at 30 minutes prior to sample collection and was conducted by Dr Nicholas Gollop at the Papworth Hospital, Cambridge UK, under the Supervision of Mr Steven Large (Chief Investigator Professor Michael Frenneaux). Only samples from Part 1 were analysed.

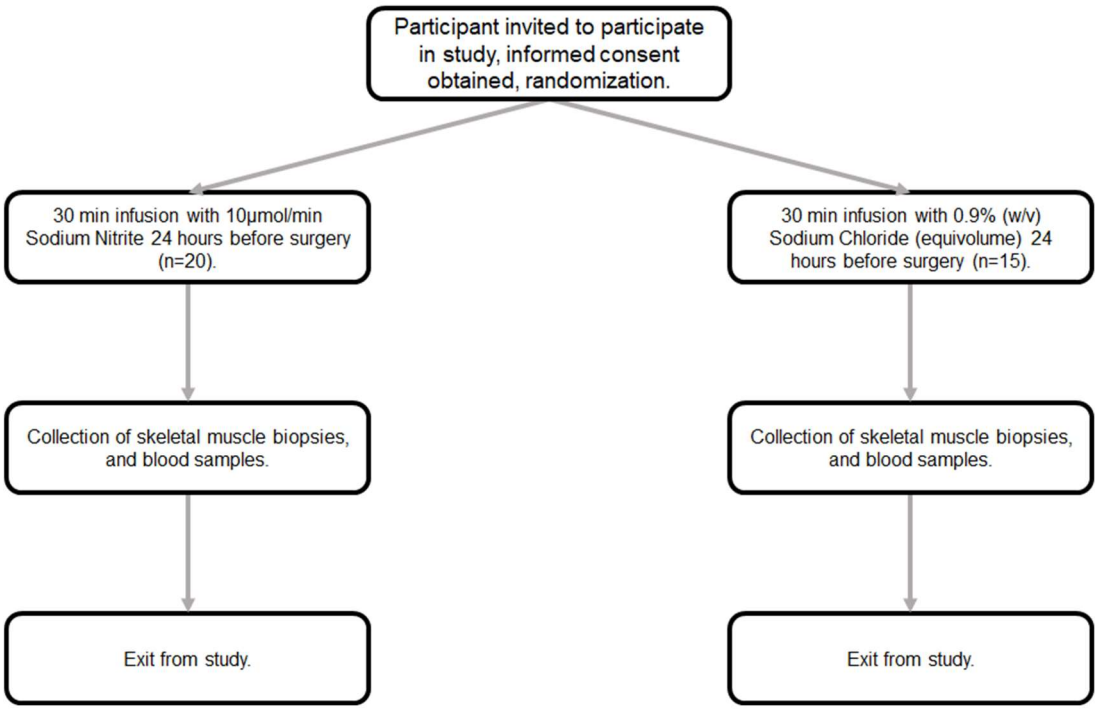

Figure 2-1: Study Design, Part 1 of the 'Effect of Nitrite on Cardiac Muscle and Blood Vessels in Patients Undergoing Coronary Artery Bypass Grafting Surgery' trial.
Patients scheduled for CABG surgery, meeting all inclusion criteria, were invited to participate by the treating clinical team. Participants were randomised to receive either a 30-minute infusion of sodium nitrite (10µmol/min) or matching normal saline (0.9%) placebo at 24hours prior to CABG surgery. Skeletal muscle (rectus abdominus) and cardiac muscle biopsies were obtained from participants during surgery, with bloods taken prior, during and after surgery, and before exiting the study (clinicalTrials.gov identifier: NCT04001283).

Briefly, eligible patients at the Aberdeen Royal Infirmary who were scheduled to undergo coronary artery bypass graft (CABG) surgery were approached by members of their treating clinical team, usually at their cardiac surgery pre-admission clinic visit. Information was provided and the study discussed in detail, with ample time afforded to consider participation (>24 hours in all cases). Written informed consent was obtained prior to study inclusion and sample collection in all cases. Exclusion criteria included inability to provide informed consent, type 1 diabetes mellitus, symptomatic heart failure (New York Heart Association class III/IV symptoms) with an ejection fraction <40%, renal impairment requiring dialysis, acute coronary syndrome (occurring within preceding 2 weeks of surgery), and pregnancy or childbearing potential. Finally, patients with G6PD deficiency (known, or measured at screening in males of African, Asian or Mediterranean descent) were excluded from the study on the basis of an increased risk of methaemoglobinaemia with nitrite treatment (see section 1.3.3.2.1). Study participants were randomly assigned to receive a 30-minute (equivolume) infusion of either sodium nitrite (10 μmol/min) or normal saline (0.9%), at 24 hours prior to scheduled CABG surgery. Blood samples were collected immediately before and after infusion, then at 6 hours post-infusion and the time of surgery (24 hours post infusion). Three, small left ventricular biopsies were obtained using Trucut biopsy needles immediately prior to aortic cross-clamping, snap-frozen in liquid nitrogen, and stored at −80°C until analysis. Skeletal muscle (*rectus abdominus*) samples, and a further blood sample, were also collected at this timepoint in all patients.

2.1.1 Western Blotting

<u>Mouse studies:</u>

The methodology for the PDH study by our group has been recently published (318). Briefly, mice were killed by cervical dislocation, and hearts and gastrocnemius muscles harvested. Mouse hearts were snap-frozen in liquid nitrogen, then stored at −80°C. Gastrocnemius muscle was first quickly cleaned of skin and fur prior to snap-

freezing. Tissue samples were homogenized in lysis buffer (100 mM Tris-HCl pH 7.4, protease inhibitors [Roche, protease Inhibitors Complete EDTA free], 2 mM sodium orthovanadate, and 5 mM sodium fluoride) using a mortar and pestle. Homogenate was subject to 3 freeze–thaw cycles using liquid nitrogen, then centrifuged at 14,000 × g for 15 min at 4°C. Supernatants were retained and stored at −20°C. Homogenate was resuspended in 2x sample buffer (250 mM Tris-HCl pH 6.8, 4% SDS [vol:vol], 10% glycerol [vol:vol], and 2% β-mercaptoethanol) to yield 10% (wt:vol) homogenate solution. Total extracted protein was determined by Bradford assay using bovine serum albumin (BSA) as standard.

Sodium Dodecyl Sulfate–Polyacrylamide Gel Electrophoresis (SDS-PAGE) was conducted under reducing conditions. Samples were loaded in Laemmli buffer containing β-mercaptoethanol, at 20µg total protein per lane in 10% acrylamide gels. Electrophoresis was conducted at 60V for 20 min, then 120V for 80 min. Separated proteins were transferred onto 0.2µm polyvinylidene difluoride (PVDF) membrane (Bio-Rad) at 100V for 75 minutes. Membranes were blocked in 5% (wt:vol) fat-free milk in 0.1% (vol:vol) Tris-buffered saline (TBS)-Tween for 1 hour at room temperature. All antibodies were diluted using 5% (wt:vol) fat-free milk in 0.1% (vol:vol) TBS-Tween. Primary antibodies (PDH E1α $pSer^{232}$, dilution 1:2000, Calbiochem; PDH E1α $pSer^{293}$, dilution 1:1000, Abcam; PDH E1α $pSer^{300}$, dilution 1:2000, Calbiochem; PDH, dilution 1:1000, Cell Signaling) were incubated overnight at 4°C, followed by incubation with goat anti-rabbit horseradish peroxidase (HRP)-conjugated secondary antibody (Cell Signaling Technology) at 1:5000 dilution for 1 hour at room temperature. Proteins were visualised using enhanced chemiluminescence substrate (ECL, GE Healthcare) and imaged in a Fusion SL imager (Peqlab). After visualisation, membranes were stained with 0.2% (wt:vol) Colloidal Coomassie Blue for normalisation to the amount of protein per lane (319). Images were analysed using ImageJ (National Institute of Health, NIH).

Human studies:

Human samples obtained from participants in Part 1 of the 'Effect of Nitrite on Cardiac Muscle and Blood Vessels in Patients Undergoing Coronary Artery Bypass Grafting Surgery' trial were analysed. As there were 3 samples of LV myocardium, 1 sample was used for the PKG1α studies and 1 sample was used for the remaining western blot targets (due to differences in sample processing). Western blotting for PDH was carried out as per the methods used for the mouse studies (see above), with the exception that antibodies were constituted in BSA rather than fat-free milk due to small biopsy samples, to prevent interference from signals due to non-specific binding of primary antibodies to phosphoproteins present in milk.

2.1.1.1 Modified Method for PKG1α Dimer Detection

Mouse studies:

The methodology specific to western blotting to assess PKG1α oxidative activation (dimer formation) has been previously reported by the King's College group, London UK, who are considered pioneers in this method (320). Our group also recently published results using this same method to assess PKG1α dimer content in murine vasculature following treatment with sodium nitrite (292). This same protocol was used for our cardiac studies in mice. Mouse hearts were ground to fine powder using a pestle and mortar in the presence of liquid nitrogen before being diluted in tissue homogenisation buffer (100 mM Tris-HCl pH 7.4, protease inhibitors [Roche, protease Inhibitors Complete EDTA free], and 100 mM maleimide). The use of maleimide importantly binds free cysteine thiols, preventing oxidisation during sample preparation (320). SDS-PAGE was conducted under non-reducing conditions. Samples were diluted into an equal volume of 2x non-reducing alkylating sample buffer (100mM Tris-HCl buffer pH 6.8, 4% SDS [vol:vol], 20% glycerol [vol:vol], 0.01% bromophenol blue [wt:vol], and 100mM maleimide [Sigma]), to yield a 10% (wt:vol) homogenate, and loaded in 8% acrylamide gels following protein determination via Bradford assay. Electrophoresis was conducted at 180V for 50 min. Separated

proteins were transferred onto 0.2µm polyvinylidene difluoride (PVDF) membrane (Bio-Rad) at 0.25 mA current (constant 10V) per membrane for 35 minutes. Membranes were blocked in 5% (wt:vol) fat-free milk in 0.1% (vol:vol) phosphate buffered saline (PBS)-Tween for 1 hour at room temperature. All antibodies were diluted using 5% (wt:vol) fat-free milk in 0.1% (vol:vol) PBS-Tween. Primary antibodies (PKG1α, 1:1000 dilution, Santa Cruz E-17; GAPDH, 1:20,000, Abcam) were incubated overnight at 4°C, followed by incubation with anti-goat (1:2500 dilution, Santa Cruz) and anti-mouse (1:2000 dilution, Dako), HRP-conjugated secondary antibody, respectively, at 1:5000 dilution for 1 hour at room temperature. Proteins were visualised on enhanced chemiluminescence (GE Healthcare). Digitized western blots were quantitatively analysed using ImageJ (NIH). The reduced form of PKG1α (the monomer) is a 75 kDa protein, whereas the oxidised dimer is 150 kDa (320). PKG1α disulfide dimer quantity was defined as a percentage of total PKG1α expression (i.e. % disulfide dimer = [intensity of dimer band/the sum of the intensity of both the monomer and dimer bands] x 100) (320).

Human studies:

Many of the human LV myocardial specimens were extremely small (range of 2-10 mg), owing to the size of the Trucut needle bore, and the reluctance of many of the cardiothoracic surgeons to make multiple passes through the LV wall. Given this, we used the experimental protocol recommended by the King's College group for use with limited sample volumes, such as for mesenteric blood vessel samples (320). This involves excluding tissue homogenisation and protein determination via Bradford assay, which minimises sample oxidation and ensures ample sample to run a Western blot. Therefore, LV myocardial samples were ground to fine powder using a mortar and pestle in the presence of liquid nitrogen and a small volume (6 µL) of 2x sample buffer (see above). Each sample was then added to equal volumes of 2x sample buffer (6 µL of each), with 10 µL added to each sample lane for SDS-PAGE.

SDS-PAGE was completed as stated above for mouse samples. However, given the limited specimens, we first determined which of the Santa Cruz or Enzo PKG1α antibody were more likely to yield reliable banding at the 75 kDa region. The Santa Cruz PKG1α primary antibody recommended by the King's College group has since changed batch and lot numbers (E-15 to E-17) (320), and has resulted in our group obtaining non-specific bands. Other primary antibodies for PKG1α have previously posed issues, as the epitopes for these antibodies are frequently within the region in which the dimer forms. Therefore, dimer content was determined by probing with an alternative PKG1α primary antibody following in-house validation (PKG1α, dilution 1:1000, Enzo KAP-PK005-D). Anti-rabbit secondary antibody (rabbit, dilution 1:2500, Cell Signaling) was used. For patients with diabetes, protein loading was determined by probing for β-actin rather than GAPDH. This is due to the fact that this protein, frequently used as a loading control in western blotting, is a glycolytic enzyme known to be altered in patients with type 2 diabetes mellitus (321).

2.1.2 PDH Activity Assay

To determine PDH activity, harvested hearts from mice supplemented with sodium nitrite in drinking water (see section 2.1) were immediately snap-frozen using tissue forceps and sent to the University of Nottingham. PDH activity is determined by phosphorylation status at the three serine residues (ser232, ser293, and ser300); dephosphorylation at these residues corresponds to an increase in PDH activity, whereas phosphorylation corresponds to reduced activity (322). Direct measurement of cardiac PDH activity was determined by rate of acetyl-CoA formation, measured following addition of radioactive oxaloacetate to form citrate, as previously reported (323).

2.1.3 Plasma Nitrate/Nitrite levels

Mouse studies:

For the PKG1α studies, mice were anaesthetized using 5% isoflurane and 4 L/min oxygen, and blood was collected via intracardiac puncture into anticoagulant tubes containing 100 µL of 10 mM N-ethylmaleimide (NEM) and 1mM EDTA. Following centrifugation at 2000 × g for 10 min at room temperature, plasma aliquots were snap-frozen in liquid nitrogen and stored at −80°C until analysis. Plasma samples were then sent to the University of Southampton for analysis. Plasma nitrate and nitrite concentrations were determined by gas phase chemiluminescence and high performance liquid chromatography (ENO-20; Eicom), as previously reported (324).

Human studies:

Plasma samples from Part 1 of the 'Effect of Nitrite on Cardiac Muscle and Blood Vessels in Patients Undergoing Coronary Artery Bypass Grafting Surgery' trial were collected at multiple timepoints as per study protocol. Plasma nitrate and nitrite concentrations were determined as for the mouse studies at the University of Southampton (see above).

2.1.4 Cell Culture

786-0 renal cell carcinoma cells (786-O [786-0], ATCC® CRL-1932™, LOT: 63530324) were purchased from the American Type Culture Collection (ATCC), Manassas USA. Cells were maintained in RPMI-1640 medium, supplemented with 10% foetal bovine serum, and 1mL of both penicillin and streptomycin, in a CO_2 incubator (ThermoFisher) maintained at a temperature of 37°C, relative humidity of 95%, and CO_2 concentration of 5%.

2.1.5 Cell Viability Studies/Luminescent ATP Assay

To test viability of 786-0 renal cell carcinoma cells following treatment with sodium nitrite (Sigma) and 5-fluorouracil (Sigma) chemotherapy, 96-well plates were plated at 10,000 cells in 200 µL culture medium per well and treated at 24 hours. The outer most columns (1 and 2) and rows (A and H) were avoided to control for potential loss of cell medium (evaporation) due to ambient conditions in the CO_2 incubator. At 24 hours (~50% confluence), cells were treated with sodium nitrite (0, 50, and 100 µM doses) and 5-fluorouracil (0, 5, 10, 25, 50, and 100 µM doses; see **Figure *2-2***).

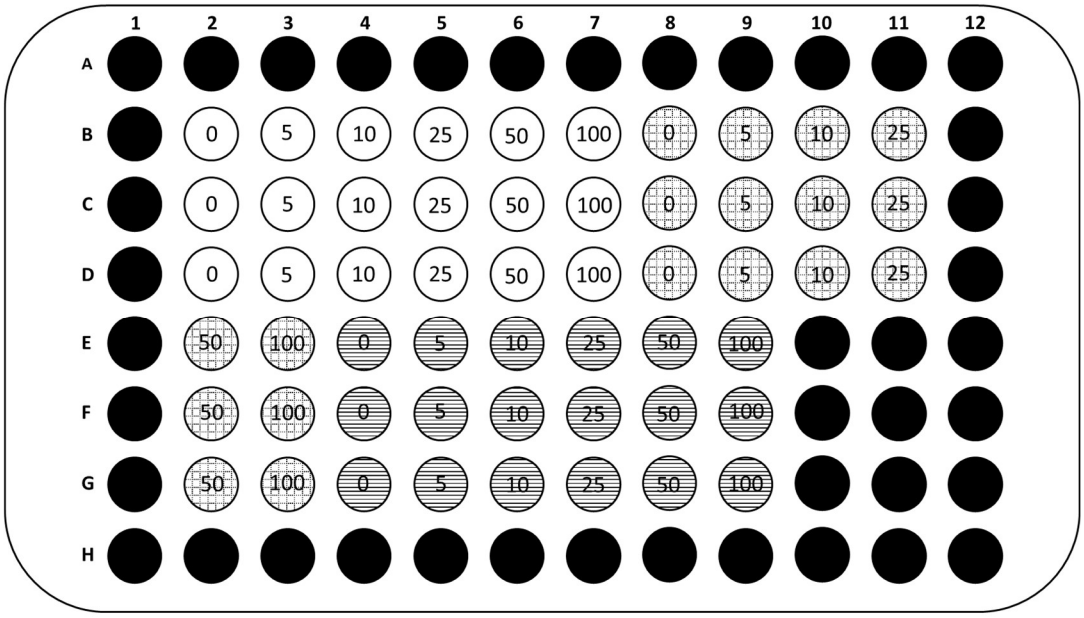

Figure 2-2: Schematic of 96-well cell culture plate used for cell viability experiments. Experimental design for cell viability studies performed at 24 hours post-treatment. 96-well plates were duplicated and placed in normoxic and hypoxic incubators for hypoxia experiments. The entire experiment was repeated with cells harvested at 48 hours post-treatment. Outer wells were not used (■ = RPMI-1640 medium only). Remaining wells dosed with 5-fluorouracil at varying concentrations (numbers in figure = µM). Note: □ = Control (0 µM sodium nitrite); ⬚ = 50 µM sodium nitrite; ▤ = 100 µM sodium nitrite.

At 24 hours post-treatment with sodium nitrite and 5-fluorouracil in normoxia or hypoxia (~80% confluence), 96-well plates were removed and 100 µL of culture medium from each well was replaced with 100 µL CellTiter-Glo® reagent (Promega). This luminescence assay determines cell viability by quantitation of ATP (i.e. luminescence is proportional to number of viable cells) (325). Plates were then covered with an opaque lid and placed on an orbital shaker at 600 rpm for 2 minutes at room temperature. At 10 minutes post addition of the CellTiter-Glo® reagent, 60 µL from each well was pipetted into white 96-well plates to maximise luminescence. Any air bubbles were first lysed with forced air from a plastic pipette bulb and the plate was read on a luminometer with a 1-second integration time. All plates were read at 10-12 minutes following addition of the CellTiter-Glo® reagent as per manufacturer specifications. Mean luminescence was determined by the mean of at least 3 replicates, and cell viability for each dose of 5-fluorouracil was expressed as a percentage of the mean luminescence of the control wells. Results were grouped by nitrite treatment concentration (0, 50 or 100 µM) in each oxygen condition (normoxia vs. hypoxia).

2.1.6 Western Blot Analysis of Cell Culture Proteins

Cells were plated into 12-well plates at 50,000 cells per well. Rows 2 and 3 were supplemented with 10 µM ODQ (1H-(1,2,4)oxadiazolo[4,3-a]quinoxalin-1-one) and 100 µM CPTIO (2-(4-Carboxyphenyl)-4,4,5,5-tetramethylimidazoline-1-oxyl-3-oxide), respectively, and placed back into the incubator for 15 minutes to stabilise (see **Figure *2-3***). ODQ is a soluble guanylate cyclase (sGC) inhibitor, whereas CPTIO is a potent nitric oxide scavenger (326). After 15 minutes of pre-treatment, columns 3 and 4 were treated with 50 µM and 100 µM sodium nitrite (from 200 mM stock constituted in distilled water), respectively. 12-well plates were then placed into a normoxic (21% O_2) or hypoxic incubator (1% O_2) for the normoxia vs. hypoxia experiments, and harvested at 24 hours (at ~80% confluence).

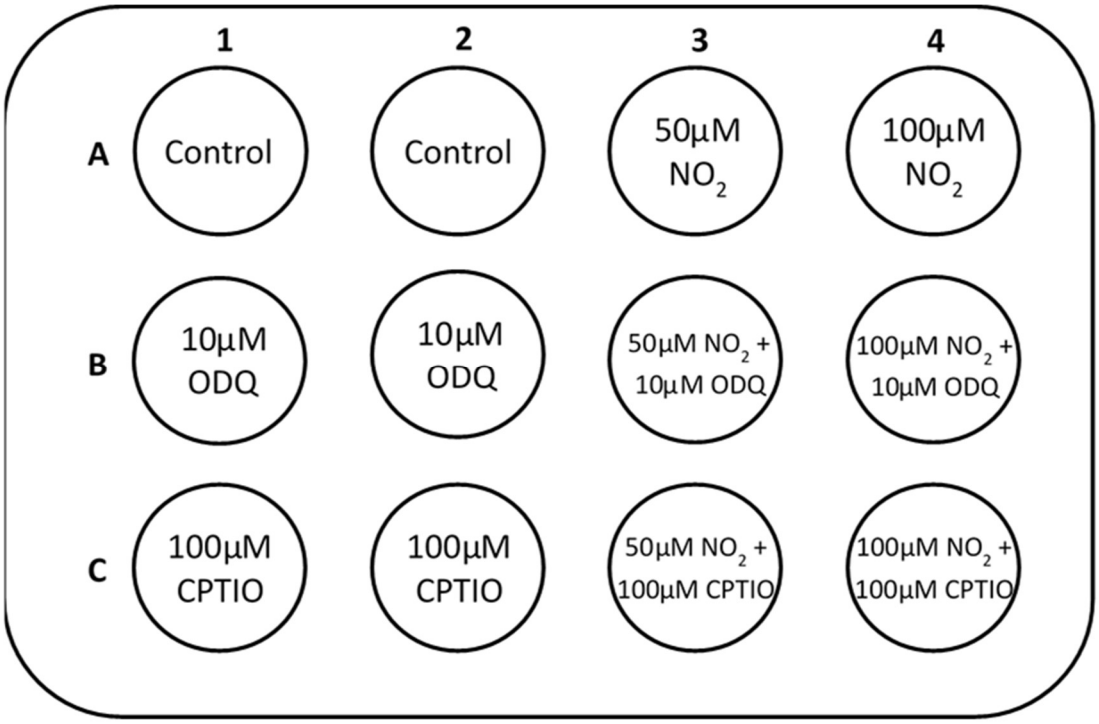

Figure 2-3: Schematic of 12-well cell culture plates used for western blotting experiments.

Experimental design for western blot studies with cells harvested at 24 hours post-treatment. 12-well plates were duplicated and placed in normoxic and hypoxic incubators for oxygen condition experiments. Note: NO_2 = (sodium) nitrite; CPTIO = 2-(4-Carboxyphenyl)-4,4,5,5-tetramethylimidazoline-1-oxyl-3-oxide; ODQ = 1H-(1,2,4)oxadiazolo[4,3-a]quinoxalin-1-one.

Adherent 786-0 cells were washed once with PBS, then detached and lysed with manual scraping, following the addition of 100 µL of lysis buffer (100 mM Tris-HCl pH 7.4, protease inhibitors [Roche, protease Inhibitors Complete EDTA free], phosphatase inhibitor cocktail [Sigma]). After chilling on ice for 15 minutes, samples were centrifuged at 4°C at 16,100 x g for a further 15 minutes, and the supernatant stored at –80°C for immunoblotting. Protein concentration was later determined via Biorad DC assay using BSA as a standard, and samples were diluted in sample buffer. SDS-PAGE was conducted at 20µg total protein per lane in 10% acrylamide gels under reducing conditions, as per the protocol for our PDH work in mice (outlined in section 2.1.1). Primary antibodies were used to detect PDH (see section 2.1.1 for details),

HIF2α (HIF2α, dilution 1:1000, Novus Biologicals), LDH (LDH, dilution 1:1000, Abcam), Akt (Akt pThr^{308}, dilution 1:1000, Abcam; Akt pSer^{473}, dilution 1:1000, Cell Signaling; Akt 1/2/3, dilution 1:1000, Abcam), and β-actin (β-actin, dilution 1:1000, Santa Cruz). HRP-conjugated anti-rabbit (dilution 1:5000, Cell Signaling) and anti-mouse (dilution 1:10000, Dako) secondary antibodies were used as appropriate.

2.1.7 Statistical Analysis

Data are expressed as either mean ± SD or mean ± SEM as stated. Differences between groups (i.e. nitrite/nitrate treatment doses, oxygen conditions, and 5-fluorouracil doses) were tested via independent Student's t test for parametric data and Mann-Whitney U test for non-parametric data. Differences in protein expression/phosphorylation status on Western Blotting and cell viability on CellTiter-Glo® assay were tested via one-way and two-way ANOVA, respectively, with appropriate *post hoc* testing. Differences in frequency between groups were tested via Chi-squared (χ^2) test.

The 'Effect of Nitrite on Cardiac Muscle and Blood Vessels in Patients Undergoing Coronary Artery Bypass Grafting Surgery' study was powered to detect a treatment difference of 20% in expression and phosphorylation status of cardiac proteins (e.g. PDH and Akt) on western blotting. Briefly, based on an assumed coefficient of variation of 20%, 14 patients would be required per group to achieve 80% power with a 2-sided α of 0.05. Statistical significance was set at $P<0.05$. GraphPad Prism version 8.4.3 or IBM SPSS Statistics version 25.0.0.1 software were used for statistical analysis.

2.2 The NICHE Trial

2.2.1 Study Design

The Nitrite In Chronic HEart failure (NICHE) Trial, was a single-centre, double-blind, randomised controlled clinical trial investigating the effects of 2-months of oral inorganic nitrate supplementation (7mmol/600mg sodium nitrate capsules taken twice daily if body weight ≥70kg or once daily if body weight <70kg) on exercise capacity in patients with heart failure with reduced ejection fraction (HFrEF) compared to matching placebo. The study was originally conceived and designed by Professor Michael Frenneaux (whilst at the University of Aberdeen) and Colleagues, to investigate the underlying mechanisms and potential therapeutic effects of nitrite in patients with cardiovascular disease. The study was approved by the Scotland A Research Ethics Committee (*Full title*: The Effects of Nitrite on cardiac and skeletal muscle: Physiology, Pharmacology and Therapeutic Potential in patients with Chronic Heart Failure; reference 12/SS/0037) and complied with the Declaration of Helsinki. Clinical trial authorisation (CTA) as a clinical trial of an investigational medicinal product (CTIMP) was also obtained from the Medicines and Healthcare products Regulatory Agency (MHRA), the competent authority in the UK (EudraCT number 2012-000788-26). The trial was placed on temporary hold in 2013 in order to source the IMP, inorganic (sodium) nitrate and placebo, which was later provided and manufactured by the Glasgow Infirmary Pharmacy Production Unit, NHS Greater Glasgow and Clyde, Scotland UK.

On Professor Frenneaux's appointment as Dean of the Norwich Medical School, University of East Anglia (UEA), in late 2014, sponsorship for the study was transferred to the Norfolk and Norwich University Hospitals (NNUH) NHS Foundation Trust, with many of the Sponsor responsibilities delegated to the Norwich Clinical Trials Unit at the UEA, as per local standard operating procedures for CTIMPs. A Trial Steering Committee was appointed to oversee the trial. An external Data and Safety

Monitoring Committee (DSMC) was appointed to advise the TSC on continuing or halting the trial based on IMP safety and efficacy data, obtained on interim analyses.

Following very substantial delays in transfer of sponsorship from the University of Aberdeen, the NNUH site was activated on 27th October 2016. Until this point we were not permitted to search the NNUH database to estimate the number of suitable patients. However, given the population drainage of the NNUH (approx. 850,000), there were no prior concerns regarding the ability to recruit. However, shortly following site activation, it was discovered that few suitable participants could be identified who fulfilled criteria on initial screening, or were willing/able to participate in the study (due to many reasons, including travel distance given the vast size of the catchment area for the NNUH) Therefore, the study was moved to the Royal Brompton Hospital (Royal Brompton and Harefield Hospitals NHS Foundation Trust, London UK), under the supervision of Professor Sanjay Prasad, and a no-cost extension was obtained from the study funder (MRC). Due to the substantial delays the UEA committed to facilitating the completion of the study, and providing funding for any shortfall associated with delayed completion. Following further delays in obtaining institutional confirmation of capability and capacity, the site was activated (N.B. the approvals process in the UK changed during this time from local site Research and Development Department approval, to a national approval by the NHS Health Research Authority [HRA], which required further submission and approval). The NICHE study was conducted at the Royal Brompton Hospital, Fulham London UK, between 17th July 2018 and 31st December 2019. Recruitment was halted by the Sponsor in October 2019. In the original study design, it was anticipated that study recruitment would take 2.5 years. Following an interim analysis, the DSMC wrote to the Sponsor to indicate that: 1) recruitment was on track; 2) the standard deviation of the primary endpoint (peak VO_2) was less than anticipated in the sample size calculations; and 3) in their view, it was inappropriate to terminate the study prematurely. The DSMC advised the Sponsor that the study should reopen, however, unfortunately, this advice was rejected and the study was closed prematurely.

2.2.2 Participant Recruitment, Selection & Randomisation

Eligible patients known to the Royal Brompton Hospital with a diagnosis of heart failure with reduced ejection fraction (HFrEF), defined as heart failure signs and symptoms with an ejection fraction ≤45% (later relaxed to <50% due to difficulties with recruitment) on transthoracic echocardiography (36), were approached by members of their treating clinical team. This usually occurred at regular clinical appointments, or via mail contact from the treating clinical team. Patients contacted by mail had previously consented to be included on a large biobank database of patients with dilated cardiomyopathy (DCM), a form of non-ischaemic HFrEF, at the Royal Brompton Hospital, and had also consented to be contacted regarding future research (327). At clinic visits, information was provided and the study discussed in detail, with ample time afforded to consider participation (>24 hours in all cases). For mail contact, a return slip was included with the provided patient information sheet (PIS) such that patients could assent to be contacted further regarding involvement in the study. Written informed consent was obtained prior to study inclusion and pre-randomisation assessment in all cases.

Inclusion criteria were age ≥18 years, a diagnosis of HFrEF defined as heart failure signs and symptoms with an ejection fraction ≤45% (later relaxed to <50% due to difficulties with recruitment) on transthoracic echocardiography or equivalent on cardiovascular magnetic resonance imaging (36), New York Heart Failure Association class II or III symptoms, on maximal tolerated standard HFrEF medication on a stable regimen for at least 6 weeks, and normal sinus rhythm. Patients were excluded on the basis of inability to provide written informed consent, HFrEF of ischaemic origin (diagnosed via cardiovascular magnetic resonance imaging or diagnostic coronary angiogram), recent (in past 3 months) hospitalisation for decompensated cardiac failure, hypotension with systolic blood pressure <90 mmHg, anaemia with a plasma haemoglobin <80 g/L, pregnancy or childbearing potential, valvular heart disease of

moderate severity or greater, or chronic peripheral vascular disease. Finally, patients with G6PD deficiency (known, or measured at screening in males of African, Asian or Mediterranean descent) were excluded from the study on the basis of an increased risk of methaemoglobinaemia with inorganic nitrate/nitrite treatment (see section 1.3.3.2.1).

Participants were individually randomised 1:1 to treatment arms via minimisation (328), using an interactive web response system (IWRS) provided by the Norwich Clinical Trials Unit (NCTU). Briefly, the number of participants already in each randomisation arm with the same value for each minimisation factor were summed, with the next patient allocated to the arm with the lower total at a probability of 75%. If the totals for each randomisation arm was equal, the arm was randomly chosen at 50% probability. Minimisation factors included those variables that were likely to have independent effects on the primary outcome, namely participant age (≥65 years vs. <65 years), BMI (≥30 kg/m^2 vs. <30 kg/m^2), and sex (male vs. female). Both the participant and study team were blinded to the drug allocation for the duration of the study.

2.2.3 Outcomes

The primary outcome of the study was the change in peak oxygen consumption (peak VO_2) on cardiopulmonary exercise (CPEX) testing from baseline visit to final visit at 2 months. Secondary outcomes included change from baseline to 2 months for the following parameters: Minnesota Living with Heart Failure Questionnaire score, six minute hall walk distance, plasma N-terminal pro B-type natriuretic peptide (NT-proBNP) level, high sensitivity C-reactive protein (hsCRP) level, fasting plasma glucose and insulin levels, plasma nitrate/nitrite/RXNO species levels, nitrated free fatty acids levels, and cardiac systolic and diastolic parameters on transthoracic echocardiography (including cardiac volumes, ejection fraction, single-beat LV end systolic elastance [Ees_{SB}], single-beat slope of the preload recruitable stroke work

relationship [SBMw], global longitudinal strain [GLS], and Doppler E/E'). Initially, measurement of cardiac and skeletal muscle energetic status on ^{31}P cardiovascular and skeletal magnetic resonance spectroscopy (^{31}P CMRS) was planned as a secondary outcome in a subgroup of participants as previously performed in patients with DCM by our group (329). Unfortunately, ^{31}P CMRS could not be established at the new RBH site, and was therefore established at the MRC London Institute of Medical Sciences (LMS), at the Hammersmith Hospital campus, under Dr Declan O'Regan as the site Principal Investigator. Unfortunately, patients declined the extra study visit to complete the ^{31}P CMRS. Similarly, skeletal muscle biopsy of the *vastus lateralis* muscle belly was planned in a subgroup of participants to assess the effects of 2 months of inorganic (sodium) nitrate on fibre type, metabolic enzyme expression/activity, and proteomics compared to baseline (330-332). However, given the already full screening/first study visit and the need for many participants to travel long distances to London for the study visit, participants declined the muscle biopsy at the time of consent.

2.2.4 Procedures

Participants presented to the Royal Brompton Hospital for their combined screening/first study visit. Participants were asked to avoid caffeine for 24 hours prior to the study visit, and to avoid nitrate/nitrite rich foods such as beetroot, lettuce etc (list provided in PIS) for 3 days prior to the study visit. Study information was re-visited and discussed again in detail. Written informed consent was confirmed, or where not already completed, obtained, and a copy of the consent form was provided to the participant. Safety bloods (full blood count [FBE], urea electrolytes & creatinine [UEC], fasting serum glucose, and liver function tests [LFTs]) were then collected and sent to the RBH Pathology Laboratory.

Fasting study bloods, including fasting insulin, NT-proBNP, and hsCRP, were also collected and immediately centrifuged at 16,100 x g at 4°C for 10 minutes, and plasma

was snap-frozen in liquid nitrogen and stored at –80°C for future analysis at the University of East Anglia. Participants then completed the Minnesota Living with Heart Failure Questionnaire (scored out of 105) and a six-minute hall walk distance test (333). The Minnesota Living with Heart Failure Questionnaire score employs a Likert scale from 0-5 (5 being most-affected) over 21 questions to assess the subjective detrimental effects of HFrEF on different aspects of a patient's quality of life, and is well-validated in HFrEF clinical trials (334). Participants then broke their fast with a nitrate/nitrite-deplete lunch and rested before the remaining screening/visit 1 study tests. Participants were then randomised via the IWRS at the end of the first study visit, and supplied with labelled medications by the hospital pharmacy. Participants were encouraged to contact the study team in the event of any issues with taking the study medication, and were provided with a 24/7 contact phone number for study team medical staff.

Participants were contacted via telephone at 4 weeks following commencement of the study IMP or placebo to check progress and record/identify any adverse reactions. Participants then returned at 2 months for the second/final study visit, which involved repeating the interventions from the first study visit.

2.2.4.1 Cardiopulmonary Exercise Testing

Following bedside spirometry, participants underwent symptom-limited cardiopulmonary exercise (CPEX) testing using a cycle ergometer employing either a 10W or 15W protocol, based on perceived exercise tolerance at the first study visit to achieve an exercise time of 10-15 minutes (335). Standard measurements were recorded including total exercise time, peak oxygen consumption (peak VO_2), anaerobic threshold, and minute ventilation/carbon dioxide production (VE/VCO_2) slope. Given issues with underestimation of predicted peak VO_2 by historical equations (336), predicted peak VO_2 was calculated using an updated equation from a recent meta-analysis to improve accuracy (337). The respiratory exchange ratio

(RER) was automatically calculated from the ratio of CO_2 output to O_2 uptake. Participants were excluded from the study if peak VO_2 was >75% of the predicted for age and gender (not truly limited), or the RER was <1.0 at the conclusion of the test, as this indicates an inadequate exertional effort as the anaerobic threshold was not reached (338).

2.2.4.2 Transthoracic Echocardiography

Transthoracic echocardiography was performed by the same operator where possible, using a commercially available system (iE33, Phillips Healthcare) with a 3.5 MHz transducer. All cardiac volumes were indexed to body surface area (BSA) and non-invasive brachial blood pressure was derived via sphygmomanometer at the conclusion of the echocardiogram in all participants. Left ventricular and left atrial volumes (biplane) were traced manually at end-diastole and end-systole in apical 4- and 2-chamber views. LV ejection fraction was calculated using the modified Simpson's biplane method (339). Stroke volume was calculated from the LV outflow tract (LVOT) velocity time integral (VTI) obtained in the apical 5-chamber view, and the LVOT cross-sectional area (CSA) calculated from the LVOT diameter using the formula for the area of a circle (340). LV end-diastolic volume (LVEDV) was calculated from SV/EF. LV mass was calculated as previously reported (341). Valvular function was assessed as per society guidelines (342,343) to exclude moderate or greater severity valvular heart disease. Diastolic parameters including early (E) and late (A) mitral diastolic velocities, E/A ratio, and mitral deceleration time were assessed. Tissue Doppler imaging was performed in the apical 4-chamber view for peak systolic (S') and early diastolic (E') velocities of the medial and lateral mitral annulus. Medial, lateral, and mean E/E' were then calculated. LV end-diastolic pressure (LVEDP) was estimated from E/E' by the formula = 11.96 + (0.596 x E/E') (344). Tricuspid annular plane systolic excursion (TAPSE) and right ventricular (RV) S' velocity were recorded on tissue Doppler imaging as measures of RV function (345). Right ventricular systolic pressure was estimated from the maximum velocity of the tricuspid regurgitant (TR)

jet (where possible), added to an assumed right atrial pressure based on collapsibility assessment of the inferior vena cava.

Speckle tracking echocardiography (STE) was performed in order to assess LV contractile function across three planes (see **Figure *2-4***). Additional LV contractile parameters were also calculated, including LV end-systolic elastance (Ees_{SB}) and slope of the preload recruitable stroke work relationship (SBMw). Global longitudinal strain was calculated from STE images using automated cardiac motion quantification ($aCMQ^{A.I.}$) software (QLAB 10.0, iE33, Phillips Healthcare) (346). As example is shown in **Figure *2-5***. Sector size and depth were adjusted to achieve visualisation at an optimal (highest possible) frame rate of at least 80 fps. A single-beat method was used to determine Ees on TTE (Ees_{SB}), which was calculated from BP, end-systolic pressure (ESP = 0.9 x SBP), SV, EF and pre-ejection and systolic ejection time intervals as previously described (347). The related measure of arterial elastance (Ea) was calculated from ESP/SV (347). The ratio of Ea/Ees was also calculated as a measure of ventricular-arterial coupling. A single-beat method was used to determine Mw on TTE (SBMw), which was calculated from SV, mean BP, LV mass, and LVEDV as previously described (348).

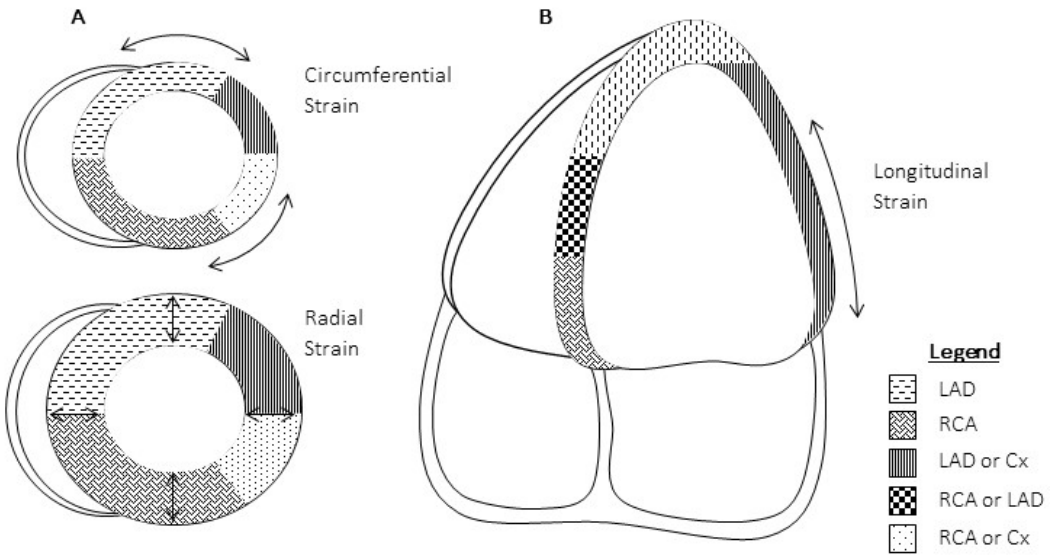

Figure 2-4: The three planes of left ventricular motion for calculating strain and corresponding coronary artery territories in a right-dominant system.
Speckle tracking echocardiography allows for tracking of the myocardium throughout the cardiac cycle. Left ventricular motion can be tracked in the circumferential (twist and untwist) and radial (thickening and thinning) planes (**A**), and longitudinal (lengthening and shortening) plane (**B**). Coronary artery supply territories for a right-dominant coronary artery system are overlaid (see legend). Note: Cx = circumflex artery, LAD = left anterior descending artery, RCA right coronary artery.

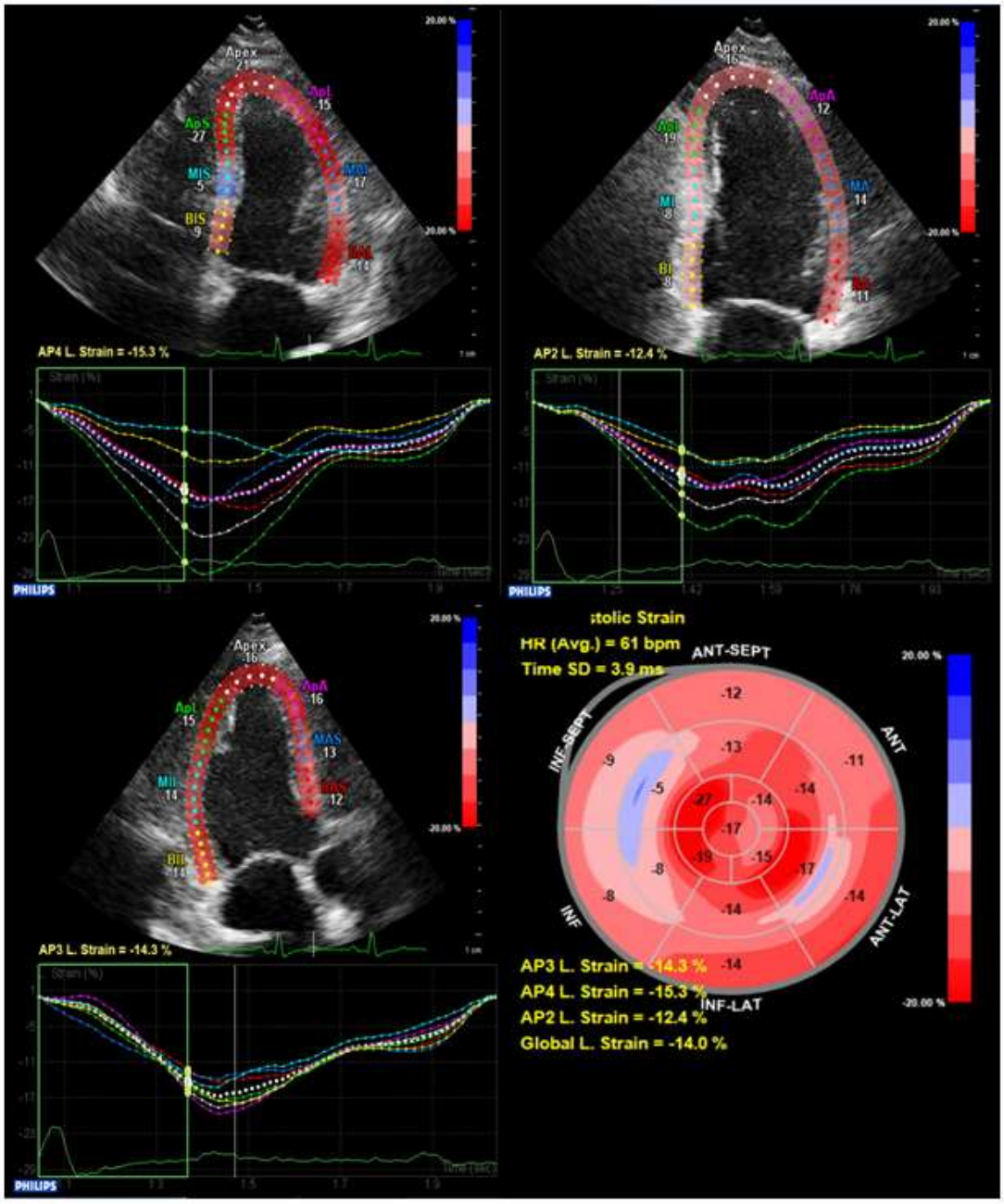

Figure 2-5: Reduced global longitudinal strain in a patient from the NICHE study. Global longitudinal strain (GLS) calculated by speckle tracking echocardiography (STE) in a patient from the NICHE study. Using the 17-segment model of the left ventricle, strain (%) is averaged across all segments in the 3 apical views to give the GLS. The GLS is -14% in this patient, which is reduced (more positive) compared to a normal value of less than -18%.

2.2.4.3 Analysis of Study Blood Tests

Plasma samples from the baseline and 2-month visits were shipped on dry ice to the University of East Anglia for analysis of fasting plasma insulin, NT-proBNP, hsCRP, and nitrated free fatty acids. Plasma samples were also sent to the University of Southampton for analysis of nitrate/nitrite levels (see section 2.1.3 for details).

2.2.5 Statistical Analysis

Data are expressed as either mean ± SD or mean ± SEM as stated. Differences between groups were tested via independent Student's t test for parametric data and Mann-Whitney U test for non-parametric data. Differences in frequency between groups were tested via Fisher's exact test given the sample size of the final number of patients recruited. GraphPad Prism version 7.01 or IBM SPSS Statistics version 25.0.0.1 software were used for statistical analysis. Based on the results of a previous study undertaken in a similar patient cohort (349) a parallel group study of 56 patients has an 80% power to detect a treatment difference of 1.5 ml/kg/min increase in peak VO_2 (the primary endpoint) with a standard deviation of 2 ml/kg/min (317) at a two-sided significance level of 0.05. We aimed to recruit a maximum of 70 patients in order to achieve 56 patients completing the primary end point in order to allow for a maximum dropout of 20%, which was deemed a necessary concession given the intervention-rich visit days proposed.

Chapter 3: Effects of Nitrite on Protein Expression in the Myocardium

3.1 Abstract

Background: Interventions that increase plasma nitrite result in alterations in cardiac metabolism, contractile function, and redox stress. We have recently described a novel redox mechanism for nitrite-mediated resistance vessel vasodilatation via cGMP-dependent protein kinase 1α (PKG1α) oxidative homodimer formation, which occurs several hours after administration of a single i.p. dose in mice, persists for approximately 24 hours, and causes delayed and sustained reductions in blood pressure. Similarly, unpublished data from our group have also demonstrated dephosphorylation of the pyruvate dehydrogenase (PDH) complex following nitrate therapy, which may increase PDH activity (a key metabolic protein). Whether these effects occurs in the myocardium following inorganic nitrate/nitrite administration is unknown.

Methods: Isolated hearts from healthy C57BL/6 wild-type (i.e. PKG1α wild-type) mice, supplemented with sodium nitrite (1g/L in drinking water for 7 days) and sodium chloride (control), were assessed for PKG1α dimer-content and PDH expression and phosphorylation status via western blotting. In a separate experiment, hearts from healthy C57BL/6 mice, treated with varying doses of intraperitoneal (i.p.) sodium nitrite or normal saline (0.9%) control at 24 hours prior to harvest, were analysed for reactive persulfide levels. Left ventricular biopsies from thirty-five patients (male %, mean age years) enrolled in Part 1 of the 'Effect of Nitrite on Cardiac Muscle and Blood Vessels in Patients Undergoing Coronary Artery Bypass Grafting Surgery' study, treated with either intravenous sodium nitrite therapy (10μmol/min for 30 minutes) or normal saline (0.9%) placebo administered 24 hours before surgery, were similarly assessed.

Results: In mice, oral sodium nitrite supplementation did not increase PKG1α dimer-content in the myocardium. Similarly, myocardial reactive persulfide levels following a single i.p. dose of sodium nitrite, were not elevated. In humans, myocardial PKG1α

dimer-content was higher in diabetics than non-diabetics, implying greater oxidative stress, and intravenous sodium nitrite therapy at 24 hours prior to sample collection resulted in a statistically significant decrease in PKG1α dimer-content compared to matching placebo in the diabetic group (P=0.01). There was also a strong trend (P=0.06) towards reduced PKG1α dimer content following nitrite therapy in non-diabetic patients. Nitrite supplementation in mice resulted in dephosphorylation of myocardial PDH at serines 232 and 300, which was not seen in the control group. However, this did not translate to increased cardiac PDH activity in the nitrite group compared to control, and this finding was not replicated in humans 24 hours following intravenous sodium nitrite therapy.

Conclusions: In contrast to our previous findings in the vasculature, nitrite caused a reduction in PKG1α oxidative dimer formation in the myocardium. This was most profound in cardiac samples from patients with type 2 diabetes mellitus, a pro-inflammatory state. Inorganic nitrate and nitrite dephosphorylated serine 232, and serines 232 and 300, respectively, of myocardial PDH in mice, but this did not translate into increased PDH activity.

Clinical Trials Registration: Effect of Nitrite on Cardiac Muscle and Blood Vessels in Patients Undergoing Coronary Artery Bypass Grafting Surgery (clinicaltrials.gov identifier: NCT04001283).

3.2 Introduction

Nitric oxide (NO) deficiency is a key feature of cardiovascular disease (9). Plasma nitrite represents a NO storage pool that can be liberated in tissues when reduced under hypoxic conditions in the presence of multiple nitrite reductases (16). There is also evidence that nitrite may work more directly without reduction to NO (i.e. independently of NO), such as via S-nitrosylation of cellular proteins (12). Whilst there are issues with oral nitrite supplementation, such as gastrointestinal inflammation and risk of cancer (216,217), oral inorganic nitrate is safe (substantial inorganic nitrate is present in the healthy Mediterranean diet) and results in a robust elevation in plasma nitrite levels in man (16). Using a proteomics approach, Perlman et al. showed that a single intraperitoneal (i.p.) dose of nitrite in rats resulted in alterations in numerous proteins that are involved in cardiac metabolism, contractile function, and redox stress (297). Cyclic GMP (guanosine 3',5'-monophosphate)-activated protein kinase or Protein kinase G (PKG) 1 alpha is a key secondary messenger protein in the cardiovascular system. Activation of PKG1α by cGMP and its phosphorylation of downstream proteins transduces the effects of NO signalling, including vasodilatation, and inhibition of platelet aggregation and of vascular smooth muscle cell proliferation (6). More recently, an alternative mechanism for PKG1α activation has been described, involving oxidation of a thiol residue/oxidant sensor within cysteine 42 of the monomer resulting in homodimer formation (282). The dimer has been shown to phosphorylate many of the same protein residues as the monomer (294), with near-identical cardiovascular effects. The most thoroughly investigated of these is oxidative dimer-mediated vasodilatation, which has important potential in the management of hypertension (280).

Nitrite has long been observed to cause vasodilatation under normoxic conditions as well (albeit to a lesser degree), however the mechanism has not been fully elucidated. As the rate of liberation of NO from nitrite by nitrite reductases is very slow in normoxia, the mechanism is most likely NO-independent. Recently, a group from

King's College London showed that (intravenous) sodium nitrite is more selective for conduit artery vasodilatation in normoxia in man, and that this is associated with increases in cGMP and, interestingly, enhanced by concomitant acetazolamide and raloxifene therapy (204). However, normoxic resistance vessel vasodilatation following inorganic nitrate or nitrite therapy has also been demonstrated. Our group recently posited a novel NO-independent mechanism whereby oxidative activation of PKG1α by nitrite in normoxia causes long-lasting resistance vessel dilatation (292). Whether this occurs in the myocardium is unknown. We therefore sought to investigate whether nitrite administration increased myocardial PKG1α dimer content in mice and human myocardial samples (**Figure *3-1***).

NO also has well-documented effects on cardiac metabolism including an important role in maintaining substrate utilisation, such that broad NOS-inhibition in healthy canine hearts causes a switch from primarily utilising free fatty acids to lactate and glucose, an effect that was reversed by a NO donor (350). Key mediators of this metabolic switch could include the pyruvate dehydrogenase (PDH) complex (the rate-limiting enzyme for glucose oxidation) (351), the phosphofructokinase (PFK) enzyme (the rate-limiting step for glycolysis) (147), and the peroxisome proliferator-activated receptor alpha (PPARα) transcriptional factor (the key regulator of β-oxidation enzymes) (156). Whether nitrite may have similar effects on metabolism is unknown. The effects of inorganic nitrate/nitrite on PPARα have been investigated elsewhere. Briefly, inorganic nitrate reversed the switch away from fatty acid oxidation in cardiac tissue from hypoxia-treated wild-type mice, but not mice that were PPARα null, indicating a PPARα-dependent effect (352). Unpublished data in mice (small numbers) from our group (PhD thesis, Dr Konstantin Schwarz, University of Aberdeen), have previously shown a dephosphorylation of PDH with inorganic (sodium) nitrate supplementation (1g/L drinking water), and an increase in PDH activity with sodium nitrite supplementation. We therefore wished to confirm the effects of inorganic nitrate and nitrite on PDH expression, phosphorylation status,

and activity in mice. Finally, we sought to investigate whether these findings are present in human cardiac samples obtained in the clinical setting (**Figure *3-1***).

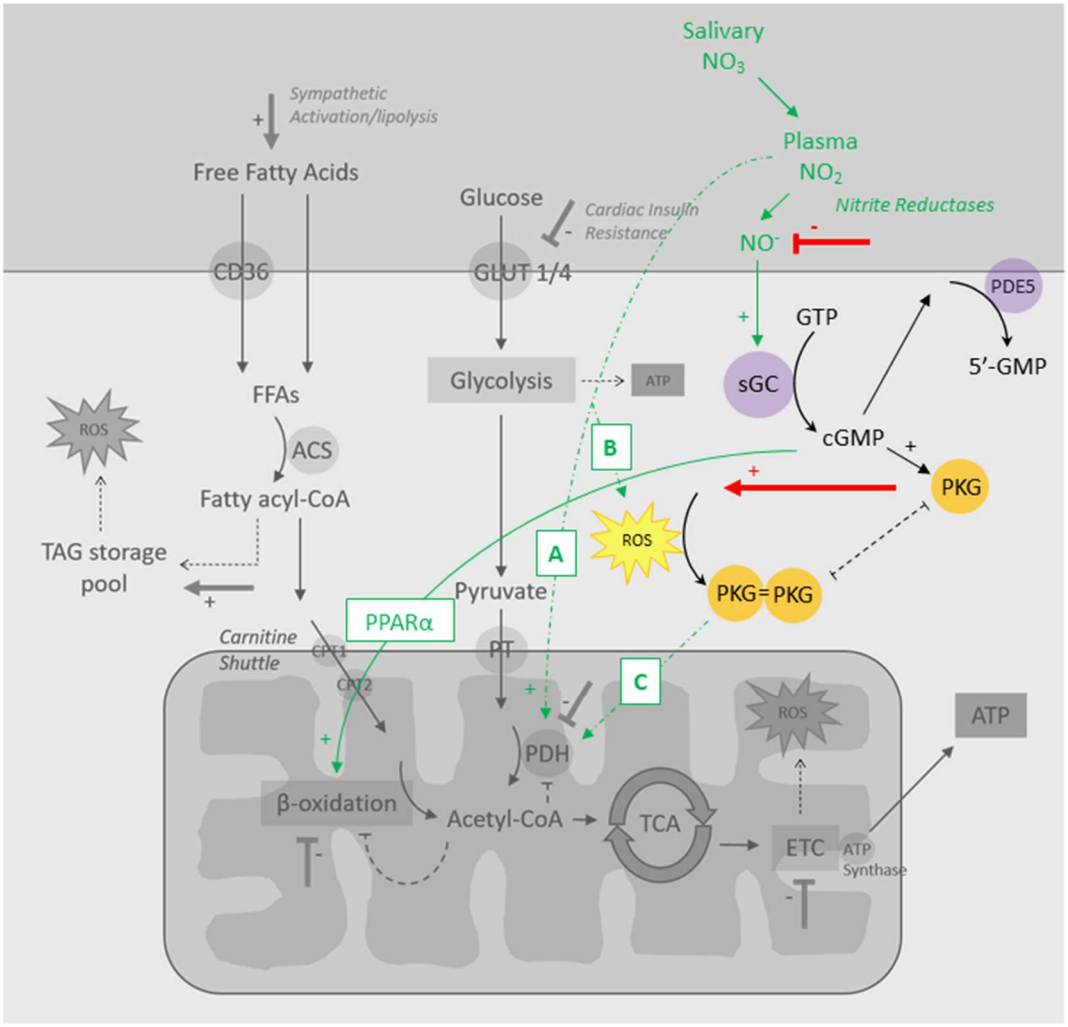

Figure 3-1: Possible Mechanisms for the Effects of Oral Inorganic Nitrate and Nitrite on Cardiac Metabolism and PKG1α Oxidative Dimer Formation.
The Nitrate-Nitrite-NO pathway supplements the nitric oxide (NO) pool available at the level of the tissues, but its effects on metabolism are unknown. The canonical NO-sGC-cGMP pathway increases fatty acid metabolism (beta-oxidation) via a mechanism involving PPARα (green arrow). Heart failure is associated with a deficiency in NO and an increase in oxidative PKG1α dimer formation via an increase in ROS (red arrow). Nitrite may also have an effect on PDH: whether this occurs directly (**A**), or via an alternative mechanism such as an increase in ROS (**B**) with oxidative PKG1α dimer formation (**C**), is not known. ACS, acyl-CoA synthetase; ATP, adenosine triphosphate; CD36, fatty acid translocase; CoQ10, co-enzyme Q10; cGMP, cyclic guanosine monophosphate; CPT, carnitine palmitoyltransferase; ETC, electron transport chain; FFA, free fatty acid; GIK, glucose, insulin, potassium; GLUT, glucose

transporter; 5'-GMP, guanosine monophosphate; NO, nitric oxide; NO_2, nitrite; NO_3, nitrate; PDE5, phosphodiesterase 5; PDH, pyruvate dehydrogenase; PKG, protein kinase G; PPARα, peroxisome proliferator-activated receptor alpha; PT, pyruvate translocase; ROS, reactive oxygen species; sGC, soluble guanylate cyclase; TCA cycle, tricarboxylic acid cycle.

3.3 Methods

The methods using in this study are detailed in section 2.1. Briefly, male C57BL/6 mice, aged between 3-5 months, were used for the PDH studies. After an acclimatisation period of 2 weeks, mice were commenced on a nitrate/nitrite-deplete diet for a further 2 weeks. Sodium nitrite, sodium nitrate, or sodium chloride (allocated 1:1:1) was added to the drinking water of each age- and body-weight-matched group at a concentration of 1g/L for 7 days. Drinking water was available *ad libitum*. For the PKG1α studies, male wild-type C57BL/6 (i.e. $PKG1\alpha^{WT}$) mice, bred and maintained in-house at the University of Birmingham, were used. All procedures were performed in accordance with the Home Office Guidance on the Operation of the United Kingdom Animals (Scientific Procedures) Act 1986. Protocols and procedures for the study were also reviewed and approved by the Institutional Animal Welfare and Ethical Review Body. Mice were killed by cervical dislocation, and hearts harvested. Mouse hearts were snap-frozen in liquid nitrogen, then stored at −80°C for western blotting of myocardial PKG1α dimer content, and PDH expression, phosphorylation status (see section 2.1.1). Additionally, hearts harvested from a separate group of mice administered either saline or sodium nitrate in drinking water were immediately snap-frozen using tissue forceps and sent to the University of Nottingham for direct measurement of cardiac PDH activity (see section 2.1.2). Plasma samples were sent to the University of Southampton for analysis of nitrate/nitrite levels (see section 2.1.3).

Human Studies:

Left ventricular (LV) myocardial biopsies and plasma samples obtained from participants in the 'Effect of Nitrite on Cardiac Muscle and Blood Vessels in Patients Undergoing Coronary Artery Bypass Grafting Surgery' study (clinicaltrials.gov identifier NCT04001283) were analysed. This was a randomised, placebo-controlled, double-blind clinical trial investigating the effects of sodium nitrite infusion on cardiac and skeletal muscle at a molecular level. In order to investigate effects on metabolic proteins, a pre-specified analysis of patients grouped by diabetic status was planned. This study was approved by the North Scotland Research Ethics Committee (reference 11/NS/0059), and complied with the Declaration of Helsinki. Part 1 of this study involved treatment at 24 hours prior to sample collection, with LV biopsies taken immediately prior to aortic cross-clamp, and was conducted by Dr Konstantin Schwarz at the Royal Infirmary, Aberdeen, Scotland UK, under the supervision of Professor Michael Frenneaux, between 21st January 2013 and 31st December 2014. Samples were analysed via western blotting of myocardial PKG1α dimer content, and PDH expression, phosphorylation status (see section 2.1.1). Plasma samples were sent to the University of Southampton for analysis of nitrate/nitrite levels (see section 2.1.3).

3.4 Results

Plasma Nitrate and Nitrite Levels

Mouse Studies

There were 10-13 mice in each intervention group (sodium nitrite, sodium nitrate, and sodium chloride). Compared to control (sodium chloride), both inorganic (sodium) nitrate ($P<0.0001$) and sodium nitrite ($P<0.05$) supplementation (1g/L drinking water for 7 days) increased plasma nitrate levels (see **Figure 3-2**). Sodium nitrite increased plasma nitrite levels compared to control and this was statistically significant ($P<0.05$). There was also an increase in plasma nitrite levels with inorganic (sodium) nitrate, but this was not statistically significant, despite a trend towards significance ($P=0.09$).

Human Samples

Patient baseline demographics data are shown in Table 3-1 (n=35). There were no statistically significant differences in baseline demographics, haemodynamics, comorbidities or drug therapy between treatment groups. Following sodium nitrite infusion (10 μmol/min for 30 minutes), plasma nitrate levels were significantly elevated immediately post-infusion, and at 6 hours post-infusion, compared to baseline ($P<0.01$). Plasma nitrite levels were elevated at 6 hours post-infusion ($P<0.01$), before returning to baseline levels (**Figure 3-3**). Whilst plasma nitrite levels were elevated to a similar extent post-infusion in patients with diabetes vs. those without diabetes (**Figure 3-2, B**), plasma nitrate levels at 6 hours post-infusion were greater in the diabetic group (**Figure 3-2, D**).

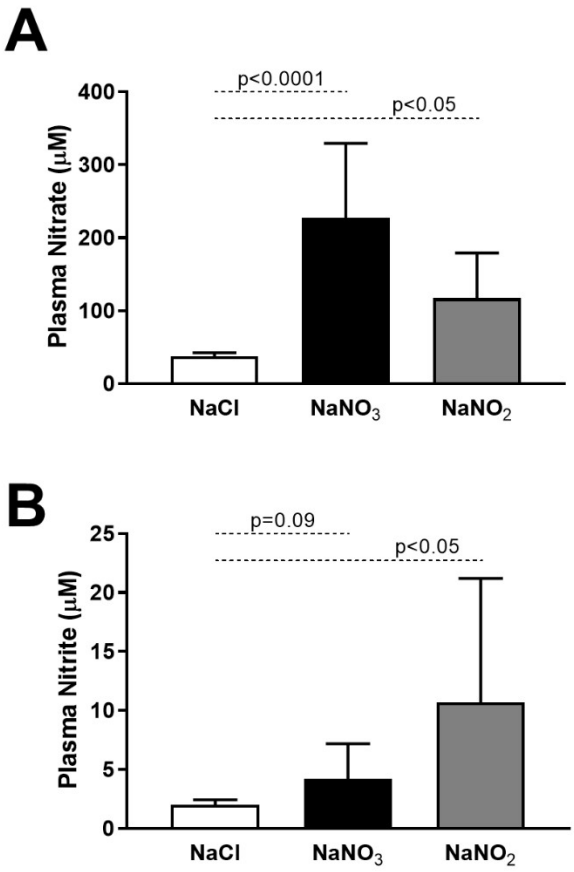

Figure 3-2: Plasma Nitrite and Nitrate Levels in mice following supplementation with oral sodium nitrate or sodium nitrite (1g/L in drinking water) for 7 days.
A; Plasma nitrate concentrations in mice supplemented with sodium nitrate (n=10-13 per group) and sodium nitrite (n=6 per group) increased significantly compared to sodium chloride (P<0.0001 and P<0.05, respectively). **B**; There was a trend towards increased plasma nitrite concentrations in mice supplemented with sodium nitrate compared to sodium chloride (P=0.09). In mice supplemented with sodium nitrite, plasma nitrite concentrations were significantly increased compared to sodium chloride (P<0.05).

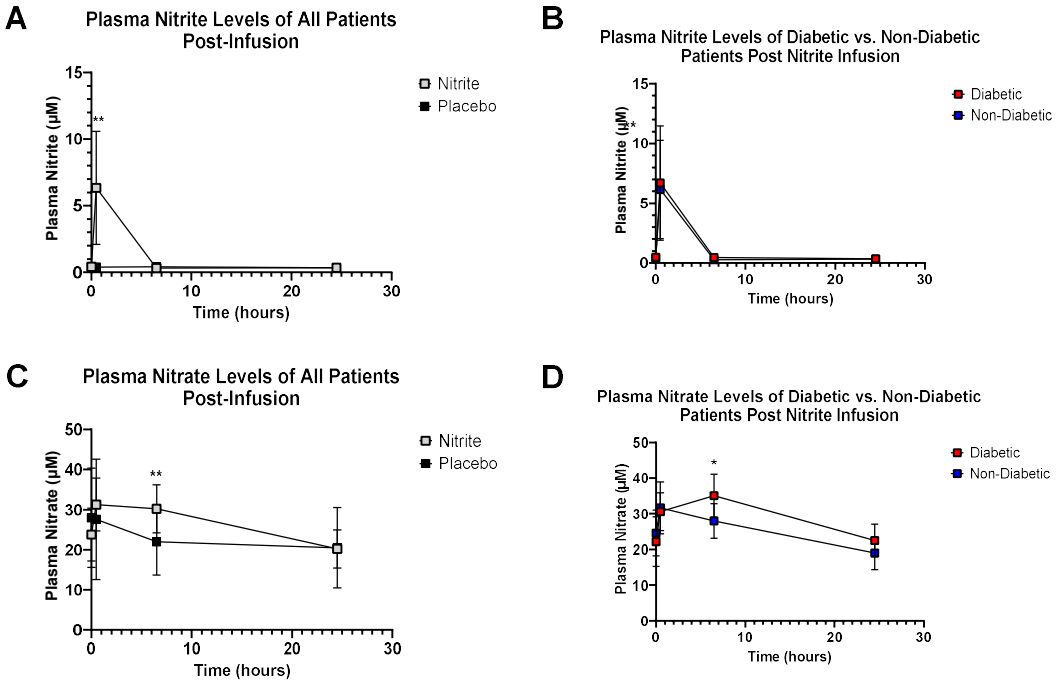

Figure 3-3: Plasma concentrations of nitrate and nitrite in humans over time following a 30-minute infusion of sodium nitrite (10 µmol/min) or normal saline placebo.

A; Plasma nitrite concentrations were significantly increased immediately post-infusion in patients receiving intravenous sodium nitrite compared to those receiving placebo ($F[1,32]=27.342$, $P<0.01$). **B**; This difference remained significant regardless of diabetes status and there was no difference between groups. **C**; Plasma nitrate concentrations were significantly increased 6 hours post-infusion in patients receiving intravenous sodium nitrite compared to those receiving placebo ($F[1,18]=9.44$, $P<0.01$). **D**; However, when grouped by diabetes status, patients with diabetes had a significantly greater increase in plasma nitrate than non-diabetic patients ($P<0.05$). **$P<0.01$, *$P<0.05$.

Disulfide Dimerisation of Protein Kinase G 1 Alpha

Mouse Studies

PKG1α dimer content increased slightly with nitrate treatment, but this was not statistically significant ($P=0.44$; **Figure 3-3**).

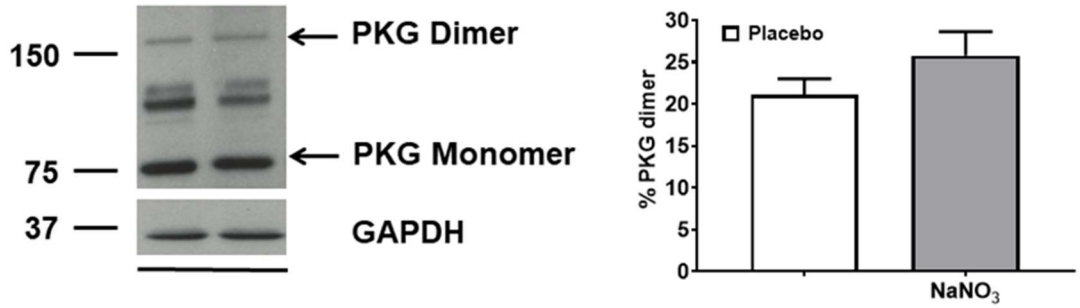

Figure 3-4: PKG1α Dimer Content in Mouse Cardiac Tissue with Oral Nitrate Supplementation.
PKG1α dimer content increased slightly with nitrate treatment, but this was not statistically significant (P=0.44).

Reactive Persulfide Levels

Preliminary data (supplied with permission by Dr Melanie Madhani with thanks) showed that reactive persulfide levels were not elevated in murine cardiac samples following varying doses of sodium nitrite (0, 0.1, 1, 10 mg/kg) at 24 hours prior to sample collection compared to saline control (**Figure 3-4**).

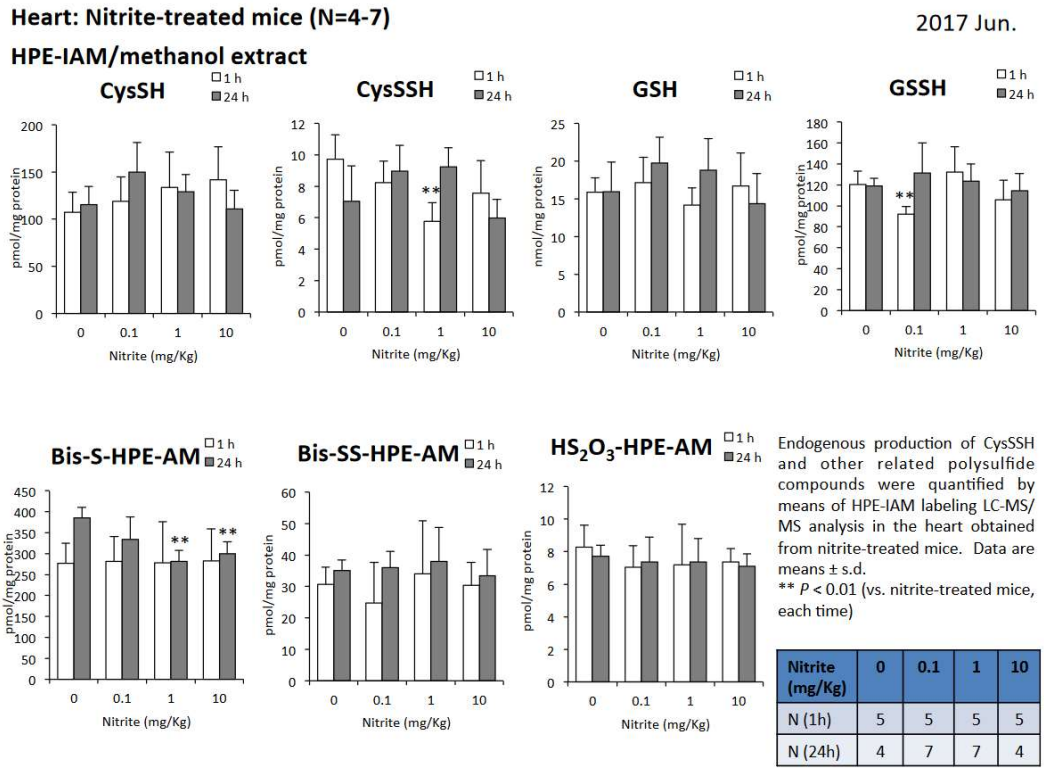

Nitrite (mg/Kg)	0	0.1	1	10
N (1h)	5	5	5	5
N (24h)	4	7	7	4

Figure 3-5: Reactive Persulfide Levels in Cardiac Samples of Mice Treated with I.p. Sodium Nitrite.

Reactive persulfide levels were not elevated in murine cardiac samples following varying doses of sodium nitrite (0, 0.1, 1, 10 mg/kg) at 24 hours prior to sample collection compared to saline control.

Human Samples

In the control group (n=15), patients with type 2 diabetes mellitus (n=5) had higher PKG1α dimer content (as a percentage of total PKG1α) than patients without diabetes (n=10) and this was statistically significant (37 ± 11.2 % vs. 20.1 ± 8.2 %, P=0.009; **Figure 3-6, A**). In all patients (n=35), sodium nitrite infusion (10μmol/min for 30 minutes, n=20) administered 24 hours prior to sample collection resulted in a statistically significant decrease in oxidative dimer expression compared to normal saline placebo (n=15; 15.6 ± 8.2 % vs. 24.3 ± 11.4 %, P=0.01; **Figure 3-6, B**). In the pre-specified analysis of patients by diabetic-status, samples from patients with diabetes showed a reduction in oxidative dimer content following nitrite treatment compared to placebo, and this was statistically significant (–16.3%, P=0.01; **Figure 3-6, C**), whereas the reduction in oxidative dimer content in non-diabetics was not statistically significant, despite a strong trend (–7%, P=0.06; **Figure 3-6, D**). Example blots are shown in **Figure 3-7**.

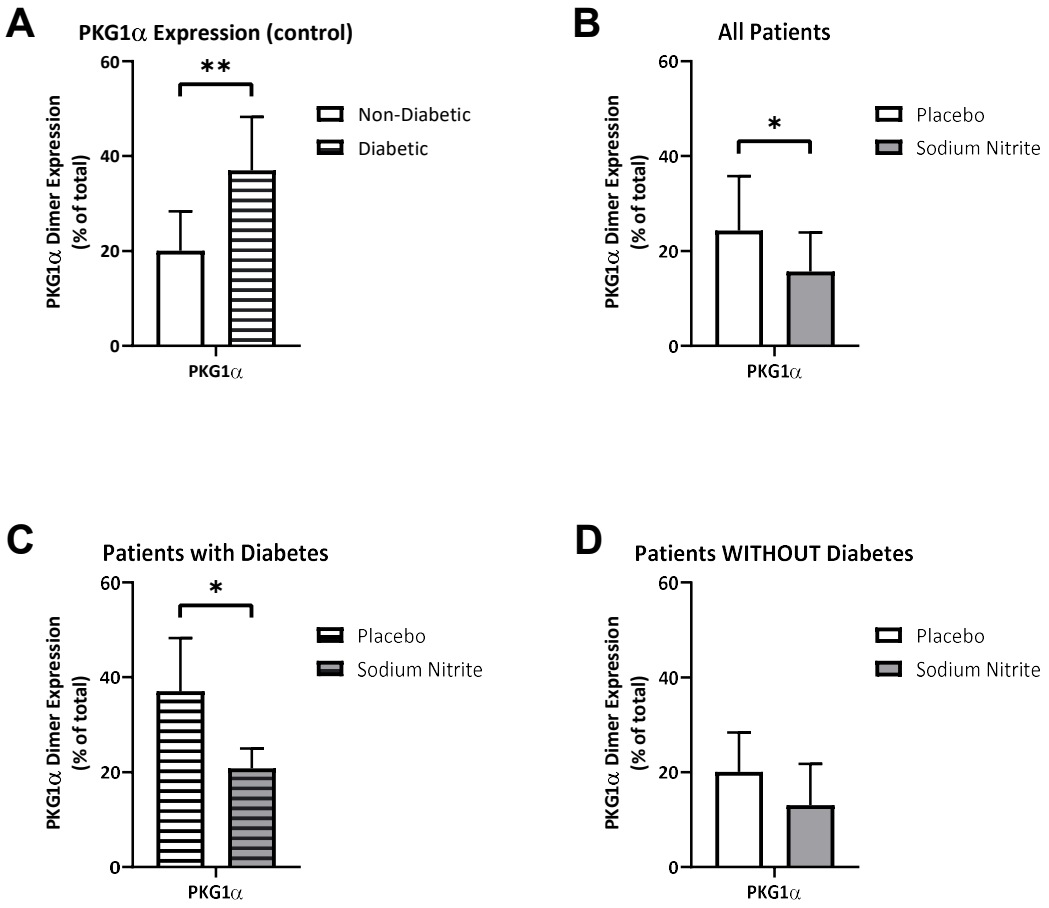

Figure 3-6: Effect of Type 2 Diabetes and Nitrite Treatment on PKG1α expression in Human LV Myocardium.

A, In patients with diabetes, expression of the PKG1α oxidative homodimer (as % of total) was significantly greater than in patients without diabetes (P=0.009). **B**, Sodium nitrite infusion (10µmol/min) resulted in a statistically significant decrease in oxidative dimer expression compared to matching normal saline placebo (P=0.01). **C**, In patients with type 2 diabetes mellitus, there was a statistically significant reduction in oxidative dimer expression following nitrite infusion at 24hours prior to LV biopsy collection, compared to placebo (P=0.01). **D**, In patients without type 2 diabetes mellitus, there was a strong trend towards a statistically significant reduction in oxidative dimer expression following nitrite infusion at 24hours prior to LV biopsy collection, compared to placebo (P=0.06). Note: *P<0.05.

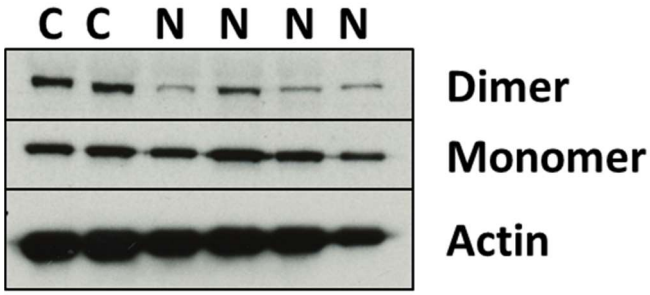

Figure 3-7: Example Blot for PKG1a Dimer Expression in Human Myocardium.
Example blot for PKG1α in human left ventricular myocardium. PKG1α disulfide dimer quantity was defined as a percentage of total PKG1α expression. Disulfide dimer % = (intensity of dimer band/the sum of the intensity of both the monomer and dimer bands) x 100. Note: C = control, N = (sodium) nitrite.

Pyruvate Dehydrogenase (PDH) Expression and Phosphorylation Status

Mouse Studies

Compared to sodium chloride control, inorganic (sodium) nitrate supplementation (1g/L of drinking water for 7 days) resulted in a statistically significant dephosphorylation at serine 232 (n=10 per group; P<0.001), but not at serines 293 or 300 in murine myocardium (see **Figure 3-8**). Total PDH expression was not affected by inorganic (sodium) nitrate supplementation. Sodium nitrite supplementation (1g/L of drinking water for 7 days), compared to control, similarly resulted in dephosphorylation of serine 232 of the PDH complex in murine myocardium (P<0.01), but also serine 300 (P<0.001) (see **Figure 3-9**). Phosphorylation status at serine 293 and total PDH expression were unchanged by sodium nitrite supplementation.

PDH complex activity, measured as acetyl coenzyme A accumulation following addition of labelled oxaloacetate (n=10 per group), was unchanged following sodium nitrite supplementation (1g/L drinking water for 7 days) compared to control (19.9 ± 1.1 vs. 19.2 ± 2.3 mmol/min/mg protein; P=0.40; **Figure 3-10**).

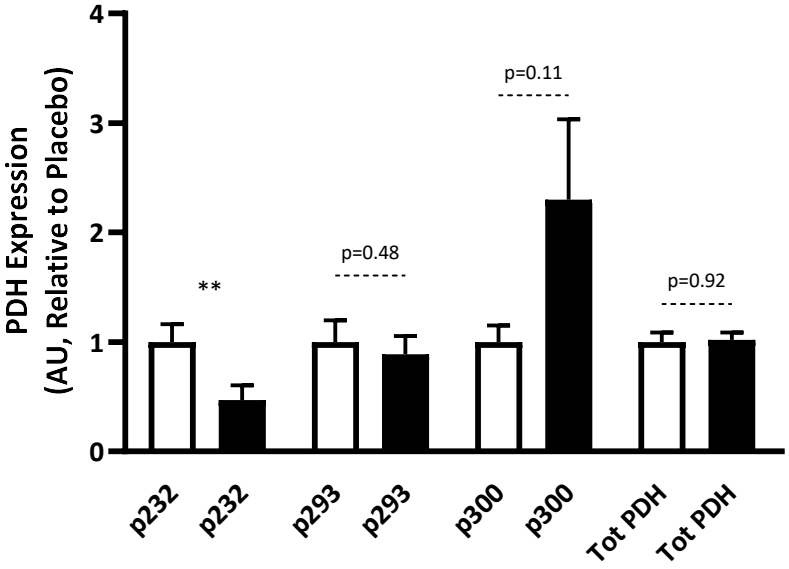

Figure 3-8: Expression and phosphorylation status of PDH in mouse cardiac muscle in response to oral inorganic (sodium) nitrate supplementation.

Oral inorganic (sodium) nitrate supplementation resulted in de-phosphorylation of serine 232 of the PDH complex compared to placebo (normalised to vinculin) in cardiac muscle in mice (n=10 per group). Note: **P<0.001, compared to placebo. Note: □ = NaCl, ■ = $NaNO_3$.

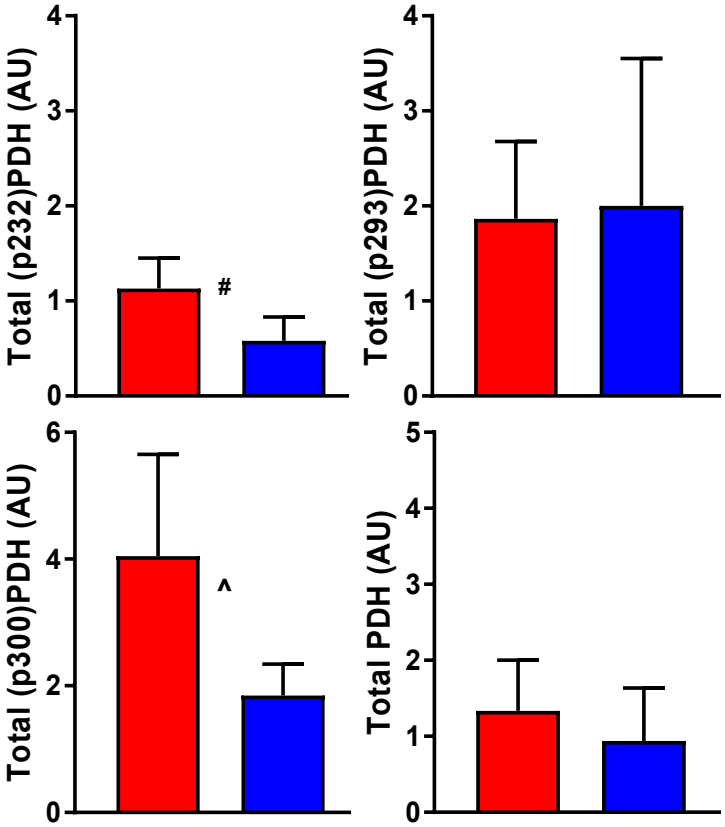

Figure 3-9: Expression and phosphorylation status of PDH in mouse cardiac muscle in response to sodium nitrite supplementation.

Sodium nitrite supplementation, compared to sodium chloride (normalised to vinculin), resulted in de-phosphorylation of serines 232 and 300 of the PDH complex in cardiac muscle in mice (n=10 per group). Note: #P<0.01, ^P<0.001, compared to control. Note: ■ = NaCl, ■ = $NaNO_2$.

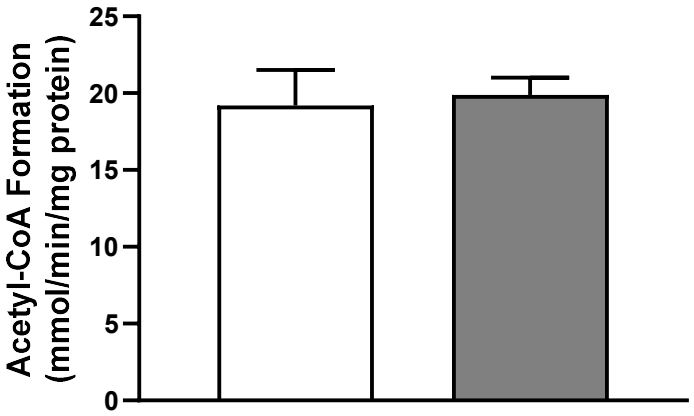

Figure 3-10: Pyruvate dehydrogenase activity in murine cardiac muscle in response to oral sodium nitrite supplementation.

Data are mean ± SEM. Pyruvate dehydrogenase activity (as reflected by the rate of acetyl coenzyme A accumulation) was unchanged in murine cardiac (left ventricular) muscle in response to nitrite. Note: □ = NaCl, ■ = $NaNO_2$.

Human Studies

In human LV myocardial samples, sodium nitrite infusion administered 24 hours prior to sample collection did not alter phosphorylation status of the pyruvate dehydrogenase (PDH) complex, nor did it affect total PDH expression (**Figure 3-11**).

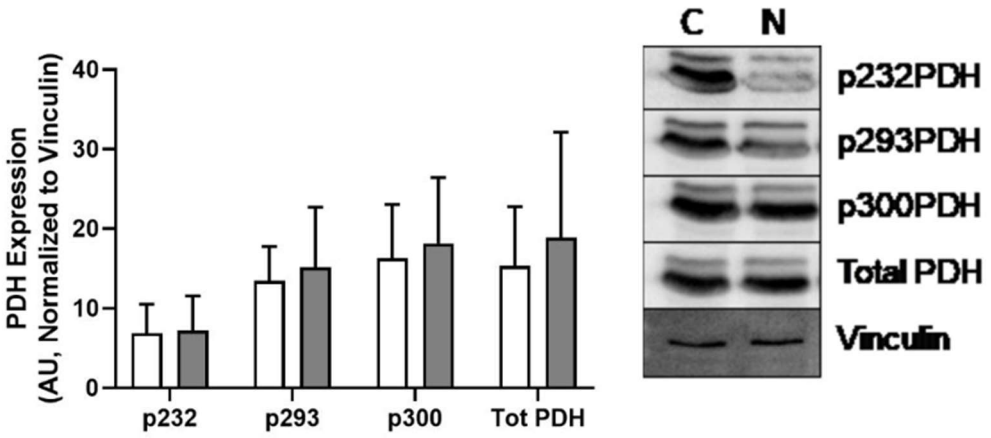

Figure 3-11: Expression and phosphorylation status of PDH in human cardiac muscle following sodium nitrite infusion or normal saline placebo.
Expression and phosphorylation status of PDH were unchanged in human cardiac (left ventricle) muscle in response to a 30-minute sodium nitrite infusion (10μmol/min) compared to normal saline placebo (n=20 and n=15, respectively). Note: □ = NaCl, ■ = $NaNO_2$.

3.5 Discussion

Both the nitrate-nitrite-nitric oxide (NO) pathway and NO-independent effects of plasma nitrite represent potentially safe and cost-effective options with numerous beneficial cardiovascular effects (16,224). We have confirmed our previous findings that both inorganic nitrate and nitrite administered in drinking water can dephosphorylate the pyruvate dehydrogenase (PDH) complex in murine myocardium. We have also shown, for the first time to our knowledge, that intravenous sodium nitrite reduces PKG1α dimer content in the myocardium of patients with type 2 diabetes mellitus, a pro-inflammatory condition, in-keeping with the previously documented anti-inflammatory effects of nitrate/nitrite (309,353,354). The 'pro-inflammatory' state of diabetic myocardium was supported in our study by a higher PKG1α dimer content compared to non-diabetic myocardium, and a higher plasma nitrate level post nitrite infusion, suggesting increased nitrite oxidation. There was also a trend towards a reduction in dimer content in the myocardium of non-diabetics but this failed to reach statistical significance (P=0.06), however, there was no change in the myocardium of healthy mice following oral nitrate supplementation. It is possible that this difference seen in mice (i.e. lack of effect on PKG1α dimer content) is due to differences in administration route and reduced enterosalivary circulation in mice compared to man.

Disulfide Dimerisation of Protein Kinase G 1 Alpha (PKG1α)

The vascular effects of oxidative activation of PKG1α have garnered great attention in the literature, especially in the context of cardiovascular disease (277,291). However, little is known about the role of the dimer in the myocardium. A key difference is the change in localisation of the PKG1α dimer following oxidative activation in the myocardium vs. the vasculature. In the vasculature, disulfide dimer formation is associated with localisation to the cell membrane to exert its effect,

whereas in cardiomyocytes, the disulfide dimer remains within the cytosol, an environment that is rich in reduced glutathione (355). Using a chemical genetic phosphoproteomic method in healthy mouse hearts to quantify phosphorylation status of the downstream targets of PKG1α, Scotcher et al. recently confirmed the activity of the oxidised PKG1α dimer at targets classically activated by the cGMP-activated monomer (294). Interestingly, they also identified a single phosphorylation site at serine 16 of the sarco(endo)plasmic reticulum calcium ATPase 2a (SERCA2a) inhibitor phospholamban, which was activated by the dimer only. The phosphorylation of phospholamban (PLN) by the PKG1α dimer was shown to relieve inhibition of SERCA2a, and improve diastolic relaxation. Given the increase in reactive oxygen species (ROS) with acute changes in cardiac stretch (such as during diastole) (356), and the observation that the amount of ROS produced related to the magnitude of stretch, it was suggested that this mechanism is important in augmenting diastolic relaxation during the normal cardiac cycle, and during acute increases in end-diastolic volume (the Frank-Starling mechanism) (294). Using the PKG1α^{C42S} knock-in mouse model (whereby a single atom substitution changing sulphur to oxygen within cysteine 42 renders the oxidant sensor within PKG1α inactive preventing dimerisation, i.e. 'redox-dead'), the authors showed that chronic absence of this mechanism is associated with reduced amplitude and slower decay of transient intracellular calcium currents and diastolic dysfunction. This mechanism highlights the importance of ROS-cycling within the healthy myocardium and the need for tight control to regulate this (357), as chronic inactivation of PLN results in excitation-contraction uncoupling. Indeed PLN genetic variants and polymorphisms in the regulator of its inhibitor (inhibitor 1, the regulator of protein phosphatase 1), are associated with inherited forms of dilated cardiomyopathy (358).

Additionally, increased dimer content impairs the action of the cGMP-activated monomer. Examples include reduced transient receptor potential canonical channel 6 (TRPC6) inhibition in heart failure models (with reduced anti-fibrotic/anti-hypertrophic effects) (276), and reduced phosphorylation of the small Rho GTPase

(RhoA) in response to doxorubicin treatment (with increased risk of doxorubicin-mediated cardiotoxicity) (296). Chronic elevations in PKG1α dimer content have been demonstrated in murine heart failure models and failing human myocardium (296), which fit with Paulus and Tschöpe's paradigm of increased myocardial ROS in heart failure with reduced ejection fraction (HFrEF) (129). However, the reduction in SERCA function and depressed contractility that is a hallmark of heart failure, in contrast to the aforementioned mechanism, is rather due to increased activity of protein phosphatase 1, which is dissociated from its inhibitor by protein kinase A (PKA) following β-adrenergic stimulation (359).

Herein, we have similarly demonstrated increased PKG1α dimer content in patients with type 2 diabetes undergoing coronary artery bypass graft (CABG) surgery, compared to non-diabetics. We note however, that myocardium from patients undergoing CABG surgery, even those without diabetes, is likely to be vastly different in terms of protein expression compared to age-matched 'healthy' myocardium, and so differences between our patient studies and mouse studies are not surprising. In the current study, nitrite therapy was associated with a decrease in PKG1α dimer content in human myocardium compared to control. By contrast, previous work by our group in murine vasculature showed increased PKG1α dimer content and dilatation of resistance vessels following sodium nitrite treatment (292). The mechanism was shown to be an elevation of reactive persulfides in the setting of elevated hydrogen peroxide (H_2O_2) levels, posited to be secondary to nitrite-mediated inhibition of catalase. The contrast is easily explained when one considers the ability of the myocardium to handle redox stress compared to the vasculature. The myocardium and large arteries produce more NO and contain higher levels of peroxiredoxins than resistance vessels, which can detoxify and quench intracellular H_2O_2/persulfides, thus preventing PKG dimerization with moderate increases in ROS (279). In-keeping with this, preliminary data by our group showed that persulfides were not elevated in murine myocardium following nitrite treatment. It seems therefore that the anti-inflammatory effects of nitrite predominate in the current

study, even in setting of ongoing catalase inhibition by nitrite, resulting in reduced ROS and therefore dimer content.

Pyruvate Dehydrogenase (PDH) Phosphorylation Status and Expression

Oral inorganic (sodium) nitrate and nitrite supplementation (1g/L drinking water for 7 days) resulted in dephosphorylation of the pyruvate dehydrogenase (PDH) complex at serine 232, and serines 232 and 300, respectively, in murine myocardium without effects on total PDH expression. This confirms previous unpublished data from our group (PhD thesis, Dr Konstantin Schwarz, University of Aberdeen). Whereas our previous work also showed an increase in PDH complex activity with sodium nitrite supplementation, this was not true for the current study. The PDH complex is regulated by phosphorylation status at serines 232, 293, and 300, and serines 232 and 300 predominate in the myocardium (152). Phosphorylation is regulated by PDH phosphatases (PDPs 1&2) which dephosphorylate and activate PDH, as well as PDH kinases (PDKs 1-4) which phosphorylate and inhibit PDH. PDH is also allosterically regulated by its products (acetyl CoA, NADH, and ATP), again via PDPs and PDKs, such that excess activates PDKs to inhibit PDH, whereas a decline in these products activates PDPs to reduce PDH activity. Phosphorylation of serine 293 is mediated by PDK2, and this has the greatest impact on enzyme activity (360). Phosphorylation of serine 232 is predominantly mediated by PDK1, the isoform that is regulated by hypoxia inducible factor 1 alpha (HIF1α) during hypoxia (360).

Importantly, terminal pyruvate oxidation via PDH in the heart is directly inhibited by mitochondrial β-oxidation of free fatty acids (FFAs), and itself inhibits β-oxidation in a process termed the ‘Randle cycle’ (150). If FFA oxidation is increased, levels of by-products such as acetyl CoA are also increased, therefore activating PDKs and reducing PDH activity. Hypoxia may also directly activate PDKs via the transcriptional effects of HIF1α, an important cellular protective mechanism preventing harmful

(oxygen-dependent) mitochondrial oxidative phosphorylation in the absence of oxygen (153). The primary regulator of FFA β-oxidation is the peroxisome proliferator activated receptor alpha (PPARα) transcriptional co-factor (157). There is now mounting evidence that inorganic nitrate and nitrite activate PPARα, and this appears to be NO-mediated (361). In a study investigating the role of PPARα in the metabolic effects of inorganic nitrate in murine myocardium, Horscroft et al. recently demonstrated conflicting results whereby inorganic (sodium) nitrate had no effect on PDH phosphorylation status in wild-type mice during normoxia (352). Unsurprisingly, hypoxia increased phosphorylation of PDH at all 3 serine residues, however, inorganic nitrate reversed this effect at all 3 residues during hypoxia. Interestingly, the effects of hypoxia appeared to be PPARα-dependent, as this effect was not observed in PPARα-null mice. As the effects of hypoxia are largely mediated by ROS, particularly produced at complex 3 of the mitochondrial electron transport chain (362), these effects could also be explained by an anti-inflammatory action of inorganic nitrate, an effect which has been well-documented (309,353,354). It is also feasible that the lack of effect of nitrite on PDH seen in the human samples in our study is due to the timing of administration of sodium nitrite compared to harvesting for immunoblotting. In the mouse studies, samples were harvested late-morning in all studies, however mice were freely able to consume the drinking water up until this time. In the human studies however, samples were harvested at 24 hours following sodium nitrite administration, and it is therefore entirely possible that any effect on PDH may have disappeared by the time the myocardial tissue samples were harvested.

Study Limitations

For the PKG1α studies, we did not determine subcellular distribution of the disulfide activated dimer. In wild-type ($PKG1\alpha^{WT}$) mice, the oxidative dimer has previously been shown to become diffusely cytosolic in distribution, as compared to the monomer which is primarily closer to the cell membrane (296). This distribution is an important factor in the differences between the mechanism of action of activators of

the membrane-bound soluble guanylate cyclase (sGC) and inhibitors of the diffusely cytosolic phosphodiesterase (PDE) 5, in heart failure, where oxidative dimer formation prevents the actions of sGC activators (276). Our human LV myocardial samples were too small to allow for this analysis, due to the small bore size of the Trucut needles and the reluctance of many of the cardiothoracic surgeons to take multiple passes of the LV wall. Similarly, the small size of the human LV myocardial samples prevented detailed analysis including reactive persulfide levels, given the need for differences in sample processing and storage.

It is difficult to determine the reason why our results for the effects of inorganic nitrate on cardiac PDH differ from those previously published by others (352), and yet agree with previous pilot data from our group (PhD thesis, Dr Konstantin Schwarz, University of Aberdeen). Identical immunoblotting methods were used for each study, with the exception of β-actin for protein loading control in the study by Horscroft et al. (352), and the use of vinculin in the current study. However, both have been validated as protein loading controls and are thus unlikely to have played a role in this variation. Perhaps the greatest differences were in the length of oral inorganic nitrate supplementation and in sample handling during cardiac harvest. In the study by Horscroft et al., mice were treated for around 35 days compared to 7 days in our study. Additionally, cardiac samples were first blotted, cleaned of fatty tissue, and separated into 3 sections before being snap-frozen in liquid nitrogen after harvest, whereas our samples were blotted to remove extra blood before being immediately snap-frozen whole in liquid nitrogen (i.e. around 1 second of handling time). Whilst the authors attempted to minimise changes in protein status by placing samples in ice-cold biopsy preservation medium, this did not include phosphatase inhibitors, and PDH is known to quickly change phosphorylation status after harvest (363). Similarly, whilst both periods (7 days and 35 days) of inorganic nitrate supplementation can be considered ‘chronic’, it is possible that a longer treatment period may be associated with changes in nitrite/nitrate handling and clearance, but

this is difficult to ascertain as plasma levels of nitrate/nitrite were not provided in the study by Horscroft et al. (352).

3.6 Conclusions

In contrast to in the vasculature, nitrite caused a reduction in PKG1α oxidative dimer formation in the myocardium. This was most profound in cardiac samples from patients with type 2 diabetes mellitus, a pro-inflammatory state. Inorganic nitrate and nitrite dephosphorylated serine 232, and serines 232 and 300, respectively, of myocardial PDH in mice, but this did not translate to increased PDH activity, and this was not seen in the human myocardial samples. Given the previously demonstrated benefits of preventing PKG1α disulfide dimer formation in the myocardium, these anti-inflammatory effects of inorganic nitrate and nitrite warrant further investigation.

Table 3-1: Baseline Demographics of the Human Study Cohort

	Placebo (*n* = 15)	**Nitrite (*n* = 20)**	***P* value**
Age (years)	67 ± 10	62 ± 9	0.19
Sex (male, %)	11 (73.3)	19 (95.0)	0.07
Height (cm)	167 ± 10	172 ± 10	0.13
Weight (kg)	89 ± 15	88 ± 16	0.95
Body surface area (m^2)	2.02 ± 0.22	2.04 ± 0.23	0.71
Baseline Haemodynamics			
SBP baseline (mmHg)	131 ± 17	125 ± 19	0.35
SBP post-infusion (mmHg)	123 ± 22	117 ± 21	0.47
DBP baseline (mmHg)	76 ± 9	73 ± 10	0.38
DBP post-infusion (mmHg)	70 ± 9	68 ± 12	0.59
HR baseline (bpm)	61 (56, 68)	64 (57, 72)	0.23
HR post-infusion (bpm)	58 (55, 63)	64 (55, 74)	0.18
Medical Comorbidities			
Diabetes mellitus	4 (26.7)	7 (35.0)	0.59
Myocardial infarction	7 (46.7)	7 (35.0)	0.48
Hypertension	11 (73.3)	10 (50.0)	0.16
Smoking status			0.32
- Never	5 (33.3)	10 (50.0)	
- Ex-smoker	9 (60.0)	7 (35.0)	
- Current	1 (6.7)	3 (15.0)	
Medications			
Aspirin	12 (80.0)	13 (65.0)	0.33
β-blockers	14 (93.3)	16 (80.0)	0.26
Oral nitrates	2 (13.3)	4 (20.0)	0.60
Calcium channel blockers	4 (26.7)	4 (20.0)	0.64
ACE-I/ARB	8 (53.3)	12 (60.0)	0.69
Statins	15 (100.0)	19 (95.0)	0.38

Data are *n* (%), mean ± SD, or median (IQR). ACE-I, angiotensin converting enzyme inhibitor; ARB, angiotensin receptor type 2 blocker; DBP, diastolic blood pressure; HR, heart rate; SBP, systolic blood pressure.

Chapter 4: Effects of Nitrite on Chemotherapy Sensitivity in 786-0 Renal Cell Carcinoma Cells

4.1 Abstract

Background: Many cancer types exhibit altered metabolism in the form of avid glucose uptake and a switch away from mitochondrial respiration and towards glycolysis, even in aerobic conditions. This 'Warburg effect' is present in 786-0 renal cell carcinoma (RCC) cells due to constitutively expressed hypoxia inducible factor (HIF), with subsequent upregulation of pyruvate dehydrogenase (PDH) kinase 1 (PDK1). PDK1 inhibits PDH via phosphorylation of serine 232, blocking the rate-limiting step for mitochondrial glucose oxidation. Our pilot data has shown that inorganic nitrate and nitrite dephosphorylate PDH at serine 232 in cardiac and skeletal muscle. We sought to investigate whether this effect occurs in 786-0 RCC cells, and whether this could reverse inhibition of mitochondrial respiration and increase susceptibility to chemotherapeutic agents.

Methods: 786-0 RCC cells were treated with varying doses of sodium nitrite (0, 50, and 100 μM) ± the nitric oxide (NO) inhibitor CPTIO or soluble guanylate cyclase inhibitor ODQ. Cells were then treated with varying doses of 5-fluorouracil (0, 5, 10, 25, 50, and 100 μM), and exposed to either normoxic (21% O_2) or hypoxic (1% O_2) conditions. Viability studies and cell harvesting for western blotting were performed at both 24 hours and 48 hours post-treatment, to determine whether there was an effect with nitrite, and whether this was NO-dependent.

Results: HIF2α was not expressed during normoxia in our 786-0 cells. Hypoxia conferred a survival benefit to 786-0 cells on assessment of viability at 24 hours (120% of normoxia; P=0.04). 100 μM nitrite increased cell viability at 24 hours in normoxia, whereas both doses increased viability at 24 hours during hypoxia. Chemotoxicity of 5-fluorouracil was re-established on the viability studies at 48 hours post-treatment. Nitrite did not affect this during normoxia or hypoxia. Mechanistically, nitrite had no effect on PDH phosphorylation status or expression, or LDH expression in normoxia. Akt phosphorylation status was slightly increased

following nitrite treatment in normoxia, but this was not statistically significant. During hypoxia, increasing doses of nitrite reduced phosphorylation of both PDH and Akt at all 3 residues compared to control, but this was not statistically significant.

Conclusions: There was significant resistance to 5-FU treatment at 24 hours in 786-0 cells. Hypoxia improved 786-0 cell survival, in association with robust increases in HIF2α expression. 100 μM sodium nitrite increased cell viability with lower dose 5-FU at 24 hours, without effects on PDH, Akt, or LDH. The mechanism is likely related to an increase in reactive oxygen species levels with higher doses of nitrite.

4.2 Introduction

Cancer cells avidly consume glucose, a phenomenon that underpins the clinical use of labelled glucose (18F-fluorodeoxyglucose/FDG) positron emission tomography (PET) imaging in medical oncology (364). In the 1920s, Otto Warburg published the observation that cancer cells preferentially ferment glucose to produce lactate, a metabolic profile previously only observed in mammalian cells in response to hypoxia (365). The mechanism was later discovered to be under the influence of hypoxia inducible factor (HIF), a transcription factor that binds to the hypoxia response element (HRE) of a range of genes, activating adaptive responses to improve cellular survival in low oxygen conditions (366,367). In clear cell renal cell carcinomas (ccRCC), a critical driver in the progression to cancer is constitutive expression of HIF due to genetic mutations in the von Hippel-Lindau (vHL) tumour suppressor gene, and loss of the functional protein (368).

This has multiple beneficial effects for cancer cells. The aforementioned increase in glucose uptake and switch towards aerobic glycolysis facilitates energy production, whilst also funnelling glucose into the hexosamine biosynthesis pathway (HBP) and pentose phosphate pathway (PPP), the end-products of which are used as cellular building blocks and quench reactive oxygen species (ROS), respectively (148,237). This also prevents the production of excessive quantities of ROS from mitochondrial oxidative phosphorylation that might otherwise trigger cellular autophagy or senescence (369). Similarly, free fatty acid (FFA) metabolism is inhibited and synthetic pathways are upregulated, promoting tumorigenesis by increasing the availability of metabolic intermediates used in cellular membrane biosynthesis and the generation of critical signalling molecules (370,371). This FFA excess and storage in fat droplets, gives ccRCC the characteristic ‘clear cell’ appearance. A key mechanism for the switch from pyruvate oxidation towards aerobic glycolysis is the inhibition of the pyruvate dehydrogenase (PDH) complex by HIF (153,372,373). PDH is the rate-limiting enzyme for the terminal oxidation of pyruvate, and is inhibited by phosphorylation at serines

232, 293, and 300 by PDH kinases (PDKs), and activated by dephosphorylation by PDH phosphatases (PDPs) (149,151). PDH Inhibition in response to hypoxia is primarily due to the action of PDK1 at serine 232, which is upregulated by HIF (372). Indeed, activation of PDH in ccRCC is associated with restoration of mitochondrial oxidative phosphorylation and ROS production, which triggers cancer cell senescence (373).

We have shown that inorganic nitrate and nitrite can dephosphorylate PDH at serine 232 in murine cardiac muscle (see **Chapter 3**) and skeletal muscle; whether this effect may be nitric oxide (NO)-dependent or independent was not explored. The direct effect of NO on HIF1α signalling has been studied previously in the setting of angiogenesis, where it was shown to activate the HIF1α complex via a mechanism that was independent of soluble guanylate cyclase (sGC) and cyclic GMP, and differed compared to the effect of hypoxia (374). Inorganic nitrate has also been shown to protect against the development of cardiomyopathy as a result of anthracycline chemotherapy in mouse models, via inhibition of mitochondrial ROS production (305). Recently, the PDK inhibitor dichloroacetate was shown to relieve inhibition of the PDH complex in 786-0 RCC cells, and this was associated with a reduction in tumour size and angiogenesis in animal models (375). The safety of inorganic nitrate in active cancer has not yet been tested. However, it could represent a cheap anticancer therapy with important cardioprotective benefits. We hypothesised that nitrite therapy would relieve the inhibition of PDH in 786-0 cells, and that this metabolic switch would increase sensitivity to chemotherapeutic agents such as 5-fluorouracil.

4.3 Methods

The methods for this study are detailed in **Chapter 2**. Briefly, 786-0 cells were plated into 96-well plates and treated with varying doses of sodium nitrite and the chemotherapeutic agent 5-fluorouracil (see **Figure 2-2**). Half of the plates were incubated for 24 hours in normoxic conditions (21% O2) and half in hypoxic

conditions (1% O2). A further replicate plate for each condition was also placed in an extended incubation of 48 hours. Cell viability was determined using the CellTiter-Glo® Luminescent ATP Assay (see section 2.1.5). To test the underlying mechanism for any effect with nitrite, 12-well plates for Western blotting were also prepared (see **Figure 2-3**). Sodium nitrite at varying doses was added following pre-treatment (15 minutes) with the soluble guanylate cyclase (sGC) inhibitor, ODQ (1H-(1,2,4)oxadiazolo[4,3-a]quinoxalin-1-one), and the nitric oxide (NO) scavenger CPTIO (2-(4-Carboxyphenyl)-4,4,5,5-tetramethylimidazoline-1-oxyl-3-oxide). Plates were left for 24 hours before harvesting of protein for Western blotting (see section 2.1.6). Data are expressed as either mean ± SD unless otherwise stated. Statistical analysis was performed as outlined in section 2.1.7.

4.4 Results

1. Effects of Nitrite on 786-0 RCC Cell Viability

Cell Viability at 24 hours

During normoxia, sodium nitrite treatment affected 786-0 cell viability at 24 hours compared to control ($F [2, 18] = 3.895$, $P=0.039$). On Tukey's multiple comparisons test, 100 µM sodium nitrite increased cell viability at lower dose (5 and 10 µM) 5-fluorouracil ($P=0.0004$ and $P=0.002$, respectively; see **Figure *4-1***).

Hypoxia significantly increased cell viability compared to control at 24 hours ($P<0.05$). During hypoxia, sodium nitrite treatment affected 786-0 cell viability at 24 hours compared to control ($F [2, 18] = 20.7$, $P<0.0001$). On Tukey's multiple comparisons test, 50 µM sodium nitrite treatment increased 786-0 cell viability at higher doses (50 and 100 µM) of 5-fluorouracil ($P=0.005$ and $P=0.019$, respectively), whereas 100 µM sodium nitrite increased cell viability at lower dose (0 and 10 µM) 5-fluorouracil ($P=0.02$ and $P=0.0003$, respectively).

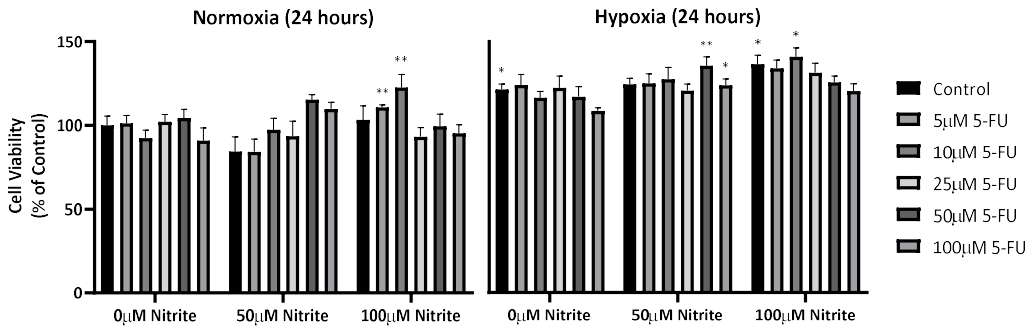

Figure 4-1: Effect of Nitrite on Viability at 24 hours of 786-0 Cells treated with 5-Fluorouracil during Normoxia and Hypoxia.

During normoxia, sodium nitrite treatment affected 786-0 cell viability at 24 hours compared to control (F [2, 18] = 3.895, P=0.039). On Tukey's multiple comparisons test, 100 µM sodium nitrite increased cell viability at lower dose (5 and 10 µM) 5-fluorouracil (P=0.0004 and P=0.002, respectively). Hypoxia significantly increased cell viability compared to control at 24 hours (P<0.05). During hypoxia, sodium nitrite treatment affected 786-0 cell viability at 24 hours compared to control (F [2, 18] = 20.7, P<0.0001). On Tukey's multiple comparisons test, 50 µM sodium nitrite treatment increased 786-0 cell viability at higher doses (50 and 100 µM) of 5-fluorouracil (P=0.005 and P=0.019, respectively), whereas 100 µM sodium nitrite increased cell viability at lower dose (0 and 10 µM) 5-fluorouracil (P=0.02 and P=0.0003, respectively). 5-FU, 5-fluorouracil.

Cell Viability at 48 hours

During normoxia, sodium nitrite treatment affected 786-0 cell viability at 48 hours compared to control (F [2, 18] = 8.994, P=0.002). On Tukey's multiple comparisons test, 50 and 100 µM sodium nitrite treatment increased 786-0 cell viability at 10 µM 5-fluorouracil (P=0.02 and P=0.001, respectively; **Figure *4-2***).

Hypoxia significantly increased cell viability compared to control (P<0.05). During hypoxia, sodium nitrite treatment did not affect 786-0 cell viability at 48 hours compared to control (F [2, 18] = 1.81, P=0.19).

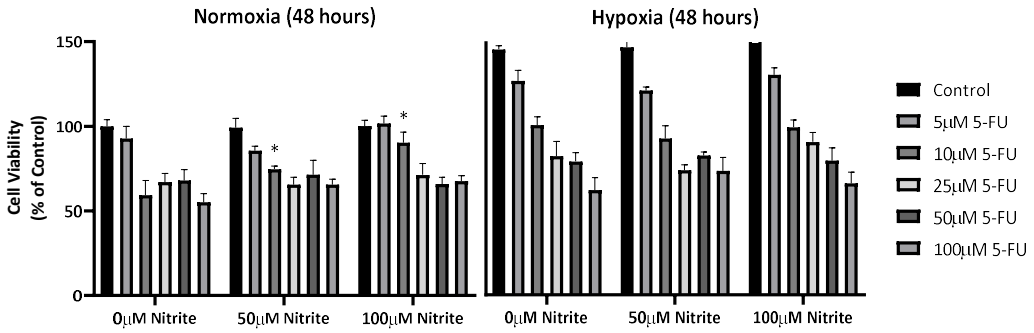

Figure 4-2: Effect of Nitrite on Viability at 48 hours of 786-0 Cells treated with 5-Fluorouracil during Normoxia and Hypoxia.

During normoxia, sodium nitrite treatment affected 786-0 cell viability at 48 hours compared to control (F [2, 18] = 8.994, P=0.002). On Tukey's multiple comparisons test, 50 and 100 µM sodium nitrite treatment increased 786-0 cell viability at 10 µM 5-fluorouracil (P=0.02 and P=0.001, respectively). Hypoxia significantly increased cell viability compared to control (P<0.05). During hypoxia, sodium nitrite treatment did not affect 786-0 cell viability at 48 hours compared to control (F [2, 18] = 1.81, P=0.19). 5-FU, 5-fluorouracil.

2. Effects of Hypoxia on Protein Expression and Phosphorylation Status

LDH and HIF2α Expression, and PDH and Akt Expression and Phosphorylation Status

Interestingly, HIF2α was not expressed during normoxia in our 786-0 cells, even following treatment with sodium nitrite (data not shown). Hypoxia robustly increased HIF2α expression (P<0.00001; see **Figure *4-3*, A**). LDH expression similarly increased during hypoxia, to 227% of normoxic expression (P=0.004; **Figure *4-3*, B**). PDH and Akt phosphorylation status and expression were also increased during hypoxia. Hypoxia phosphorylated PDH at all 3 residues, but this was only statistically significant at serine 293 (P=0.03). Total PDH expression also increased during hypoxia (P=0.049; **Figure *4-3*, C**). Akt phosphorylation increased during hypoxia at threonine 308 (P<0.001), and there was a strong trend at serine 473, but this was not statistically significant (P=0.08). Total Akt expression also increased during hypoxia (P=0.001; **Figure *4-3*, D**).

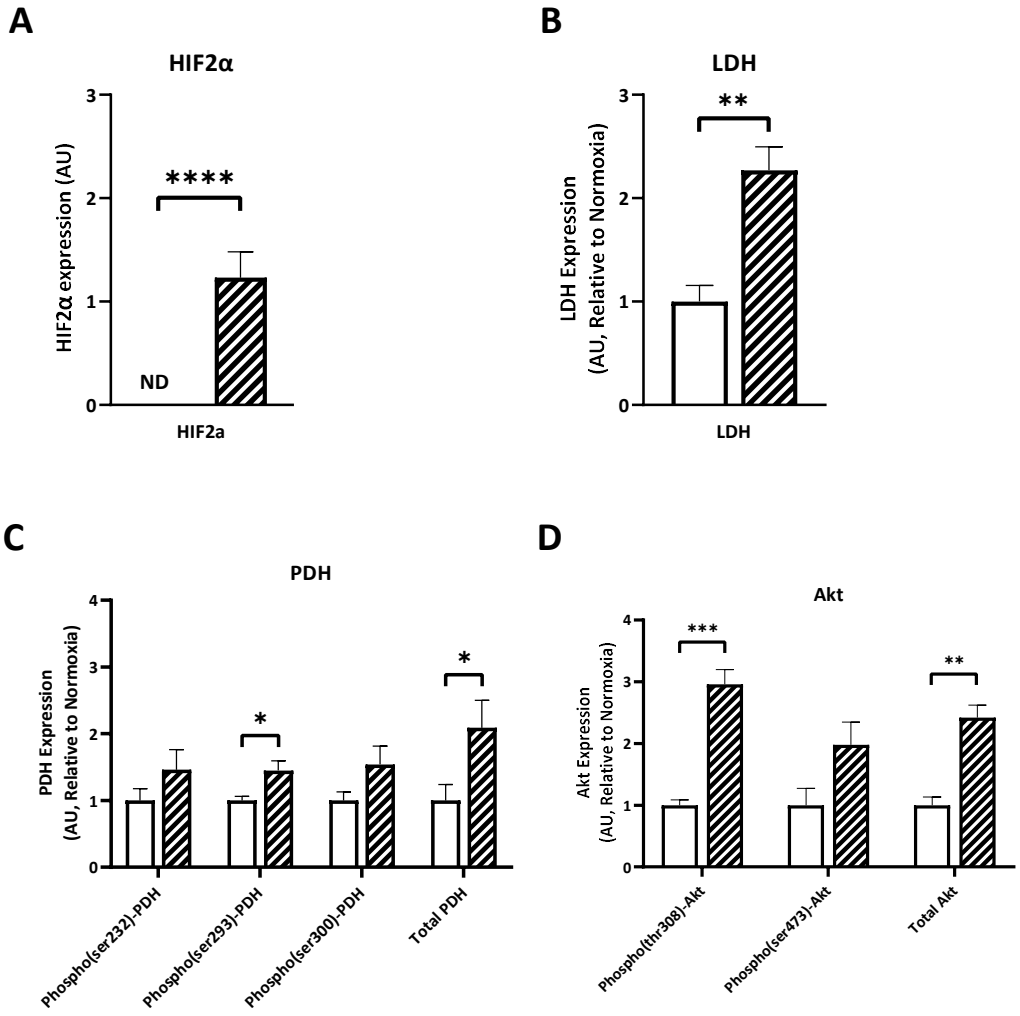

Figure 4-3: Effect of Hypoxia on Protein Expression in 786-0 Cells.
Interestingly, HIF2α was not expressed during normoxia in our 786-0 cells, even following treatment with sodium nitrite (data not shown). Hypoxia robustly increased HIF2α expression (P<0.00001; see Figure 4 3, A). LDH expression similarly increased during hypoxia, to 227% of normoxic expression (P=0.004; Figure 4 3, B). PDH and Akt phosphorylation status and expression were also increased during hypoxia. Hypoxia phosphorylated PDH at all 3 residues, but this was only statistically significant at serine 293 (P=0.03). Total PDH expression also increased during hypoxia (P=0.049; Figure 4 3, C). Akt phosphorylation increased during hypoxia at threonine 308 (P<0.001), and there was a strong trend at serine 473, but this was not statistically significant (P=0.08). Total Akt expression also increased during hypoxia (P=0.001; Figure 4 3, D). AU, arbitrary units; HIF2a, hypoxia inducible factor 2 alpha; LDH, lactate dehydrogenase; PDH, pyruvate dehydrogenase.

3. Effects of Nitrite on Protein Expression and Phosphorylation Status

Normoxia

Pyruvate Dehydrogenase (PDH) Expression and Phosphorylation Status

Under normal oxygen conditions (21% O_2), sodium nitrite treatment at 50 and 100 µM doses did not alter phosphorylation status of PDH at serine 232 (P=0.92), serine 239 (P=0.56), or serine 300 (P=0.84), nor did it significantly affect total PDH expression (P=0.55; see **Figure *4-4***). The addition of ODQ and CPTIO, inhibitors of sGC and NO respectively, did not alter the lack of effect seen with nitrite therapy (see **Figure *4-5***).

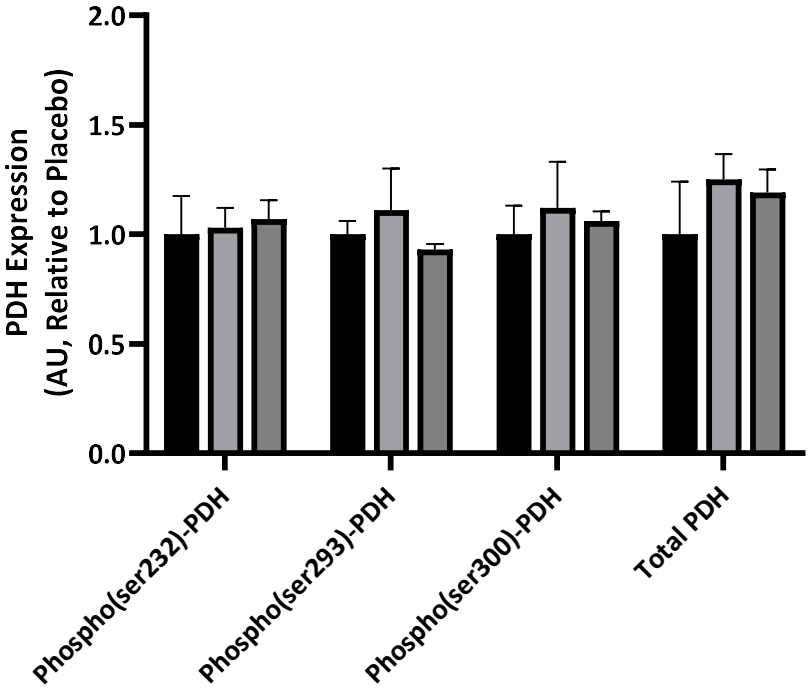

Figure 4-4: Effect of Sodium Nitrite on PDH Expression and phosphorylation status in 786-0 cells in Normoxia.
Under normal oxygen conditions (21% O_2), sodium nitrite treatment at 50 and 100 µM doses did not alter phosphorylation status of PDH at serine 232 (P=0.92), serine 239 (P=0.56), or serine 300 (P=0.84), nor did it significantly affect total PDH expression (P=0.55). AU, arbitrary units; PDH, pyruvate dehydrogenase.

NO and sGC inhibition

PDH Serine 232 Phosphorylation

At the 50 μM dose of sodium nitrite, ODQ did not significantly alter the effect of nitrite on phosphorylation status of PDH at serine 232 (P=0.95), and nor did CPTIO (P=0.67; see **Figure *4-5*, A**). At the 100 μM dose of sodium nitrite, ODQ treatment was associated with a trend towards a reduction in PDH phosphorylation at serine 232, but this was not statistically significant (P=0.15); CPTIO treatment did not alter the effect of nitrite (P=0.79).

PDH Serine 293 Phosphorylation

ODQ did not significantly alter the effect of 50 μM nitrite sodium on phosphorylation status of PDH at serine 293 (P=0.81), and nor did CPTIO (P=0.57; see **Figure *4-5*, B**). At the 100 μM dose of sodium nitrite however, CPTIO treatment was associated with a reduction in phosphorylation of PDH at serine 293 (P=0.048). There was a trend towards an increase in PDH phosphorylation at serine 293 with ODQ, but this was not statistically significant (P=0.12).

PDH Serine 300 Phosphorylation

ODQ did not significantly alter the effect of 50 μM sodium nitrite on the phosphorylation status of PDH at serine 300 (P=0.91), and nor did CPTIO (P=0.63; see **Figure *4-5*, C**). At the 100 μM dose of sodium nitrite however, CPTIO treatment was associated with a reduction in phosphorylation of PDH at serine 300 (P=0.045). ODQ treatment did not alter the effect of nitrite (P=0.27).

Total PDH Expression

At the 50 μM dose of sodium nitrite, ODQ did not significantly alter the effect of nitrite on total PDH expression (P=0.41), and nor did CPTIO (P=0.98; see **Figure *4-5*, D**). Similarly, at the 100 μM dose of sodium nitrite, neither ODQ nor CPTIO altered the effect of nitrite on total PDH expression (P=0.21 and P=0.28, respectively).

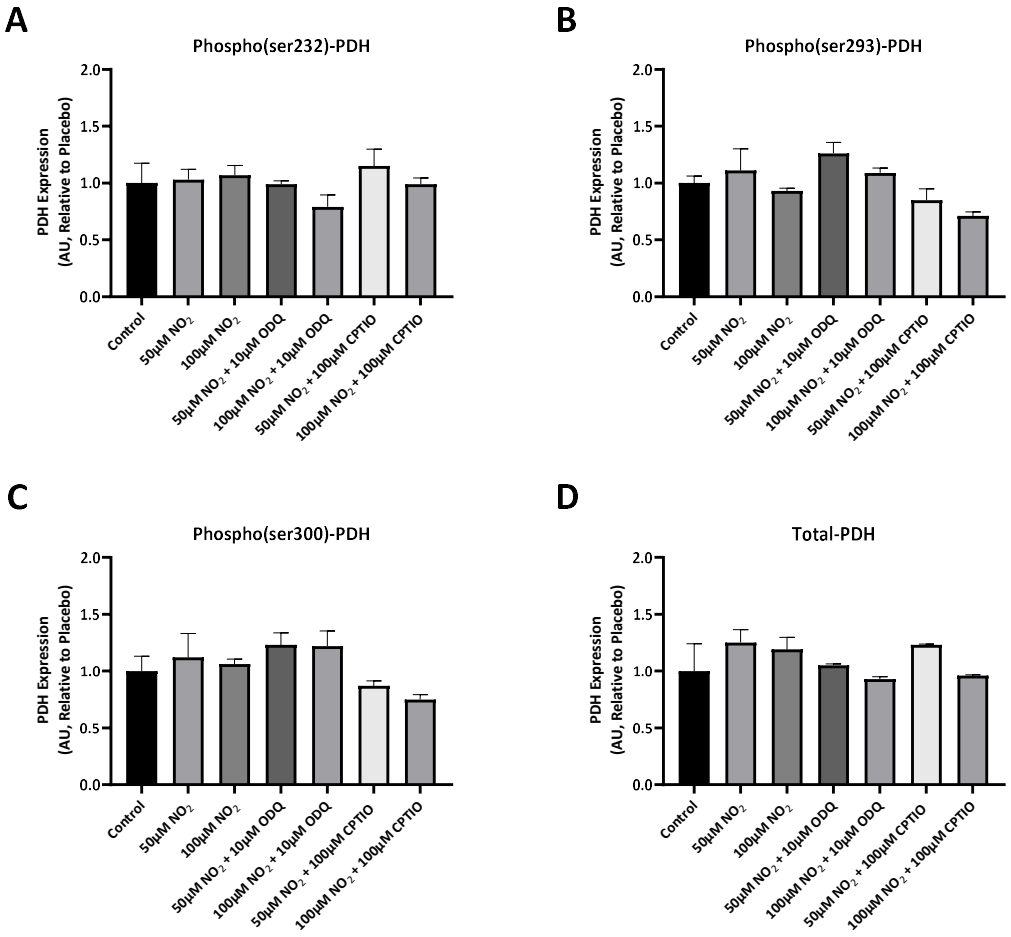

Figure 4-5: Effect of Sodium Nitrite on PDH Expression and Phosphorylation Status in 786-0 Cells in Normoxia with inhibitors.

A: At the 50 µM dose of sodium nitrite, ODQ did not significantly alter the effect of nitrite on phosphorylation status of PDH at serine 232 (P=0.95), and nor did CPTIO (P=0.67). At the 100 µM dose of sodium nitrite, ODQ treatment was associated with a trend towards a reduction in PDH phosphorylation at serine 232, but this was not statistically significant (P=0.15); CPTIO treatment did not alter the effect of nitrite (P=0.79). **B:** ODQ did not significantly alter the effect of 50 µM nitrite sodium on phosphorylation status of PDH at serine 293 (P=0.81), and nor did CPTIO (P=0.57). At the 100 µM dose of sodium nitrite however, CPTIO treatment was associated with a reduction in phosphorylation of PDH at serine 293 (P=0.048). There was a trend towards an increase in PDH phosphorylation at serine 293 with ODQ, but this was not statistically significant (P=0.12). **C:** ODQ did not significantly alter the effect of 50 µM sodium nitrite on the phosphorylation status of PDH at serine 300 (P=0.91), and nor did CPTIO (P=0.63). At the 100 µM dose of sodium nitrite however, CPTIO treatment was associated with a reduction in phosphorylation of PDH at serine 300 (P=0.045). ODQ treatment did not alter the effect of nitrite (P=0.27). **D:** At the 50 µM dose of sodium nitrite, ODQ did not significantly alter the effect of nitrite on total PDH expression (P=0.41), and nor did CPTIO (P=0.98). Similarly, at the 100 µM dose of sodium nitrite, neither ODQ nor CPTIO altered the effect of nitrite on total PDH

expression (P=0.21 and P=0.28, respectively). AU, arbitrary units; PDH, pyruvate dehydrogenase.

Lactate Dehydrogenase Expression and Akt Phosphorylation Status and Expression

Under normoxic conditions, lactate dehydrogenase (LDH) expression was not significantly increased following treatment with 50 or 100 µM sodium nitrite (P=0.52 and P=0.78, respectively). Similarly, sodium nitrite treatment at 50 or 100 µM under normoxic conditions did not alter Akt phosphorylation at threonine 308 (P=0.18) or serine 473 (P=0.71), nor did it affect total Akt expression (P=0.34; see **Figure *4-6***).

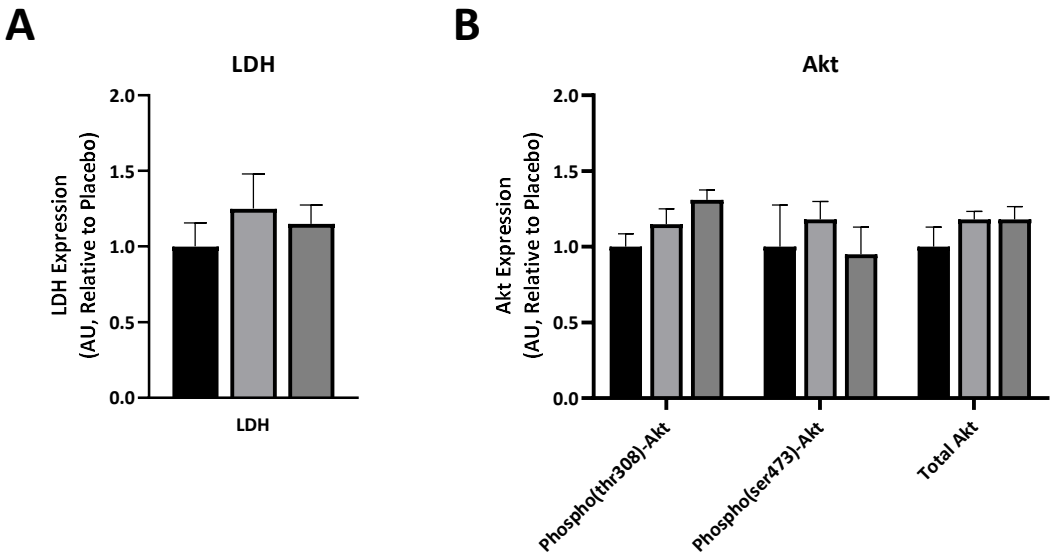

Figure 4-6: Effect of Sodium Nitrite on LDH and Akt Expression and Phosphorylation Status in 786-0 Cells in Normoxia.

Under normoxic conditions, lactate dehydrogenase (LDH) expression was not significantly increased following treatment with 50 or 100 µM sodium nitrite (P=0.52 and P=0.78, respectively). Similarly, sodium nitrite treatment at 50 or 100 µM under normoxic conditions did not alter Akt phosphorylation at threonine 308 (P=0.18) or serine 473 (P=0.71), nor did it affect total Akt expression (P=0.34). AU, arbitrary units; LDH, lactate dehydrogenase.

NO and sGC inhibition

LDH Expression

At the 50 μM dose of sodium nitrite, ODQ did not significantly alter the effect of nitrite on LDH expression (P=0.85) and nor did CPTIO (P=0.85; see **Figure *4-7*, A**). Similarly, ODQ did not alter the effect of the 100 μM dose of sodium nitrite on LDH expression (P=0.81) and CPTIO (P=0.98).

Akt Threonine 308 Phosphorylation

At the 50 μM sodium nitrite dose, ODQ treatment was associated with a statistically significant increase in Akt phosphorylation at threonine 308 (P=0.02), whereas CPTIO did not alter the effect of nitrite (P=0.77; see **Figure *4-7*, B**). At the 100 μM dose of sodium nitrite, ODQ did not alter the effect of nitrite (P=0.96), however, CPTIO treatment was associated with a trend towards a reduction in phosphorylation of Akt at threonine 308 that was not statistically significant (P=0.10).

Akt Serine 473 Phosphorylation

Under normoxic conditions, ODQ did not alter the effect of 50 μM sodium nitrite on phosphorylation of Akt at serine 473 (P=0.30), and nor did CPTIO (P=0.85; see **Figure *4-7*, C**). Similarly, at the 100 μM dose of sodium nitrite, ODQ did not significantly alter the effect of nitrite on Akt phosphorylation at serine 473 (P=0.98), and nor did CPTIO (P=0.85).

Total Akt Expression

At the 50 μM sodium nitrite dose, ODQ treatment was associated with a statistically significant increase in Akt expression (P=0.02), whereas CPTIO treatment was associated with a trend towards a decrease in phosphorylation status that was not statistically significant (P=0.11; see **Figure *4-7*, D**). At the 100 μM dose of sodium nitrite, ODQ did not significantly alter the effect of nitrite on Akt expression (P=0.40), and nor did CPTIO (P=0.20).

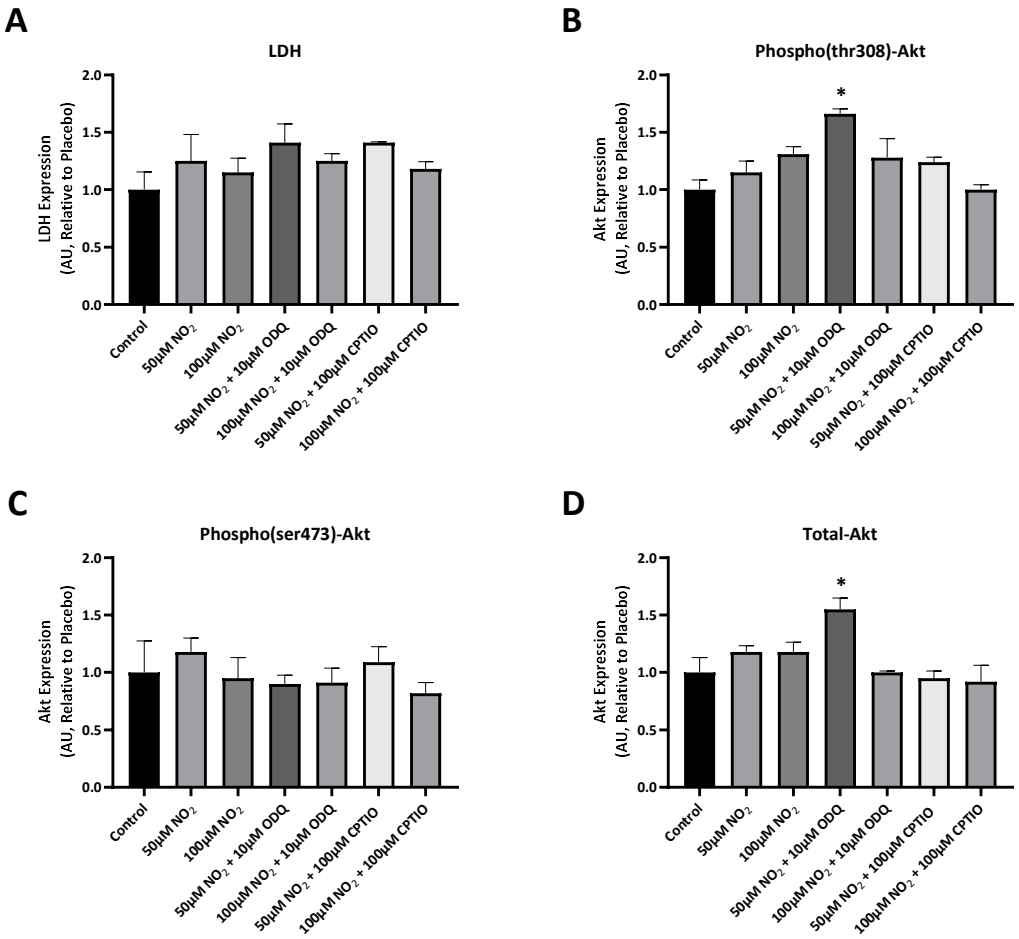

Figure 4-7: Effect of Nitrite on LDH and Akt Expression and Phosphorylation status in 786-0 Cells in Normoxia with inhibitors.

A: At the 50 µM dose of sodium nitrite, ODQ did not significantly alter the effect of nitrite on LDH expression (P=0.85) and nor did CPTIO (P=0.85). Similarly, ODQ did not alter the effect of the 100 µM dose of sodium nitrite on LDH expression (P=0.81) and CPTIO (P=0.98). **B:** At the 50 µM sodium nitrite dose, ODQ treatment was associated with a statistically significant increase in Akt phosphorylation at threonine 308 (P=0.02), whereas CPTIO did not alter the effect of nitrite (P=0.77). At the 100 µM dose of sodium nitrite, ODQ did not alter the effect of nitrite (P=0.96), however, CPTIO treatment was associated with a trend towards a reduction in phosphorylation of Akt at threonine 308 that was not statistically significant (P=0.10). **C:** Under normoxic conditions, ODQ did not alter the effect of 50 µM sodium nitrite on phosphorylation of Akt at serine 473 (P=0.30), and nor did CPTIO (P=0.85). Similarly, at the 100 µM dose of sodium nitrite, ODQ did not significantly alter the effect of nitrite on Akt phosphorylation at serine 473 (P=0.98), and nor did CPTIO (P=0.85). **D:** At the 50 µM sodium nitrite dose, ODQ treatment was associated with a statistically significant increase in Akt expression (P=0.02), whereas CPTIO treatment was associated with a trend towards a decrease in phosphorylation status that was not

statistically significant (P=0.11). At the 100 μM dose of sodium nitrite, ODQ did not significantly alter the effect of nitrite on Akt expression (P=0.40), and nor did CPTIO (P=0.20). AU, arbitrary units; LDH, lactate dehydrogenase.

Hypoxia

Pyruvate Dehydrogenase (PDH) Expression and Phosphorylation Status

Under hypoxic conditions (1% O_2), sodium nitrite treatment at 50 and 100 µM doses did not alter phosphorylation status of PDH at serine 232 (P=0.65), serine 239 (P=0.35), or serine 300 (P=0.56), nor did it significantly affect total PDH expression (P=0.96; see **Figure *4-8***). The addition of ODQ and CPTIO, inhibitors of sGC and NO respectively, did not alter the lack of effect seen with nitrite therapy (see **Figure *4-9***).

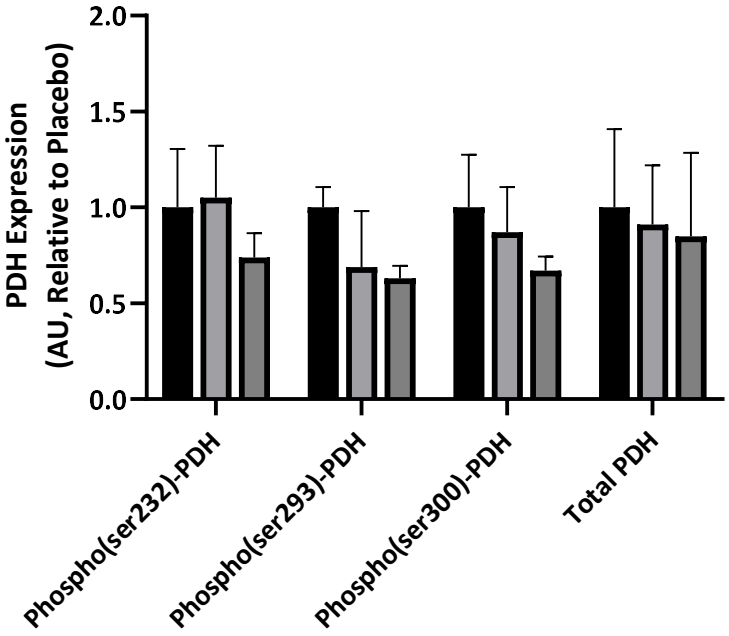

Figure 4-8: Effect of Nitrite on PDH Expression and Phosphorylation Status in 786-0 Cells in Hypoxia.
Under hypoxic conditions (1% O_2), sodium nitrite treatment at 50 and 100 µM doses did not alter phosphorylation status of PDH at serine 232 (P=0.65), serine 239 (P=0.35), or serine 300 (P=0.56), nor did it significantly affect total PDH expression (P=0.96). AU, arbitrary units; PDH, pyruvate dehydrogenase.

NO and sGC inhibition

PDH Serine 232 Phosphorylation

At the 50 µM dose of sodium nitrite, ODQ did not significantly alter the effect of nitrite on phosphorylation status of PDH at serine 232 (P=0.30), and nor did CPTIO (P=0.74; see **Figure *4-9*, A**). Similarly, at the 100 µM dose of sodium nitrite, ODQ did not significantly alter the effect of nitrite on phosphorylation status of PDH at serine 232 (P=0.65), and nor did CPTIO (P=0.88).

PDH Serine 293 Phosphorylation

ODQ did not significantly alter the effect of 50 µM nitrite sodium on phosphorylation status of PDH at serine 293 (P=0.99), and nor did CPTIO (P=0.76; see **Figure *4-9*, B**). At the 100 µM dose of sodium nitrite, ODQ did not significantly alter the effect of nitrite on phosphorylation status of PDH at serine 293 (P=0.34), however there was a strong trend towards a reduction in PDH phosphorylation at serine 293 with CPTIO treatment, but this did not reach statistical significance (P=0.07).

PDH Serine 300 Phosphorylation

ODQ did not significantly alter the effect of 50 µM sodium nitrite on the phosphorylation status of PDH at serine 300 (P=0.65), and nor did CPTIO (P=0.78; see **Figure *4-9*, C**). Similarly, at the 100 µM dose of sodium nitrite, ODQ did not significantly alter the effect of nitrite on phosphorylation status of PDH at serine 300 (P=0.99), and nor did CPTIO (P=0.97).

Total PDH Expression

At the 50 µM dose of sodium nitrite, ODQ did not significantly alter the effect of nitrite on total PDH expression (P=0.91), and nor did CPTIO (P=0.73; see **Figure *4-9*, D**). Similarly, at the 100 µM dose of sodium nitrite, neither ODQ nor CPTIO altered the effect of nitrite on total PDH expression (P=0.98 and P=0.84, respectively).

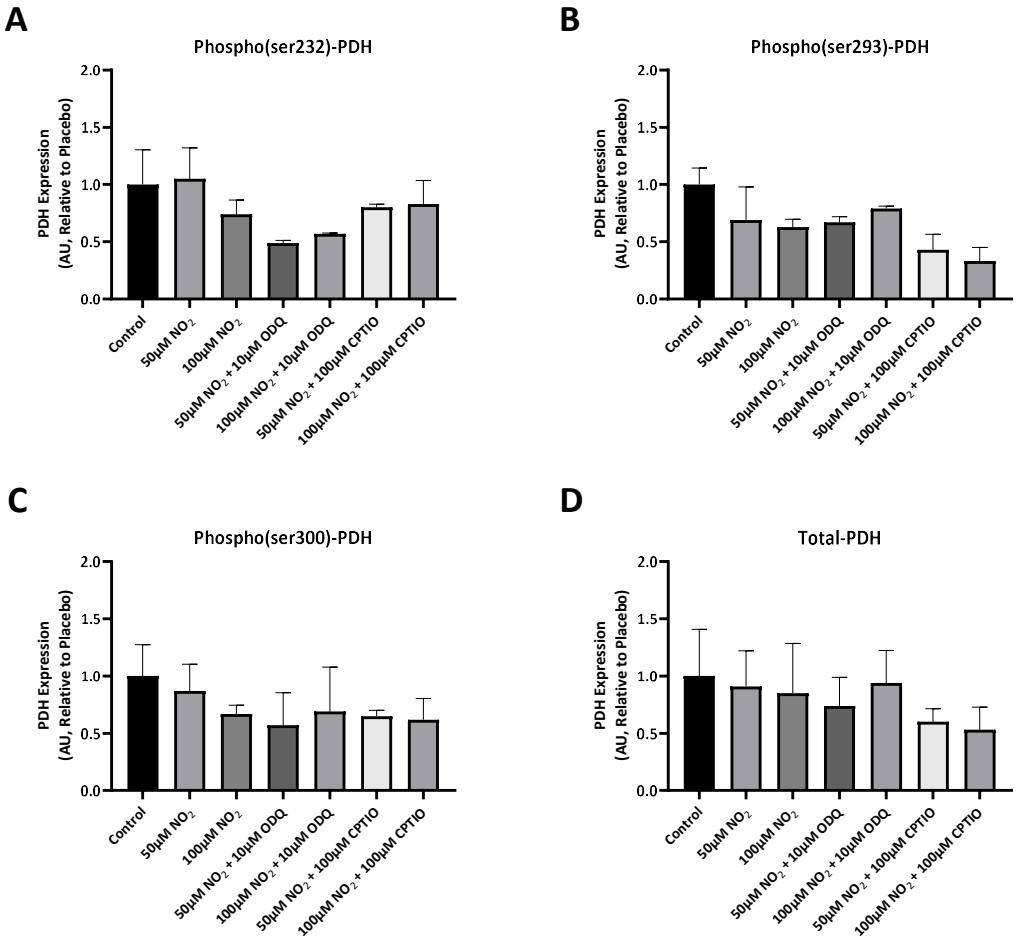

Figure 4-9: Effect of Nitrite on PDH Expression and Phosphorylation status in 786-0 Cells in Hypoxia.

A: At the 50 µM dose of sodium nitrite, ODQ did not significantly alter the effect of nitrite on phosphorylation status of PDH at serine 232 (P=0.30), and nor did CPTIO (P=0.74). Similarly, at the 100 µM dose of sodium nitrite, ODQ did not significantly alter the effect of nitrite on phosphorylation status of PDH at serine 232 (P=0.65), and nor did CPTIO (P=0.88). **B:** ODQ did not significantly alter the effect of 50 µM nitrite sodium on phosphorylation status of PDH at serine 293 (P=0.99), and nor did CPTIO (P=0.76). At the 100 µM dose of sodium nitrite, ODQ did not significantly alter the effect of nitrite on phosphorylation status of PDH at serine 293 (P=0.34), however there was a strong trend towards a reduction in PDH phosphorylation at serine 293 with CPTIO treatment, but this did not reach statistical significance (P=0.07). **C:** ODQ did not significantly alter the effect of 50 µM sodium nitrite on the phosphorylation status of PDH at serine 300 (P=0.65), and nor did CPTIO (P=0.78). Similarly, at the 100 µM dose of sodium nitrite, ODQ did not significantly alter the effect of nitrite on phosphorylation status of PDH at serine 300 (P=0.99), and nor did CPTIO (P=0.97). **D:** At the 50 µM dose of sodium nitrite, ODQ did not significantly alter the effect of nitrite on total PDH expression (P=0.91), and nor did CPTIO (P=0.73; see Figure 4 9, D). Similarly, at the 100 µM dose of sodium nitrite, neither ODQ nor CPTIO altered

the effect of nitrite on total PDH expression (P=0.98 and P=0.84, respectively). AU, arbitrary units; PDH, pyruvate dehydrogenase.

Hypoxia Inducible Factor (HIF) 2α and LDH Expression, and NO and sGC inhibition

Neither the 50 nor 100 μM doses of sodium nitrite altered the expression of HIF2α in hypoxia (P=0.91 and P=0.97, respectively; see **Figure *4-10*, A**). At the 50 μM dose of sodium nitrite, neither ODQ nor CPTIO altered the change in HIF2α with nitrite in hypoxia (P=0.60 and P=0.30, respectively). Similarly, at the 100 μM dose of sodium nitrite, neither ODQ nor CPTIO altered the change in HIF2α with nitrite in hypoxia (P=0.93 and P=0.56, respectively; see **Figure *4-10*, B**).

Neither the 50 nor 100 μM doses of sodium nitrite altered the expression of LDH in hypoxia (P=0.99 and P=0.67, respectively; see **Figure *4-10*, C**). At the 50 μM dose of sodium nitrite, neither ODQ nor CPTIO altered the change in LDH expression with nitrite in hypoxia (P=0.68 and P=0.51, respectively). Similarly, at the 100 μM dose of sodium nitrite, neither ODQ nor CPTIO altered the change in LDH expression with nitrite in hypoxia (P=0.99 and P=0.26, respectively; see **Figure *4-10*, D**).

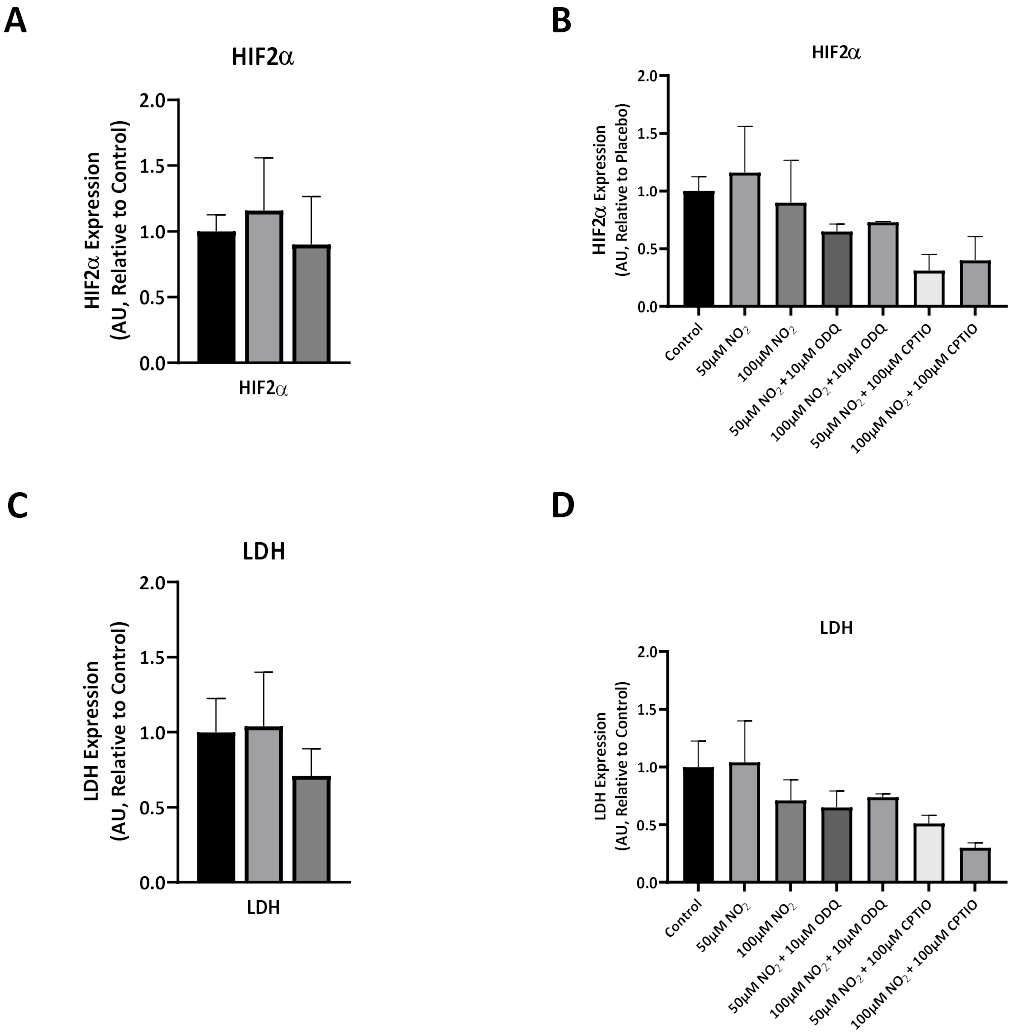

Figure 4-10: Effect of Nitrite on LDH and HIF2α Expression in 786-0 Cells in Hypoxia. **A:** Neither the 50 nor 100 μM doses of sodium nitrite altered the expression of HIF2α in hypoxia (P=0.91 and P=0.97, respectively). **B:** At the 50 μM dose of sodium nitrite, neither ODQ nor CPTIO altered the change in HIF2α with nitrite in hypoxia (P=0.60 and P=0.30, respectively). Similarly, at the 100 μM dose of sodium nitrite, neither ODQ nor CPTIO altered the change in HIF2α with nitrite in hypoxia (P=0.93 and P=0.56, respectively). **C:** Neither the 50 nor 100 μM doses of sodium nitrite altered the expression of LDH in hypoxia (P=0.99 and P=0.67, respectively). **D:** At the 50 μM dose of sodium nitrite, neither ODQ nor CPTIO altered the change in LDH expression with nitrite in hypoxia (P=0.68 and P=0.51, respectively). Similarly, at the 100 μM dose of sodium nitrite, neither ODQ nor CPTIO altered the change in LDH expression with nitrite in hypoxia (P=0.99 and P=0.26, respectively). AU, arbitrary units; HIF2a, hypoxia inducible factor 2 alpha; LDH, lactate dehydrogenase.

Akt Expression and Phosphorylation Status

Sodium nitrite at doses of 50 and 100 µM did not alter Akt phosphorylation at threonine 308 (P=0.78 and P=0.70) and serine 473 (P=0.99 and P=0.87), nor total Akt expression (P=0.94 and P=0.73; see **Figure *4-11*, A**). Similarly, neither ODQ nor CPTIO altered the (lack of) effect of nitrite on Akt expression and phosphorylation status.

Akt Threonine 308 Phosphorylation

At the 50 µM dose of sodium nitrite, ODQ did not alter the effect of nitrite on Akt phosphorylation at threonine 308 (P=0.78), and nor did CPTIO (P=0.61). Similarly, at the 100 µM dose of sodium nitrite, ODQ did not alter the effect of nitrite on Akt phosphorylation at threonine 308 (P=0.97), and nor did CPTIO (P=0.74; see **Figure *4-11*, B**).

Akt Serine 473 Phosphorylation

At the 50 µM dose of sodium nitrite, ODQ did not alter the effect of nitrite on Akt phosphorylation at serine 473 (P=0.68), and nor did CPTIO (P=0.57). Similarly, at the 100 µM dose of sodium nitrite, ODQ did not alter the effect of nitrite on Akt phosphorylation at serine 473 (P=0.99), and nor did CPTIO (P=0.87; see **Figure *4-11*, C**).

Total Akt Expression

At the 50 µM dose of sodium nitrite, ODQ did not alter the effect of nitrite on Akt expression (P=0.77), and nor did CPTIO (P=0.75). Similarly, at the 100 µM dose of sodium nitrite, ODQ did not alter the effect of nitrite on Akt expression (P=0.99), and nor did CPTIO (P=0.89; see **Figure *4-11*, D**).

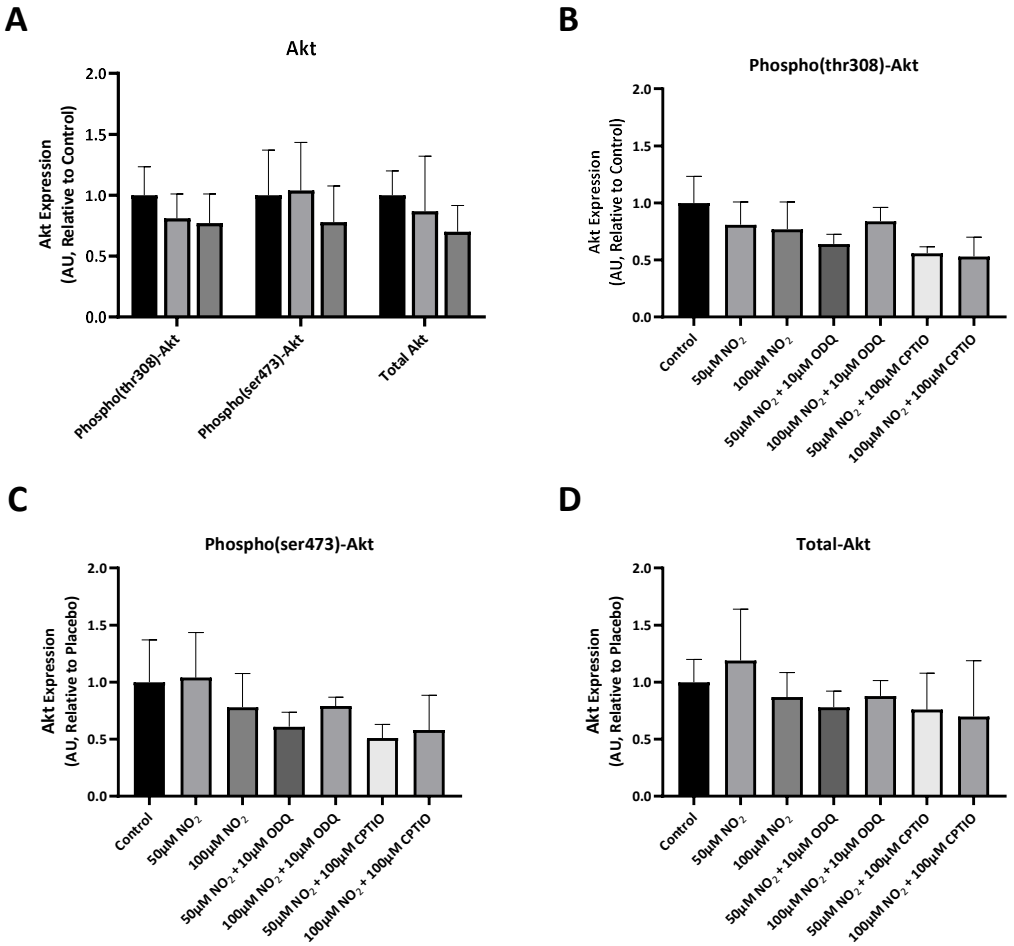

Figure 4-11: Effect of Nitrite on Akt Expression and Phosphorylation status in 786-0 Cells in Hypoxia.

A: Sodium nitrite at doses of 50 and 100 μM did not alter Akt phosphorylation at threonine 308 (P=0.78 and P=0.70) and serine 473 (P=0.99 and P=0.87), nor total Akt expression (P=0.94 and P=0.73). Similarly, neither ODQ nor CPTIO altered the (lack of) effect of nitrite on Akt expression and phosphorylation status. **B:** At the 50 μM dose of sodium nitrite, ODQ did not alter the effect of nitrite on Akt phosphorylation at threonine 308 (P=0.78), and nor did CPTIO (P=0.61). Similarly, at the 100 μM dose of sodium nitrite, ODQ did not alter the effect of nitrite on Akt phosphorylation at threonine 308 (P=0.97), and nor did CPTIO (P=0.74). **C:** At the 50 μM dose of sodium nitrite, ODQ did not alter the effect of nitrite on Akt phosphorylation at serine 473 (P=0.68), and nor did CPTIO (P=0.57). Similarly, at the 100 μM dose of sodium nitrite, ODQ did not alter the effect of nitrite on Akt phosphorylation at serine 473 (P=0.99), and nor did CPTIO (P=0.87). **D:** At the 50 μM dose of sodium nitrite, ODQ did not alter the effect of nitrite on Akt expression (P=0.77), and nor did CPTIO (P=0.75). Similarly, at the 100 μM dose of sodium nitrite, ODQ did not alter the effect of nitrite on Akt expression (P=0.99), and nor did CPTIO (P=0.89). AU, arbitrary units.

4.5 Discussion

Many cancers are dependent on a metabolic switch away from glucose oxidation towards glycolysis (the Warburg effect), and the causative mechanism for this is blockade of pyruvate dehydrogenase (PDH), the rate-limiting enzyme for pyruvate oxidation (372,373). We have shown that sodium nitrite can dephosphorylate and activate PDH in mouse hearts (see **Chapter 3**). If nitrite could 'unblock' PDH in cancer cells it could increase susceptibility to chemotherapeutic agents, representing a cheap anticancer agent in addition to its important cardioprotective effects (305). Paradoxically, we show that nitrite treatment is associated with increases in viability of 786-0 RCC cells treated with 5-fluorouracil (5-FU) at 24 hours. In normoxic conditions, 100 μM sodium nitrite increased cell viability of 786-0 RCC cells treated with lower dose (i.e. 0-10 μM) 5-FU. In hypoxia, both doses increased cell viability. These effects occurred independently of changes in protein expression and phosphorylation status of a range of targets, including PDH, Akt, HIF2α, and LDH. Nitrite did not alter the effect of 5-FU on cell viability at 48 hours.

Interestingly, on immunoblotting, our 786-0 RCC cells did not demonstrate constitutive HIF2α expression in normoxia (characteristic of this cell line), indicating absence of the critical driver of the Warburg effect. It was somewhat unsurprising therefore, that sodium nitrite treatment did not alter PDH phosphorylation status or protein expression in normoxia in this study. Hypoxia (1% O_2) was associated with robust increases in HIF2α levels, and this was associated with predictable increases in LDH expression (376), Akt phosphorylation (activation) and expression (377), and PDH phosphorylation (inhibition) and expression (153). This suggests that the hypoxic environment in these experiments was satisfactorily achieved and maintained. Nitrite treatment in hypoxia was associated with dephosphorylation of PDH at all 3 residues, and decreased PDH expression, as well as Akt dephosphorylation and decreased expression, but this was not statistically significant.

Hypoxia inducible factor (HIF) is the primary transducer of the cellular response to hypoxia. During normoxia, the alpha and beta subunits pair to form the HIF protein, but this is quickly degraded following hydroxylation by the prolyl hydroxylase (PHD) enzyme, which marks HIF for proteolytic degradation by the vHL-E3-ubiquitin ligase complex (378,379). During hypoxic conditions, mitochondrial respiration results in the production of a large amount of ROS, particularly at complex III of the electron transport chain (380). This ROS is converted by Cu,Zn-superoxide dismutase (SOD) in the cytosol into hydrogen peroxide (H_2O_2), which inhibits the PHD enzyme, allowing for HIF stabilisation (362). Stabilised HIF then enters the nucleus where it binds to the hypoxia response element (HRE) on a range of genes, triggering the adaptive response to hypoxia. 786-0 RCC cells constitutively express the HIF2α isoform due to an acquired genetic loss of the vHL protein (368), which is responsible for the Warburg metabolism observed in these cells (381). Constitutive HIF expression conveys a survival advantage for cancer cells. The upregulation of pyruvate dehydrogenase kinase (PDK) 1 by HIF phosphorylates and inactivates PDH, preventing the production of ROS from mitochondrial oxidative phosphorylation that might otherwise trigger cellular autophagy or senescence responses, preventing cancer growth and/or spread (369,372,373). HIF expression also increases glucose uptake, with excess glucose funnelled into the hexosamine biosynthesis pathway (HBP) and pentose phosphate pathway (PPP), the end-products of which are used as cellular building blocks and to quench reactive oxygen species (ROS), respectively (237). Excess glucose is also associated with post-translational modification of multiple cellular proteins via O-GlcNAcylation (148). Upregulation of the HIF isoforms also directly and indirectly opposes the effects of the tumour suppressor gene p53 (382,383), and inhibits the mTOR (autophagy) pathway via activation of oncogenes such as the PI3K/Akt pathway (384).

HIF1α activation in cancers upregulates genes for glucose transport (GLUT1), glycolysis (HK2, PFK, ALDA, PGK1, LDHA etc), and lipid metabolism (ADRP), as well as angiogenesis (VEGF) and autophagy (BNIP3) (383). HIF1α expression varies

significantly across RCC types (385,386). 786-0 clear cell RCC cells however, constitutively express the HIF2α rather than HIF1α isoform, which upregulates all of the aforementioned targets with the exception of enzymes involved in glycolysis, but also genes involved in cell cycle progression (CCND1) and growth factor levels (TGFα) (387). In ccRCC, terminal oxidation of both glucose and free fatty acids (FFAs) by the mitochondria is suppressed. The inhibition of FFA oxidation results in FFA accumulation and deposition, giving the characteristic 'clear cell' appearance. The mechanism for this is related to HIF-mediated CPT1A inhibition (388). Similarly, fatty acid synthesis is increased due to conversion of glutamine to citrate via α-ketoglutarate, which may occur via forward-flux through the Krebs cycle via oxaloacetate or reverse-activity of the isocitrate dehydrogenase and aconitase enzymes (371,389,390). In a study using 786-0 cells and a human ccRCC biopsy sample (later transfected into mouse models), Kinnaird et al. demonstrated that dichloroacetate, a pyruvate analogue and therefore blocker of PDK, relieved PDH blockade and reduced tumour size and angiogenesis *in vivo* (375). This was associated with an increase in mitochondrial ROS and the Krebs cycle metabolite α-ketoglutarate, as well as increased p53 activity. However, this hypothesis that modulation of metabolism in 786-0 RCC cells via a HIF2α-PDH pathway may have anticancer effects appears in opposition to previous reports by others investigating HIF in 786-0 RCC xenografts (391).

The active metabolites of 5-FU cause instability and prevent cellular replication via incorporation into DNA and RNA, as well as inhibition of the thymidylate synthase enzyme (392). The specificity for cancer cells is improved by the rapid cellular division and avid uptake of pyrimidines and their precursors that is characteristic of cancers, however toxic effects in non-cancerous cells is a common side effect of all chemotherapies. 5-FU mediated cytotoxicity has been shown to be dependent on p53 levels, with studies demonstrating a direct link between p53 tumour suppressor gene inactivation and 5-FU resistance in many cancers (393,394). P53-dependent apoptosis of cancer cells occurs via a pathway involving mitochondrial ROS

production (395). Given the key role of ROS in the stabilisation of HIF and in p53-dependent apoptosis, the effects seen with nitrite in 786-0 RCC cells treated with 5-FU in the current study may be explained by its documented effects on ROS, including as seen in our previous studies (see **Chapter 3**). Higher doses of nitrite have been shown to increase ROS (396), whereas lower doses of nitrite (i.e. those approaching physiological levels in the plasma) exert anti-inflammatory effects, reducing ROS (309,353,354). The lack of effect of nitrite on the Western blotting targets is likely explained by the apparent heterogeneity in gene expression of these proteins in 786-0 ccRCC cells (even in the literature as discussed), particularly of HIF1α/2α and PDK1. It appears that careful genotyping of this cell line is required in the event that future studies are undertaken, despite assurances from the manufacturer. In our 786-0 RCC cells, lacking constitutive HIF2α expression, sodium nitrite treatment increased resistance to 5-FU in normoxia, but particularly hypoxia. It is likely that the mechanism was increased ROS-related stabilisation of HIF2α with resultant reductions in p53. This suggests that caution ought to be used when employing redox-modulating adjunctive therapies in cancers, especially those that are largely influenced by redox status.

Study limitations

Our 786-0 RCC cells did not constitutively express HIF2α in normoxia. As such, any assessment of the effect of nitrite on Warburg metabolism in 786-0 RCC cells is limited. There appears to be unexpected heterogeneity in gene expression in this cell line, necessitating careful genotyping and assessment of protein expression prior to future experiments in order to be able to accurately interpret the results. However, our selection of the 786-0 RCC cell line was based on previous studies demonstrating unblocking of PDH with dichloroacetate treatment in these cells, and the resultant increase in p53-dependent apoptosis (375). Initially, this study was planned using the anthracycline Daunorubicin in the place of 5-FU, given the previously demonstrated cardioprotective benefits of inorganic nitrate and nitrite in anthracycline treated mice (305). However, a recent study has shown that anthracycline sensitivity in ccRCC

cells is mediated by downregulation of ALDH2 in a manner that is independent of HIF, which occurs as a result of vHL deficiency (397). As nitrite has proven effects on ALDH2 (398,399), it would have been difficult to separate this from the effects on HIF in our study.

4.6 Conclusions

Sodium nitrite treatment in 786-0 RCC cells was associated with increased rather than decreased resistance to the anticancer effects of 5-FU. This occurred independently of PDH, Akt, HIF, or LDH. The mechanism is likely related to an increase in reactive oxygen species levels with higher doses of nitrite. Higher ROS levels increase HIF stabilisation, with resultant reductions in p53. Caution should be used when employing redox-modulating adjunctive therapies in cancers that are largely influenced by redox status.

Chapter 5: The Nitrite In Chronic HEart failure (NICHE) Trial

5.1 Abstract

Background: The cardinal feature of heart failure is exercise impairment due to reduced cardiovascular reserve, and key causative mechanisms include reduced skeletal muscle blood flow, skeletal muscle loss and dysfunction, and pulmonary venous and arterial hypertension. The vasodilator effects of nitrite are significantly augmented by hypoxia, increasing its selectivity for the pulmonary vasculature, and for the skeletal muscle vasculature during exercise. Furthermore, additional purported benefits of nitrite, such as anti-inflammatory properties and its effects on metabolism, may also increase exercise tolerance in patients with heart failure, and this is supported by evidence from small-scale studies. Inhaled nitrite recently failed to improve exercise tolerance in patients with heart failure with preserved ejection fraction (HFpEF) in a large clinical trial. We sought to investigate the effects of an alternative method for increasing plasma nitrite, oral inorganic nitrate, on exercise capacity in patients with heart failure with reduced ejection fraction (HFrEF), and compare this to matching placebo.

Methods: We designed a multicentre randomised, placebo-controlled trial to investigate the effects of 7 mmol oral inorganic (sodium) nitrate twice daily or placebo on peak oxygen consumption (peak VO_2) on cardiopulmonary exercise (CPEX) testing in 56 patients at 2 months compared to baseline. Secondary outcomes included a quality of life questionnaire (Minnesota Living with Heart Failure), 6 minute hall walk distance, blood tests including fasting glucose and markers of systemic inflammation, and echocardiographic measures of resting diastolic and systolic function. In the original trial design, recruitment was anticipated to take 2.5 years. The study opened but recruited from a single site, the Royal Brompton Hospital in London, with recruitment running from July 2018 until end of October 2019. The study was sponsored by the Norfolk and Norwich University Hospitals NHS Foundation Trust (NNUH).

Results: Nineteen (19) patients completed the study before recruitment was halted early by the study Sponsor due to concerns regarding study feasibility, despite a letter from the DSMC stating that recruitment was on track, and that the standard deviation of peak VO_2 was smaller than in the sample size calculations, and therefore the study should continue. Groups were well-matched on demographics data, however, patients in the active treatment arm had greater diastolic dysfunction (E/E', 6.9 ± 2.2 vs. 10.4 ± 3.8, p=0.04), and a trend towards higher (worse) quality of life scores (8.4 ± 8.0 vs. 22.3 ± 19.9, p=0.06), and poorer exercise tolerance (peak VO_2, 18.8 ± 4.2 vs. 15.9 ± 3.3 $ml.kg^{-1}.min^{-1}$, p=0.11), at baseline. At 2 months, peak VO_2 became more similar between the groups (peak VO2, 18.5 ± 5.4 vs. 16.6 ± 3.7 $ml.kg^{-1}.min^{-1}$, p=0.41), due to a greater fall compared to baseline in the placebo group compared to the active treatment arm (Δpeak VO_2, –1.49 ± 1.9 vs. +0.48 ± 1.3 $ml.kg^{-1}.min^{-1}$, p=0.03). There were no significant differences in the change in plasma glucose or in quality of life scores, however there was a greater worsening of diastolic function in the placebo group compared to the nitrate group, which was statistically significant (ΔE/E', +1.76 ± 2.2 vs. –0.72 ± 1.6, p=0.03). There was a statistically significant negative correlation between the change in E/E' and change in peak VO_2 (r^2=0.43, p=0.03). Unfortunately, other blood test results from patient plasma samples were not available due to delays experienced in processing these in Southampton as a result of the COVID-19 global pandemic.

Conclusion: In our study, inorganic nitrate treatment was not associated with a deterioration in exercise capacity, unlike that seen in the placebo group, and the delta differed significantly between the groups. The change in respiratory exchange ratio was not different between groups, excluding effects from differences in exertional effort. The fall in peak VO_2 correlated with an increase in resting E/E', suggesting a worsening of diastolic function or increase in LVEDP as the likely cause for reduced cardiovascular reserve and worsening exercise tolerance in the placebo group. However, baseline exercise capacity and diastolic function were slightly better in the placebo group, with the groups becoming more similar at 2 months. A definitive large

scale clinical trial is still sorely needed to confirm the effects seen with inorganic nitrate therapy in smaller-scale studies of patients with HFrEF.

Clinical Trials Registration: Effects of inorganic nitrite on cardiac and skeletal muscle (ISRCTN clinical trial registration number: 16356908).

5.2 Introduction

Heart failure affects more than 900,000 people in the United Kingdom, and this number is likely to increase as the population continues to age (38). Various forms of cardiovascular disease may culminate in heart failure. The cardinal feature of heart failure is exercise intolerance. Symptoms (typically dyspnoea) are typically present on exercise, but may be present even at rest, and are caused by an inability of the heart to pump sufficient blood to meet the metabolic needs of the body, or to do so only by raising left ventricular end diastolic pressure (LVEDP) (36). There is an established evidence-base for drug treatments targeting neurohormonal activation in heart failure with reduced ejection fraction (HFrEF), such as ACE-inhibitors, Beta-blockers, and Mineralocorticoid Receptor Antagonists (MRAs) etc, which, together, can robustly reduce patient morbidity and mortality (36). However, the real-world initiation and optimisation of these medications is often complicated by intolerable side effects, resulting in many patients remaining symptomatic and on doses well below those shown to be beneficial in clinical trials (36). Further treatments are still sorely needed for many of these patients.

Dysfunctional nitric oxide (NO) signalling is a key feature of heart failure. Nitrite (NO_2^-), previously thought to be an inert by-product of NO metabolism in the tissues, is now recognised as a NO storage pool from which NO may be liberated by nitrite reductases, especially during hypoxia (16). Inorganic nitrate (NO_3) was similarly regarded as a by-product created by the oxidation of nitrite that is then excreted by the kidneys, due to the absence of a nitrate reductase in man (182). However, critically, commensal bacteria on the dorsum of the tongue possess this enzyme, making them an integral part of the nitrate-nitrite-NO pathway in man. Ingested inorganic nitrate, for example from beetroot or green leafy vegetables in the diet, is absorbed in the stomach into the bloodstream (16). Plasma nitrate is then concentrated in the salivary glands and secreted onto the tongue, where it is reduced to nitrite. This nitrite is then absorbed in the stomach, resulting in an increase in

plasma nitrite levels; small amounts are also reduced to NO by the stomach acid (termed acid disproportionation), which is important for gastric mucosal integrity and has antibacterial properties (183).

Intravenous sodium nitrite (to increase plasma nitrite levels) has been shown to be a potent vasodilator and source of NO in the human forearm circulation in the presence of deoxyhaemoglobin (194). Building on this, Frenneaux et al. demonstrated that nitrite is a potent venodilator in both normoxia and hypoxia, but that the vasodilator effects are only modest in normoxia, with hypoxia significantly augmenting nitrite-induced vasodilatation (300). Inhaled nitrite also showed promise in early studies as a selective, hypoxic pulmonary vasodilator (301). This is of particular interest to the heart failure community given the high prevalence of pulmonary hypertension caused by left-sided cardiac failure (302). Inorganic nitrate also prevented progression to heart failure following a toxic dose of doxorubicin in mice, via transient blockade (nitrosylation) of mitochondrial ROS generation at complex I of the mitochondrial electron transport chain (305). The same mechanism is thought to be responsible for nitrite-induced cardioprotection from ischaemia reperfusion injury. However, in the large, randomised-controlled 'NIAMI' Trial by Frenneaux et al., 70 µmol intravenous nitrite infused for 5 minutes prior to reperfusion at percutaneous coronary intervention for acute myocardial infarction failed to reduce the primary endpoint of myocardial infarct size on cardiovascular magnetic resonance imaging at 6-8 days post-presentation (306). Furthermore, additional purported benefits of nitrite, such as anti-inflammatory properties (309,353,354) and effects on metabolism (304), may also increase exercise tolerance in patients with heart failure. Some of these effects have been shown to be independent of NO (204,292), and may involve other mechanisms such as direct S-nitrosylation of proteins by nitrite (12).

Several small studies have now demonstrated either a significant or equivocal improvement in peak oxygen consumption (peak VO_2) on cardiopulmonary exercise (CPEX) testing with acute doses of oral inorganic nitrate, but these were

underpowered and larger studies are needed (312,313). In 25 patients with severe chronic heart failure, intravenous sodium nitrite infusion at 50μg/kg/min for 5 minutes significantly reduced pulmonary vascular resistance (p=0.03) and increased LV stroke volume (p=0.003) (314). Interestingly, the increase in stroke volume correlated with the increase in transmural LVEDP (r=0.67; p=0.003), prompting the authors to suggest that nitrite may be relieving DVI in these patients (previously shown to be present in ~40% of HFrEF patients at rest (93)). Very recently, a large randomised controlled, crossover trial of inhaled nebulised nitrite in patients with heart failure with a *preserved* ejection fraction (HFpEF) was completed. In this study, nitrite failed to demonstrate an improvement in peak VO_2 vs. placebo (13.5 vs. 13.7 $ml.kg^{-1}.min^{-1}$, p=0.27) (317). The 'Inorganic Nitrite Delivery to Improve Exercise Capacity in Heart Failure with Preserved Ejection Fraction' or 'INDIE-HFpEF' study randomised 105 patients in a random-order crossover design to 4 weeks of nitrite and placebo, with a primary end point of peak VO_2. Inhaled nitrite also failed to improve the secondary endpoints of daily activity levels, quality of life scores, diastolic function on echocardiogram (E/E'), or NT pro BNP levels (317). Despite questions related to dosing, route of administration, and duration of therapy, this study has largely quelled interest in nitrite as a therapy for HFpEF, but left the question of its potential use in HFrEF largely unanswered, particularly given the differences in pathophysiology between the two conditions (129) and the longer-lasting effects of using an alternative administration route, such as with oral inorganic nitrate. We sought to investigate the effects of oral inorganic nitrate, to increased plasma nitrite levels, on exercise capacity in patients with HFrEF compared to matching placebo.

5.3 Methods

The methods used for this study are described in more detail in **section 2.2**. Briefly, patients with non-ischaemic dilated cardiomyopathy (previously assessed via cardiovascular magnetic resonance imaging or diagnostic coronary angiogram) were

recruited from clinics at the Royal Brompton Hospital in London, UK, and by post from a database maintained by the Cardiovascular Biomedical Research Centre at the Royal Brompton Hospital (see section 2.2.2). After allowing adequate time to read the study patient information sheet (at least 24 hours in all cases), patients were invited to attend a screening visit at the Royal Brompton Hospital. After obtaining written informed consent, patients underwent screening/baseline cardiopulmonary exercise (CPEX) testing (see section 2.2.4.1) and transthoracic echocardiography (TTE, see section 2.2.4.2). Patients were excluded on the basis of atrial fibrillation or ejection fraction >50% on TTE, and/or a respiratory exchange ratio <1.0 on CPEX testing. Other inclusion criteria included: age ≥18 years; a diagnosis of HFrEF with New York Heart Failure Association (NYHA) class II or III symptoms; and on maximally-tolerated standard HFrEF medication on a stable regimen for at least 6 weeks. Additional exclusion criteria included: inability to provide written informed consent; recent (past 3 months) hospitalisation for decompensated cardiac failure; hypotension with baseline systolic blood pressure <90 mmHg; anaemia with a plasma haemoglobin <80 g/L; pregnancy or childbearing potential; valvular heart disease of moderate severity or greater; or chronic peripheral vascular disease. Finally, patients with G6PD deficiency (known, or measured at screening in males of African, Asian or Mediterranean descent) were excluded from the study on the basis of an increased risk of methaemoglobinaemia with inorganic nitrate/nitrite treatment (see section 1.3.3.2.1).

Participants then completed baseline testing for the study outcomes (see section 2.2.3) including blood tests (see section 2.2.4.3), a Minnesota Living with Heart Failure quality of life questionnaire (see section 2.2.4), and 6 minute hall walk test (see section 2.2.4). Finally, participants were randomised via minimisation (see section 2.2.2) in a double-blind fashion to either 7 mmol inorganic (sodium) nitrate twice daily or matching placebo for 2 months, at which time participants returned for repeat testing, with results compared to baseline.

5.4 Results

Nineteen (19) patients completed the study before recruitment was halted early by the study Sponsor due to concerns regarding study feasibility. This was despite a strongly worded letter from the DSMC objecting to this. In the study design approved by the MRC, recruitment was anticipated to take 2.5 years. The DSMC noted that the recruitment rate at the time of the interim analysis was satisfactory, and furthermore that the SD for the primary end point was lower than that used for the original sample size calculations. They therefore requested that the study be reopened but the sponsor declined. The study opened but recruited from a single site only, the Royal Brompton Hospital in London, with recruitment at this site running from July 2018 until end of October 2019. Two (2) further patients were randomised but failed to complete the study. One patient withdrew due to a severe adverse event (SAE) in the form of symptomatic ventricular ectopics, which was deemed to be unrelated to the study drug. On unblinding, this patient was found to be in the placebo arm. The other patient withdrew from the study due to intolerable nausea, which was deemed related to the study drug. On unblinding, this patient was in the inorganic (sodium) nitrate arm of the study.

Baseline Demographics

The 2 participant groups were well-matched on demographics data, however, patients in the active treatment arm had greater diastolic dysfunction (E/E', 6.9 ± 2.2 vs. 10.4 ± 3.8, p=0.04), and a trend towards higher (worse) quality of life scores (8.4 ± 8.0 vs. 22.3 ± 19.9, p=0.06), and poorer exercise tolerance (peak VO_2, 18.8 ± 4.2 vs. 15.9 ± 3.3 $ml.kg^{-1}.min^{-1}$, p=0.11), at baseline (**Table 5-1**). This difference was not considered to be due to differences in exertional effort, as patients were excluded if RER was <1.0, and RER for placebo and nitrate groups was similar (1.10 ± 0.05 vs. 1.12 ± 0.06, p=0.28).

Change in Primary Outcome at 2 months vs. Baseline

At 2 months, peak VO_2 became more similar between the groups (peak VO_2 at 2 months, 18.5 ± 5.4 vs. 16.6 ± 3.7 $ml.kg^{-1}.min^{-1}$, p=0.41, **Figure 5-1**), due to a greater fall compared to baseline in the placebo group compared to the active treatment arm (Δpeak VO_2, –1.49 ± 1.9 vs. +0.48 ± 1.3 $ml.kg^{-1}.min^{-1}$, p=0.03, **Figure 5-2**). The slight increase in the inorganic nitrate arm was not statistically significant compared to baseline (p=0.33), however there was a trend towards statistical significance for the fall in the placebo arm (p=0.08). There was no change in respiratory exchange ratio (RER) for either group between baseline and at 2 months, and the difference in the change in RER was not statistically significant between groups (nitrate vs. placebo, +0.02 ± 0.06 vs. 0 ± 0.10, p=0.52).

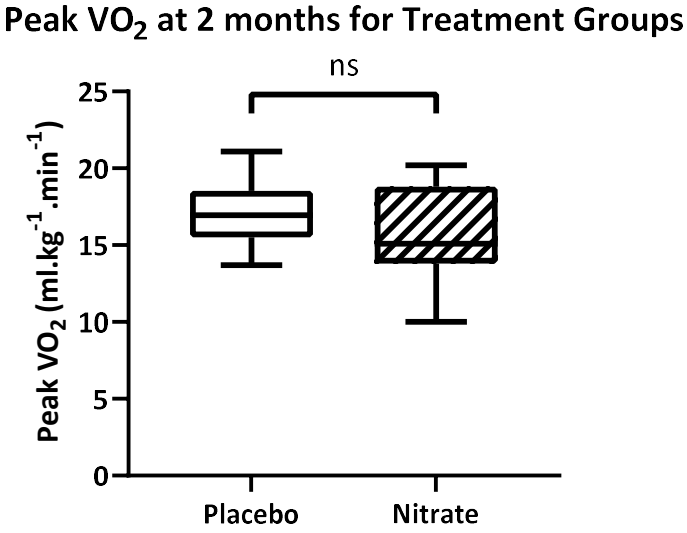

Figure 5-1: Peak VO_2 Following 2 months of Treatment by Intervention Arm.
Peak VO_2 on CPEX testing at 2 months was higher in the placebo group, but this was not statistically significant (peak VO2, 18.5 ± 5.4 vs. 16.6 ± 3.7 $ml.kg^{-1}.min^{-1}$, p=0.41). CPEX testing, cardiopulmonary exercise testing; NS, not significant; VO_2, oxygen consumption.

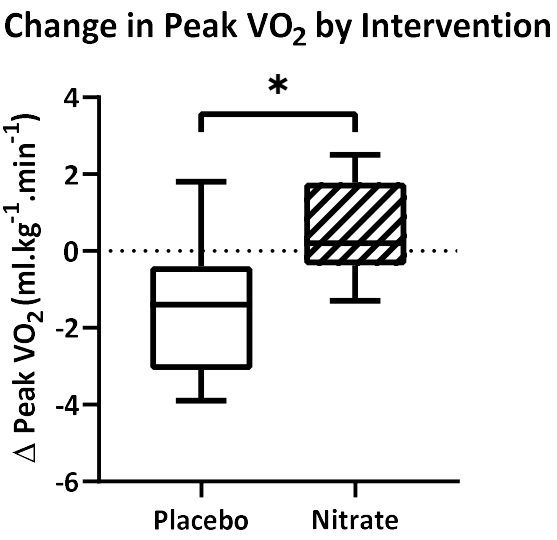

Figure 5-2: Change in Peak VO2 at 2 months by Intervention Arm.
After 2 months of treatment, the *change* in peak VO_2 on CPEX testing was greater in the placebo group, due to a fall compared to baseline in the placebo group and a slight increase in the active treatment arm, and this was statistically significant (Δpeak VO_2, –1.49 ± 1.9 vs. +0.48 ± 1.3 $ml.kg^{-1}.min^{-1}$, p=0.03). CPEX testing, cardiopulmonary exercise testing; VO_2, oxygen consumption.

Change in Secondary Outcomes at 2 months vs. Baseline

Minnesota Living with Heart Failure Questionnaire

There was essentially no change in Minnesota Living with Heart Failure quality of life questionnaire scores (MLWHF) for the placebo (ΔMLWHF, –2 ± 9.4, p=0.56) and nitrate groups (ΔMLWHF, –1 ± 12.5, p=0.59) at 2 months, and the difference in the change between intervention arms was also not statistically significant (ΔMLWHF, placebo vs. nitrate, p=0.91, **Figure 5-3**).

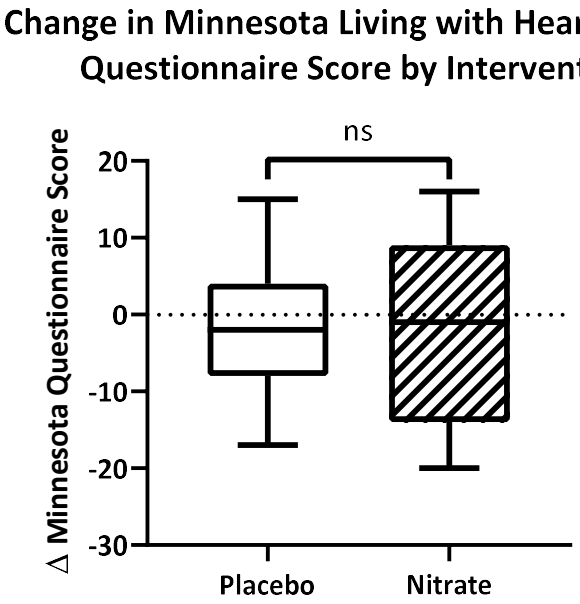

Figure 5-3: Change in Minnesota Living with Heart Failure Questionnaire Score at 2 months by Intervention Arm.

There was no difference in the change in the Minnesota Living with Heart Failure quality of life questionnaire scores between intervention arms (–2 ± 9.4 vs. –1 ± 12.5, p=0.91) at 2 months.

6 Minute Hall Walk Test

There was a slight improvement in 6 minute hall walk test distance (6MWT) for the placebo group (placebo Δ6MWT, +30 ± 22.1 m, p=0.007), and this was statistically significant. In the nitrate group, there was a trend towards an improvement in 6MWT, but this was not statistically significant (Δ6MWT, +63 ± 66.9 m, p=0.17). The difference in the change between intervention arms was also not statistically significant (Δ6MWT, placebo vs. nitrate, p=0.79, **Figure 5-4**).

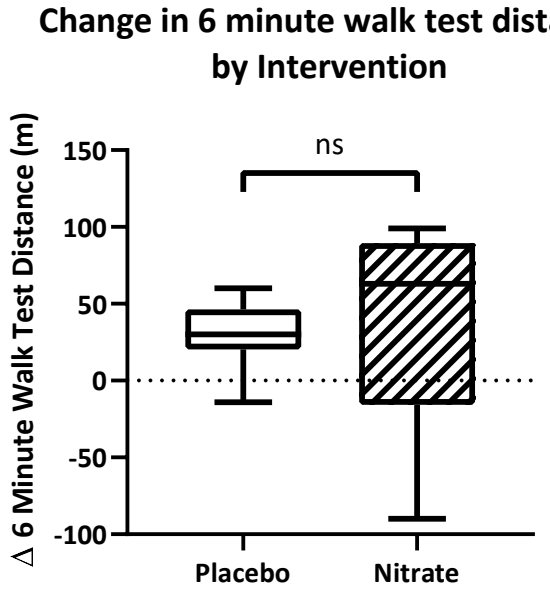

Figure 5-4: Change in 6 Minute Hall Walk Test Distance at 2 months by Intervention Arm.
There was no difference in the change in 6 minute hall walk test distance between intervention arms (+30 ± 22.1 vs. +63 ± 66.9 m, p=0.79).

Exercise Time on CPEX Testing

There was a slight increase exercise time (ET) for both the placebo (ΔET, +26.5 ± 113 s, p=0.20) and nitrate groups (ΔET, +19.5 ± 57 s, p=39) at 2 months, but this was not statistically significant. The difference in the change between intervention arms was also not statistically significant (ΔET, placebo vs. nitrate, p=0.57, **Figure 5-5**).

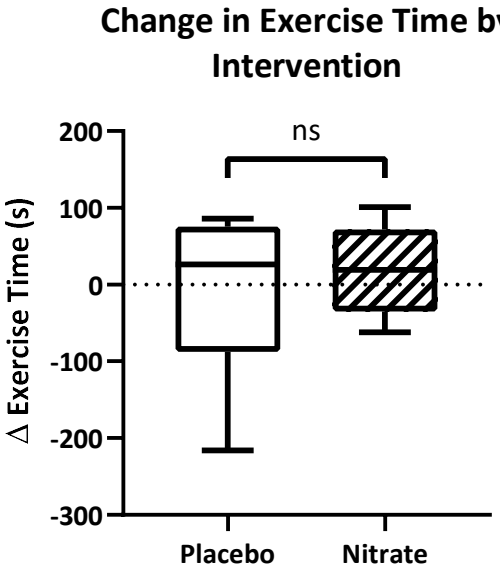

Figure 5-5: Change in Exercise Time at 2 months by Intervention Arm.
There was no difference in the change in exercise time between intervention arms (+26.5 ± 113 vs. +19.5 ± 57 s, p=0.57).

Fasting Plasma Glucose

There was no change in fasting plasma glucose levels (FG) for either placebo (ΔFG, 0 ± 0.85 mmol/L, p=0.73) or nitrate groups (ΔFG, –0.15 ± 0.95 mmol/L, p=0.55) at 2 months. The difference in the change between intervention arms was also not statistically significant (ΔFG, placebo vs. nitrate, p=0.80, **Figure 5-6**).

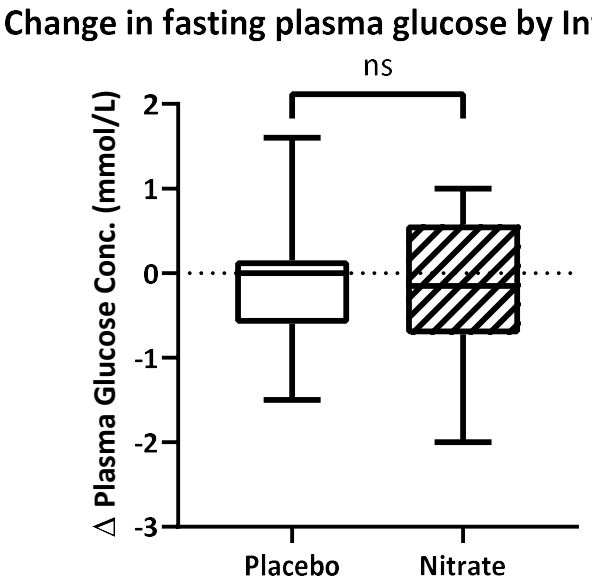

Figure 5-6: Change in Fasting Plasma Glucose Levels at 2 months by Intervention Arm.
There was no difference in the change in fasting plasma glucose levels between intervention arms (0 ± 0.85 vs. –0.15 ± 0.95 mmol/L, p=0.80).

Resting Blood Pressure

There was a larger change in systolic blood pressure (SBP) at 2 months in the inorganic nitrate arm compared to placebo but this failed to reach statistical significance (ΔSBP, placebo vs. nitrate, 0 ± 20.5 vs. –8 ± 14.9 mmHg, p=0.11, **Figure 5-7**). There was no change in SBP in the placebo group (ΔSBP, 0 ± 20.5 mmHg, p=0.43) at 2 months, however, there was a fall in the nitrate group (ΔSBP, –8 ± 14.9 mmHg, p=0.23), but this was not statistically significant. Similarly, there was a larger change in diastolic blood pressure (DBP) at 2 months in the inorganic nitrate arm compared to placebo, but this failed to reach statistical significance (ΔDBP, placebo vs. nitrate, +0.5 ± 13.5 vs. –4 ± 5.7 mmHg, p=0.09, **Figure 5-8**). There was no change in DBP in the placebo group (ΔDBP, +0.5 ± 13.5 mmHg, p=0.48) at 2 months, however, there was a fall in the nitrate group (ΔDBP, –4 ± 5.7 mmHg, p=0.09), but, despite a trend, this was not statistically significant.

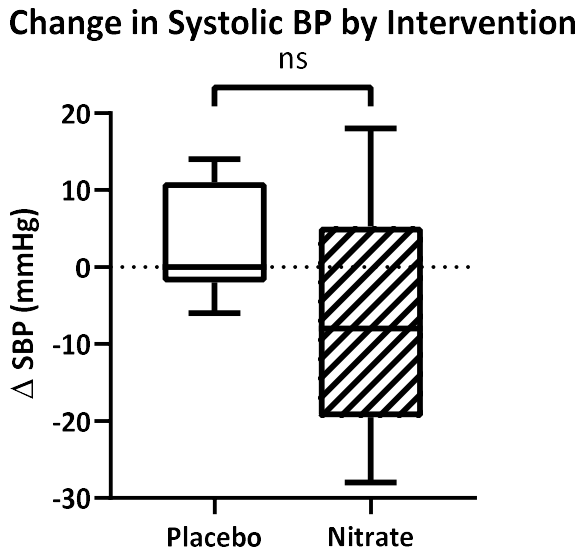

Figure 5-7: Change in Systolic Blood Pressure at 2 months by Intervention Arm.
There was a larger fall in systolic blood pressure at 2 months in the inorganic nitrate arm compared to placebo but this failed to reach statistical significance (0 ± 20.5 vs. –8 ± 14.9 mmHg, p=0.11).

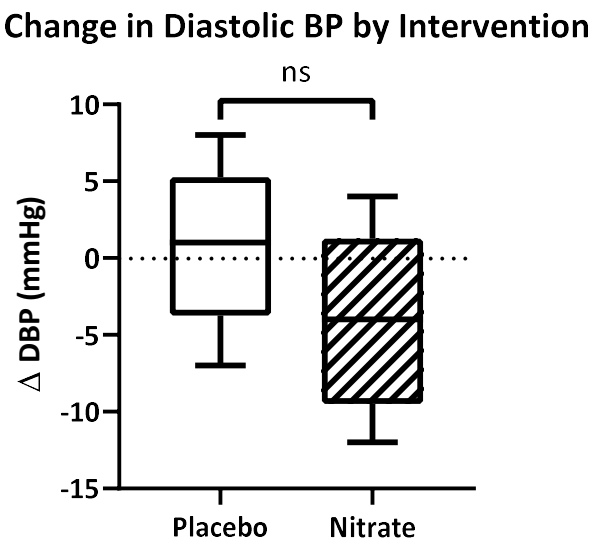

Figure 5-8: Change in Systolic Blood Pressure at 2 months by Intervention Arm. There was a larger fall in diastolic blood pressure at 2 months in the inorganic nitrate arm compared to placebo but this failed to reach statistical significance (+0.5 ± 13.5 vs. –4 ± 5.7 mmHg, p=0.09).

Echocardiographic Data

Cardiac Volumes

There was an increase in left ventricular end diastolic volume (LVEDV) in the placebo group and not in the inorganic nitrate group, but this difference was not statistically significant (ΔLVEDV, placebo vs. nitrate, +36.9 ± 74.9 vs. +1.7 ± 64.6 mL, p=0.51, **Figure 5-9**). However, the change in LVEDV at 2 months was not statistically significant for either the placebo (ΔLVEDV, +36.9 ± 74.9 mL, p=0.43) or nitrate groups (ΔLVEDV, +1.7 ± 64.6 mL, p=0.95). Similarly, left ventricular end systolic volume (LVESV) increased in the placebo group and decreased in the inorganic nitrate group, but this difference was not statistically significant (ΔLVESV, +18.5 ± 51.3 vs. –23.9 ± 51.9 mL, p=0.80, **Figure 5-10**). The change in LVESV at 2 months was not statistically significant for either the placebo (ΔLVESV, +18.5 ± 51.3 mL, p=0.78) or nitrate groups (ΔLVEDV, –23.9 ± 51.9 mL, p=0.94).

Left ventricular ejection fraction (EF) increased in the placebo group at 2 months (due to a greater increase in LVEDV compared to LVESV), and remained unchanged in the inorganic nitrate group, but the difference in the change in EF was not statistically significant (ΔEF, placebo vs. nitrate, +5 ± 10.9 vs. –1.8 ± 19.5 %, p=0.94, **Figure 5-11**). The change in EF at 2 months was not statistically significant compared to baseline for either the placebo (ΔEF, +5 ± 10.9 %, p=0.67) or nitrate groups (ΔLVEDV, –1.8 ± 19.5 %, p=0.88).

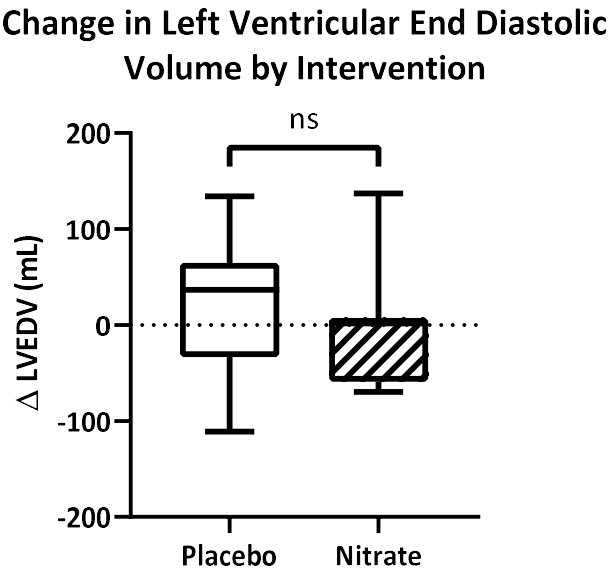

Figure 5-9: Change in Left Ventricular End Diastolic Volume at 2 months by Intervention Arm.
There was an increase in left ventricular end diastolic volume (LVEDV) in the placebo group and not in the inorganic nitrate group, but this difference was not statistically significant (ΔLVEDV, +36.9 ± 74.9 vs. +1.7 ± 64.6 mL, p=0.51).

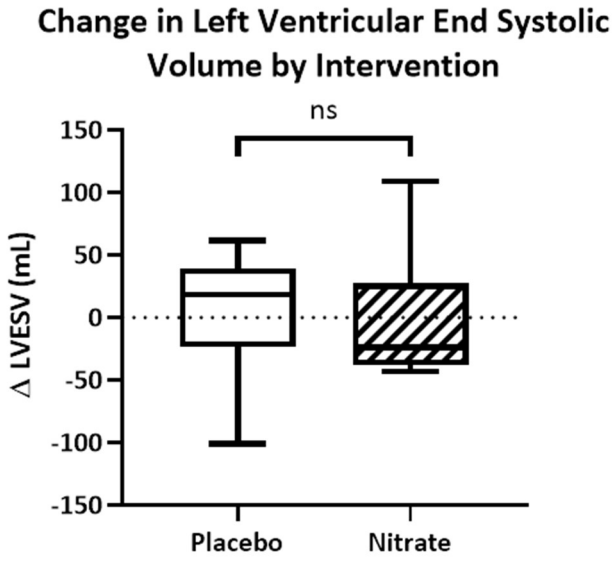

Figure 5-10: Change in Left Ventricular End Systolic Volume at 2 months by Intervention Arm.
Left ventricular end systolic volume (LVESV) increased in the placebo group and decreased in the inorganic nitrate group, but this difference was not statistically significant (ΔLVESV, +18.5 ± 51.3 vs. –23.9 ± 51.9 mL, p=0.80).

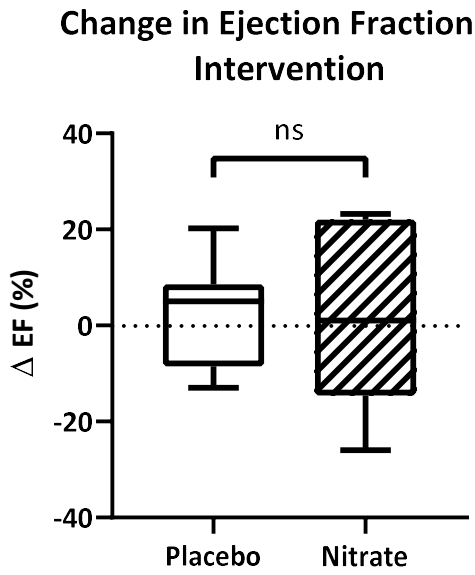

Figure 5-11: Change in Left Ventricular Ejection Fraction at 2 months by Intervention Arm.
Left ventricular ejection fraction (EF) increased in the placebo group, but remained unchanged in the inorganic nitrate group, but the difference in change in EF was not statistically significant (+5 ± 10.9 vs. –1.8 ± 19.5 mL, p=0.94).

Systolic Function

Left ventricular end systolic elastance (Ees_{SB}) fell slightly in the placebo group at 2 months and remained unchanged in the nitrate group but the difference in change in Ees_{SB} was not statistically significant (ΔEes_{SB}, placebo vs. nitrate, –0.1 ± 0.9 vs. 0 ± 0.7, p=0.94, **Figure 5-12**). The change in Ees_{SB} at 2 months was not statistically significant for either the placebo (ΔEes_{SB}, –0.1 ± 0.9, p=0.75) or nitrate groups (ΔEes_{SB}, 0 ± 0.7, p=0.79). V100, a measure of LV pressure when volume is 100 mL (a surrogate for V0 – the x-axis intercept of Ees_{SB}), increased in the placebo group and fell in the nitrate group, but the difference was not statistically significant despite a strong trend (ΔV100, placebo vs. nitrate, +16.1 ± 30.2 vs. –17.8 ± 32.8, p=0.07, **Figure 5-13**). There was a trend towards a statistically significant increase in V100 in the placebo group, but this failed to reach statistical significance (ΔV100, +16.1 ± 30.2, p=0.07). The fall

in V100 in the nitrate group was not statistically significant (ΔV100, –17.8 ± 32.8, p=0.50).

The slope of the left ventricular preload recruitable stroke work relationship (SBMw) fell slightly in the placebo group and increased slightly in the nitrate group at 2 months, however the difference in the change in SBMw was not statistically significant (ΔSBMw, placebo vs. nitrate, –2.2 ± 16.2 vs. +5.5 ± 20.2, p=0.68, **Figure 5-14**). The change in SBMw at 2 months was not significant in either the placebo (ΔSBMw, –2.2 ± 16.2, p=0.74) or nitrate groups (ΔSBMw, +5.5 ± 20.2, p=0.70).

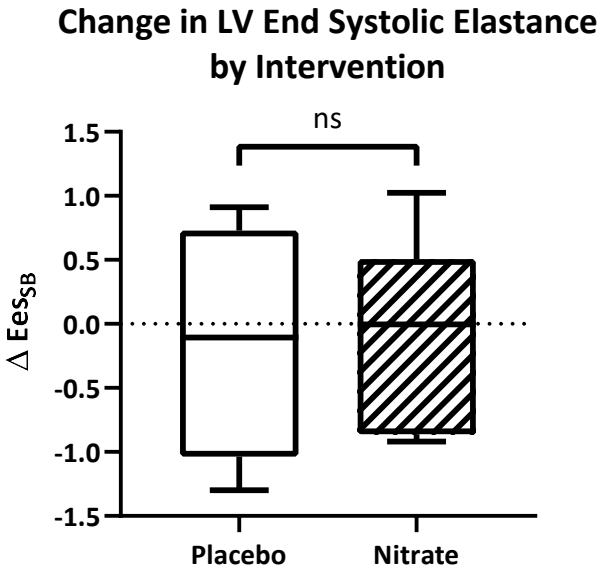

Figure 5-12: Change in LV End Systolic Elastance at 2 months by Intervention Arm. Left ventricular end systolic elastance (Ees_{SB}) fell slightly in the placebo group at 2 months and remained unchanged in the nitrate group, but the difference in change in Ees_{SB} was not statistically significant (–0.1 ± 0.9 vs. 0 ± 0.7, p=0.94).

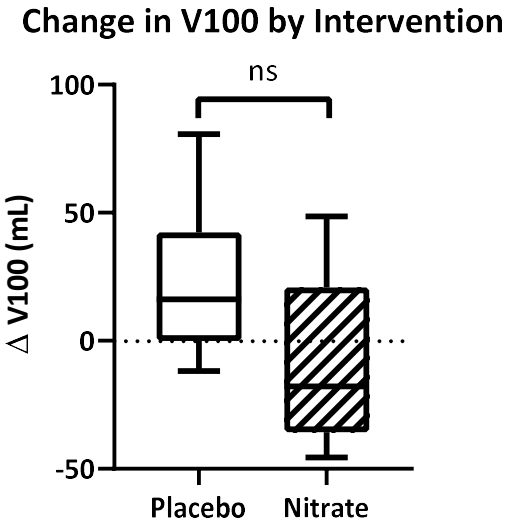

Figure 5-13: Change in Left Ventricular V100 at 2 months by Intervention Arm.
V100, a measure of LV volume when LV pressure is 100 mmHg (a surrogate for V0 – the x-axis intercept of Ees_{SB}), increased in the placebo group and fell in the nitrate group, but the difference was not statistically significant despite a strong trend (+16.1 ± 30.2 vs. –17.8 ± 32.8, p=0.07).

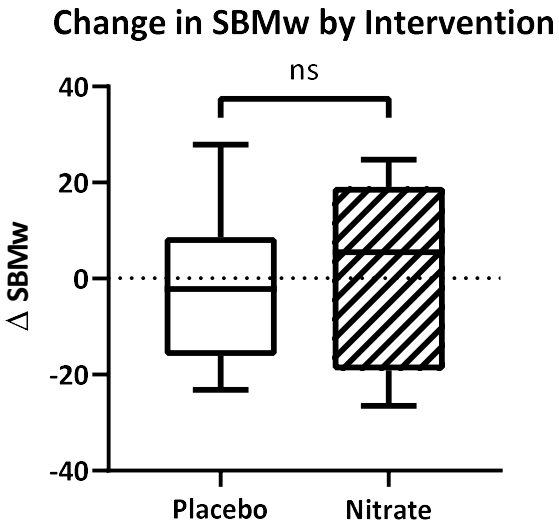

Figure 5-14: Change in the Slope of the Preload Recruitable Stroke Work Relationship (SBMw) at 2 months by Intervention Arm.
The slope of the left ventricular preload recruitable stroke work relationship (SBMw) fell slightly in the placebo group and increased slightly in the nitrate group, however the difference in the change in SBMw was not statistically significant (–2.2 ± 16.2 vs. +5.5 ± 20.2, p=0.68).

Diastolic Function

There was a worsening in diastolic function in the placebo group compared to no change in the nitrate group at 2 months, and this difference was statistically significant (ΔE/E', placebo vs. nitrate, +1.76 ± 2.2 vs. –0.72 ± 1.6, p=0.03, **Figure 5-15**). The change in E/E' at 2 months compared to baseline was statistically significant in the placebo group (ΔE/E', +1.76 ± 2.2, p=0.03), but not the nitrate group (ΔE/E', –0.72 ± 1.6, p=0.26).

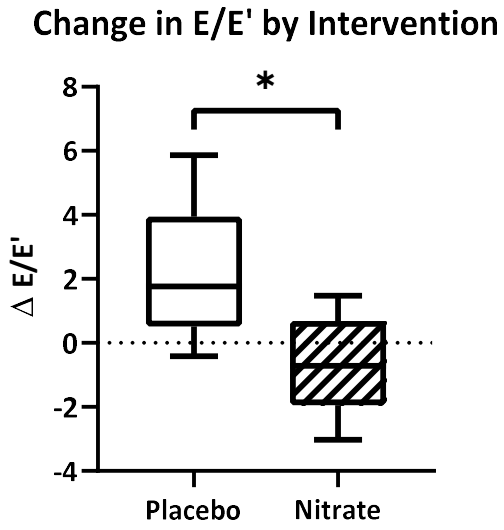

Figure 5-15: Change in Left Ventricular E/E' at 2 months by Intervention Arm.
There was a greater worsening of diastolic function in the placebo group compared to the nitrate group at 2 months, and this difference was statistically significant (ΔE/E', +1.76 ± 2.2 vs. –0.72 ± 1.6, p=0.03).

Global Longitudinal Strain and Right Ventricular Assessment

Unfortunately, there were insufficient sets of paired data to assess global longitudinal strain (GLS) or to assess the right ventricle (due to poor TR jets and RV windows) in either group.

Blood Tests

Results from other blood tests performed on participant plasma samples were, unfortunately, not available due to delays experienced in processing these in Southampton as a result of the COVID-19 global pandemic.

Correlation between E/E' and Delta Peak VO_2

There was a statistically significant negative correlation between the change in E/E' on transthoracic echocardiography and change in peak VO_2 on CPEX testing (r^2=0.43, p=0.03, **Figure 5-16**).

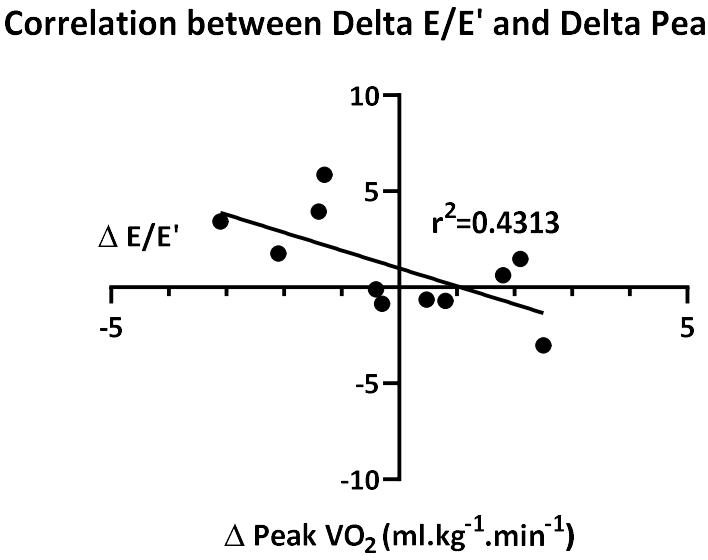

Figure 5-16: Correlation between Change in Left Ventricular E/E' and Peak VO_2 at 2 months by Intervention Arm.
There was a statistically significant negative correlation between the change in E/E' and change in peak VO_2 on CPEX testing at 2 months compared to baseline (r^2=0.43, p=0.03). CPEX testing, cardiopulmonary exercise testing. VO_2, oxygen consumption.

5.5 Discussion

We have demonstrated a statistically significant difference in delta peak VO_2 on CPEX testing following oral inorganic (sodium) nitrate therapy for 2 months in patients with heart failure with reduced ejection fraction (HFrEF) compared to placebo. This appears to be in agreement with the results of other studies of shorter duration. However, interestingly, the difference in our study was due more to a deterioration in exercise capacity in the placebo group, rather than a statistically significant improvement in the active treatment group. The RER in each of the groups was similar both at baseline and at end of study, suggesting that a difference in exertional effort between the 2 groups was not responsible for the observed difference. Similarly, the difference in change in peak HR between groups was not statistically significant, and there were similar rates of beta-blocker therapy use between groups, and they were adequately withheld prior to CPEX testing.

On unblinding, our placebo and nitrate groups were found to be well-matched in terms of baseline demographics (**Table 5-1**). Despite this, diastolic function on transthoracic echocardiography at the baseline visit was worse in patients in the nitrate arm, and this was accompanied by a strong trend towards both worse quality of life scores and peak VO_2 on CPEX at baseline, suggesting poorer baseline functional capacity. After 2 months of treatment, the primary end point (peak VO_2) improved in the nitrate arm (by 0.48 $ml.kg^{-1}.min^{-1}$), but fell in the placebo arm (by 1.49 $ml.kg^{-1}.min^{-1}$). Whilst the difference between nitrate and placebo groups was statistically significant (p=0.03), there was also a strong trend towards statistical significance for the difference in peak VO_2 between baseline and 2 months in the placebo arm. The change in the placebo arm is thought to be due to the effects of time and disease progression (i.e. a fall to the level of the nitrate group), especially given how closely-matched the groups were in terms of patient demographics, NYHA class, and time since diagnosis with HFrEF (**Table 5-1**).

The change in peak VO_2 at 2 months correlated with E/E', the ratio of the early mitral inflow peak velocity (E) to the mitral annular early diastolic velocity (E'). E/E' has been shown to correlate with invasive left ventricular end diastolic pressure (LVEDP), making it an easy-to-measure, non-invasive surrogate for diastolic function on echocardiogram (400). In HFrEF, changes in LVEDP over this timeframe might be expected to be related to a decline in cardiac function (i.e. worsening pump failure), an increase in interstitial fibrosis (e.g. secondary to increased activity of the tissue renin-angiotensin-aldosterone system from neurohormonal activation) (52), or changes in left ventricular chamber dimensions (remodelling) (98). In the current study, cardiac volumes increased slightly in the placebo group at 2 months compared to baseline but this was not statistically significant, and 'chamber-level' measures of LV systolic function remained unchanged (EF, Ees_{SB}, and SBMw). V100, a measure of LV volume when LV pressure is 100 mmHg, increased in the placebo group at 2 months but fell in the nitrate group. There was a strong trend towards statistical significance for the difference in V100 between the two groups (p=0.07), and between the placebo group at 2 months compared to baseline (p=0.07). V100 is a surrogate for V0, the x-axis intercept of the end systolic pressure volume relationship (ESPVR) (347). Despite not reaching statistical significance, an increase in V100 in the placebo arm denotes a rightwards shift in the ESPVR, i.e. a reduction in LV contractility, and an increase in LV volume (see **Figure 1-1**). The latter is supported by the observed increases in LVEDV and LVESV in the placebo group at 2 months. This likely explains the reduction in exercise capacity in the placebo group, and the increase in E/E'.

Unfortunately, the study was halted early by the Sponsor due to doubts regarding study feasibility in terms of recruitment (see section 2.2.1). This was despite an interim analysis performed by the study Data Safety and Monitoring Committee (DSMC) in January 2020 recommending that the study not be terminated prematurely. This was based on recruitment projections indicating that the study was on track, and results of the interim analysis indicating a smaller standard deviation

for the primary endpoint (change in peak VO_2) than anticipated in the original sample size calculations, suggesting that fewer patients would be required to achieve the desired statistical power.

In a clinical study involving 9 patients with HFrEF, inorganic nitrate (beetroot juice containing 11.2 mmol of nitrate) increased knee extension strength (maximal power) on isokinetic dynamometry (310). Small studies have since also demonstrated either an improvement or no difference in peak oxygen consumption (peak VO_2) on cardiopulmonary exercise (CPEX) testing with acute doses of oral inorganic nitrate (312,313,401,402). In a randomised, double-blind, placebo-controlled crossover study of 8 patients with HFrEF, oral inorganic nitrate supplementation with a single dose of beetroot juice (containing 11.2 mmol of nitrate) increased peak VO_2 on CPEX testing at 2 hours post ingestion from 21.4 ± 2.1 to 23.0 ± 2.3 $ml.kg^{-1}.min^{-1}$ ($p<0.05$), with no difference seen with placebo (nitrate-deplete beetroot juice) (312). In another study, 13 patients with HFrEF were randomised in a double-blind crossover fashion to 9 days of beetroot juice or placebo (nitrate-deplete beetroot juice), with a primary endpoint of time to exercise intolerance on constant-load CPEX testing; there was no difference between beetroot juice and placebo in this study (313). Using a primary endpoint of distance walked during incremental shuttle walk tests, a further study demonstrated an improvement in exercise tolerance after a single dose of beetroot juice (with 12.9 mmol inorganic nitrate) compared to placebo (nitrate-deplete beetroot juice) in 11 patients with HFrEF ($p=0.006$) (401). Finally, a small pilot study of 5 patients with HFrEF has also shown an improvement in exercise cardiac output and stroke volume (both $p<0.05$) following an acute dose of inorganic nitrate (beetroot juice) compared to placebo (nitrate deplete beetroot juice) on three-stage submaximal exercise stress echocardiography (402).

Very recently, a definitive randomised controlled, crossover trial of inhaled nebulised nitrite in patients with heart failure with a *preserved* ejection fraction (HFpEF) was completed. The 'Inorganic Nitrite Delivery to Improve Exercise Capacity in Heart

Failure with Preserved Ejection Fraction' or 'INDIE-HFpEF' study randomised 105 patients in a random-order crossover design to 4 weeks of both nitrite and placebo, with a primary end point of peak VO_2. In this study, nitrite failed to demonstrate an improvement in peak VO_2 vs. placebo (13.5 vs. 13.7 $ml.kg^{-1}.min^{-1}$, p=0.27) (317). Inhaled nitrite also failed to improve the secondary endpoints of daily activity levels, quality of life scores, diastolic function on echocardiogram (E/E'), or NT pro BNP levels (317). Despite questions related to dosing, route of administration, and duration of therapy, this study has largely quelled interest in nitrite as a therapy for HFpEF, but left the question of its potential use in HFrEF largely unanswered, particularly given the differences in pathophysiology between the two conditions (129) and the longer-lasting effects of using an alternative administration route, such as with oral inorganic nitrate. It is therefore clear that a large scale trial of inorganic nitrate in HFrEF is needed to confirm the findings of smaller studies. Whilst the current study was designed to be powered to answer this question, it was unfortunately halted early. Fortunately, other large scale trials of inorganic nitrate in HFrEF are underway (e.g. the INIX-HF trial, clinicaltrials.org identifier NCT02797184).

Study Limitations

Due to being halted early, the study is currently inadequately powered to determine whether inorganic nitrate can improve exercise tolerance in patients with HFrEF. However, as discussed, an interim analysis by the study DSMC indicated that fewer patients would be required than stated in the original sample size calculations. The revised number based on these data was 36 patients in total (down from 56 patients), which would have been quite achievable. However, due to the global coronavirus (COVID-19) pandemic, it is clear that the study would have been halted again only months later if reopened. Despite being stopped prematurely, 19 patients completed the study protocol, bringing this study at least on-par with any of the studies to come before it. Additionally, this is the only study to examine the effects of chronic nitrate therapy (2 months), with other studies investigating a single acute dose or a week of treatment. Unfortunately, the COVID-19 pandemic has also caused delays with the

processing of participant blood samples taken during the study. Due to this, we were unable to confirm the expected elevation in plasma nitrate and nitrite levels from inorganic nitrate in the study, thereby complicating our interpretation of the observed lack of effect on peak VO_2 in the nitrate arm. Similarly, other secondary outcomes such as change in nitrated fatty acids, high sensitivity CRP, and NT pro BNP cannot be assessed. Finally, there were insufficient paired GLS data to assess the change in GLS with nitrate or placebo, as well as insufficient RV views and TR jets to assess RV function, and so these data were not included.

5.6 Conclusions

Exercise capacity (peak VO_2) fell at 2 months in the placebo arm in our study, but remained unchanged in the inorganic nitrate arm. The fall in peak VO_2 correlated with an increase in E/E' and was associated with an increase in V100, implying worsening diastolic function, reduced LV contractility, and increased LV size (chamber dilatation). Baseline exercise capacity and diastolic function were slightly better in the placebo group, with the groups becoming more similar at 2 months. Thus, our data indicate an effect from time and disease progression in the placebo arm, and a lack of effect from inorganic nitrate in the treatment arm. A definitive large scale clinical trial is still sorely needed to confirm the effects of oral inorganic nitrate therapy in patients with HFrEF.

Table 5-1: Demographics, Baseline Symptoms, and CMR Data

	Placebo (n=10)	**Inorganic Nitrate (n=9)**	**P value**
Demographics Data			
Age (years)	64 ± 10.6	64 ± 13.0	0.98
Male (n [%])	8 (80)	7 (78)	0.99
BMI (kg/m^2)	30.2 ± 4.1	29.2 ± 5.4	0.65
SBP (mmHg)	118.1 ± 17.4	124.5 ± 18.0	0.44
DBP (mmHg)	75.2 ± 10.6	73.6 ± 10.8	0.75
Heart Rate (bpm)	73 ± 7.3	68 ± 7.5	0.15
Fasting Glucose (mmol/L)	5.21 ± 0.62	5.34 ± 0.55	0.35
Time since diagnosis (years)	8.0 ± 4.6	7.8 ± 3.7	0.90
MLWHF Questionnaire Score	8.4 ± 8.0	22.3 ± 19.9	0.06
NYHA Class II Sx	10 (100)	9 (100)	1.00
6 Minute Walk Distance (m)	554.5 ± 104	474.3 ± 75	0.30
Aetiology of DCM (n [%])			
Idiopathic	5 (50)	3 (33.3)	0.65
Genetic (TTNtv)	1 (10)	1 (11.1)	0.99
Myocarditis	3 (30)	0 (0)	0.21
Alcohol	0 (0)	2 (22.2)	0.21
Tachycardia	0 (0)	2 (22.2)	0.21
Chemotherapy	1 (10)	1 (11.1)	0.99
Comorbidities (n [%])			
Hypertension	3 (30)	3 (33.3)	0.99
Type 2 Diabetes Mellitus	2 (20)	0 (0)	0.47
History of AF	1 (10)	3 (33.3)	0.30
Obesity	2 (20)	3 (33.3)	0.63
Hypercholesterolaemia	4 (40)	4 (44.4)	0.99
Renal Failure	1 (10)	0 (0)	0.99
History of CVA	2 (20)	2 (22.2)	0.99
Drug Therapy (n [%])			
Aspirin	2 (20)	1 (11.1)	0.99
Beta-blocker	9 (90)	8 (88.8)	0.99
ACE-I or ARB	8 (80)	8 (88.8)	0.99
Entresto	2 (20)	1 (11.1)	0.99
Ivabradine	0 (0)	1 (11.1)	0.47
Statin	6 (60)	5 (55.5)	0.99
Ca^{2+} channel blocker	0 (0)	0 (0)	1.00
Loop diuretic	4 (40)	4 (44.4)	0.99

MRA	4 (40)	7 (77.7)	0.17
PPI	1 (10)	4 (44.4)	0.14
Allopurinol	1 (0)	0 (0)	0.99
PDE blocker	1 (0)	0 (0)	0.99
Cardiac Device (n [%])			
CRT-D	3 (30)	2 (22.2)	0.99
ICD	1 (10)	1 (11.1)	0.99
Cardiovascular Magnetic Resonance Imaging Data (at diagnosis)			
Fibrosis Pattern on CMR (n [%])			
Any Fibrosis	7 (70)	5 (55.5)	0.65
Mid Wall Fibrosis	5 (50)	5 (55.5)	0.99
Subepicardial Fibrosis	2 (20)	0 (0)	0.47
Infarction Pattern Fibrosis	0 (0)	0 (0)	1.00

Values are mean ± SD or n (%).Demographics, Baseline Symptoms, and CMR Data. ACE-I, angiotensin converting enzyme inhibitor; AF, atrial fibrillation; ARB, angiotensin receptor blocker; BMI, body mass index; CRT-D, cardiac resynchronisation therapy device with defibrillator; CVA, cerebrovascular accident; DBP, diastolic blood pressure; DCM, dilated cardiomyopathy; ICD, implantable cardiac defibrillator; MLWHF, Minnesota Living with Heart Failure; MRA, mineralocorticoid receptor antagonist; NYHA, New York Heart Association; PDE, phosphodiesterase inhibitor; PPI, proton pump inhibitor; SBP, systolic blood pressure; TTNtv, titin truncating variant.

Table 5-2: Baseline Echocardiography and Exercise Data

	Placebo (n=10)	**Inorganic Nitrate (n=9)**	**P value**
Echocardiography Data			
IVSd (cm)	0.96 ± 0.3	0.91 ± 0.1	0.62
PWd (cm)	0.91 ± 0.2	0.89 ± 0.1	0.80
LVIDd (cm)	5.53 ± 0.7	5.57 ± 0.7	0.89
LVIDs (cm)	4.34 ± 0.6	4.37 ± 0.7	0.90
LVOT diameter (cm)	2.38 ± 0.2	2.32 ± 0.2	0.53
LVEDV (mL)	136.4 ± 38.1	140.2 ± 41.2	0.84
LVESV (mL)	76.0 ± 18.2	83.7 ± 42.8	0.61
SV (mL)	73.4 ± 19.3	71.5 ± 18.0	0.83
EF (%)	43 ± 7.3	43 ± 10.9	0.89
E (m/s)	0.40 ± 0.12	0.62 ± 0.17	0.007*
A (m/s)	0.68 ± 0.13	0.78 ± 0.13	0.13
E/A ratio	0.62 ± 0.27	0.80 ± 0.20	0.17
E'_{septal}	5.15 ± 1.2	5.69 ± 1.1	0.37
$E'_{lateral}$	7.91 ± 1.8	7.21 ± 2.0	0.48
$E/E'_{average}$	6.9 ± 2.2	10.4 ± 3.8	0.04*
Ees_{SB}	1.62 ± 0.44	1.91 ± 0.51	0.20
V_{100}	42.4 ± 21.2	43.1 ± 28.4	0.95
SBMw	62.4 ± 14.4	61.3 ± 12.5	0.86
Cardiopulmonary Exercise Testing Data			
Exercise Time (s)	834 ± 135	833 ± 174	0.98
Peak VO_2 ($ml.kg^{-1}.min^{-1}$)	18.8 ± 4.2	15.9 ± 3.3	0.11
% of predicted Peak VO_2	58 ± 14.7	48 ± 10.3	0.12
Peak HR (bpm)	139 ± 17.6	141 ± 25.3	0.84
VE/VCO_2 slope	26.5 ± 3.4	30.9 ± 6.5	0.07
RER	1.10 ± 0.06	1.12 ± 0.05	0.33

Values are mean ± SD. Baseline Echocardiography and Exercise Data. A, late mitral inflow peak velocity; E, early mitral inflow peak velocity; E', mitral annular early diastolic peak velocity; Ees_{SB}, single beat LV end systolic elastance; EF, ejection fraction; HR, heart rate; IVSd, interventricular septum thickness in diastole; LVEDV, left ventricular end diastolic volume; LVESV, left ventricular end systolic velocity; LVIDd, left ventricular internal diameter in diastole; LVIDs, left ventricular internal diameter in systole; LVOT, left ventricular outflow tract; PWd, LV posterior wall thickness in diastole; RER, respiratory exchange ratio; SBMw, slope of the preload recruitable stroke work relationship; SV, stroke volume; VE/VCO_2, minute ventilation to carbon dioxide production; V100, LV volume when LV pressure is 100 mmHg.

Chapter 6: Myocardial Energetic Deficiency in Non-obstructive Hypertrophic Cardiomyopathy and Association with Vasculoventricular Coupling and Exercise Capacity

6.1 Abstract:

Background: Cardiac energetic status is reduced in patients with non-obstructive hypertrophic cardiomyopathy (HCM) compared to controls. We hypothesized that this would result in dynamic impairment of both left ventricular (LV) diastolic and systolic function on exercise, and contribute to exercise limitation.

Methods: Fifty-one patients with symptomatic non-obstructive HCM (39 males; mean age 54 years), and thirty-three age- and sex-matched controls were enrolled, and underwent resting ^{31}P cardiovascular magnetic resonance spectroscopy to assess myocardial energetic status (PCr/γATP ratio). Cardiopulmonary exercise testing to measure peak oxygen consumption (peak VO_2) and radionuclide ventriculography to assess the changes in contractile function (LV end systolic elastance index, $E_{LV}I$), vasculoventricular coupling (VVC) ratio and time to peak filling (normalized to RR interval; nTTPF) with exercise, were then performed and tested for their associations with resting PCr/γATP ratio.

Results: Compared to controls, HCM patients exhibited markedly reduced peak VO_2 (24±6 ml/kg/min vs. 38±8 ml/kg/min; $p<0.0001$) and cardiac PCr/γATP ratios (1.41±0.48 vs. 2.26±0.59; $p<0.0001$). During exercise, nTTPF shortened in controls but increased in patients (0.19±0.09s to 0.16±0.08s vs. 0.17±0.07s to 0.32±0.09s; $p<0.0001$). VVC ratio fell in controls during exercise but much less so in HCM patients (δVVC, −0.25±0.19 vs. −0.06±0.24, $p=0.006$), due to a greater relative increase in $E_{LV}I$ in controls (1.7±0.7 vs. 1.24±0.68; $p<0.05$). In HCM patients, resting PCr/γATP ratio correlated with peak VO_2 ($r=0.52$; $p<0.001$), and with the change in nTTPF ($r=–0.47$; $p=0.003$) and VVC ratio ($r=–0.40$; $p=0.02$) with exercise.

Conclusion: Impaired myocardial energetic status in HCM is associated with dynamic diastolic and systolic dysfunction, and correlates significantly with reduced exercise capacity.

6.2 Introduction

Hypertrophic cardiomyopathy (HCM) is a common inherited cardiac condition, frequently caused by genetic mutations in cardiac sarcomere proteins (403). Updated estimates now suggest that HCM may affect around 1 in 200 people (404). While sudden cardiac death is the most important complication of the disease, patients may also experience debilitating symptoms (including dyspnoea) that limit exercise capacity, sometimes profoundly. In patients with provocable left ventricular outflow tract (LVOT) obstruction, this is the primary mechanism for exercise limitation, and septal reduction therapies have proven highly effective (405,406). Patients without obstruction may also be severely symptomatic however, and management of their symptoms remains challenging. Diastolic dysfunction represents a significant contribution to exercise limitation in these patients. Left ventricular (LV) relaxation is typically slowed and filling rate is diminished at rest (407). Furthermore, we have showed there is frequently failure to increase the rate of LV active relaxation with exercise in patients with non-obstructive HCM; indeed in some patients, active relaxation paradoxically slowed on exertion (408). Although resting measures of diastolic function poorly correlated with peak oxygen consumption (VO_2), time to peak filling, a measure of the rate of LV active relaxation assessed during submaximal exercise, was inversely related to peak VO_2 (408). We have also showed that Perhexiline, a metabolic modulating agent, increased cardiac PCr/ATP ratio on 31P cardiovascular magnetic resonance spectroscopy (CMRS) in patients with non-obstructive HCM, and this was associated with a correction of the abnormal slowing of LV active relaxation on exercise and, in turn, an increase in peak VO_2 (409).

There has also been increasing interest in the role of exercise-induced systolic dysfunction in the pathophysiology of HCM. In the majority of patients, resting left ventricular ejection fraction (LVEF) is normal or supernormal, yet subtle impairment of systolic function (such as impaired long axis systolic function and strain) are frequently present (410). A subgroup of patients may also develop a progressive

impairment of LVEF, usually associated with worsening of symptom status (411). Compared to LVEF as a measure of LV contractile function, non-invasively derived end-systolic elastance (ELV) is less affected by loading conditions (347). In order to maximize myocardial efficiency and thereby prevent energy wastage, LV contractility and afterload are normally closely matched at rest. The ratio of LV afterload, represented by the arterial elastance (Ea), and ELV is called the vasculoventricular coupling (VVC) ratio and describes myocardial efficiency/performance. On exercise in healthy subjects, Ea increases slightly, but there is a much larger increase in ELV resulting in a fall in the VVC ratio (412), thereby increasing stroke work and cardiac output. Increased resting large artery stiffness was reported to be associated with reduced exercise capacity in patients with HCM, presumably by disturbing VVC (413).

In this study we sought to determine the relationship between severity of resting cardiac energetic deficiency on 31P CMRS and measures of systolic and diastolic and function and VVC during submaximal exercise using radionuclide ventriculography, and with peak VO2. In order to control for the important effects of betablockers on cardiac inotropy and lusitropy, group comparisons were repeated after excluding patients on betablockers.

6.3 Methods

The data from this study was obtained by Dr Ibrar Ahmed, Dr Khalid Abozguia, and Dr Thanh Phan at the University of Birmingham. Briefly, fifty-one patients with non-obstructive HCM (39 males) and 33 age and sex-matched controls (20 males) were included in the study following written informed consent. The Local National Health Service (NHS) Research Ethics Committee approved the study, which conformed to the principles outlined in the Declaration of Helsinki. All study participants underwent baseline electrocardiogram (ECG), echocardiogram, and cardiopulmonary exercise testing.

6.3.1 Patient selection

All HCM patients were in sinus rhythm and fulfilled conventional echocardiographic criteria for the diagnosis of HCM as previously described (414,415). All patients underwent assessment for left ventricular outflow tract (LVOT) obstruction, and those with a resting or provocable gradient >30mmHg were excluded. Significant epicardial coronary artery disease had been excluded in all patients with a history of chest pain by coronary angiography. Controls had no history or symptoms of cardiovascular disease, with normal ECGs and echocardiograms (LV ejection fraction ≥ 55%).

6.3.2 Cardiopulmonary exercise testing

Cardiopulmonary exercise (CPEX) testing was performed using a Schiller CS-200 Ergo-Spiro exercise machine, which was calibrated prior to each study. Subjects first underwent spirometry, which was followed by symptom-limited erect treadmill exercise testing using a standard ramp protocol with simultaneous respiratory gas analysis (416,417). Sampling of expired gases was performed continuously, and data were expressed as 30-second means. Minute ventilation (VE), oxygen consumption (VO_2), carbon dioxide production (VCO_2), and respiratory exchange ratio (RER) were obtained. Peak oxygen consumption (peak VO_2) was defined as the highest VO_2 achieved during exercise and was expressed in ml/kg/min. Blood pressure and ECG were monitored throughout. Patients were encouraged to exercise to exhaustion with a minimal RER requirement of 1.0.

6.3.3 Resting echocardiography

Echocardiography was performed with participants in the left lateral decubitus position using a GE Vivid 7 echocardiographic machine with a 2.5MHz transducer. Measurements were averaged over 3 beats and were stored digitally and analyzed

offline. Resting standard parasternal long and short-axis views, as well as apical 4-chamber and apical 2-chamber views, were acquired as previously described (418), and left ventricular ejection fraction (LVEF) was calculated from a modified Simpson's biplane formula (419). A pulse wave Doppler sample volume was placed at the tip of the mitral valve leaflets and averaged over 3 cardiac cycles. Mitral annular velocities (acquired from tissue Doppler imaging, TDI) were recorded from the basal anterolateral and basal inferoseptal walls in the apical 4-chamber view. LA volumes were measured by the area-length method from apical 2-chamber and 4-chamber views as previously described (419).

6.3.4 Radionuclide ventriculography

Equilibrium R-wave gated blood pool scintigraphy at rest and during graded semierect exercise on a cycle ergometer was used to measure LVEF and diastolic filling as previously described by our group (408,420,421). Three minutes of data were acquired at rest and during exercise (after a 1-minute period for stabilization of heart rate at the commencement of the exercise). Exercise was performed at a workload designed to achieve 50% of heart rate reserve. Data were analysed using LinkMedical MAPS software (Sun Microsystems, Hampshire, UK). Peak left ventricular filling rate was calculated in terms of end-diastolic count per second (EDC/s) and time to peak filling after end-systole normalized for R-R interval (nTTPF) was calculated from the first derivative of the diastolic activity-time curve.

Stroke volume indexed to body surface area (SVI), and end systolic pressure (estimated as 90% of brachial artery systolic blood pressure), were used to calculate the arterial elastance index (i.e. EaI = ESP/SVI) (412,421). The LV end-systolic elastance index ($E_{LV}I$) was calculated from the end systolic pressure and end systolic volume index (i.e. ESP/ESVI). The VVC ratio (EaI/$E_{LV}I$) was calculated from the LV end systolic volume index and stroke volume index (ESVI/SVI). Relative changes in $E_{LV}I$ and

EaI from rest to exercise (i.e. exercise/rest) and net change in VVC ratio (i.e. exercise–rest) were then calculated.

6.3.5 ^{31}P cardiovascular magnetic resonance spectroscopy

^{31}P cardiovascular magnetic resonance spectroscopy (CMRS) was performed using a Phillips Achieva 3T scanner to measure *in vivo* myocardial energetics both in controls and HCM patients as previously validated by us (422). Using the pre-processing operations within jMRUI, signals were Fourier transformed, phase corrected, and apodized by 15Hz. The AMARES (advanced method of accurate, robust and efficient spectroscopic fitting) algorithm was used to fit for phosphocreatine (PCr), adenosine triphosphate (ATP), phosphodiesters, and 2,3-diphosphoglycerate (**Figure 6-1**). The PCr/γATP ratio was then calculated as a measure of resting cardiac energetic state (423).

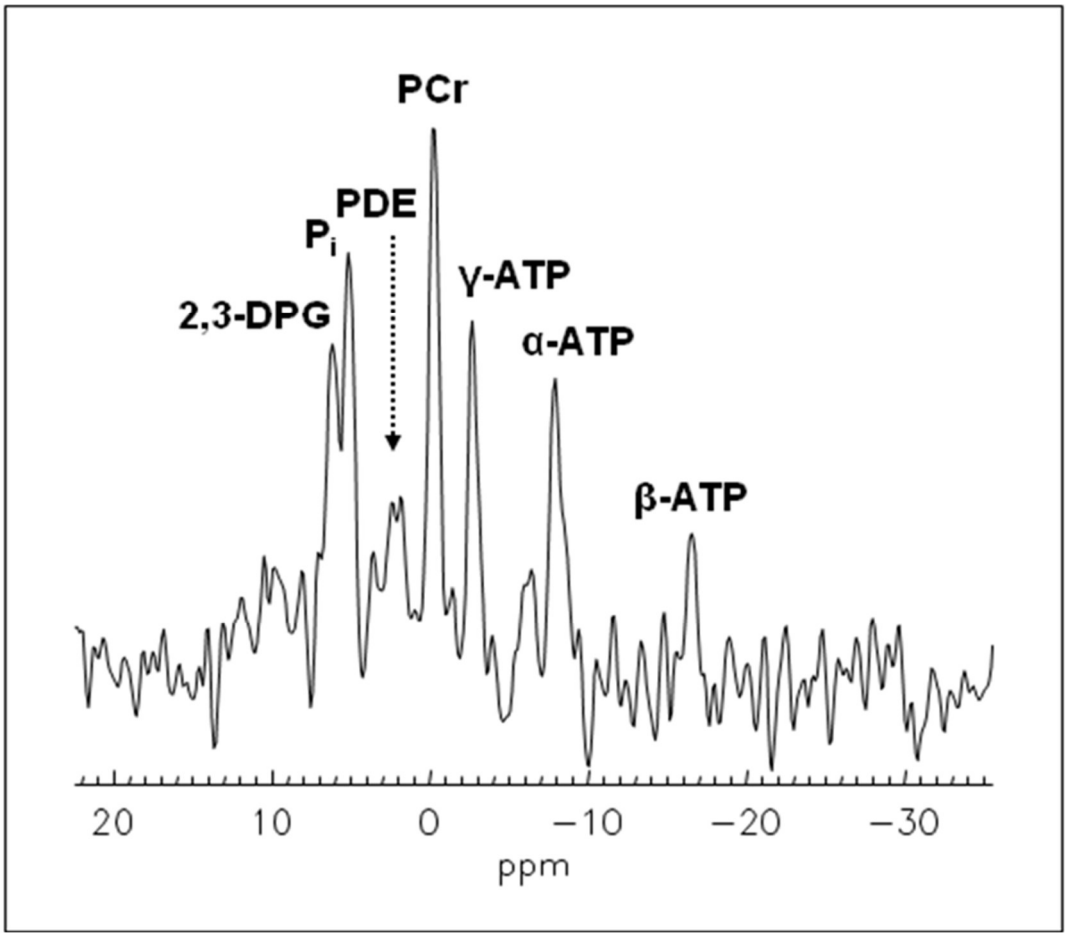

Figure 6-1: An Example of a ^{31}P Cardiac Spectrum.
2,3-DPG, 2,3-diphosphoglycerate; ATP, adenosine triphosphate; PDE, phosphodiesters; PCr, phosphocreatine; Pi, inorganic phosphorus; α, β,γ indicate the three phosphorus nuclei of ATP.

6.3.6 Statistics

Data were analyzed using SPSS version 23.0 for Windows. Data were normally distributed and expressed as mean $\pm$ standard deviation (SD). Comparisons of variables were made using the Student's t-test (2-tail). Categorical variables were compared with the Pearson chi-squared test. A value of $p<0.05$ was taken to indicate statistical significance. Pearson's correlation coefficient was used to describe the relationship between variables. Analyses were repeated after excluding HCM patients who were on betablocker therapy where indicated.

6.4 Results

The clinical characteristics and CPEX test results of HCM patients and controls are shown in **Table 6-1**. Groups were well-matched with respect to age and sex. Patients exhibited marked exercise limitation compared to controls, whereas left ventricular ejection fraction was similar between groups. Heart rate was lower in the HCM group compared to controls, likely due to differences in the prescription of rate-limiting medications (betablockers and non-dihydropyridine calcium channel blockers).

Conventional echocardiographic measurements

Standard, Doppler, and TDI echocardiographic findings of HCM and control groups are listed in **Table 6-2**. Transmitral Doppler measurements showed no significant differences in peak trans-mitral early diastolic velocity (E), trans-mitral late diastolic velocity (A), and E/A ratio in HCM patients versus controls. However, myocardial peak systolic velocity (S'), myocardial peak early diastolic velocity (E'), and myocardial peak late diastolic velocity (A') of the inferoseptal and anterolateral basal segments were significantly lower in HCM patients compared to controls (**Table 6-2**).

Cardiac energetic status

Five healthy controls were unable to complete the CMRS studies due to claustrophobia. Fifteen HCM patients were excluded from the CMRS studies: 8 due to claustrophobia, 4 due to poor quality spectra (either due to inadequate ECG-gating or shimming), and 3 due to high risk history for potential metallic foreign bodies in their eyes. In the remaining patients, resting cardiac PCr/γATP ratio was significantly reduced in HCM patients compared to controls (1.41$\pm$0.48 vs. 2.26$\pm$0.59; $p<0.0001$), and this remained true after excluding those patients on betablockers (1.35$\pm$0.48 vs 2.26$\pm$0.59, respectively; $p<0.0001$; **Figure 6-2**).

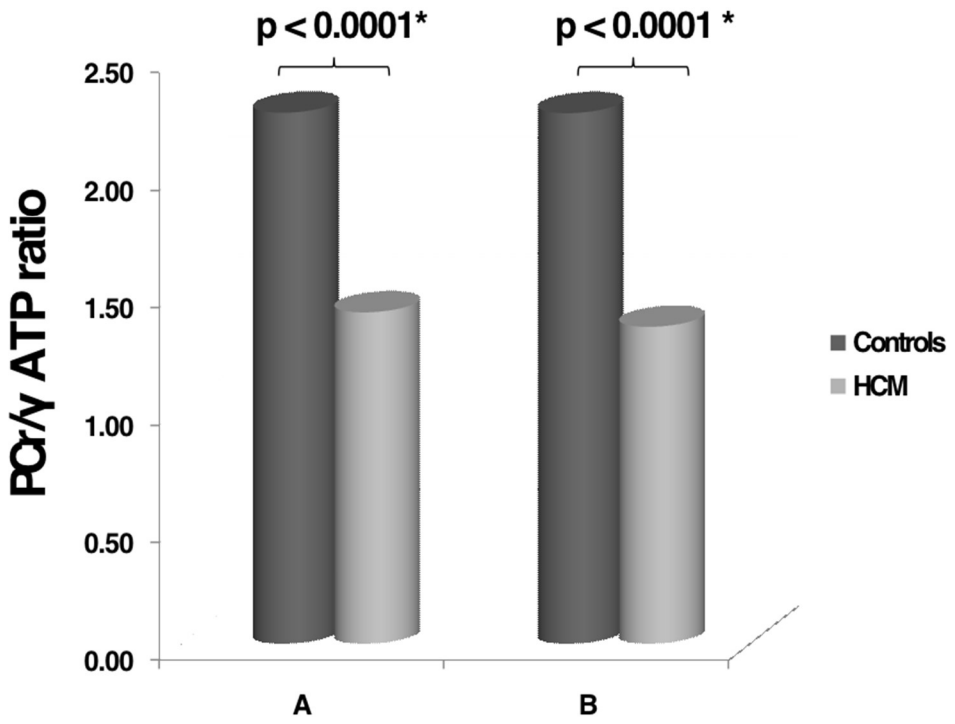

Figure 6-2: Cardiac PCr/γATP Ratio in HCM Patients and Controls.
A – all HCM patients and controls; B – HCM patients excluding those on betablockers and controls. Both HCM groups exhibit significant reductions in cardiac energetics compared to controls. γATP, adenosine triphosphate gamma peak; PCr, phosphocreatine.

Contractile function and vasculoventricular coupling at rest and during submaximal exercise

VVC ratio decreased significantly on exercise in healthy control subjects (from 0.60±0.21 to 0.41±0.15; p=0.003). A reduction in VVC ratio was also seen in HCM patients on exercise, however this did not reach statistical significance (from 0.55±0.3 to 0.46±0.24; p=0.28; **Table 6-3**). The difference between patients and controls was significant (**Figure 6-3, panel A**), and this was principally due to a greater increase in LV contractility during exercise in controls versus patients (relative $\Delta E_{LV}I$, 1.7±0.7 vs. 1.2±0.7; p<0.05; **Figure 6-3, panel B**). There was no significant difference in the

change in arterial elastance during exercise between patients and controls (relative ΔEaI, 1.43±0.73 vs. 1.28±0.44; p=0.27; **Table 6-3; Figure 6-3, panel C**). LVEF significantly increased during exercise in controls (64±9% to 72±8%; p=0.005) but not in patients (68±13% to 70±11%; p=0.40).

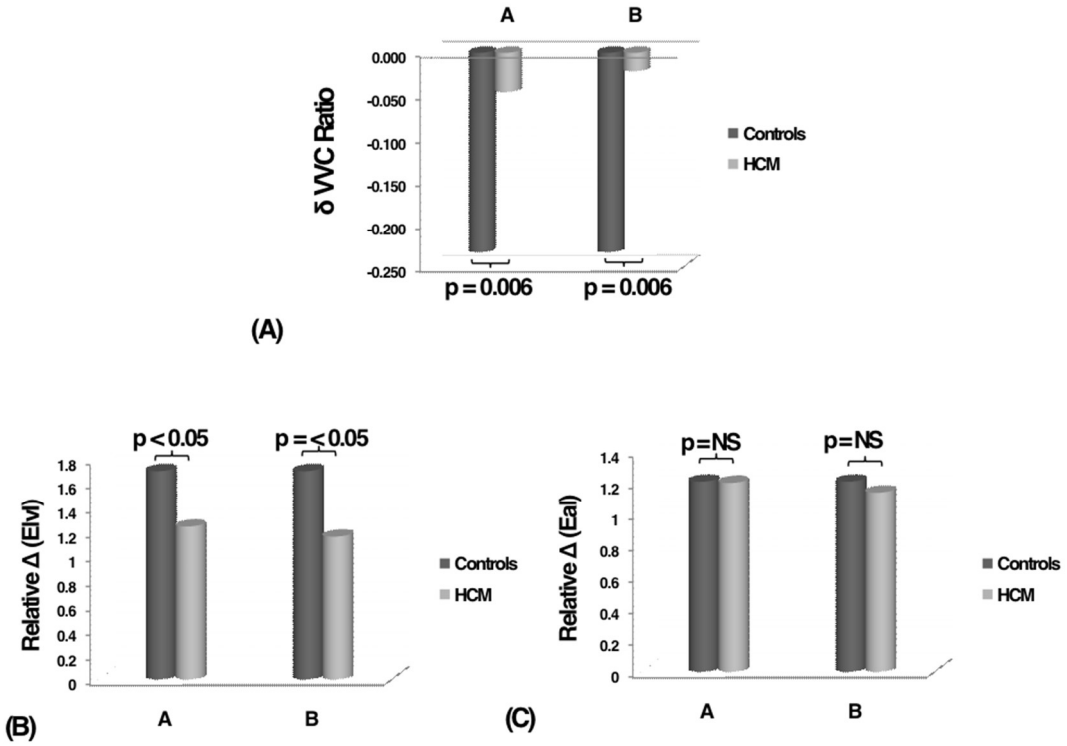

Figure 6-3: Vasculoventricular Coupling (VVC) in HCM Patients and Controls with Exercise.
(A) change in VVC ratio with exercise; (B) relative change in $E_{LV}I$; (C) relative change in EaI; A – comparison between all HCM patients and controls; B – comparison between HCM patients not on betablockers and controls. EaI, arterial elastance index; $E_{LV}I$, LV end-systolic elastance index; NS, non-significant; Relative ΔEaI = exercise elastance / resting elastance; Relative $\Delta E_{LV}I$ = exercise elastance / resting elastance; δVVC Ratio = exercise – rest.

LVEF fell by 5% or more during exercise in 8 HCM patients. In this subgroup, VVC ratio paradoxically increased with exercise (0.45±0.21 vs. 0.64±0.24; p<0.001), due to a significantly greater increase in arterial elastance (relative ΔEaI, 2.09±0.73 vs.

1.17±0.56; p=0.005). The change in LV contractility on exercise in this subgroup did not differ from that observed in the other HCM patients (relative $\Delta E_{LV}I$, 1.43±0.67 vs. 1.52±0.64; p=0.75). Patients with a fall in LVEF did not differ significantly from those without a fall in LVEF in terms of age (52±11years vs 57±12years; p=0.32), peak systolic blood pressure (158±27mmHg vs 172±37mmHg; p=0.25), or peak heart rate (140±29bpm vs 135±24 bpm; p=0.67). In contrast, no controls exhibited a fall in LVEF. These results remained statistically similar after excluding HCM patients who were on betablockers (**Table 6-4**).

Resting and exercise diastolic function

At rest, normalized time to peak filling (nTTPF) was similar between HCM patients and controls (0.17±0.07s vs. 0.19±0.09s; p=0.38). During submaximal exercise however, nTTPF shortened in controls (0.19±0.09s to 0.16±0.08s), but lengthened in patients (0.17±0.07s to 0.32±0.09s). The difference in the change in nTTPF on exercise between patients and controls was statistically significant (p<0.0001; **Table 6-3; Figure 6-4, panel A**). These results remained significant after excluding patients on betablockers (p<0.0001; **Figure 6-4, panel B**).

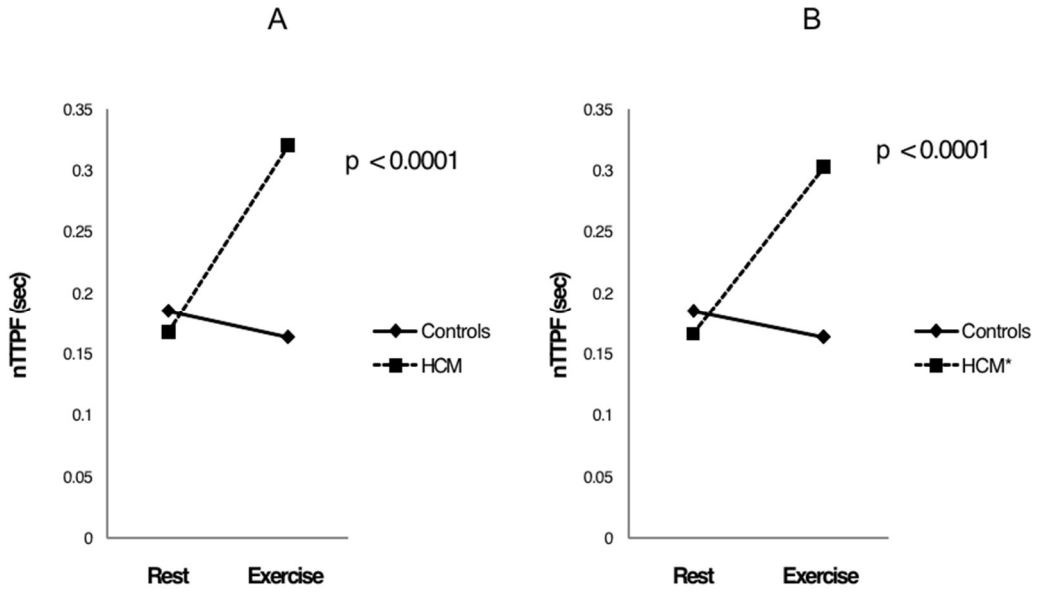

Figure 6-4: Time to Peak Filling Normalized for RR Interval (nTTPF) at Rest and During Exercise (50% Workload of Heart Rate Reserve).

A – comparison between all HCM patients and controls; B – comparison between HCM patients not on betablockers and controls. During exercise, nTTPF shortened in controls but lengthened in HCM patients. *These results remained statistically significant after excluding patients on betablockers. HCM, hypertrophic cardiomyopathy; nTTPF, normalized time to peak filling.

Relationship between change in contractile and diastolic function during exercise and in vivo cardiac energetic status

In HCM patients, resting cardiac PCr/γATP ratio inversely correlated with nTTPF during exercise (r=–0.47, p=0.003), and with the change in VVC ratio (δVVC ratio; r=–0.40, p=0.02; **Table 6-4**). These correlations remained significant after excluding patients on betablockers (r=–0.48, p=0.007; and r=–0.40, p=0.03; respectively; **Table 6-4**). There was no correlation between resting PCr/γATP ratio and relative $\Delta E_{LV}I$ or relative ΔEaI (r=0.15, p=0.44; and r=–0.21, p=0.27; respectively; **Table 6-4**). Similarly, there was no correlation between resting PCr/γATP ratio and the change in LVEF during exercise (r=0.13; p=0.45). PCr/γATP did not differ between HCM patients in whom LVEF increased during exercise and those in whom it fell during exercise.

Relationship between peak VO_2 and measures of contractile and diastolic function during exercise, and cardiac energetic status

Peak VO_2 correlated with resting PCr/γATP ratio (r=0.52; p<0.001) and with the change in nTTPF during exercise (r=0.70; p<0.001) in HCM patients, but not with changes in relative E_{LV}I (r=0.20; p=0.2), relative EaI (r=–0.07; p=0.65), or LVEF during exercise (r=–0.20; p=0.1). Peak VO_2 did not differ between patients in whom LVEF increased during exercise and those in whom it fell during exercise.

6.5 Discussion

The principal aim of this study was to investigate the relationship between cardiac energetic impairment and changes in contractile and diastolic function (and of vasculoventricular interaction) with exercise in patients with non-obstructive HCM. We confirmed that, consistent with previous studies, HCM patients demonstrate reduced resting myocardial energetic status (409,424,425), and a paradoxical slowing of LV active relaxation on exercise (408). In healthy controls, LV contractile status increased during exercise, resulting in a marked reduction in the vasculoventricular coupling ratio, whereas in nonobstructive HCM, augmentation of LV contractile function on exercise was markedly blunted (and accordingly vasculoventricular coupling ratio was unchanged). Cardiac energetic status correlated positively with exercise capacity and was inversely correlated with exercise nTTPF, a measure of the rate of LV active relaxation, and with δVVC ratio, a measure of the coupling of the heart and vasculature. Peak VO_2 correlated with the change in nTTPF during exercise but not with changes in LV end-systolic elastance or arterial elastance.

Impaired exercise relaxation correlates with energy depletion

The pathophysiology of HCM is complex. A substantial proportion of patients complain of breathlessness and/or fatigue and most have reduced exercise capacity (408). These patients typically exhibit impaired LV active relaxation at rest and/or during exercise. This has led many to conclude that exercise limitation is primarily a result of impaired LV diastolic filling. Somewhat surprisingly, our data show no significant difference in nTTPF at rest between HCM and controls. This could be at least in part because the mean age of our population of patients (and in consequence controls) was rather older than previously studied populations (408,426,427). Nevertheless, on exercise, patients and controls behaved very differently, with nTTPF shortening in healthy controls during submaximal exercise but lengthening in patients, consistent with our previous study (408). The change in nTTPF on exercise

was inversely related to resting cardiac PCr/ATP ratio, a measure of cardiac energetic status. In both HCM and heart failure, PCr is depleted to a greater extent than ATP resulting in a fall in the PCr/ATP ratio (425,428). PCr represents a rapid source of ATP under conditions of stress such as exercise. The rate at which ATP can be regenerated from PCr is approximately 10-fold faster than the rate of *de novo* synthesis of ATP. The presence of a reduced resting PCr/ATP ratio therefore indicates a reduction in energy 'reserves'. A previous study has shown that PCr/ATP ratio is maintained during low-level exercise in healthy subjects, whereas it falls in patients with HCM (429). This energetic impairment may be partly a consequence of microvascular dysfunction (430) but it is also known that cross bridge cycling by the mutant sarcomeric proteins in HCM is abnormal, resulting in an energy wasting effect (431)**,** and this energetic impairment is manifest before phenotypic evidence of the disease is present (432).

Impaired exercise systolic performance correlates with energy depletion

We also observed significant differences in contractile responses to exercise in patients vs. controls. There was a failure to increase LVEF during exercise in the HCM patients, which was not seen in the controls. In 8 patients, LVEF fell by 5% or more. In our study, the change in LVEF on exercise was not significantly related to resting PCr/ATP ratio but, as discussed, this ratio falls on exercise in HCM, and exercise PCr/ATP ratio may therefore be more relevant (429).

LVEF is a highly imperfect measure of cardiac contractile function especially in HCM. Firstly, it is profoundly influenced by loading conditions, and secondly, the lower LVEDV at rest in HCM and failure to increase LVEDV during exercise may result in LVEF giving a falsely high impression of contractile performance. We therefore sought to assess a load-independent measure of contractile function ($E_{LV}I$), and also a global measure of cardiac afterload (EaI), and derived the vasculoventricular coupling ratio (EaI/$E_{LV}I$), which is inversely related to EF as VVC ratio = (1/EF) – 1 (412). Cardiac efficiency is dependent on maintaining this coupling ratio within a physiological

range. In a canine model, optimal stroke work and metabolic efficiency is seen in the range 0.3 to 1.3. When VVC was higher than 1.3, stroke work and cardiac mechanical efficiency fell substantially, and at values below 0.3, both fell modestly (433). In our healthy controls, the VVC ratio fell during exercise due to a combination of a substantial increase in LV end-systolic elastance (indicating increased contractile performance) and a modest increase in arterial elastance (i.e. global cardiac afterload). These observations are consistent with previous studies in healthy subjects (412).

In HCM patients there was a blunted increase in LV end-systolic elastance (i.e. a loss of contractile enhancement during exercise). Accordingly, whereas the VVC ratio fell significantly during exercise in healthy controls, it did not change significantly in patients with HCM. Arterial elastance also increased modestly on exercise in patients with HCM, which was similar to that observed in the healthy controls. It may seem counterintuitive that arterial elastance increases on exercise despite systemic vascular resistance falling substantially on exercise in healthy subjects and even more so in many patients with HCM (434). However arterial elastance is a global measure of afterload that is influenced by both static load (systemic vascular resistance), and by pulsatile load, in turn influenced by heart rate. The increase in heart rate on exercise is therefore responsible for the increase in arterial elastance, and the similar increment in HCM and controls despite a (presumed) greater fall in systemic vascular resistance can be explained by the lower heart rate on exercise in HCM patients. Unlike LV active relaxation, relative $\Delta E_{LV}I$ and ΔEaI did not correlate with resting PCr/ATP ratio. However, the change in VVC on exercise significantly correlated with resting PCr/ATP ratio. In the subgroup of 8 patients in whom LVEF fell on exercise, VVC paradoxically increased, and this was due to an exaggerated increase in arterial elastance compared to the remaining HCM patients, rather than a more blunted increase in ventricular end-systolic elastance. This suggests that abnormal large artery function on exercise may play an important role in the fall in LVEF.

Beta blockade does not explain diastolic or systolic observations

Beta adrenergic stimulation increases contractile performance and also has significant lusitropic effects (435). We explored the possibility that some of the differences in contractile and diastolic function observed on exercise between HCM patients and controls might be explained by the use of betablocker therapy. However, we found similar changes even after excluding those patients taking betablockers.

Energy depletion

The importance of cardiac energetic impairment and of the associated impairment of contractile function in the pathophysiology of exercise limitation in HCM is underscored by the fact that peak VO_2 correlated with PCr/ATP ratio, with nTTPF during exercise, and with the change in VVC during exercise. This is consistent with our previous observations following partial correction of the cardiac energetic abnormality in patients with HCM using the metabolic modulator Perhexiline (409). Interestingly, in a recent randomized controlled trial by our group, an alternative metabolic modulator Trimetazidine failed to improved exercise tolerance in patients with HCM, perhaps due to weaker inhibition of fatty acid β-oxidation compared to Perhexiline, and a shorter trial duration (436).

In summary, in the present study, exercise led to a paradoxical reduction in the rate of LV active relaxation in HCM patients, compared to an increase in controls. Furthermore, compared to controls, there was a failure to increase contractility during exercise. Resting cardiac energetic status was substantially reduced in HCM patients, which is supported by other studies (424,425). Based on prior pathophysiologic data (409,437), we propose that energetic impairment may underlie these dynamic changes in active relaxation and contractility, and thus contribute significantly to exercise limitation. These findings may indicate the

potential for therapeutic benefit from 'metabolic agents' that improve myocardial energetic status by altering cardiac substrate use (438). These agents have shown promise in ischemic heart disease (439-443) and in heart failure (349,444). In the subgroup of patients in whom LVEF fell on exercise, abnormal large artery function on exercise appeared to play a role.

Study Limitations

One limitation of our trial is that the changes in end-systolic elastance were 'relative' rather than absolute. EaI and E_{LV}I are measured using end systolic pressure, which is estimated from brachial blood pressures, divided by end systolic volume index (ESVI) and stroke volume index (SVI), respectively. There is however, substantial heterogeneity in methodology between studies measuring VVC ratio and its components (102). We therefore measured and reported relative changes, which are likely to be more useful. Additionally, although provocation with Valsalva was performed on all patients, we did not routinely perform exercise echocardiography on all patients. It is possible that some of our observations could be related to exercise related LVOT obstruction. This does not detract from our observations about the fall in EF, abnormal VVC, impaired relaxation, and energy depletion in HCM however, as LVOT obstruction, if it had occurred here, would only exacerbate the underlying energy depletion.

6.6 Conclusions

Impaired myocardial energetic status in HCM correlates significantly with exercise capacity, and deficiency is associated with dynamic diastolic and systolic dysfunction. Based on prior pathophysiologic data we propose that energetic impairment may underlie these dynamic changes in active relaxation and contractility.

Table 6-1: Baseline Characteristics

	HCM	**Controls**	**p value**
Age (years)	54 ± 12	52 ± 15	0.40
Number (Male)	51 (35)	33 (20)	0.64
Heart Rate (bpm)	69 ± 14	82 ± 16	<0.001†
Systolic BP (mm Hg)	126 ± 21	126 ± 21	0.91
Diastolic BP (mm Hg)	75 ± 12	78 ± 11	0.30
Peak VO_2 (ml/kg/min)	24 ± 6	38 ± 8	<0.001†
Medications			
Diuretic	10 (20)	0	0.006*
ACE inhibitor	6 (12)	0	0.04*
ARB	1 (2)	0	0.42
Beta-blocker	20 (39)	0	<0.001†
Calcium channel blocker	26 (51)	0	<0.001†
Aspirin	13 (25)	0	0.001*
Warfarin	5 (10)	0	0.06
Nitrate	2 (4)	0	0.25
Statin	15 (29)	0	<0.001†

Values are mean ± SD or n (%). * p<0.05, † p<0.001. Baseline Demographics. ACE, angiotensin-converting enzyme; ARB, angiotensin II receptor blockers; VO_2, oxygen consumption.

Table 6-2: Baseline Echocardiography Data

	HCM	**Controls**	**P value**
EF Biplane (%)	65 ± 9	63 ± 6	0.2
Biplane LA Volume (ml)	78 ± 30	39 ± 20	<0.001†
LA Volume Index (ml/m2)	37 ± 17	15 ± 13	<0.001†
MV E (m/s)	0.70 ± 0.17	0.66 ± 0.15	0.34
MV A (m/s)	0.67 ± 0.24	0.59 ± 0.14	0.06
MV E/A ratio	1.16 ± 0.5	1.17 ± 0.38	0.89
MV Dec Time (ms)	239 ± 76	260 ± 70	0.27
Antlat S' (cm/s)	0.06 ± 0.02	0.09 ± 0.02	<0.001†
Antlat E' (cm/s)	0.08 ± 0.03	0.10 ± 0.04	<0.001†
Antlat A' (cm/s)	0.06 ± 0.03	0.10 ± 0.03	<0.001†
Infsep S' (cm/s)	0.06 ± 0.02	0.08 ± 0.02	<0.001†
Infsep E' (cm/s)	0.05 ± 0.02	0.07± 0.03	<0.001†
Infsep A' (cm/s)	0.07 ± 0.02	0.09 ± 0.02	<0.001†
Average S' (cm/s)	0.06 ± 0.02	0.08 ± 0.02	<0.001†
Average E' (cm/s)	0.06 ± 0.02	0.09 ± 0.04	0.01*
E/E'_{antlat}	9.84 ± 4.09	6.94 ± 2.28	0.001*
E/E'_{infsep}	17.28 ± 7.32	9.55 ± 3.79	<0.001†
$E/E'_{average}$	11.93 ± 4.39	8.03 ± 3.28	<0.001†

Values are mean ± SD. * p<0.05, † p<0.001. Baseline Echocardiography Data. A', myocardial (TDI) peak late diastolic velocity; E', myocardial (TDI) peak early diastolic velocity; Dec, deceleration; LA, left atrium; MV, mitral valve; MV A, trans-mitral late diastolic velocity; MV E, trans-mitral early diastolic velocity; S', myocardial (TDI) peak systolic velocity.

Table 6-3: Exercise Radionuclide Ventriculography

	HCM	Controls	P value
Rest			
Heart rate (bpm)	69 ± 14	82 ± 16	<0.001†
Systolic BP (mmHg)	126 ± 21	126 ± 21	0.91
LVEF (%)	68 ± 13	64 ± 9	0.09
VVC ratio	0.55 ± 0.3	0.60 ± 0.21	0.32
nTTPF (s)	0.17 ± 0.07	0.19 ± 0.09	0.44
Exercise			
Heart rate (bpm)	137 ± 25	114 ± 11	<0.0001†
Systolic BP (mmHg)	168 ± 34	198 ± 27	<0.0001†
LVEF (%)	70 ± 11	72 ± 8	0.34
Relative $\Delta E_{LV}I$	1.24 ± 0.68	1.7 ± 0.7	0.004*
Relative ΔEaI	1.43 ± 0.73	1.28 ± 0.44	0.27
VVC ratio	0.46 ± 0.24	0.41 ± 0.15	0.02*
ΔVVC ratio	−0.06 ± 0.24	−0.25 ± 0.19	0.006*
nTTPF (s)	0.32 ± 0.09	0.16 ± 0.08	<0.0001†
ΔnTTPF (s)	+0.13 ± 0.11	−0.01 ± 0.10	<0.0001†

Values are mean ± SD. * $p<0.05$, † $p<0.001$. Exercise Radionuclide Ventriculography Data. BP, blood pressure; EaI, arterial elastance index; $E_{LV}I$, LV end-systolic elastance index; HCM, hypertrophic cardiomyopathy; nTTPF, normalized time to peak filling; ΔnTTPF = exercise – rest; Relative ΔEaI = exercise elastance / resting elastance; Relative $\Delta E_{LV}I$ = exercise elastance / resting elastance; VVC ratio, vasculoventricular coupling ratio; δVVC Ratio = exercise – rest.

Table 6-4: Correlations between Resting PCr/γATP Ratio with Exercise and Vasculoventricular Data

Exercise Variables	**HCM patients (all)**		**HCM patients (excluding those on BB)**	
	PCr/γATP		**PCr/γATP**	
Correlations	r	p	r	p
Peak VO_2 (ml/kg/min)	0.52	<0.001†	0.48	0.001*
Exercise nTTPF (s)	–0.47	0.003*	–0.48	0.007*
ΔVVC Ratio	–0.40	0.02*	–0.40	0.03*
Relative $\Delta E_{LV}I$	0.15	0.44	0.18	0.43
Relative ΔEaI	–0.21	0.27	–0.29	0.21

* p<0.05, † p<0.001. Correlations between resting PCr/γATP ratio with exercise and vasculoventricular data. BB, beta blockers; EaI, arterial elastance index; $E_{LV}I$, LV end-systolic elastance index; nTTPF, normalized time to peak filling; Peak VO_2, peak oxygen consumption; Relative ΔEaI = exercise elastance / resting elastance; Relative $\Delta E_{LV}I$ = exercise elastance / resting elastance; VVC ratio, vasculoventricular coupling ratio; δVVC Ratio = exercise – rest.

Conclusions

Inorganic nitrate and nitrite represent cheap and well-tolerated therapeutic options that have been shown to be effective in cardiovascular diseases such as hypertension and *angina pectoris* (16). The beneficial effects are related to both liberation of nitric oxide (NO) from nitrite in the presence of various reductases, as well as direct mechanisms such as S-nitrosylation of important subcellular proteins (12). We focused primarily on the effects of this nitrate-nitrite-NO pathway on cellular metabolism, and potential benefit in patients with chronic heart failure.

In heart failure with reduced ejection fraction (HFrEF), protein kinase G1α (PKG1α) oxidative dimer formation is increased in the myocardium, reflecting elevated levels of reactive oxygen species (ROS) (276). Myocardial metabolism is also reduced, due to impairments in both free fatty acid oxidation and glucose oxidation, reducing energy production from oxidative phosphorylation (152). Although the failing heart shifts towards glucose oxidation via the Randle Cycle and attempts to make up for the energy deficit, primarily by increasing glycolysis, these mechanisms are inefficient and indeed, insufficient. Others in our group have previously generated pilot data in murine myocardium demonstrating a dephosphorylation (disinhibition) of the pyruvate dehydrogenase (PDH) complex, the key regulator of glucose oxidation, following treatment with nitrite (unpublished data, Dr Konstantin Schwarz, PhD thesis presented to the University of Aberdeen). This was associated with an increase in PDH activity and an improvement in oxidative phosphorylation. In our study, we investigated the effect of nitrite on myocardial PKG1α dimer content and attempted to confirm the effects on nitrite on PDH. We then translated this to human myocardium, obtained from patients (without heart failure) undergoing coronary artery bypass grafting surgery. The effect of nitrite on PKG1α dimer content in healthy mouse myocardium was not statistically significant compared to placebo. In human myocardium, nitrite reduced PKG1α oxidative dimer content compared to placebo in the myocardium of patients with type 2 diabetes mellitus, but not in the myocardium of non-diabetics. This implies a selective anti-inflammatory effect of nitrite in myocardium with high ROS content and, as such, is likely to translate to patients with

chronic heart failure. In keeping with the inflammatory paradigm proposed by Paulus and Tschöpe (2013) in the pathogenesis of HFrEF (129), and the observed association between diabetes and forms of cardiomyopathy (162), these results are intriguing and merit further investigation. Although nitrite dephosphorylated (disinhibited) PDH, disappointingly, this was not associated with an increase in PDH activity in our study. However, it is important to note that we did not measure the effects of nitrite on 'absolute' glucose oxidation levels or glucose uptake, nor on mitochondrial oxidative phosphorylation.

Building on the same pilot data regarding the effects of nitrite on PDH, we conducted a concurrent study to delineate a potential mechanism, specifically related to potential effects of nitrite on the hypoxia inducible factor (HIF) pathway. The HIF pathway importantly inhibits glucose oxidation in all cells during hypoxia, by inhibiting PDH via pyruvate dehydrogenase kinases (PDK) (153). A direct effect of NO on HIF has also been shown in some tissues. In many cancer types, constitutive expression of HIF actually confers a survival benefit and aids in progression of metastasis, producing a glycolytic phenotype present in aerobic conditions, termed the Warburg effect (365). We chose the 786-0 renal cell carcinoma cell line for our experimental model, as HIF is constitutively activated in this cell line due to a mutation in the von Hippel Lindau protein, allowing for measurement of an oppositional effect of nitrite on PDH. A recent study using Dichloroacetate to directly inhibit PDK in 786-0 renal cell carcinoma cells demonstrated a successful suppression of HIF signalling, relieving mitochondrial 'blockade' at the level of PDH (375). It was further hypothesised by us that unblocking PDH may increase 786-0 renal cell carcinoma cell sensitivity to chemotherapeutic agents. In our study, nitrite, disappointingly, did not significantly affect phosphorylation status of PDH in 786-0 renal cell carcinoma cells on western blotting, nor of the important cancer cell survival protein Akt (384). Sensitivity to 5-fluorouracil chemotherapy was similarly unaffected. However, there was a paradoxical survival benefit noted at low-dose chemotherapy, and whilst the mechanism was not explored, it is possible that this

was related to the known antioxidant properties of nitrite, as ROS are important in the transduction of chemotoxic effects (392). Whilst the survival benefit was small and inconsistent, it does caution that care ought to be taken when conducting trials in cancer cells with agents that interact with redox signalling pathways.

In our randomised controlled trial of inorganic nitrate therapy to elevate plasma nitrite levels in patients with HFrEF due to dilated cardiomyopathy (the NICHE trial), we investigated the effects of nitrite on exercise capacity (peak VO_2 on CPEX) and measures of cardiac function on transthoracic echocardiography at 2 months. Unfortunately, our study was halted early by the study Sponsor, despite a recommendation from the study DSMC to continue recruitment. In fact, an interim analysis by the external study statistician demonstrated a smaller standard deviation for the primary endpoint (peak VO_2) than in the sample size calculations, suggesting that fewer patients than the original target of 56 would be required. Analysing data from the 19 patients who completed both study visits before the study was halted, there was a statistically significant deterioration in exercise capacity in the placebo group, but not in the inorganic nitrate group (ΔPeak VO_2, placebo –1.49 ± 1.9 vs. nitrate +0.48 ± 1.3 $mL.kg^{-1}.min^{-1}$, P=0.03). The change in respiratory exchange ratio was not different between groups, excluding major differences in exertional effort. However, baseline exercise capacity was slightly better in the placebo group compared to the treatment group (Peak VO_2, 18.8 ± 4.2 vs. 15.9 ± 3.3 $mL.kg^{-1}.min^{-1}$, P=0.11), as was diastolic function (E/E', 6.9 ± 2.2 vs. 10.4 ± 3.8, P=0.04), with the two groups converging at 2 months. The fall in peak VO2 correlated with an increase in resting E/E' (r^2=0.43, P=0.03), suggesting a worsening of diastolic dysfunction, and therefore a reduced ability to recruit the Frank-Starling mechanism to augment exercise cardiac output, as the likely cause for reduced cardiovascular reserve and worsening exercise tolerance in the placebo group. A definitive large scale clinical trial is still sorely needed to confirm the effects seen with inorganic nitrate therapy in smaller-scale studies of patients with HFrEF. A recent large RCT investigating inhaled nitrite therapy vs. placebo in patients with HFpEF showed no difference in

exercise capacity in the treatment group (317), and this has largely curbed interest in nitrite as a therapy for patients with HFpEF. However, inorganic nitrate studies in HFpEF have previously demonstrated benefit (316), suggesting that differences in dosing and route may play a significant role.

Finally, I analysed ^{31}P CMR spectroscopy and exercise (CPEX and radionuclide ventriculography) data previously obtained by others in our group in patients with symptomatic non-obstructive hypertrophic cardiomyopathy (often considered to be a unique endotype of HFpEF). Exercise impairment in patients with HCM has previously been shown to be related to dynamic diastolic dysfunction (particularly active relaxation), thus impairing utility of the Frank-Starling mechanism to increase exercise cardiac output (408). We showed that patients with HCM, compared to age-matched healthy controls, exhibited marked resting energetic impairment (PCr/γATP ratio, 1.41±0.48 vs. 2.26±0.59; P<0.0001), exercise impairment/intolerance (Peak VO_2, 24 ± 6 vs. 38 ± 8 $mL.kg^{-1}.min^{-1}$; P<0.0001), loss of the typical fall in vasculoventricular coupling ratio normally seen with exercise (δVVC, −0.25 ± 0.19 vs. −0.06 ± 0.24; P=0.006), reduced diastolic active relaxation (change in normalised time to peak filling, 0.19 ± 0.09s to 0.16 ± 0.08s vs. 0.17 ± 0.07s to 0.32 ± 0.09s; P<0.0001), and reduced systolic function (relative change in end systolic elastance or ELVI, 1.7 ± 0.7 vs. 1.24 ± 0.68; P<0.05). Energetic impairment (i.e. reduced PCr/γATP ratio on 31P CMR spectroscopy), was correlated positively with all of these changes, and was statistically significant (P<0.05 for all). Previous findings from basic science studies would support the conclusion that energetic impairment is therefore a significant contributor to exercise impairment in patients with HCM, and a key therapeutic target for improving quality of life and possibly mortality in these patients. There are currently no available therapies for these patients. Whilst nitrite is unlikely to be useful in patients with HCM, given the recent disappointing results of a definitive trial of inhaled nitrite in HFpEF (317), other metabolic modulators remain attractive despite mixed results (409,436).

This thesis, investigating the effects of nitrite on myocardial metabolism and potential therapeutic benefits in HFrEF, comprises part of a larger group of works to explore the benefits of nitrite in cardiovascular diseases. Whilst our data do not support a significant effect of nitrite on myocardial glucose metabolism, the effects on myocardial redox status are intriguing. Our attempts to investigate nitrite as a therapy in HFrEF due to DCM were, unfortunately, cut short prematurely. Definitive trials are still sorely needed.

1. Ignarro LJ. Biosynthesis and metabolism of endothelium-derived nitric oxide. (1990) *Annu Rev Pharmacol Toxicol* **30**:535-60.

2. Borland C. Endothelium in control. (1991) *Br Heart J* **66**:405.

3. Rassaf T, Preik M, Kleinbongard P et al. Evidence for in vivo transport of bioactive nitric oxide in human plasma. (2002) *J Clin Invest* **109**:1241-8.

4. Griffith OW, Stuehr DJ. Nitric oxide synthases: properties and catalytic mechanism. (1995) *Annu Rev Physiol* **57**:707-36.

5. Forstermann U, Closs EI, Pollock JS et al. Nitric oxide synthase isozymes. Characterization, purification, molecular cloning, and functions. (1994) *Hypertension* **23**:1121-31.

6. Naseem KM. The role of nitric oxide in cardiovascular diseases. (2005) *Mol Aspects Med* **26**:33-65.

7. Feron O, Balligand JL. Caveolins and the regulation of endothelial nitric oxide synthase in the heart. (2006) *Cardiovasc Res* **69**:788-97.

8. Feron O, Saldana F, Michel JB, Michel T. The endothelial nitric-oxide synthase-caveolin regulatory cycle. (1998) *J Biol Chem* **273**:3125-8.

9. Panza JA, Casino PR, Kilcoyne CM, Quyyumi AA. Role of endothelium-derived nitric oxide in the abnormal endothelium-dependent vascular relaxation of patients with essential hypertension. (1993) *Circulation* **87**:1468-74.

10. Forstermann U, Munzel T. Endothelial nitric oxide synthase in vascular disease: from marvel to menace. (2006) *Circulation* **113**:1708-14.

11. Global, regional, and national age-sex specific mortality for 264 causes of death, 1980-2016: a systematic analysis for the Global Burden of Disease Study 2016. (2017) *Lancet* **390**:1151-1210.

12. Martinez-Ruiz A, Cadenas S, Lamas S. Nitric oxide signaling: classical, less classical, and nonclassical mechanisms. (2011) *Free Radic Biol Med* **51**:17-29.

13. Bolotina VM, Najibi S, Palacino JJ, Pagano PJ, Cohen RA. Nitric oxide directly activates calcium-dependent potassium channels in vascular smooth muscle. (1994) *Nature* **368**:850-3.

14. Lugnier C, Komas N. Modulation of vascular cyclic nucleotide phosphodiesterases by cyclic GMP: role in vasodilatation. (1993) *Eur Heart J* **14 Suppl I**:141-8.

15. Lauer T, Preik M, Rassaf T et al. Plasma nitrite rather than nitrate reflects regional endothelial nitric oxide synthase activity but lacks intrinsic vasodilator action. (2001) *Proc Natl Acad Sci U S A* **98**:12814-9.

16. Lundberg JO, Weitzberg E, Gladwin MT. The nitrate-nitrite-nitric oxide pathway in physiology and therapeutics. (2008) *Nat Rev Drug Discov* **7**:156-67.

17. Shiva S, Wang X, Ringwood LA et al. Ceruloplasmin is a NO oxidase and nitrite synthase that determines endocrine NO homeostasis. (2006) *Nat Chem Biol* **2**:486-93.

18. Kelm M. Nitric oxide metabolism and breakdown. (1999) *Biochim Biophys Acta* **1411**:273-89.

19. Castiglione N, Rinaldo S, Giardina G, Stelitano V, Cutruzzola F. Nitrite and nitrite reductases: from molecular mechanisms to significance in human health and disease. (2012) *Antioxid Redox Signal* **17**:684-716.

20. Gladwin MT, Kim-Shapiro DB. The functional nitrite reductase activity of the heme-globins. (2008) *Blood* **112**:2636-47.

21. Furchgott RF, Zawadzki JV. The obligatory role of endothelial cells in the relaxation of arterial smooth muscle by acetylcholine. (1980) *Nature* **288**:373-376.

22. Garg UC, Hassid A. Nitric oxide-generating vasodilators and 8-bromo-cyclic guanosine monophosphate inhibit mitogenesis and proliferation of cultured rat vascular smooth muscle cells. (1989) *J Clin Invest* **83**:1774-7.

23. Radomski MW, Palmer RM, Moncada S. An L-arginine/nitric oxide pathway present in human platelets regulates aggregation. (1990) *Proc Natl Acad Sci U S A* **87**:5193-7.

24. Gkaliagkousi E, Ritter J, Ferro A. Platelet-derived nitric oxide signaling and regulation. (2007) *Circ Res* **101**:654-62.

25. Radomski MW, Palmer RM, Moncada S. The role of nitric oxide and cGMP in platelet adhesion to vascular endothelium. (1987) *Biochem Biophys Res Commun* **148**:1482-9.

26. Kubes P, Suzuki M, Granger DN. Nitric oxide: an endogenous modulator of leukocyte adhesion. (1991) *Proc Natl Acad Sci U S A* **88**:4651-5.

27. Bath PM, Hassall DG, Gladwin AM, Palmer RM, Martin JF. Nitric oxide and prostacyclin. Divergence of inhibitory effects on monocyte chemotaxis and adhesion to endothelium in vitro. (1991) *Arterioscler Thromb* **11**:254-60.

28. Ziche M, Morbidelli L, Masini E et al. Nitric oxide mediates angiogenesis in vivo and endothelial cell growth and migration in vitro promoted by substance P. (1994) *J Clin Invest* **94**:2036-44.

29. Dulak J, Józkowicz A, Dembinska-Kiec A et al. Nitric oxide induces the synthesis of vascular endothelial growth factor by rat vascular smooth muscle cells. (2000) *Arterioscler Thromb Vasc Biol* **20**:659-66.

30. Cooke JP, Losordo DW. Nitric oxide and angiogenesis. (2002) *Circulation* **105**:2133-5.

31. Kolpakov V, Gordon D, Kulik TJ. Nitric oxide-generating compounds inhibit total protein and collagen synthesis in cultured vascular smooth muscle cells. (1995) *Circ Res* **76**:305-9.

32. Calderone A, Thaik CM, Takahashi N, Chang DL, Colucci WS. Nitric oxide, atrial natriuretic peptide, and cyclic GMP inhibit the growth-promoting effects of norepinephrine in cardiac myocytes and fibroblasts. (1998) *J Clin Invest* **101**:812-8.

33. Massion PB, Feron O, Dessy C, Balligand JL. Nitric oxide and cardiac function: ten years after, and continuing. (2003) *Circ Res* **93**:388-98.

34. Shah AM. Paracrine modulation of heart cell function by endothelial cells. (1996) *Cardiovasc Res* **31**:847-67.

35. Dagenais GR, Leong DP, Rangarajan S et al. Variations in common diseases, hospital admissions, and deaths in middle-aged adults in 21 countries from five continents (PURE): a prospective cohort study. (2019) *Lancet*.

36. Ponikowski P, Voors AA, Anker SD et al. 2016 ESC Guidelines for the diagnosis and treatment of acute and chronic heart failure: The Task Force for the diagnosis and treatment of acute and chronic heart failure of the European Society of Cardiology (ESC)Developed with the special contribution of the Heart Failure Association (HFA) of the ESC. (2016) *Eur Heart J* **37**:2129-2200.

37. Mamas MA, Sperrin M, Watson MC et al. Do patients have worse outcomes in heart failure than in cancer? A primary care-based cohort study with 10-year follow-up in Scotland. (2017) *Eur J Heart Fail* **19**:1095-1104.

38. Cowie MR. The heart failure epidemic: a UK perspective. (2017) *Echo Res Pract* **4**:R15-r20.

39. Berry C, Murdoch DR, McMurray JJ. Economics of chronic heart failure. (2001) *Eur J Heart Fail* **3**:283-91.

40. Owan TE, Hodge DO, Herges RM, Jacobsen SJ, Roger VL, Redfield MM. Trends in prevalence and outcome of heart failure with preserved ejection fraction. (2006) *N Engl J Med* **355**:251-9.

41. Kitzman DW, Little WC, Brubaker PH et al. Pathophysiological characterization of isolated diastolic heart failure in comparison to systolic heart failure. (2002) *Jama* **288**:2144-50.

42. Packer M. Abnormalities of diastolic function as a potential cause of exercise intolerance in chronic heart failure. (1990) *Circulation* **81**:Iii78-86.

43. Tan YT, Wenzelburger F, Lee E et al. The pathophysiology of heart failure with normal ejection fraction: exercise echocardiography reveals complex abnormalities of both systolic and diastolic ventricular function involving torsion, untwist, and longitudinal motion. (2009) *J Am Coll Cardiol* **54**:36-46.

44. Hsu JJ, Ziaeian B, Fonarow GC. Heart Failure With Mid-Range (Borderline) Ejection Fraction: Clinical Implications and Future Directions. (2017) *JACC Heart Fail* **5**:763-771.

45. Sagawa K. The end-systolic pressure-volume relation of the ventricle: definition, modifications and clinical use. (1981) *Circulation* **63**:1223-7.

46. Baicu CF, Zile MR, Aurigemma GP, Gaasch WH. Left ventricular systolic performance, function, and contractility in patients with diastolic heart failure. (2005) *Circulation* **111**:2306-12.

47. van der Velde ET, Burkhoff D, Steendijk P, Karsdon J, Sagawa K, Baan J. Nonlinearity and load sensitivity of end-systolic pressure-volume relation of canine left ventricle in vivo. (1991) *Circulation* **83**:315-27.

48. Jacob R, Dierberger B, Kissling G. Functional significance of the Frank-Starling mechanism under physiological and pathophysiological conditions. (1992) *Eur Heart J* **13 Suppl E**:7-14.

49. Glower DD, Spratt JA, Snow ND et al. Linearity of the Frank-Starling relationship in the intact heart: the concept of preload recruitable stroke work. (1985) *Circulation* **71**:994-1009.

50. Elliott P, Andersson B, Arbustini E et al. Classification of the cardiomyopathies: a position statement from the European Society Of Cardiology Working Group on Myocardial and Pericardial Diseases. (2008) *Eur Heart J* **29**:270-6.

51. Hartupee J, Mann DL. Neurohormonal activation in heart failure with reduced ejection fraction. (2017) *Nat Rev Cardiol* **14**:30-38.

52. Lymperopoulos A, Rengo G, Koch WJ. Adrenergic nervous system in heart failure: pathophysiology and therapy. (2013) *Circ Res* **113**:739-53.

53. Gresham KS, Stelzer JE. The contributions of cardiac myosin binding protein C and troponin I phosphorylation to beta-adrenergic enhancement of in vivo cardiac function. (2016) *J Physiol* **594**:669-86.

54. Rona G. Catecholamine cardiotoxicity. (1985) *J Mol Cell Cardiol* **17**:291-306.

55. Mann DL, Kent RL, Parsons B, Cooper Gt. Adrenergic effects on the biology of the adult mammalian cardiocyte. (1992) *Circulation* **85**:790-804.

56. Haeusler KG, Laufs U, Endres M. Chronic heart failure and ischemic stroke. (2011) *Stroke* **42**:2977-82.

57. The Cardiac Insufficiency Bisoprolol Study II (CIBIS-II): a randomised trial. (1999) *Lancet* **353**:9-13.

58. Effect of metoprolol CR/XL in chronic heart failure: Metoprolol CR/XL Randomised Intervention Trial in Congestive Heart Failure (MERIT-HF). (1999) *Lancet* **353**:2001-7.

59. Packer M, Fowler MB, Roecker EB et al. Effect of carvedilol on the morbidity of patients with severe chronic heart failure: results of the carvedilol prospective randomized cumulative survival (COPERNICUS) study. (2002) *Circulation* **106**:2194-9.

60. Flather MD, Shibata MC, Coats AJ et al. Randomized trial to determine the effect of nebivolol on mortality and cardiovascular hospital admission in elderly patients with heart failure (SENIORS). (2005) *Eur Heart J* **26**:215-25.

61. Effects of enalapril on mortality in severe congestive heart failure. Results of the Cooperative North Scandinavian Enalapril Survival Study (CONSENSUS). (1987) *N Engl J Med* **316**:1429-35.

62. Yusuf S, Pitt B, Davis CE, Hood WB, Jr., Cohn JN. Effect of enalapril on mortality and the development of heart failure in asymptomatic patients with reduced left ventricular ejection fractions. (1992) *N Engl J Med* **327**:685-91.

63. Pfeffer MA, Braunwald E, Moye LA et al. Effect of captopril on mortality and morbidity in patients with left ventricular dysfunction after myocardial infarction. Results of the survival and ventricular enlargement trial. The SAVE Investigators. (1992) *N Engl J Med* **327**:669-77.

64. Effect of ramipril on mortality and morbidity of survivors of acute myocardial infarction with clinical evidence of heart failure. The Acute Infarction Ramipril Efficacy (AIRE) Study Investigators. (1993) *Lancet* **342**:821-8.

65. Granger CB, McMurray JJ, Yusuf S et al. Effects of candesartan in patients with chronic heart failure and reduced left-ventricular systolic function intolerant to angiotensin-converting-enzyme inhibitors: the CHARM-Alternative trial. (2003) *Lancet* **362**:772-6.

66. Cohn JN, Tognoni G. A randomized trial of the angiotensin-receptor blocker valsartan in chronic heart failure. (2001) *N Engl J Med* **345**:1667-75.

67. Pfeffer MA, McMurray JJ, Velazquez EJ et al. Valsartan, captopril, or both in myocardial infarction complicated by heart failure, left ventricular dysfunction, or both. (2003) *N Engl J Med* **349**:1893-906.

68. Pitt B, Zannad F, Remme WJ et al. The effect of spironolactone on morbidity and mortality in patients with severe heart failure. Randomized Aldactone Evaluation Study Investigators. (1999) *N Engl J Med* **341**:709-17.

69. Zannad F, McMurray JJ, Krum H et al. Eplerenone in patients with systolic heart failure and mild symptoms. (2011) *N Engl J Med* **364**:11-21.

70. Vardeny O, Miller R, Solomon SD. Combined neprilysin and renin-angiotensin system inhibition for the treatment of heart failure. (2014) *JACC Heart Fail* **2**:663-70.

71. McMurray JJ, Packer M, Desai AS et al. Angiotensin-neprilysin inhibition versus enalapril in heart failure. (2014) *N Engl J Med* **371**:993-1004.

72. Cleland JG, Daubert JC, Erdmann E et al. The effect of cardiac resynchronization on morbidity and mortality in heart failure. (2005) *N Engl J Med* **352**:1539-49.

73. Bristow MR, Saxon LA, Boehmer J et al. Cardiac-resynchronization therapy with or without an implantable defibrillator in advanced chronic heart failure. (2004) *N Engl J Med* **350**:2140-50.

74. Moss AJ, Hall WJ, Cannom DS et al. Cardiac-resynchronization therapy for the prevention of heart-failure events. (2009) *N Engl J Med* **361**:1329-38.

75. Fox K, Ford I, Steg PG, Tendera M, Ferrari R. Ivabradine for patients with stable coronary artery disease and left-ventricular systolic dysfunction (BEAUTIFUL): a randomised, double-blind, placebo-controlled trial. (2008) *Lancet* **372**:807-16.

76. Swedberg K, Komajda M, Bohm M et al. Ivabradine and outcomes in chronic heart failure (SHIFT): a randomised placebo-controlled study. (2010) *Lancet* **376**:875-85.

77. The effect of digoxin on mortality and morbidity in patients with heart failure. (1997) *N Engl J Med* **336**:525-33.

78. Packer M, Anker SD, Butler J et al. Cardiovascular and Renal Outcomes with Empagliflozin in Heart Failure. (2020) *N Engl J Med* **383**:1413-1424.

79. Chilton R, Tikkanen I, Cannon CP et al. Effects of empagliflozin on blood pressure and markers of arterial stiffness and vascular resistance in patients with type 2 diabetes. (2015) *Diabetes Obes Metab* **17**:1180-93.

80. Packer M. Activation and Inhibition of Sodium-Hydrogen Exchanger Is a Mechanism That Links the Pathophysiology and Treatment of Diabetes Mellitus With That of Heart Failure. (2017) *Circulation* **136**:1548-1559.

81. Mordi NA, Mordi IR, Singh JS, McCrimmon RJ, Struthers AD, Lang CC. Renal and Cardiovascular Effects of SGLT2 Inhibition in Combination With Loop Diuretics in Patients With Type 2 Diabetes and Chronic Heart Failure: The RECEDE-CHF Trial. (2020) *Circulation* **142**:1713-1724.

82. Bailey CJ. Uric acid and the cardio-renal effects of SGLT2 inhibitors. (2019) *Diabetes Obes Metab* **21**:1291-1298.

83. Packer M. Are the benefits of SGLT2 inhibitors in heart failure and a reduced ejection fraction influenced by background therapy? Expectations and realities of a new standard of care. (2020) *Eur Heart J* **41**:2393-2396.

84. Kingma I, Tyberg JV, Smith ER. Effects of diastolic transseptal pressure gradient on ventricular septal position and motion. (1983) *Circulation* **68**:1304-14.

85. Patterson SW, Starling EH. On the mechanical factors which determine the output of the ventricles. (1914) *J Physiol* **48**:357-79.

86. Horwitz LD, Atkins JM, Leshin SJ. Role of the Frank-Starling mechanism in exercise. (1972) *Circ Res* **31**:868-75.

87. Chantler PD, Melenovsky V, Schulman SP et al. Use of the Frank-Starling mechanism during exercise is linked to exercise-induced changes in arterial load. (2012) *Am J Physiol Heart Circ Physiol* **302**:H349-58.

88. Schwinger RH, Bohm M, Koch A et al. The failing human heart is unable to use the Frank-Starling mechanism. (1994) *Circ Res* **74**:959-69.

89. Lee JM, Boughner DR. Mechanical properties of human pericardium. Differences in viscoelastic response when compared with canine pericardium. (1985) *Circ Res* **57**:475-81.

90. Belenkie I, Dani R, Smith ER, Tyberg JV. Ventricular interaction during experimental acute pulmonary embolism. (1988) *Circulation* **78**:761-8.

91. Howarth S, Mc MJ, Sharpey-Schafer EP. Effects of venesection in low output heart failure. (1946) *Clin Sci* **6**:41-50.

92. Moore TD, Frenneaux MP, Sas R et al. Ventricular interaction and external constraint account for decreased stroke work during volume loading in CHF. (2001) *Am J Physiol Heart Circ Physiol* **281**:H2385-91.

93. Atherton JJ, Moore TD, Lele SS et al. Diastolic ventricular interaction in chronic heart failure. (1997) *Lancet* **349**:1720-4.

94. Little RC, Little WC. Cardiac preload, afterload, and heart failure. (1982) *Arch Intern Med* **142**:819-22.

95. Cingolani HE, Perez NG, Cingolani OH, Ennis IL. The Anrep effect: 100 years later. (2013) *Am J Physiol Heart Circ Physiol* **304**:H175-82.

96. Maroto R, Raso A, Wood TG, Kurosky A, Martinac B, Hamill OP. TRPC1 forms the stretch-activated cation channel in vertebrate cells. (2005) *Nat Cell Biol* **7**:179-85.

97. Zou Y, Akazawa H, Qin Y et al. Mechanical stress activates angiotensin II type 1 receptor without the involvement of angiotensin II. (2004) *Nat Cell Biol* **6**:499-506.

98. Katz AM, Rolett EL. Heart failure: when form fails to follow function. (2016) *Eur Heart J* **37**:449-54.

99. Colombo PC, Onat D, Sabbah HN. Acute heart failure as "acute endothelitis"--Interaction of fluid overload and endothelial dysfunction. (2008) *Eur J Heart Fail* **10**:170-5.

100. Kelly RP, Ting CT, Yang TM et al. Effective arterial elastance as index of arterial vascular load in humans. (1992) *Circulation* **86**:513-21.

101. Borlaug BA, Kass DA. Ventricular-vascular interaction in heart failure. (2008) *Heart Fail Clin* **4**:23-36.

102. Ikonomidis I, Aboyans V, Blacher J et al. The role of ventricular-arterial coupling in cardiac disease and heart failure: assessment, clinical implications and therapeutic interventions. A consensus document of the European Society of Cardiology Working Group on Aorta & Peripheral Vascular Diseases, European Association of Cardiovascular Imaging, and Heart Failure Association. (2019) *Eur J Heart Fail* **21**:402-424.

103. Chantler PD, Lakatta EG, Najjar SS. Arterial-ventricular coupling: mechanistic insights into cardiovascular performance at rest and during exercise. (2008) *J Appl Physiol (1985)* **105**:1342-51.

104. Zile MR, Baicu CF, Gaasch WH. Diastolic heart failure--abnormalities in active relaxation and passive stiffness of the left ventricle. (2004) *N Engl J Med* **350**:1953-9.

105. Hogg K, Swedberg K, McMurray J. Heart failure with preserved left ventricular systolic function; epidemiology, clinical characteristics, and prognosis. (2004) *J Am Coll Cardiol* **43**:317-27.

106. Lam CS, Donal E, Kraigher-Krainer E, Vasan RS. Epidemiology and clinical course of heart failure with preserved ejection fraction. (2011) *Eur J Heart Fail* **13**:18-28.

107. Borlaug BA, Lam CS, Roger VL, Rodeheffer RJ, Redfield MM. Contractility and ventricular systolic stiffening in hypertensive heart disease insights into the pathogenesis of heart failure with preserved ejection fraction. (2009) *J Am Coll Cardiol* **54**:410-8.

108. McEniery CM, Yasmin, Hall IR, Qasem A, Wilkinson IB, Cockcroft JR. Normal vascular aging: differential effects on wave reflection and aortic pulse wave velocity: the Anglo-Cardiff Collaborative Trial (ACCT). (2005) *J Am Coll Cardiol* **46**:1753-60.

109. Belz GG. Elastic properties and Windkessel function of the human aorta. (1995) *Cardiovasc Drugs Ther* **9**:73-83.

110. Davies JE, Whinnett ZI, Francis DP et al. Evidence of a dominant backward-propagating "suction" wave responsible for diastolic coronary filling in humans, attenuated in left ventricular hypertrophy. (2006) *Circulation* **113**:1768-78.

111. Reddy YNV, Andersen MJ, Obokata M et al. Arterial Stiffening With Exercise in Patients With Heart Failure and Preserved Ejection Fraction. (2017) *J Am Coll Cardiol* **70**:136-148.

112. Torjesen AA, Wang N, Larson MG et al. Forward and backward wave morphology and central pressure augmentation in men and women in the Framingham Heart Study. (2014) *Hypertension* **64**:259-65.

113. Zile MR, Baicu CF, Ikonomidis JS et al. Myocardial stiffness in patients with heart failure and a preserved ejection fraction: contributions of collagen and titin. (2015) *Circulation* **131**:1247-59.

114. Schafer S, de Marvao A, Adami E et al. Titin-truncating variants affect heart function in disease cohorts and the general population. (2017) *Nat Genet* **49**:46-53.

115. Williams L, Howell N, Pagano D et al. Titin isoform expression in aortic stenosis. (2009) *Clin Sci (Lond)* **117**:237-42.

116. LeWinter MM, Granzier HL. Cardiac titin and heart disease. (2014) *J Cardiovasc Pharmacol* **63**:207-12.

117. Schwartzenberg S, Redfield MM, From AM, Sorajja P, Nishimura RA, Borlaug BA. Effects of vasodilation in heart failure with preserved or reduced ejection fraction implications of distinct pathophysiologies on response to therapy. (2012) *J Am Coll Cardiol* **59**:442-51.

118. Shah SJ. Precision Medicine for Heart Failure with Preserved Ejection Fraction: An Overview. (2017) *J Cardiovasc Transl Res* **10**:233-244.

119. Pitt B, Pfeffer MA, Assmann SF et al. Spironolactone for heart failure with preserved ejection fraction. (2014) *N Engl J Med* **370**:1383-92.

120. Yusuf S, Pfeffer MA, Swedberg K et al. Effects of candesartan in patients with chronic heart failure and preserved left-ventricular ejection fraction: the CHARM-Preserved Trial. (2003) *Lancet* **362**:777-81.

121. Massie BM, Carson PE, McMurray JJ et al. Irbesartan in patients with heart failure and preserved ejection fraction. (2008) *N Engl J Med* **359**:2456-67.

122. Redfield MM, Chen HH, Borlaug BA et al. Effect of phosphodiesterase-5 inhibition on exercise capacity and clinical status in heart failure with preserved ejection fraction: a randomized clinical trial. (2013) *Jama* **309**:1268-77.

123. Redfield MM, Anstrom KJ, Levine JA et al. Isosorbide Mononitrate in Heart Failure with Preserved Ejection Fraction. (2015) *N Engl J Med* **373**:2314-24.

124. Shah SJ, Kitzman DW, Borlaug BA et al. Phenotype-Specific Treatment of Heart Failure With Preserved Ejection Fraction: A Multiorgan Roadmap. (2016) *Circulation* **134**:73-90.

125. Gorter TM, Obokata M, Reddy YNV, Melenovsky V, Borlaug BA. Exercise unmasks distinct pathophysiologic features in heart failure with preserved ejection fraction and pulmonary vascular disease. (2018) *Eur Heart J* **39**:2825-2835.

126. Parasuraman SK, Loudon BL, Lowery C et al. Diastolic Ventricular Interaction in Heart Failure With Preserved Ejection Fraction. (2019) *J Am Heart Assoc* **8**:e010114.

127. Borlaug BA, Carter RE, Melenovsky V et al. Percutaneous Pericardial Resection: A Novel Potential Treatment for Heart Failure With Preserved Ejection Fraction. (2017) *Circ Heart Fail* **10**:e003612.

128. Bleasdale RA, Turner MS, Mumford CE et al. Left ventricular pacing minimizes diastolic ventricular interaction, allowing improved preload-dependent systolic performance. (2004) *Circulation* **110**:2395-400.

129. Paulus WJ, Tschope C. A novel paradigm for heart failure with preserved ejection fraction: comorbidities drive myocardial dysfunction and remodeling through coronary microvascular endothelial inflammation. (2013) *J Am Coll Cardiol* **62**:263-71.

130. Seshiah PN, Weber DS, Rocic P, Valppu L, Taniyama Y, Griendling KK. Angiotensin II stimulation of NAD(P)H oxidase activity: upstream mediators. (2002) *Circ Res* **91**:406-13.

131. Ennezat PV, Malendowicz SL, Testa M et al. Physical training in patients with chronic heart failure enhances the expression of genes encoding antioxidative enzymes. (2001) *J Am Coll Cardiol* **38**:194-8.

132. Markousis-Mavrogenis G, Tromp J, Ouwerkerk W et al. The clinical significance of interleukin-6 in heart failure: results from the BIOSTAT-CHF study. (2019) *Eur J Heart Fail* **21**:965-973.

133. Chung ES, Packer M, Lo KH, Fasanmade AA, Willerson JT. Randomized, double-blind, placebo-controlled, pilot trial of infliximab, a chimeric monoclonal antibody to tumor necrosis factor-alpha, in patients with moderate-to-severe heart failure: results of the anti-TNF Therapy Against Congestive Heart Failure (ATTACH) trial. (2003) *Circulation* **107**:3133-40.

134. Everett BM, Cornel JH, Lainscak M et al. Anti-Inflammatory Therapy With Canakinumab for the Prevention of Hospitalization for Heart Failure. (2019) *Circulation* **139**:1289-1299.

135. Neubauer S. The failing heart--an engine out of fuel. (2007) *N Engl J Med* **356**:1140-51.

136. Taegtmeyer H. Carbohydrate interconversions and energy production. (1985) *Circulation* **72**:Iv1-8.

137. Doenst T, Nguyen TD, Abel ED. Cardiac metabolism in heart failure: implications beyond ATP production. (2013) *Circ Res* **113**:709-24.

138. Loudon BL, Noordali H, Gollop ND, Frenneaux MP, Madhani M. Present and future pharmacotherapeutic agents in heart failure: an evolving paradigm. (2016) *Br J Pharmacol* **173**:1911-24.

139. Noordali H, Loudon BL, Frenneaux MP, Madhani M. Cardiac metabolism - A promising therapeutic target for heart failure. (2018) *Pharmacol Ther* **182**:95-114.

140. Kennedy JA, Unger SA, Horowitz JD. Inhibition of carnitine palmitoyltransferase-1 in rat heart and liver by perhexiline and amiodarone. (1996) *Biochem Pharmacol* **52**:273-80.

141. Carley AN, Bi J, Wang X et al. Multiphasic triacylglycerol dynamics in the intact heart during acute in vivo overexpression of CD36. (2013) *J Lipid Res* **54**:97-106.

142. Rosca MG, Vazquez EJ, Kerner J et al. Cardiac mitochondria in heart failure: decrease in respirasomes and oxidative phosphorylation. (2008) *Cardiovasc Res* **80**:30-9.

143. Rousset S, Alves-Guerra MC, Mozo J et al. The biology of mitochondrial uncoupling proteins. (2004) *Diabetes* **53 Suppl 1**:S130-5.

144. Redza-Dutordoir M, Averill-Bates DA. Activation of apoptosis signalling pathways by reactive oxygen species. (2016) *Biochim Biophys Acta* **1863**:2977-2992.

145. Bouche C, Serdy S, Kahn CR, Goldfine AB. The cellular fate of glucose and its relevance in type 2 diabetes. (2004) *Endocr Rev* **25**:807-30.

146. Agledal L, Niere M, Ziegler M. The phosphate makes a difference: cellular functions of NADP. (2010) *Redox Rep* **15**:2-10.

147. Yi W, Clark PM, Mason DE et al. Phosphofructokinase 1 glycosylation regulates cell growth and metabolism. (2012) *Science* **337**:975-80.

148. Yang X, Qian K. Protein O-GlcNAcylation: emerging mechanisms and functions. (2017) *Nat Rev Mol Cell Biol* **18**:452-465.

149. Gudi R, Bowker-Kinley MM, Kedishvili NY, Zhao Y, Popov KM. Diversity of the pyruvate dehydrogenase kinase gene family in humans. (1995) *J Biol Chem* **270**:28989-94.

150. Randle PJ, Garland PB, Hales CN, Newsholme EA. The glucose fatty-acid cycle. Its role in insulin sensitivity and the metabolic disturbances of diabetes mellitus. (1963) *Lancet* **1**:785-9.

151. Huang B, Gudi R, Wu P, Harris RA, Hamilton J, Popov KM. Isoenzymes of pyruvate dehydrogenase phosphatase. DNA-derived amino acid sequences, expression, and regulation. (1998) *J Biol Chem* **273**:17680-8.

152. Stanley WC, Recchia FA, Lopaschuk GD. Myocardial substrate metabolism in the normal and failing heart. (2005) *Physiol Rev* **85**:1093-129.

153. Kim JW, Tchernyshyov I, Semenza GL, Dang CV. HIF-1-mediated expression of pyruvate dehydrogenase kinase: a metabolic switch required for cellular adaptation to hypoxia. (2006) *Cell Metab* **3**:177-85.

154. Yin X, Dwyer J, Langley SR et al. Effects of perhexiline-induced fuel switch on the cardiac proteome and metabolome. (2013) *J Mol Cell Cardiol* **55**:27-30.

155. Owen OE, Kalhan SC, Hanson RW. The key role of anaplerosis and cataplerosis for citric acid cycle function. (2002) *J Biol Chem* **277**:30409-12.

156. Turer AT, Hill JA, Elmquist JK, Scherer PE. Adipose tissue biology and cardiomyopathy: translational implications. (2012) *Circ Res* **111**:1565-77.

157. Muoio DM, Way JM, Tanner CJ et al. Peroxisome proliferator-activated receptor-alpha regulates fatty acid utilization in primary human skeletal muscle cells. (2002) *Diabetes* **51**:901-9.

158. Shoag J, Arany Z. Regulation of hypoxia-inducible genes by PGC-1 alpha. (2010) *Arterioscler Thromb Vasc Biol* **30**:662-6.

159. Drosatos K, Schulze PC. Cardiac lipotoxicity: molecular pathways and therapeutic implications. (2013) *Curr Heart Fail Rep* **10**:109-21.

160. Ardehali H, Sabbah HN, Burke MA et al. Targeting myocardial substrate metabolism in heart failure: potential for new therapies. (2012) *Eur J Heart Fail* **14**:120-9.

161. Laplante M, Sabatini DM. mTOR signaling in growth control and disease. (2012) *Cell* **149**:274-93.

162. Solang L, Malmberg K, Ryden L. Diabetes mellitus and congestive heart failure. Further knowledge needed. (1999) *Eur Heart J* **20**:789-95.

163. Jeon SM. Regulation and function of AMPK in physiology and diseases. (2016) *Exp Mol Med* **48**:e245.

164. Zhang Y, Lee TS, Kolb EM et al. AMP-activated protein kinase is involved in endothelial NO synthase activation in response to shear stress. (2006) *Arterioscler Thromb Vasc Biol* **26**:1281-7.

165. Ding WX, Yin XM. Mitophagy: mechanisms, pathophysiological roles, and analysis. (2012) *Biol Chem* **393**:547-64.

166. Zhu H, Tannous P, Johnstone JL et al. Cardiac autophagy is a maladaptive response to hemodynamic stress. (2007) *J Clin Invest* **117**:1782-93.

167. Tanno M, Kuno A, Horio Y, Miura T. Emerging beneficial roles of sirtuins in heart failure. (2012) *Basic Res Cardiol* **107**:273.

168. Webster BR, Lu Z, Sack MN, Scott I. The role of sirtuins in modulating redox stressors. (2012) *Free Radic Biol Med* **52**:281-90.

169. Longo VD, Kennedy BK. Sirtuins in aging and age-related disease. (2006) *Cell* **126**:257-68.

170. Cherry AD, Piantadosi CA. Regulation of mitochondrial biogenesis and its intersection with inflammatory responses. (2015) *Antioxid Redox Signal* **22**:965-76.

171. Sabbah HN. Targeting mitochondrial dysfunction in the treatment of heart failure. (2016) *Expert Rev Cardiovasc Ther* **14**:1305-1313.

172. Manganelli V, Capozzi A, Recalchi S et al. Altered Traffic of Cardiolipin during Apoptosis: Exposure on the Cell Surface as a Trigger for "Antiphospholipid Antibodies". (2015) *J Immunol Res* **2015**:847985.

173. Daubert MA, Yow E, Dunn G et al. Novel Mitochondria-Targeting Peptide in Heart Failure Treatment: A Randomized, Placebo-Controlled Trial of Elamipretide. (2017) *Circ Heart Fail* **10**.

174. Butler J, Khan MS, Anker SD et al. Effects of Elamipretide on Left Ventricular Function in Patients With Heart Failure With Reduced Ejection Fraction: The PROGRESS-HF Phase 2 Trial. (2020) *J Card Fail* **26**:429-437.

175. Carreras MC, Franco MC, Peralta JG, Poderoso JJ. Nitric oxide, complex I, and the modulation of mitochondrial reactive species in biology and disease. (2004) *Mol Aspects Med* **25**:125-39.

176. Shiva S, Sack MN, Greer JJ et al. Nitrite augments tolerance to ischemia/reperfusion injury via the modulation of mitochondrial electron transfer. (2007) *J Exp Med* **204**:2089-102.

177. Ingwall JS. Energy metabolism in heart failure and remodelling. (2009) *Cardiovasc Res* **81**:412-9.

178. Hirsch GA, Bottomley PA, Gerstenblith G, Weiss RG. Allopurinol acutely increases adenosine triphospate energy delivery in failing human hearts. (2012) *J Am Coll Cardiol* **59**:802-8.

179. Chirinos JA, Zamani P. The Nitrate-Nitrite-NO Pathway and Its Implications for Heart Failure and Preserved Ejection Fraction. (2016) *Curr Heart Fail Rep* **13**:47-59.

180. Zweier JL, Wang P, Samouilov A, Kuppusamy P. Enzyme-independent formation of nitric oxide in biological tissues. (1995) *Nat Med* **1**:804-9.

181. Spiegelhalder B, Eisenbrand G, Preussmann R. Influence of dietary nitrate on nitrite content of human saliva: possible relevance to in vivo formation of N-nitroso compounds. (1976) *Food Cosmet Toxicol* **14**:545-8.

182. Duncan C, Dougall H, Johnston P et al. Chemical generation of nitric oxide in the mouth from the enterosalivary circulation of dietary nitrate. (1995) *Nat Med* **1**:546-51.

183. Petersson J, Phillipson M, Jansson EA, Patzak A, Lundberg JO, Holm L. Dietary nitrate increases gastric mucosal blood flow and mucosal defense. (2007) *Am J Physiol Gastrointest Liver Physiol* **292**:G718-24.

184. Webb AJ, Patel N, Loukogeorgakis S et al. Acute blood pressure lowering, vasoprotective, and antiplatelet properties of dietary nitrate via bioconversion to nitrite. (2008) *Hypertension* **51**:784-90.

185. Govoni M, Jansson EA, Weitzberg E, Lundberg JO. The increase in plasma nitrite after a dietary nitrate load is markedly attenuated by an antibacterial mouthwash. (2008) *Nitric Oxide* **19**:333-7.

186. Benjamin N, O'Driscoll F, Dougall H et al. Stomach NO synthesis. (1994) *Nature* **368**:502.

187. Carlsson S, Wiklund NP, Engstrand L, Weitzberg E, Lundberg JO. Effects of pH, nitrite, and ascorbic acid on nonenzymatic nitric oxide generation and bacterial growth in urine. (2001) *Nitric Oxide* **5**:580-6.

188. Gago B, Lundberg JO, Barbosa RM, Laranjinha J. Red wine-dependent reduction of nitrite to nitric oxide in the stomach. (2007) *Free Radic Biol Med* **43**:1233-42.

189. Feelisch M, Fernandez BO, Bryan NS et al. Tissue processing of nitrite in hypoxia: an intricate interplay of nitric oxide-generating and -scavenging systems. (2008) *J Biol Chem* **283**:33927-34.

190. Godber BL, Doel JJ, Sapkota GP et al. Reduction of nitrite to nitric oxide catalyzed by xanthine oxidoreductase. (2000) *J Biol Chem* **275**:7757-63.

191. Li H, Cui H, Kundu TK, Alzawahra W, Zweier JL. Nitric oxide production from nitrite occurs primarily in tissues not in the blood: critical role of xanthine oxidase and aldehyde oxidase. (2008) *J Biol Chem* **283**:17855-63.

192. Gautier C, van Faassen E, Mikula I, Martasek P, Slama-Schwok A. Endothelial nitric oxide synthase reduces nitrite anions to NO under anoxia. (2006) *Biochem Biophys Res Commun* **341**:816-21.

193. Rassaf T, Flogel U, Drexhage C, Hendgen-Cotta U, Kelm M, Schrader J. Nitrite reductase function of deoxymyoglobin: oxygen sensor and regulator of cardiac energetics and function. (2007) *Circ Res* **100**:1749-54.

194. Cosby K, Partovi KS, Crawford JH et al. Nitrite reduction to nitric oxide by deoxyhemoglobin vasodilates the human circulation. (2003) *Nat Med* **9**:1498-505.

195. Ormerod JO, Ashrafian H, Maher AR et al. The role of vascular myoglobin in nitrite-mediated blood vessel relaxation. (2011) *Cardiovasc Res* **89**:560-5.

196. Castello PR, David PS, McClure T, Crook Z, Poyton RO. Mitochondrial cytochrome oxidase produces nitric oxide under hypoxic conditions: implications for oxygen sensing and hypoxic signaling in eukaryotes. (2006) *Cell Metab* **3**:277-87.

197. Basu S, Azarova NA, Font MD et al. Nitrite reductase activity of cytochrome c. (2008) *J Biol Chem* **283**:32590-7.

198. Aamand R, Dalsgaard T, Jensen FB, Simonsen U, Roepstorff A, Fago A. Generation of nitric oxide from nitrite by carbonic anhydrase: a possible link between metabolic activity and vasodilation. (2009) *Am J Physiol Heart Circ Physiol* **297**:H2068-74.

199. Trandafir F, Van Doorslaer S, Dewilde S, Moens L. Temperature dependence of NO binding modes in human neuroglobin. (2004) *Biochim Biophys Acta* **1702**:153-61.

200. Tiso M, Tejero J, Basu S et al. Human neuroglobin functions as a redox-regulated nitrite reductase. (2011) *J Biol Chem* **286**:18277-89.

201. Deem S, Min JH, Moulding JD, Eveland R, Swenson ER. Red blood cells prevent inhibition of hypoxic pulmonary vasoconstriction by nitrite in isolated, perfused rat lungs. (2007) *Am J Physiol Heart Circ Physiol* **292**:H963-70.

202. Munzel T, Daiber A, Mulsch A. Explaining the phenomenon of nitrate tolerance. (2005) *Circ Res* **97**:618-28.

203. Gould N, Doulias PT, Tenopoulou M, Raju K, Ischiropoulos H. Regulation of protein function and signaling by reversible cysteine S-nitrosylation. (2013) *J Biol Chem* **288**:26473-9.

204. Omar SA, Fok H, Tilgner KD et al. Paradoxical normoxia-dependent selective actions of inorganic nitrite in human muscular conduit arteries and related selective actions on central blood pressures. (2015) *Circulation* **131**:381-9; discussion 389.

205. Charles RL, Rudyk O, Prysyazhna O et al. Protection from hypertension in mice by the Mediterranean diet is mediated by nitro fatty acid inhibition of soluble epoxide hydrolase. (2014) *Proc Natl Acad Sci U S A* **111**:8167-72.

206. Raat NJ, Noguchi AC, Liu VB et al. Dietary nitrate and nitrite modulate blood and organ nitrite and the cellular ischemic stress response. (2009) *Free Radic Biol Med* **47**:510-7.

207. Appel LJ, Moore TJ, Obarzanek E et al. A clinical trial of the effects of dietary patterns on blood pressure. DASH Collaborative Research Group. (1997) *N Engl J Med* **336**:1117-24.

208. Hord NG, Tang Y, Bryan NS. Food sources of nitrates and nitrites: the physiologic context for potential health benefits. (2009) *Am J Clin Nutr* **90**:1-10.

209. Kapil V, Khambata RS, Robertson A, Caulfield MJ, Ahluwalia A. Dietary nitrate provides sustained blood pressure lowering in hypertensive patients: a randomized, phase 2, double-blind, placebo-controlled study. (2015) *Hypertension* **65**:320-7.

210. Butler AR, Feelisch M. Therapeutic uses of inorganic nitrite and nitrate: from the past to the future. (2008) *Circulation* **117**:2151-9.

211. Fields S. Global nitrogen: cycling out of control. (2004) *Environ Health Perspect* **112**:A556-63.

212. Keith NM, Binger MW. DIuretic action of potassium salts. (1935) *Journal of the American Medical Association* **105**:1584-1591.

213. Cammack R, Joannou CL, Cui XY, Torres Martinez C, Maraj SR, Hughes MN. Nitrite and nitrosyl compounds in food preservation. (1999) *Biochim Biophys Acta* **1411**:475-88.

214. Lauder Brunton T. ON THE USE OF NITRITE OF AMYL IN ANGINA PECTORIS. *The Lancet* **90**:97-98.

215. Bryan NS, Alexander DD, Coughlin JR, Milkowski AL, Boffetta P. Ingested nitrate and nitrite and stomach cancer risk: an updated review. (2012) *Food Chem Toxicol* **50**:3646-65.

216. Ansari FA, Ali SN, Arif H, Khan AA, Mahmood R. Acute oral dose of sodium nitrite induces redox imbalance, DNA damage, metabolic and histological changes in rat intestine. (2017) *PLoS One* **12**:e0175196.

217. Lijinsky W. Induction of tumours in rats by feeding nitrosatable amines together with sodium nitrite. (1984) *Food Chem Toxicol* **22**:715-20.

218. Ward MH. Too much of a good thing? Nitrate from nitrogen fertilizers and cancer. (2009) *Rev Environ Health* **24**:357-63.

219. Bradbury KE, Appleby PN, Key TJ. Fruit, vegetable, and fiber intake in relation to cancer risk: findings from the European Prospective Investigation into Cancer and Nutrition (EPIC). (2014) *Am J Clin Nutr* **100 Suppl 1**:394s-8s.

220. Gonzalez CA, Lujan-Barroso L, Bueno-de-Mesquita HB et al. Fruit and vegetable intake and the risk of gastric adenocarcinoma: a reanalysis of the European Prospective Investigation into Cancer and Nutrition (EPIC-EURGAST) study after a longer follow-up. (2012) *Int J Cancer* **131**:2910-9.

221. Song P, Wu L, Guan W. Dietary Nitrates, Nitrites, and Nitrosamines Intake and the Risk of Gastric Cancer: A Meta-Analysis. (2015) *Nutrients* **7**:9872-95.

222. Keszei AP, Goldbohm RA, Schouten LJ, Jakszyn P, van den Brandt PA. Dietary N-nitroso compounds, endogenous nitrosation, and the risk of esophageal and gastric cancer subtypes in the Netherlands Cohort Study. (2013) *Am J Clin Nutr* **97**:135-46.

223. Dellavalle CT, Xiao Q, Yang G et al. Dietary nitrate and nitrite intake and risk of colorectal cancer in the Shanghai Women's Health Study. (2014) *Int J Cancer* **134**:2917-26.

224. Ahluwalia A, Gladwin M, Coleman GD et al. Dietary Nitrate and the Epidemiology of Cardiovascular Disease: Report From a National Heart, Lung, and Blood Institute Workshop. (2016) *J Am Heart Assoc* **5**.

225. Yawata Y, Ding L, Tanishima K, Tomoda A. New variant of cytochrome b5 reductase deficiency (b5RKurashiki) in red cells, platelets, lymphocytes, and cultured fibroblasts with congenital methemoglobinemia, mental and neurological retardation, and skeletal anomalies. (1992) *Am J Hematol* **40**:299-305.

226. Greer FR, Shannon M. Infant methemoglobinemia: the role of dietary nitrate in food and water. (2005) *Pediatrics* **116**:784-6.

227. Kanady JA, Aruni AW, Ninnis JR et al. Nitrate reductase activity of bacteria in saliva of term and preterm infants. (2012) *Nitric Oxide* **27**:193-200.

228. Timby N, Domellof M, Hernell O et al. Effects of age, sex and diet on salivary nitrate and nitrite in infants. (2019) *Nitric Oxide* **94**:73-78.

229. Allen K, Chuter KM, Fithon K, Marshall L, Hauton D. Modulation of the orthostatic blood pressure response by acute nitrate consumption is dependent upon ethnic origin. (2018) *Clin Exp Pharmacol Physiol* **45**:1106-1117.

230. Kapil V, Rathod KS, Khambata RS et al. Sex differences in the nitrate-nitrite-NO(*) pathway: Role of oral nitrate-reducing bacteria. (2018) *Free Radic Biol Med* **126**:113-121.

231. Lidder S, Webb AJ. Vascular effects of dietary nitrate (as found in green leafy vegetables and beetroot) via the nitrate-nitrite-nitric oxide pathway. (2013) *Br J Clin Pharmacol* **75**:677-96.

232. Saito T, Takeichi S, Osawa M, Yukawa N, Huang XL. A case of fatal methemoglobinemia of unknown origin but presumably due to ingestion of nitrate. (2000) *Int J Legal Med* **113**:164-7.

233. Avery AA. Infantile methemoglobinemia: reexamining the role of drinking water nitrates. (1999) *Environ Health Perspect* **107**:583-6.

234. Percy MJ, Lappin TR. Recessive congenital methaemoglobinaemia: cytochrome b(5) reductase deficiency. (2008) *Br J Haematol* **141**:298-308.

235. Gibson QH. The reduction of methaemoglobin in red blood cells and studies on the cause of idiopathic methaemoglobinaemia. (1948) *Biochem J* **42**:13-23.

236. Howes RE, Piel FB, Patil AP et al. G6PD deficiency prevalence and estimates of affected populations in malaria endemic countries: a geostatistical model-based map. (2012) *PLoS Med* **9**:e1001339.

237. Stanton RC. Glucose-6-phosphate dehydrogenase, NADPH, and cell survival. (2012) *IUBMB Life* **64**:362-9.

238. Schuurman M, van Waardenburg D, Da Costa J, Niemarkt H, Leroy P. Severe hemolysis and methemoglobinemia following fava beans ingestion in glucose-6-phosphatase dehydrogenase deficiency: case report and literature review. (2009) *Eur J Pediatr* **168**:779-82.

239. Beutler E, Duparc S. Glucose-6-phosphate dehydrogenase deficiency and antimalarial drug development. (2007) *Am J Trop Med Hyg* **77**:779-89.

240. Ruwende C, Khoo SC, Snow RW et al. Natural selection of hemi- and heterozygotes for G6PD deficiency in Africa by resistance to severe malaria. (1995) *Nature* **376**:246-9.

241. Baskin SI, Horowitz AM, Nealley EW. The antidotal action of sodium nitrite and sodium thiosulfate against cyanide poisoning. (1992) *J Clin Pharmacol* **32**:368-75.

242. Ignarro LJ, Buga GM, Wood KS, Byrns RE, Chaudhuri G. Endothelium-derived relaxing factor produced and released from artery and vein is nitric oxide. (1987) *Proc Natl Acad Sci U S A* **84**:9265-9.

243. Ichinose F, Roberts JD, Jr., Zapol WM. Inhaled nitric oxide: a selective pulmonary vasodilator: current uses and therapeutic potential. (2004) *Circulation* **109**:3106-11.

244. Young JD, Sear JW, Valvini EM. Kinetics of methaemoglobin and serum nitrogen oxide production during inhalation of nitric oxide in volunteers. (1996) *Br J Anaesth* **76**:652-6.

245. Michael JR, Barton RG, Saffle JR et al. Inhaled nitric oxide versus conventional therapy: effect on oxygenation in ARDS. (1998) *Am J Respir Crit Care Med* **157**:1372-80.

246. Loh E, Stamler JS, Hare JM, Loscalzo J, Colucci WS. Cardiovascular effects of inhaled nitric oxide in patients with left ventricular dysfunction. (1994) *Circulation* **90**:2780-5.

247. Rix PJ, Vick A, Attkins NJ et al. Pharmacokinetics, pharmacodynamics, safety, and tolerability of nebulized sodium nitrite (AIR001) following repeat-dose inhalation in healthy subjects. (2015) *Clin Pharmacokinet* **54**:261-72.

248. Borlaug BA, Melenovsky V, Koepp KE. Inhaled Sodium Nitrite Improves Rest and Exercise Hemodynamics in Heart Failure With Preserved Ejection Fraction. (2016) *Circ Res* **119**:880-6.

249. Liu D, Fernandez BO, Hamilton A et al. UVA irradiation of human skin vasodilates arterial vasculature and lowers blood pressure independently of nitric oxide synthase. (2014) *J Invest Dermatol* **134**:1839-1846.

250. Munzel T, Daiber A, Gori T. Nitrate therapy: new aspects concerning molecular action and tolerance. (2011) *Circulation* **123**:2132-44.

251. Chen Z, Zhang J, Stamler JS. Identification of the enzymatic mechanism of nitroglycerin bioactivation. (2002) *Proc Natl Acad Sci U S A* **99**:8306-11.

252. Li H, Liu X, Cui H, Chen YR, Cardounel AJ, Zweier JL. Characterization of the mechanism of cytochrome P450 reductase-cytochrome P450-mediated nitric oxide and nitrosothiol generation from organic nitrates. (2006) *J Biol Chem* **281**:12546-54.

253. Munzel T, Giaid A, Kurz S, Stewart DJ, Harrison DG. Evidence for a role of endothelin 1 and protein kinase C in nitroglycerin tolerance. (1995) *Proc Natl Acad Sci U S A* **92**:5244-8.

254. Munzel T, Sayegh H, Freeman BA, Tarpey MM, Harrison DG. Evidence for enhanced vascular superoxide anion production in nitrate tolerance. A novel mechanism underlying tolerance and cross-tolerance. (1995) *J Clin Invest* **95**:187-94.

255. Heitzer T, Just H, Brockhoff C, Meinertz T, Olschewski M, Munzel T. Long-term nitroglycerin treatment is associated with supersensitivity to vasoconstrictors in men with stable coronary artery disease: prevention by concomitant treatment with captopril. (1998) *J Am Coll Cardiol* **31**:83-8.

256. Horowitz JD, Antman EM, Lorell BH, Barry WH, Smith TW. Potentiation of the cardiovascular effects of nitroglycerin by N-acetylcysteine. (1983) *Circulation* **68**:1247-53.

257. Pasupathy S, Tavella R, Grover S et al. Early Use of N-acetylcysteine With Nitrate Therapy in Patients Undergoing Primary Percutaneous Coronary Intervention for ST-Segment-Elevation Myocardial Infarction Reduces

Myocardial Infarct Size (the NACIAM Trial [N-acetylcysteine in Acute Myocardial Infarction]). (2017) *Circulation* **136**:894-903.

258. Taylor AL, Ziesche S, Yancy C et al. Combination of isosorbide dinitrate and hydralazine in blacks with heart failure. (2004) *N Engl J Med* **351**:2049-57.

259. Tinker JH, Michenfelder JD. Sodium nitroprusside: pharmacology, toxicology and therapeutics. (1976) *Anesthesiology* **45**:340-54.

260. Hottinger DG, Beebe DS, Kozhimannil T, Prielipp RC, Belani KG. Sodium nitroprusside in 2014: A clinical concepts review. (2014) *J Anaesthesiol Clin Pharmacol* **30**:462-71.

261. Rector TS, Bank AJ, Mullen KA et al. Randomized, double-blind, placebo-controlled study of supplemental oral L-arginine in patients with heart failure. (1996) *Circulation* **93**:2135-41.

262. Bode-Boger SM, Boger RH, Alfke H et al. L-arginine induces nitric oxide-dependent vasodilation in patients with critical limb ischemia. A randomized, controlled study. (1996) *Circulation* **93**:85-90.

263. Schulman SP, Becker LC, Kass DA et al. L-arginine therapy in acute myocardial infarction: the Vascular Interaction With Age in Myocardial Infarction (VINTAGE MI) randomized clinical trial. (2006) *Jama* **295**:58-64.

264. Boerrigter G, Burnett JC, Jr. Nitric oxide-independent stimulation of soluble guanylate cyclase with BAY 41-2272 in cardiovascular disease. (2007) *Cardiovasc Drug Rev* **25**:30-45.

265. Boerrigter G, Costello-Boerrigter LC, Cataliotti A, Lapp H, Stasch JP, Burnett JC, Jr. Targeting heme-oxidized soluble guanylate cyclase in experimental heart failure. (2007) *Hypertension* **49**:1128-33.

266. Simonneau G, D'Armini AM, Ghofrani HA et al. Riociguat for the treatment of chronic thromboembolic pulmonary hypertension: a long-term extension study (CHEST-2). (2015) *Eur Respir J* **45**:1293-302.

267. Ghofrani HA, D'Armini AM, Grimminger F et al. Riociguat for the treatment of chronic thromboembolic pulmonary hypertension. (2013) *N Engl J Med* **369**:319-29.

268. Gheorghiade M, Greene SJ, Filippatos G et al. Cinaciguat, a soluble guanylate cyclase activator: results from the randomized, controlled, phase IIb COMPOSE programme in acute heart failure syndromes. (2012) *Eur J Heart Fail* **14**:1056-66.

269. Boswell-Smith V, Spina D, Page CP. Phosphodiesterase inhibitors. (2006) *Br J Pharmacol* **147 Suppl 1**:S252-7.

270. Castro LR, Schittl J, Fischmeister R. Feedback control through cGMP-dependent protein kinase contributes to differential regulation and compartmentation of cGMP in rat cardiac myocytes. (2010) *Circ Res* **107**:1232-40.

271. Ballard SA, Gingell CJ, Tang K, Turner LA, Price ME, Naylor AM. Effects of sildenafil on the relaxation of human corpus cavernosum tissue in vitro and on the activities of cyclic nucleotide phosphodiesterase isozymes. (1998) *J Urol* **159**:2164-71.

272. Movsesian MA, Kukreja RC. Phosphodiesterase inhibition in heart failure. (2011) *Handb Exp Pharmacol*:237-49.

273. Packer M, Carver JR, Rodeheffer RJ et al. Effect of oral milrinone on mortality in severe chronic heart failure. The PROMISE Study Research Group. (1991) *N Engl J Med* **325**:1468-75.

274. Hasenfuss G, Pieske B. Calcium cycling in congestive heart failure. (2002) *J Mol Cell Cardiol* **34**:951-69.

275. Guazzi M, Tumminello G, Di Marco F, Fiorentini C, Guazzi MD. The effects of phosphodiesterase-5 inhibition with sildenafil on pulmonary hemodynamics and diffusion capacity, exercise ventilatory efficiency, and oxygen uptake kinetics in chronic heart failure. (2004) *J Am Coll Cardiol* **44**:2339-48.

276. Nakamura T, Zhu G, Ranek MJ et al. Prevention of PKG-1alpha Oxidation Suppresses Antihypertrophic/Antifibrotic Effects From PDE5 Inhibition but not sGC Stimulation. (2018) *Circ Heart Fail* **11**:e004740.

277. Prysyazhna O, Eaton P. Redox regulation of cGMP-dependent protein kinase Ialpha in the cardiovascular system. (2015) *Front Pharmacol* **6**:139.

278. Burgoyne JR, Madhani M, Cuello F et al. Cysteine redox sensor in PKGIa enables oxidant-induced activation. (2007) *Science* **317**:1393-7.

279. Burgoyne JR, Prysyazhna O, Rudyk O, Eaton P. cGMP-dependent activation of protein kinase G precludes disulfide activation: implications for blood pressure control. (2012) *Hypertension* **60**:1301-8.

280. Burgoyne JR, Prysyazhna O, Richards DA, Eaton P. Proof of Principle for a Novel Class of Antihypertensives That Target the Oxidative Activation of PKG Ialpha (Protein Kinase G Ialpha). (2017) *Hypertension* **70**:577-586.

281. Matoba T, Shimokawa H, Nakashima M et al. Hydrogen peroxide is an endothelium-derived hyperpolarizing factor in mice. (2000) *J Clin Invest* **106**:1521-30.

282. Prysyazhna O, Rudyk O, Eaton P. Single atom substitution in mouse protein kinase G eliminates oxidant sensing to cause hypertension. (2012) *Nat Med* **18**:286-90.

283. Rudyk O, Prysyazhna O, Burgoyne JR, Eaton P. Nitroglycerin fails to lower blood pressure in redox-dead Cys42Ser PKG1alpha knock-in mouse. (2012) *Circulation* **126**:287-95.

284. Stubbert D, Prysyazhna O, Rudyk O, Scotcher J, Burgoyne JR, Eaton P. Protein kinase G Ialpha oxidation paradoxically underlies blood pressure lowering by the reductant hydrogen sulfide. (2014) *Hypertension* **64**:1344-51.

285. Prysyazhna O, Wolhuter K, Switzer C et al. Blood Pressure-Lowering by the Antioxidant Resveratrol Is Counterintuitively Mediated by Oxidation of cGMP-Dependent Protein Kinase. (2019) *Circulation* **140**:126-137.

286. Friederich-Persson M, Nguyen Dinh Cat A, Persson P, Montezano AC, Touyz RM. Brown Adipose Tissue Regulates Small Artery Function Through NADPH Oxidase 4-Derived Hydrogen Peroxide and Redox-Sensitive Protein Kinase G-1alpha. (2017) *Arterioscler Thromb Vasc Biol* **37**:455-465.

287. Mitschke MM, Hoffmann LS, Gnad T et al. Increased cGMP promotes healthy expansion and browning of white adipose tissue. (2013) *Faseb j* **27**:1621-30.

288. Crabtree MJ, Channon KM. Synthesis and recycling of tetrahydrobiopterin in endothelial function and vascular disease. (2011) *Nitric Oxide* **25**:81-88.

289. Kroncke KD, Fehsel K, Kolb-Bachofen V. Inducible nitric oxide synthase in human diseases. (1998) *Clin Exp Immunol* **113**:147-56.

290. Rudyk O, Phinikaridou A, Prysyazhna O, Burgoyne JR, Botnar RM, Eaton P. Protein kinase G oxidation is a major cause of injury during sepsis. (2013) *Proc Natl Acad Sci U S A* **110**:9909-13.

291. Rudyk O, Rowan A, Prysyazhna O et al. Oxidation of PKGIalpha mediates an endogenous adaptation to pulmonary hypertension. (2019) *Proc Natl Acad Sci U S A* **116**:13016-13025.

292. Feelisch M, Akaike T, Griffiths K et al. Long-lasting blood pressure lowering effects of nitrite are NO-independent and mediated by hydrogen peroxide, persulfides, and oxidation of protein kinase G1α redox signalling. (2020) *Cardiovasc Res* **116**:51-62.

293. Roberts LD, Ashmore T, Kotwica AO et al. Inorganic nitrate promotes the browning of white adipose tissue through the nitrate-nitrite-nitric oxide pathway. (2015) *Diabetes* **64**:471-484.

294. Scotcher J, Prysyazhna O, Boguslavskyi A et al. Disulfide-activated protein kinase G Ialpha regulates cardiac diastolic relaxation and fine-tunes the Frank-Starling response. (2016) *Nat Commun* **7**:13187.

295. Bers DM. Cardiac excitation-contraction coupling. (2002) *Nature* **415**:198-205.

296. Prysyazhna O, Burgoyne JR, Scotcher J, Grover S, Kass D, Eaton P. Phosphodiesterase 5 Inhibition Limits Doxorubicin-induced Heart Failure by Attenuating Protein Kinase G Ialpha Oxidation. (2016) *J Biol Chem* **291**:17427-36.

297. Perlman DH, Bauer SM, Ashrafian H et al. Mechanistic insights into nitrite-induced cardioprotection using an integrated metabolomic/proteomic approach. (2009) *Circ Res* **104**:796-804.

298. Larsen FJ, Weitzberg E, Lundberg JO, Ekblom B. Effects of dietary nitrate on oxygen cost during exercise. (2007) *Acta Physiol (Oxf)* **191**:59-66.

299. Larsen FJ, Schiffer TA, Borniquel S et al. Dietary inorganic nitrate improves mitochondrial efficiency in humans. (2011) *Cell Metab* **13**:149-59.

300. Maher AR, Milsom AB, Gunaruwan P et al. Hypoxic modulation of exogenous nitrite-induced vasodilation in humans. (2008) *Circulation* **117**:670-7.

301. Hunter CJ, Dejam A, Blood AB et al. Inhaled nebulized nitrite is a hypoxia-sensitive NO-dependent selective pulmonary vasodilator. (2004) *Nat Med* **10**:1122-7.

302. Rosenkranz S, Gibbs JS, Wachter R, De Marco T, Vonk-Noordegraaf A, Vachiery JL. Left ventricular heart failure and pulmonary hypertension. (2016) *Eur Heart J* **37**:942-54.

303. Lam CS, Roger VL, Rodeheffer RJ, Borlaug BA, Enders FT, Redfield MM. Pulmonary hypertension in heart failure with preserved ejection fraction: a community-based study. (2009) *J Am Coll Cardiol* **53**:1119-26.

304. Lai YC, Tabima DM, Dube JJ et al. SIRT3-AMP-Activated Protein Kinase Activation by Nitrite and Metformin Improves Hyperglycemia and Normalizes Pulmonary Hypertension Associated With Heart Failure With Preserved Ejection Fraction. (2016) *Circulation* **133**:717-31.

305. Zhu SG, Kukreja RC, Das A, Chen Q, Lesnefsky EJ, Xi L. Dietary nitrate supplementation protects against Doxorubicin-induced cardiomyopathy by improving mitochondrial function. (2011) *J Am Coll Cardiol* **57**:2181-9.

306. Siddiqi N, Neil C, Bruce M et al. Intravenous sodium nitrite in acute ST-elevation myocardial infarction: a randomized controlled trial (NIAMI). (2014) *Eur Heart J* **35**:1255-62.

307. Freeman BA, Baker PR, Schopfer FJ, Woodcock SR, Napolitano A, d'Ischia M. Nitro-fatty acid formation and signaling. (2008) *J Biol Chem* **283**:15515-9.

308. Cui T, Schopfer FJ, Zhang J et al. Nitrated fatty acids: Endogenous anti-inflammatory signaling mediators. (2006) *J Biol Chem* **281**:35686-98.

309. Chang S, Hu L, Xu Y et al. Inorganic Nitrate Alleviates Total Body Irradiation-Induced Systemic Damage by Decreasing Reactive Oxygen Species Levels. (2019) *Int J Radiat Oncol Biol Phys* **103**:945-957.

310. Coggan AR, Leibowitz JL, Spearie CA et al. Acute Dietary Nitrate Intake Improves Muscle Contractile Function in Patients With Heart Failure: A Double-Blind, Placebo-Controlled, Randomized Trial. (2015) *Circ Heart Fail* **8**:914-20.

311. Maher AR, Arif S, Madhani M et al. Impact of chronic congestive heart failure on pharmacokinetics and vasomotor effects of infused nitrite. (2013) *Br J Pharmacol* **169**:659-70.

312. Coggan AR, Broadstreet SR, Mahmood K et al. Dietary Nitrate Increases VO2peak and Performance but Does Not Alter Ventilation or Efficiency in

Patients With Heart Failure With Reduced Ejection Fraction. (2018) *J Card Fail* **24**:65-73.

313. Hirai DM, Zelt JT, Jones JH et al. Dietary nitrate supplementation and exercise tolerance in patients with heart failure with reduced ejection fraction. (2017) *Am J Physiol Regul Integr Comp Physiol* **312**:R13-r22.

314. Ormerod JO, Arif S, Mukadam M et al. Short-term intravenous sodium nitrite infusion improves cardiac and pulmonary hemodynamics in heart failure patients. (2015) *Circ Heart Fail* **8**:565-71.

315. Borlaug BA, Koepp KE, Melenovsky V. Sodium Nitrite Improves Exercise Hemodynamics and Ventricular Performance in Heart Failure With Preserved Ejection Fraction. (2015) *J Am Coll Cardiol* **66**:1672-82.

316. Zamani P, Rawat D, Shiva-Kumar P et al. Effect of inorganic nitrate on exercise capacity in heart failure with preserved ejection fraction. (2015) *Circulation* **131**:371-80; discussion 380.

317. Borlaug BA, Anstrom KJ, Lewis GD et al. Effect of Inorganic Nitrite vs Placebo on Exercise Capacity Among Patients With Heart Failure With Preserved Ejection Fraction: The INDIE-HFpEF Randomized Clinical Trial. (2018) *Jama* **320**:1764-1773.

318. Ntessalen M, Procter NEK, Schwarz K et al. Inorganic nitrate and nitrite supplementation fails to improve skeletal muscle mitochondrial efficiency in mice and humans. (2020) *Am J Clin Nutr* **111**:79-89.

319. Welinder C, Ekblad L. Coomassie staining as loading control in Western blot analysis. (2011) *J Proteome Res* **10**:1416-9.

320. Burgoyne JR, Eaton P. Approaches for Monitoring PKG1α Oxidative Activation. In: Krieg T, Lukowski R, editors. Guanylate Cyclase and Cyclic GMP: Methods and Protocols. Totowa, NJ: Humana Press, 2013:163-173.

321. Kanwar M, Kowluru RA. Role of glyceraldehyde 3-phosphate dehydrogenase in the development and progression of diabetic retinopathy. (2009) *Diabetes* **58**:227-34.

322. Linn TC, Pettit FH, Reed LJ. Alpha-keto acid dehydrogenase complexes. X. Regulation of the activity of the pyruvate dehydrogenase complex from beef kidney mitochondria by phosphorylation and dephosphorylation. (1969) *Proc Natl Acad Sci U S A* **62**:234-41.

323. Constantin-Teodosiu D, Cederblad G, Hultman E. A sensitive radioisotopic assay of pyruvate dehydrogenase complex in human muscle tissue. (1991) *Anal Biochem* **198**:347-51.

324. Rassaf T, Bryan NS, Kelm M, Feelisch M. Concomitant presence of N-nitroso and S-nitroso proteins in human plasma. (2002) *Free Radic Biol Med* **33**:1590-6.

325. Riss TL, Moravec RA, Niles AL et al. Cell Viability Assays. In: Markossian S, Sittampalam GS, Grossman A, et al., editors. Assay Guidance Manual. Bethesda (MD): Eli Lilly & Company and the National Center for Advancing Translational Sciences, 2004.

326. Borgognone A, Shantsila E, Worrall SM et al. Nitrite circumvents platelet resistance to nitric oxide in patients with heart failure preserved ejection fraction and chronic atrial fibrillation. (2018) *Cardiovasc Res* **114**:1313-1323.

327. Herman DS, Lam L, Taylor MR et al. Truncations of titin causing dilated cardiomyopathy. (2012) *N Engl J Med* **366**:619-28.

328. Altman DG, Bland JM. Treatment allocation by minimisation. (2005) *Bmj* **330**:843.

329. Beadle RM, Williams LK, Kuehl M et al. Improvement in cardiac energetics by perhexiline in heart failure due to dilated cardiomyopathy. (2015) *JACC Heart Fail* **3**:202-11.

330. Bradley H, Shaw CS, Bendtsen C et al. Visualization and quantitation of GLUT4 translocation in human skeletal muscle following glucose ingestion and exercise. (2015) *Physiol Rep* **3**.

331. Bergstrom J. Percutaneous needle biopsy of skeletal muscle in physiological and clinical research. (1975) *Scand J Clin Lab Invest* **35**:609-16.

332. Camera DM, Burniston JG, Pogson MA, Smiles WJ, Hawley JA. Dynamic proteome profiling of individual proteins in human skeletal muscle after a high-fat diet and resistance exercise. (2017) *Faseb j* **31**:5478-5494.

333. ATS statement: guidelines for the six-minute walk test. (2002) *Am J Respir Crit Care Med* **166**:111-7.

334. Rector TS, Cohn JN. Assessment of patient outcome with the Minnesota Living with Heart Failure questionnaire: reliability and validity during a randomized, double-blind, placebo-controlled trial of pimobendan. Pimobendan Multicenter Research Group. (1992) *Am Heart J* **124**:1017-25.

335. ATS/ACCP Statement on cardiopulmonary exercise testing. (2003) *Am J Respir Crit Care Med* **167**:211-77.

336. Hansen JE, Sue DY, Wasserman K. Predicted values for clinical exercise testing. (1984) *American Review of Respiratory Disease* **129**:S49-S55.

337. Schneider J. Age dependency of oxygen uptake and related parameters in exercise testing: an expert opinion on reference values suitable for adults. (2013) *Lung* **191**:449-58.

338. Gibbons RJ, Balady GJ, Beasley JW et al. ACC/AHA Guidelines for Exercise Testing. A report of the American College of Cardiology/American Heart Association Task Force on Practice Guidelines (Committee on Exercise Testing). (1997) *J Am Coll Cardiol* **30**:260-311.

339. Lang RM, Badano LP, Mor-Avi V et al. Recommendations for cardiac chamber quantification by echocardiography in adults: an update from the American Society of Echocardiography and the European Association of Cardiovascular Imaging. (2015) *J Am Soc Echocardiogr* **28**:1-39.e14.

340. Lam CS, Roger VL, Rodeheffer RJ et al. Cardiac structure and ventricular-vascular function in persons with heart failure and preserved ejection fraction from Olmsted County, Minnesota. (2007) *Circulation* **115**:1982-90.

341. Devereux RB, Reichek N. Echocardiographic determination of left ventricular mass in man. Anatomic validation of the method. (1977) *Circulation* **55**:613-8.

342. Baumgartner H, Hung J, Bermejo J et al. Echocardiographic assessment of valve stenosis: EAE/ASE recommendations for clinical practice. (2009) *J Am Soc Echocardiogr* **22**:1-23; quiz 101-2.

343. Lancellotti P, Tribouilloy C, Hagendorff A et al. Recommendations for the echocardiographic assessment of native valvular regurgitation: an executive summary from the European Association of Cardiovascular Imaging. (2013) *Eur Heart J Cardiovasc Imaging* **14**:611-44.

344. Burkhoff D. Pressure-volume loops in clinical research: a contemporary view. (2013) *J Am Coll Cardiol* **62**:1173-6.

345. Rudski LG, Lai WW, Afilalo J et al. Guidelines for the echocardiographic assessment of the right heart in adults: a report from the American Society of Echocardiography endorsed by the European Association of Echocardiography, a registered branch of the European Society of Cardiology, and the Canadian Society of Echocardiography. (2010) *J Am Soc Echocardiogr* **23**:685-713; quiz 786-8.

346. Mor-Avi V, Lang RM, Badano LP et al. Current and evolving echocardiographic techniques for the quantitative evaluation of cardiac mechanics: ASE/EAE consensus statement on methodology and indications endorsed by the Japanese Society of Echocardiography. (2011) *J Am Soc Echocardiogr* **24**:277-313.

347. Chen CH, Fetics B, Nevo E et al. Noninvasive single-beat determination of left ventricular end-systolic elastance in humans. (2001) *J Am Coll Cardiol* **38**:2028-34.

348. Lee WS, Huang WP, Yu WC, Chiou KR, Ding PY, Chen CH. Estimation of preload recruitable stroke work relationship by a single-beat technique in humans. (2003) *Am J Physiol Heart Circ Physiol* **284**:H744-50.

349. Lee L, Campbell R, Scheuermann-Freestone M et al. Metabolic modulation with perhexiline in chronic heart failure: a randomized, controlled trial of short-term use of a novel treatment. (2005) *Circulation* **112**:3280-8.

350. Recchia FA, McConnell PI, Loke KE, Xu X, Ochoa M, Hintze TH. Nitric oxide controls cardiac substrate utilization in the conscious dog. (1999) *Cardiovasc Res* **44**:325-32.

351. Liu LX, Rowe GC, Yang S et al. PDK4 Inhibits Cardiac Pyruvate Oxidation in Late Pregnancy. (2017) *Circ Res* **121**:1370-1378.

352. Horscroft JA, O'Brien KA, Clark AD et al. Inorganic nitrate, hypoxia, and the regulation of cardiac mitochondrial respiration-probing the role of PPARα. (2019) *Faseb j* **33**:7563-7577.

353. Waltz P, Escobar D, Botero AM, Zuckerbraun BS. Nitrate/Nitrite as Critical Mediators to Limit Oxidative Injury and Inflammation. (2015) *Antioxid Redox Signal* **23**:328-39.

354. Khambata RS, Ghosh SM, Rathod KS et al. Antiinflammatory actions of inorganic nitrate stabilize the atherosclerotic plaque. (2017) *Proc Natl Acad Sci U S A* **114**:E550-e559.

355. Rainer PP, Kass DA. Old dog, new tricks: novel cardiac targets and stress regulation by protein kinase G. (2016) *Cardiovasc Res* **111**:154-62.

356. Prosser BL, Khairallah RJ, Ziman AP, Ward CW, Lederer WJ. X-ROS signaling in the heart and skeletal muscle: stretch-dependent local ROS regulates $[Ca^{2+}]i$. (2013) *J Mol Cell Cardiol* **58**:172-81.

357. Burgoyne JR, Mongue-Din H, Eaton P, Shah AM. Redox signaling in cardiac physiology and pathology. (2012) *Circ Res* **111**:1091-106.

358. Schmitt JP, Kamisago M, Asahi M et al. Dilated cardiomyopathy and heart failure caused by a mutation in phospholamban. (2003) *Science* **299**:1410-3.

359. Kranias EG, Hajjar RJ. Modulation of cardiac contractility by the phospholamban/SERCA2a regulatome. (2012) *Circ Res* **110**:1646-60.

360. Kato M, Li J, Chuang JL, Chuang DT. Distinct structural mechanisms for inhibition of pyruvate dehydrogenase kinase isoforms by AZD7545, dichloroacetate, and radicicol. (2007) *Structure* **15**:992-1004.

361. Ashmore T, Roberts LD, Morash AJ et al. Nitrate enhances skeletal muscle fatty acid oxidation via a nitric oxide-cGMP-PPAR-mediated mechanism. (2015) *BMC Biol* **13**:110.

362. Chandel NS, McClintock DS, Feliciano CE et al. Reactive oxygen species generated at mitochondrial complex III stabilize hypoxia-inducible factor-1alpha during hypoxia: a mechanism of O2 sensing. (2000) *J Biol Chem* **275**:25130-8.

363. Rardin MJ, Wiley SE, Naviaux RK, Murphy AN, Dixon JE. Monitoring phosphorylation of the pyruvate dehydrogenase complex. (2009) *Anal Biochem* **389**:157-64.

364. Beyer T, Townsend DW, Brun T et al. A combined PET/CT scanner for clinical oncology. (2000) *J Nucl Med* **41**:1369-79.

365. Warburg O, Wind F, Negelein E. THE METABOLISM OF TUMORS IN THE BODY. (1927) *J Gen Physiol* **8**:519-30.

366. Semenza GL, Wang GL. A nuclear factor induced by hypoxia via de novo protein synthesis binds to the human erythropoietin gene enhancer at a site required for transcriptional activation. (1992) *Mol Cell Biol* **12**:5447-54.

367. Courtnay R, Ngo DC, Malik N, Ververis K, Tortorella SM, Karagiannis TC. Cancer metabolism and the Warburg effect: the role of HIF-1 and PI3K. (2015) *Mol Biol Rep* **42**:841-51.

368. Gossage L, Eisen T, Maher ER. VHL, the story of a tumour suppressor gene. (2015) *Nat Rev Cancer* **15**:55-64.

369. Poillet-Perez L, Despouy G, Delage-Mourroux R, Boyer-Guittaut M. Interplay between ROS and autophagy in cancer cells, from tumor initiation to cancer therapy. (2015) *Redox Biol* **4**:184-92.

370. Currie E, Schulze A, Zechner R, Walther TC, Farese RV, Jr. Cellular fatty acid metabolism and cancer. (2013) *Cell Metab* **18**:153-61.

371. Röhrig F, Schulze A. The multifaceted roles of fatty acid synthesis in cancer. (2016) *Nat Rev Cancer* **16**:732-749.

372. Golias T, Papandreou I, Sun R et al. Hypoxic repression of pyruvate dehydrogenase activity is necessary for metabolic reprogramming and growth of model tumours. (2016) *Sci Rep* **6**:31146.

373. Kaplon J, Zheng L, Meissl K et al. A key role for mitochondrial gatekeeper pyruvate dehydrogenase in oncogene-induced senescence. (2013) *Nature* **498**:109-12.

374. Kimura H, Weisz A, Kurashima Y et al. Hypoxia response element of the human vascular endothelial growth factor gene mediates transcriptional regulation by nitric oxide: control of hypoxia-inducible factor-1 activity by nitric oxide. (2000) *Blood* **95**:189-97.

375. Kinnaird A, Dromparis P, Saleme B et al. Metabolic Modulation of Clear-cell Renal Cell Carcinoma with Dichloroacetate, an Inhibitor of Pyruvate Dehydrogenase Kinase. (2016) *Eur Urol* **69**:734-744.

376. Firth JD, Ebert BL, Ratcliffe PJ. Hypoxic regulation of lactate dehydrogenase A. Interaction between hypoxia-inducible factor 1 and cAMP response elements. (1995) *J Biol Chem* **270**:21021-7.

377. Zhang Z, Yao L, Yang J, Wang Z, Du G. PI3K/Akt and HIF-1 signaling pathway in hypoxia-ischemia (Review). (2018) *Mol Med Rep* **18**:3547-3554.

378. Semenza GL. Hypoxia-inducible factor 1: master regulator of O2 homeostasis. (1998) *Curr Opin Genet Dev* **8**:588-94.

379. Masson N, Ratcliffe PJ. HIF prolyl and asparaginyl hydroxylases in the biological response to intracellular O(2) levels. (2003) *J Cell Sci* **116**:3041-9.

380. Guzy RD, Hoyos B, Robin E et al. Mitochondrial complex III is required for hypoxia-induced ROS production and cellular oxygen sensing. (2005) *Cell Metab* **1**:401-8.

381. Semenza GL. HIF-1 mediates the Warburg effect in clear cell renal carcinoma. (2007) *J Bioenerg Biomembr* **39**:231-4.

382. Roberts AM, Watson IR, Evans AJ, Foster DA, Irwin MS, Ohh M. Suppression of hypoxia-inducible factor 2alpha restores p53 activity via Hdm2 and reverses chemoresistance of renal carcinoma cells. (2009) *Cancer Res* **69**:9056-64.

383. Keith B, Johnson RS, Simon MC. HIF1α and HIF2α: sibling rivalry in hypoxic tumour growth and progression. (2011) *Nat Rev Cancer* **12**:9-22.

384. Agani F, Jiang BH. Oxygen-independent regulation of HIF-1: novel involvement of PI3K/AKT/mTOR pathway in cancer. (2013) *Curr Cancer Drug Targets* **13**:245-51.

385. Lidgren A, Hedberg Y, Grankvist K, Rasmuson T, Vasko J, Ljungberg B. The expression of hypoxia-inducible factor 1alpha is a favorable independent prognostic factor in renal cell carcinoma. (2005) *Clin Cancer Res* **11**:1129-35.

386. Hoefflin R, Harlander S, Schäfer S et al. HIF-1α and HIF-2α differently regulate tumour development and inflammation of clear cell renal cell carcinoma in mice. (2020) *Nat Commun* **11**:4111.

387. Hu CJ, Wang LY, Chodosh LA, Keith B, Simon MC. Differential roles of hypoxia-inducible factor 1alpha (HIF-1alpha) and HIF-2alpha in hypoxic gene regulation. (2003) *Mol Cell Biol* **23**:9361-74.

388. Du W, Zhang L, Brett-Morris A et al. HIF drives lipid deposition and cancer in ccRCC via repression of fatty acid metabolism. (2017) *Nat Commun* **8**:1769.

389. Martínez-Reyes I, Chandel NS. Mitochondrial TCA cycle metabolites control physiology and disease. (2020) *Nat Commun* **11**:102.

390. Metallo CM, Gameiro PA, Bell EL et al. Reductive glutamine metabolism by IDH1 mediates lipogenesis under hypoxia. (2011) *Nature* **481**:380-4.

391. Biswas S, Troy H, Leek R et al. Effects of HIF-1alpha and HIF2alpha on Growth and Metabolism of Clear-Cell Renal Cell Carcinoma 786-0 Xenografts. (2010) *J Oncol* **2010**:757908.

392. Longley DB, Harkin DP, Johnston PG. 5-fluorouracil: mechanisms of action and clinical strategies. (2003) *Nat Rev Cancer* **3**:330-8.

393. O'Connor PM, Jackman J, Bae I et al. Characterization of the p53 tumor suppressor pathway in cell lines of the National Cancer Institute anticancer drug screen and correlations with the growth-inhibitory potency of 123 anticancer agents. (1997) *Cancer Res* **57**:4285-300.

394. Lowe SW, Bodis S, McClatchey A et al. p53 status and the efficacy of cancer therapy in vivo. (1994) *Science* **266**:807-10.

395. Johnson TM, Yu ZX, Ferrans VJ, Lowenstein RA, Finkel T. Reactive oxygen species are downstream mediators of p53-dependent apoptosis. (1996) *Proc Natl Acad Sci U S A* **93**:11848-52.

396. Lai YC, Tabima DM, Dube JJ et al. SIRT3-AMP-Activated Protein Kinase Activation by Nitrite and Metformin Improves Hyperglycemia and Normalizes Pulmonary Hypertension Associated With Heart Failure With Preserved Ejection Fraction. (2016) *Circulation* **133**:717-31.

397. Gao YH, Wu ZX, Xie LQ et al. VHL deficiency augments anthracycline sensitivity of clear cell renal cell carcinomas by down-regulating ALDH2. (2017) *Nat Commun* **8**:15337.

398. Arif S, Borgognone A, Lin EL et al. Role of aldehyde dehydrogenase in hypoxic vasodilator effects of nitrite in rats and humans. (2015) *Br J Pharmacol* **172**:3341-52.

399. Ormerod JO, Evans JD, Contractor H et al. Human Second Window Pre-Conditioning and Post-Conditioning by Nitrite Is Influenced by a Common Polymorphism in Mitochondrial Aldehyde Dehydrogenase. (2017) *JACC Basic Transl Sci* **2**:13-21.

400. Park JH, Marwick TH. Use and Limitations of E/e' to Assess Left Ventricular Filling Pressure by Echocardiography. (2011) *J Cardiovasc Ultrasound* **19**:169-73.

401. Kerley CP, O'Neill JO, Reddy Bijjam V, Blaine C, James PE, Cormican L. Dietary nitrate increases exercise tolerance in patients with non-ischemic, dilated cardiomyopathy-a double-blind, randomized, placebo-controlled, crossover trial. (2016) *J Heart Lung Transplant* **35**:922-6.

402. Woessner MN, Levinger I, Allen JD, McIlvenna LC, Neil C. The Effect of Dietary Inorganic Nitrate Supplementation on Cardiac Function during Submaximal Exercise in Men with Heart Failure with Reduced Ejection Fraction (HFrEF): A Pilot Study. (2020) *Nutrients* **12**.

403. Maron BJ, Maron MS. Hypertrophic cardiomyopathy. (2013) *Lancet* **381**:242-55.

404. Semsarian C, Ingles J, Maron MS, Maron BJ. New perspectives on the prevalence of hypertrophic cardiomyopathy. (2015) *J Am Coll Cardiol* **65**:1249-1254.

405. Qin JX, Shiota T, Lever HM et al. Outcome of patients with hypertrophic obstructive cardiomyopathy after percutaneous transluminal septal myocardial ablation and septal myectomy surgery. (2001) *J Am Coll Cardiol* **38**:1994-2000.

406. Veselka J, Jensen MK, Liebregts M et al. Long-term clinical outcome after alcohol septal ablation for obstructive hypertrophic cardiomyopathy: results from the Euro-ASA registry. (2016) *Eur Heart J* **37**:1517-23.

407. Bonow RO, Rosing DR, Bacharach SL et al. Effects of verapamil on left ventricular systolic function and diastolic filling in patients with hypertrophic cardiomyopathy. (1981) *Circulation* **64**:787-96.

408. Lele SS, Thomson HL, Seo H, Belenkie I, McKenna WJ, Frenneaux MP. Exercise capacity in hypertrophic cardiomyopathy. Role of stroke volume limitation, heart rate, and diastolic filling characteristics. (1995) *Circulation* **92**:2886-94.

409. Abozguia K, Elliott P, McKenna W et al. Metabolic modulator perhexiline corrects energy deficiency and improves exercise capacity in symptomatic hypertrophic cardiomyopathy. (2010) *Circulation* **122**:1562-9.

410. MacIver DH, Clark AL. Contractile Dysfunction in Sarcomeric Hypertrophic Cardiomyopathy. (2016) *J Card Fail*.

411. Spirito P, Maron BJ, Bonow RO, Epstein SE. Occurrence and significance of progressive left ventricular wall thinning and relative cavity dilatation in hypertrophic cardiomyopathy. (1987) *Am J Cardiol* **60**:123-9.

412. Najjar SS, Schulman SP, Gerstenblith G et al. Age and gender affect ventricular-vascular coupling during aerobic exercise. (2004) *J Am Coll Cardiol* **44**:611-7.

413. Austin BA, Popovic ZB, Kwon DH et al. Aortic stiffness independently predicts exercise capacity in hypertrophic cardiomyopathy: a multimodality imaging study. (2010) *Heart* **96**:1303-10.

414. Maron BJ, Gottdiener JS, Epstein SE. Patterns and significance of distribution of left ventricular hypertrophy in hypertrophic cardiomyopathy. A wide angle, two dimensional echocardiographic study of 125 patients. (1981) *Am J Cardiol* **48**:418-28.

415. Shapiro LM, Kleinebenne A, McKenna WJ. The distribution of left ventricular hypertrophy in hypertrophic cardiomyopathy: comparison to athletes and hypertensives. (1985) *Eur Heart J* **6**:967-74.

416. Bruce RA, McDonough JR. Stress testing in screening for cardiovascular disease. (1969) *Bull N Y Acad Med* **45**:1288-305.

417. Davies NJ, Denison DM. The measurement of metabolic gas exchange and minute volume by mass spectrometry alone. (1979) *Respir Physiol* **36**:261-7.

418. Notomi Y, Setser RM, Shiota T et al. Assessment of left ventricular torsional deformation by Doppler tissue imaging: validation study with tagged magnetic resonance imaging. (2005) *Circulation* **111**:1141-7.

419. Lang RM, Bierig M, Devereux RB et al. Recommendations for chamber quantification: a report from the American Society of Echocardiography's Guidelines and Standards Committee and the Chamber Quantification Writing Group, developed in conjunction with the European Association of Echocardiography, a branch of the European Society of Cardiology. (2005) *J Am Soc Echocardiogr* **18**:1440-63.

420. Lele SS, Macfarlane D, Morrison S, Thomson H, Khafagi F, Frenneaux M. Determinants of exercise capacity in patients with coronary artery disease and mild to moderate systolic dysfunction. Role of heart rate and diastolic filling abnormalities. (1996) *Eur Heart J* **17**:204-12.

421. Phan TT, Abozguia K, Nallur Shivu G et al. Heart failure with preserved ejection fraction is characterized by dynamic impairment of active relaxation and contraction of the left ventricle on exercise and associated with myocardial energy deficiency. (2009) *J Am Coll Cardiol* **54**:402-9.

422. Shivu GN, Abozguia K, Phan TT, Ahmed I, Henning A, Frenneaux M. (31)P magnetic resonance spectroscopy to measure in vivo cardiac energetics in normal myocardium and hypertrophic cardiomyopathy: Experiences at 3T. (2010) *Eur J Radiol* **73**:255-9.

423. Neubauer S, Krahe T, Schindler R et al. 31P magnetic resonance spectroscopy in dilated cardiomyopathy and coronary artery disease. Altered cardiac high-energy phosphate metabolism in heart failure. (1992) *Circulation* **86**:1810-8.

424. Crilley JG, Boehm EA, Blair E et al. Hypertrophic cardiomyopathy due to sarcomeric gene mutations is characterized by impaired energy metabolism irrespective of the degree of hypertrophy. (2003) *J Am Coll Cardiol* **41**:1776-82.

425. Jung WI, Sieverding L, Breuer J et al. 31P NMR spectroscopy detects metabolic abnormalities in asymptomatic patients with hypertrophic cardiomyopathy. (1998) *Circulation* **97**:2536-42.

426. Betocchi S, Bonow RO, Bacharach SL, Rosing DR, Maron BJ, Green MV. Isovolumic relaxation period in hypertrophic cardiomyopathy: assessment by radionuclide angiography. (1986) *J Am Coll Cardiol* **7**:74-81.

427. Chen YT, Chang KC, Hu WS, Wang SJ, Chiang BN. Left ventricular diastolic function in hypertrophic cardiomyopathy: assessment by radionuclide angiography. (1987) *Int J Cardiol* **15**:185-93.

428. Neubauer S, Horn M, Cramer M et al. Myocardial phosphocreatine-to-ATP ratio is a predictor of mortality in patients with dilated cardiomyopathy. (1997) *Circulation* **96**:2190-6.

429. Dass S, Cochlin LE, Suttie JJ et al. Exacerbation of cardiac energetic impairment during exercise in hypertrophic cardiomyopathy: a potential mechanism for diastolic dysfunction. (2015) *Eur Heart J* **36**:1547-54.

430. Cecchi F, Olivotto I, Gistri R, Lorenzoni R, Chiriatti G, Camici PG. Coronary microvascular dysfunction and prognosis in hypertrophic cardiomyopathy. (2003) *N Engl J Med* **349**:1027-35.

431. Frey N, Brixius K, Schwinger RH et al. Alterations of tension-dependent ATP utilization in a transgenic rat model of hypertrophic cardiomyopathy. (2006) *J Biol Chem* **281**:29575-82.

432. Jagatheesan G, Rajan S, Petrashevskaya N et al. Rescue of tropomyosin-induced familial hypertrophic cardiomyopathy mice by transgenesis. (2007) *Am J Physiol Heart Circ Physiol* **293**:H949-58.

433. De Tombe PP, Jones S, Burkhoff D, Hunter WC, Kass DA. Ventricular stroke work and efficiency both remain nearly optimal despite altered vascular loading. (1993) *Am J Physiol* **264**:H1817-24.

434. Frenneaux MP, Counihan PJ, Caforio AL, Chikamori T, McKenna WJ. Abnormal blood pressure response during exercise in hypertrophic cardiomyopathy. (1990) *Circulation* **82**:1995-2002.

435. Kranias EG, Solaro RJ. Phosphorylation of troponin I and phospholamban during catecholamine stimulation of rabbit heart. (1982) *Nature* **298**:182-4.

436. Coats CJ, Pavlou M, Watkinson OT et al. Effect of Trimetazidine Dihydrochloride Therapy on Exercise Capacity in Patients With Nonobstructive Hypertrophic Cardiomyopathy: A Randomized Clinical Trial. (2019) *JAMA Cardiol* **4**:230-235.

437. Heitner SB, Jacoby D, Lester SJ et al. Mavacamten Treatment for Obstructive Hypertrophic Cardiomyopathy: A Clinical Trial. (2019) *Ann Intern Med* **170**:741-748.

438. Abozguia K, Clarke K, Lee L, Frenneaux M. Modification of myocardial substrate use as a therapy for heart failure. (2006) *Nat Clin Pract Cardiovasc Med* **3**:490-8.

439. Di Napoli P, Taccardi AA, Barsotti A. Long term cardioprotective action of trimetazidine and potential effect on the inflammatory process in patients with ischaemic dilated cardiomyopathy. (2005) *Heart* **91**:161-5.

440. Horgan JH, O'Callaghan WG, Teo KK. Therapy of angina pectoris with low-dose perhexiline. (1981) *J Cardiovasc Pharmacol* **3**:566-72.

441. Horowitz JD, Mashford ML. Perhexiline maleate in the treatment of severe angina pectoris. (1979) *Med J Aust* **1**:485-8.

442. Horowitz JD, Sia ST, Macdonald PS, Goble AJ, Louis WJ. Perhexiline maleate treatment for severe angina pectoris--correlations with pharmacokinetics. (1986) *Int J Cardiol* **13**:219-29.

443. Rosano GM, Vitale C, Sposato B, Mercuro G, Fini M. Trimetazidine improves left ventricular function in diabetic patients with coronary artery disease: a double-blind placebo-controlled study. (2003) *Cardiovasc Diabetol* **2**:16.

444. Fragasso G, Perseghin G, De Cobelli F et al. Effects of metabolic modulation by trimetazidine on left ventricular function and phosphocreatine/adenosine triphosphate ratio in patients with heart failure. (2006) *Eur Heart J* **27**:942-8.

Appendices

Appendix A: Major Clinical Trials of NO-modulation in Heart Failure

Appendix A-Table 1: List of Major Clinical Trials Exploring the Benefits of NO Modulation in Heart Failure

Mechanism of NO Modulation	Clinical Trial Name(s)	Type of Heart Failure	Clinical Trial Phase and Type	No. of patients (% male)	Effect(s) vs. Placebo (or comparator)	Reference(s)
Enhanced NOS-derived NO						
L-arginine	**-**	HFrEF (NYHA II/III)	Phase 2 random-order crossover, placebo-controlled, double-blind trial	15 (93%)	Increased FBF during exercise, increased 6-min walk distance, and reduced LWHF questionnaire scores.	Rector et al. 1996 Circulation
	-	HFrEF (NYHA III/IV)	Phase 2 randomised, placebo-controlled, double-blind trial	20 (95%)	FBF response to ACh and sodium nitroprusside not affected by L-arginine or placebo.	Chin-Dusting et al. 1996 JACC
Exercise	**-**	HFrEF (NYHA II/III)	Cochrane review of exercise-based cardiac rehab	4,740 (-)	*<1-year follow-up:* no change in mortality, but trend towards reduced hospitalisations (RR 0.88; 95% CI 0.75 to 1.02).	Taylor et al. 2014 Cochrane Database Systematic Reviews

Mechanism of NO Modulation	Clinical Trial Name(s)	Type of Heart Failure	Clinical Trial Phase and Type	No. of patients (% male)	Effect(s) vs. Placebo (or comparator)	Reference(s)
					>1-year follow-up: trend towards reduced mortality (RR 0.88; 95% CI 0.75 to 1.02), and reduced HF hospitalisations (RR 0.61; 95% CI 0.46 to 0.80).	
	HF-ACTION	HFrEF (NYHA II-IV)	Phase 2 randomised, placebo-controlled, double-blind trial	2,331 (72%)	*Intention-to-treat analysis:* reduced all-cause mortality or hospitalisation (HR 0.89; 95% CI 0.81 to 0.99), and reduced cardiovascular mortality or heart failure hospitalisation (HR 0.85; 95% CI 0.74 to 0.99).	O'Connor et al. 2009 JAMA
NO Donors						
Inhaled NO	- (Inhaled NO vs. Sodium Nitroprusside)	HFrEF / PH associated with LVSD (NYHA III/IV)	Phase 2 randomised, placebo-controlled, double-blind trial	16 (81%)	Reduction in PVR ($p<0.05$), but an increase in PCWP ($p<0.05$). No change in MAP.	Semigran et al. 1994 JACC
	- (Inhaled NO vs. Placebo)	HFrEF / PH associated	Phase 2 non-randomised,	19 (79%)	Reduction in PVR ($p<0.05$), but an increase in PCWP ($p<0.05$) and reduction in	Loh et al. 1994 Circulation

Mechanism of NO Modulation	Clinical Trial Name(s)	Type of Heart Failure	Clinical Trial Phase and Type	No. of patients (% male)	Effect(s) vs. Placebo (or comparator)	Reference(s)
		with LVSD (NYHA III/IV)	open-label, single-arm trial		cardiac index (p<0.05). No change in MAP.	
ISMN	NEAT-HFpEF	HFpEF (NYHA II/III)	Phase 2 random-order crossover, placebo-controlled, double-blind trial	110 (43%)	No change in QOL or submaximal exercise capacity, and a reduction in activity levels (−439 accelerometer units; 95% CI, −792 to −86; p = 0.02).	Redfield et al. 2015 NEJM
ISDN + Hydralazine	V-HeFT I (ISDN + Hydralazine vs. prazosin vs. placebo)	HFrEF (-)	Phase 2 randomised, placebo-controlled, double-blind trial	642 (100%)	34% RR in mortality at 2 years (p<0.028) and increased LVEF.	Cohn et al. 1986 NEJM NB: pre-dates Beta-Blocker and ACE-I trials
	V-HeFT II (ISDN + Hydralazine vs. Enalapril)	HFrEF (NYHA II/III)	Phase 2 randomised, placebo-controlled, double-blind trial	804 (100%)	*Enalapril vs. ISDN + Hydralazine:* 28% RR in mortality in the Enalapril arm (p = 0.016).	Cohn et al. 1991 NEJM
	A-HeFT (ISDN + Hydralazine vs. placebo in patients self-	HFrEF (NYHA III/IV)	Phase 2 randomised, placebo-controlled,	1,050 (60%)	Lower rates of all-cause mortality (HR 0.57; p = 0.01), heart failure hospitalisations (p = 0.001)	Taylor et al. 2004 NEJM

Mechanism of NO Modulation	Clinical Trial Name(s)	Type of Heart Failure	Clinical Trial Phase and Type	No. of patients (% male)	Effect(s) vs. Placebo (or comparator)	Reference(s)
	identifying as black)		double-blind trial		and improved QOL scores (p = 0.02).	
Sodium Nitroprusside	-	HFrEF / LVSD due to AMI	Phase 2 randomised, placebo-controlled, double-blind trial	18 (-)	Reduced PCWP, and slight fall in MAP. Significantly increased cardiac output, SV, and LVEF.	Guiha et al. 1974 NEJM
	-	LVSD in setting of severe AS	Phase 2 non-randomised, open-label, single-arm trial	25 (64%)	Increase in cardiac index (p<0.001). Well-tolerated with minimal side effects.	Khot et al. 2003 NEJM
	-	Low-output ADHF	Phase 2 non-randomised, retrospective review of patient notes	175 (81%)	Lower rates of all-cause mortality (OR 0.48; 95% CI: 0.29 to 0.80; p = 0.005), without an increase in rehospitalization rates (58% vs. 56%; p = NS).	Mullens et al. 2008 JACC
GTN	VMAC (Nesiritide vs. GTN vs. placebo)	ADHF	Phase 2 randomised, placebo-controlled,	489 (69%)	GTN reduced PCWP, and improved dyspnoea and global clinical status.	Publication Committee for the VMAC

Mechanism of NO Modulation	Clinical Trial Name(s)	Type of Heart Failure	Clinical Trial Phase and Type	No. of patients (% male)	Effect(s) vs. Placebo (or comparator)	Reference(s)
			double-blind trial		*GTN vs. Nesiritide:* Nesiritide further reduced PCWP (p<0.001 vs. GTN) but no difference in dyspnoea and only modest improvement in global clinical status.	Investigators 2002 JAMA
		ADHF with HTN	Phase 2 non-randomised, open-label, single-arm trial	74 (61%) = 29 (65%) GTN + 45 (58%) no intervention	Fewer endotracheal intubations, use of BiPAP, and ICU admissions.	Levy et al. 2007 Ann Emerg Med
sGC Stimulators						
Riociguat	LEPHT	HFrEF / PH associated with LVSD (NYHA II-IV)	Phase 2b randomised, placebo-controlled, double-blind trial	201 (86%)	Trend towards reduced primary endpoint of PASP (p = 0.10). Significantly reduced cardiac index (p = 0.0001), stroke volume index (p = 0.0018), and LWHF scores (p = 0.0002).	Bonderman et al. 2013 Circulation

Mechanism of NO Modulation	Clinical Trial Name(s)	Type of Heart Failure	Clinical Trial Phase and Type	No. of patients (% male)	Effect(s) vs. Placebo (or comparator)	Reference(s)
Vericiguat	VICTORIA	HFrEF (NYHA II-IV)	Phase 3 randomised, placebo-controlled, double-blind trial	5,050 (-)	Reduced primary outcome events (HR 0.90; 95% CI 0.82 to 0.98; P=0.02). *Primary outcome =* composite of cardiovascular mortality or first hospitalization for heart failure.	Armstrong et al. 2020 NEJM
sGC Activators						
Cinaciguat	-	ADHF	Phase 2b randomised (2:1), placebo-controlled, double-blind trial	146 (85%)	Reduced PCWP ($p<0.0001$), RAP ($p = 0.0019$), and cardiac index and MAP ($p<0.0001$). The trial was stopped prematurely due to an increased occurrence of hypotension.	Erdmann et al. 2013 Eur J Heart Fail
	COMPOSE	ADHF	Phase 2b randomised, placebo-controlled, double-blind trial programme	78 (83%)	Short-term use of intravenous Cinaciguat decreased blood pressure without improving dyspnoea or cardiac index.	Gheorghiade et al. 2012 Eur J Heart Fail

Mechanism of NO Modulation	Clinical Trial Name(s)	Type of Heart Failure	Clinical Trial Phase and Type	No. of patients (% male)	Effect(s) vs. Placebo (or comparator)	Reference(s)
PDE Inhibitors						
Sildenafil (PDE5 inhibitor)	-	HFrEF (NYHA II/III)	Phase 2 randomised, placebo-controlled, double-blind trial	45 (100%)	Improved peak VO_2 (+2.7 ml/kg/min vs. baseline) and ventilation efficiency on CPEX, and QOL scores (all $p<0.01$).	Guazzi et al. 2011 Circulation
	RELAX	HFpEF (NYHA II/III)	Phase 3 randomised, placebo-controlled, double-blind trial	216 (52%)	Did not alter exercise capacity or clinical status compared to placebo.	Redfield et al. 2013 JAMA
PDE3 Inhibitors	-	HFrEF (II-IV)	Cochrane review	8,408 (-)	Increased all-cause mortality (HR 1.17; 95% CI 1.06 to 1.30; $p<0.001$).	Amsallem et al. 2013 Cochrane Database Systematic Reviews

ACE-I, angiotensin converting enzyme inhibitor; ACh, acetylcholine; ADHF, acute decompensated heart failure; AMI, acute myocardial infarction; BiPAP, bilevel positive airways pressure; FBF, forearm blood flow; GTN, glyceryl trinitrate; HFpEF, heart failure with preserved ejection fraction; HFrEF, heart failure with reduced ejection fraction; ICU, intensive care unit; ISDN, isosorbide dinitrate; LVEF, left ventricular ejection fraction; MAP, mean arterial pressure; PCWP, pulmonary capillary wedge pressure; PVR, pulmonary vascular resistance; QOL, quality of life; RHF, right heart failure.

References

Amsallem E, Kasparian C, Haddour G, Boissel JP and Nony P. Phosphodiesterase III inhibitors for heart failure. (2013) *Cochrane Database Syst Rev*. Issue **1**. DOI: 10.1002/14651858.CD002230.pub2.

Armstrong PW, Pieske B, Anstrom KJ et al; VICTORIA Study Group. Vericiguat in Patients with Heart Failure and Reduced Ejection Fraction. (2020) *N Engl J Med* **382**:1883-1893.

Bonderman D, Ghio S, Felix SB et al; Left Ventricular Systolic Dysfunction Associated With Pulmonary Hypertension Riociguat Trial (LEPHT) Study Group. Riociguat for patients with pulmonary hypertension caused by systolic left ventricular dysfunction: a phase IIb double-blind, randomized, placebo-controlled, dose-ranging hemodynamic study. (2013) *Circulation* **128**:502-11.

Chin-Dusting JP, Kaye DM, Lefkovits J, Wong J, Bergin P, Jennings GL. Dietary supplementation with L-arginine fails to restore endothelial function in forearm resistance arteries of patients with severe heart failure. (1996) *J Am Coll Cardiol* **27**:1207-13.

Cohn JN, Archibald DG, Ziesche S et al. Effect of vasodilator therapy on mortality in chronic congestive heart failure. Results of a Veterans Administration Cooperative Study. (1986) *N Engl J Med* **314**:1547-52.

Cohn JN, Johnson G, Ziesche S et al. A comparison of enalapril with hydralazine-isosorbide dinitrate in the treatment of chronic congestive heart failure. (1991) *N Engl J Med* **325**:303-10.

Erdmann E, Semigran MJ, Nieminen MS et al. Cinaciguat, a soluble guanylate cyclase activator, unloads the heart but also causes hypotension in acute decompensated heart failure. (2013) *Eur Heart J* **34**:57-67.

Gheorghiade M, Greene SJ, Filippatos G et al; COMPOSE Investigators and Coordinators. Cinaciguat, a soluble guanylate cyclase activator: results from the randomized, controlled, phase IIb COMPOSE programme in acute heart failure syndromes. (2012) *Eur J Heart Fail* **14**:1056-66.

Guazzi M, Vicenzi M, Arena R, Guazzi MD. Pulmonary hypertension in heart failure with preserved ejection fraction: a target of phosphodiesterase-5 inhibition in a 1-year study. (2011) *Circulation* **124**:164-74.

Guiha NH, Cohn JN, Mikulic E, Franciosa JA, Limas CJ. Treatment of refractory heart failure with infusion of nitroprusside. (1974) *N Engl J Med* **291**:587-92.

Khot UN, Novaro GM, Popović ZB et al. Nitroprusside in critically ill patients with left ventricular dysfunction and aortic stenosis. (2003) *N Engl J Med* **348**:1756-63.

Levy P, Compton S, Welch R et al. Treatment of severe decompensated heart failure with high-dose intravenous nitroglycerin: a feasibility and outcome analysis. (2007) *Ann Emerg Med* **50**:144-52.

Loh E, Stamler JS, Hare JM, Loscalzo J, Colucci WS. Cardiovascular effects of inhaled nitric oxide in patients with left ventricular dysfunction. (1994) *Circulation* **90**:2780-5.

Mullens W, Abrahams Z, Francis GS et al. Sodium nitroprusside for advanced low-output heart failure. (2008) *J Am Coll Cardiol* **52**:200-7.

O'Connor CM, Whellan DJ, Lee KL et al; HF-ACTION Investigators. Efficacy and safety of exercise training in patients with chronic heart failure: HF-ACTION randomized controlled trial. (2009) *JAMA* **301**:1439-50.

Publication Committee for the VMAC Investigators (Vasodilatation in the Management of Acute CHF). Intravenous nesiritide vs nitroglycerin for treatment of decompensated congestive heart failure: a randomized controlled trial. (2002) *JAMA* **287**:1531-40.

Rector TS, Bank AJ, Mullen KA et al. Randomized, double-blind, placebo-controlled study of supplemental oral L-arginine in patients with heart failure. (1996) *Circulation* **93**:2135-41.

Redfield MM, Anstrom KJ, Levine JA et al; NHLBI Heart Failure Clinical Research Network. Isosorbide Mononitrate in Heart Failure with Preserved Ejection Fraction. (2015) *N Engl J Med* **373**:2314-24.

Redfield MM, Chen HH, Borlaug BA et al; RELAX Trial. Effect of phosphodiesterase-5 inhibition on exercise capacity and clinical status in heart failure with preserved ejection fraction: a randomized clinical trial. (2013) *JAMA* **309**:1268-77.

Semigran MJ, Cockrill BA, Kacmarek R et al. Hemodynamic effects of inhaled nitric oxide in heart failure. (1994) *J Am Coll Cardiol* **24**:982-8.

Taylor AL, Ziesche S, Yancy C et al; African-American Heart Failure Trial Investigators. Combination of isosorbide dinitrate and hydralazine in blacks with heart failure. (2004) *N Engl J Med* **351**:2049-57.

Taylor RS, Sagar VA, Davies EJ et al. Exercise-based rehabilitation for heart failure. (2014) *Cochrane Database Syst Rev* **2014**:CD003331.

Appendix B: Published Original Research Articles

1. Article/s from Chapter 1:

Loudon BL, Noordali H, Gollop ND, Frenneaux MP, Madhani M. Present and future pharmacotherapeutic agents in heart failure: an evolving paradigm. Br J Pharmacol. 2016 Jun; 173(12):1911-24. Doi: 10.1111/bph.13480. Epub 2016 May 6. Review.

Noordali H, **Loudon BL**, Frenneaux MP, Madhani M. Cardiac metabolism - A promising therapeutic target for heart failure. Pharmacol Ther. 2018 Feb; 182:95-114. Doi: 10.1016/j.pharmthera.2017.08.001. Epub 2017 Aug 15. Review.

2. Article/s from Chapter 3 data:

Ntessalen M, Procter NEK, Schwarz K, **Loudon BL**, Minnion M, Fernandez BO, Vassiliou VS, Vauzour D, Madhani M, Constantin-Teodosiu D, Horowitz JD, Feelisch M, Dawson D, Crichton PG, Frenneaux MP. Inorganic nitrate and nitrite supplementation fails to improve skeletal muscle mitochondrial efficiency in mice and humans. Am J Clin Nutr. 2020 Jan 1; 111(1):79-89. Doi: 10.1093/ajcn/nqz245.

3. Article/s from Chapter 6 data:

Currently under Review:

Loudon BL, Abozguia K, Ahmed I, Phan TT, McKiddie F, Cameron D, Elliott P, McKenna WJ, Vassiliou VS, Sherrid MV, Frenneaux MP. Myocardial Energy Deficiency is associated with Exercise-Induced Diastolic and Systolic Dysfunction in Symptomatic Hypertrophic Cardiomyopathy.